平成 26～28 年度労災疾病臨床研究事業

胸膜中皮腫の的確な診断方法に関する研究
―鑑別診断方法と症例収集―

平成 29 年 3 月

胸膜中皮腫の的確な診断方法に関する研究班

胸膜中皮腫の的確な診断方法に関する研究
―鑑別診断方法と症例収集―

研究者一覧

研究代表者	労働者健康安全機構岡山労災病院副院長	岸本 卓巳
研究分担者	国立病院機構山口宇部医療ｾﾝﾀｰ統括診療部内科系診療部長	青江 啓介
	長崎大学大学院医歯薬学総合研究科臨床腫瘍学教授	芦澤 和人
	広島大学名誉教授	井内 康輝
	川崎医科大学衛生学教授	大槻 剛巳
	労働者健康安全機構北海道中央労災病院病理診断科部長	岡本 賢三
	川崎医科大学放射線医学教授	加藤 勝也
	国立学校共済組合中国中央病院腫瘍内科部長	玄馬 顕一
	広島大学大学院医歯薬保健学研究科病理学研究室教授	武島 幸男
	労働者健康安全機構岡山労災病院腫瘍内科部長	藤本 伸一
	労働者健康安全機構千葉労災病院ｱｽﾍﾞｽﾄ疾患センター長	由佐 俊和
研究協力者	広島大学大学院医歯薬保健学研究科病理学研究室講師	Amatya V. Jeet
	JA 愛知厚生連海南病院病理診断科	石川 操
	労働者健康安全機構北海道中央労災病院副院長	大塚 義紀
	社会医療法人北海道恵愛会札幌南三条病院副院長	加地 苗人
	広島大学大学院医歯薬保健学研究科病理学研究室助教	櫛谷 桂
	玉野三井病院内科	筒井 英太
	国立病院機構近畿中央胸部疾患センター院長	林 清二
	労働者健康安全機構富山労災病院ｱｽﾍﾞｽﾄ疾患センター長	水橋 啓一
	労働者健康安全機構香川労災病院副院長	丸川 將臣
	労働者健康安全機構岡山労災病院臨床病理科	藤木 正昭
	労働者健康安全機構岡山労災病院臨床病理科	妹尾 純江
	労働者健康安全機構岡山労災病院臨床検査部	宮原 基平
	労働者健康安全機構岡山労災病院ｱｽﾍﾞｽﾄ関連疾患研究ｾﾝﾀｰ	児島 葉子
	労働者健康安全機構岡山労災病院ｱｽﾍﾞｽﾄ関連疾患研究ｾﾝﾀｰ	藤村 敬子
	労働者健康安全機構岡山労災病院ｱｽﾍﾞｽﾄ関連疾患研究ｾﾝﾀｰ	佐藤 史織
	労働者健康安全機構岡山労災病院ｱｽﾍﾞｽﾄ関連疾患研究ｾﾝﾀｰ	安井 利枝

目　次

はじめに　・・・・・・　1

1. 胸膜中皮腫の CT 画像に関する研究　・・・・・・　2
岸本　卓巳、青江　啓介、芦澤　和人、
岡本　賢三、加藤　勝也

2. 悪性胸膜中皮腫の診断における胸水中の Secretory leukocyte protease inhibitor（SLPI）の有用性について　・・・・・・　21
藤本　伸一、岸本　卓巳

3. 中皮腫の病理学的鑑別診断の為の新規免疫組織化学マーカーの探索　・・・・・・　33
櫛谷　桂、Amatya V. Jeet、武島　幸男

4. 胸膜中皮腫の的確な診断に資するための ICT を用いた遠隔病理及び画像診断の応用　・・・・・・　60
井内　康輝、由佐　俊和

5. 中皮腫の症例において他疾患との鑑別が困難な症例の収集、的確な鑑別診断の方法に関する研究、及び胸水の症例において石綿によるものと他の原因によるものとの鑑別が困難な症例の収集、的確な鑑別診断の方法に関する研究　・・・・・・　71
大槻　剛巳

6. 石綿健康管理手帳健診受診者を対象とした低線量 CT についての検討　-長期経過観察後の解析-　・・・・・・　87
玄馬　顕一、加藤　勝也、芦澤　和人、
由佐　俊和、岸本　卓巳

研究成果の刊行に関する一覧表　・・・・・・　105

研究成果の刊行物・別刷　・・・・・・　107

はじめに

胸膜中皮腫の鑑別診断では、肺癌や肉腫のような悪性腫瘍から胸膜炎のような良性疾患までと幅広いため、現在でもなお確定診断が難しいのが現状である。

我々の研究班はその診断率を高めるための画像、胸水マーカー及び病理診断等を中心とした診断方法についての研究を開始して 3 年が経過した。

平成 28 年度は岡山労災病院のみならず、山口宇部医療センター及び札幌南三条病院の症例を併せた 782 例について画像パターンデータを集積して、胸膜中皮腫画像のパターンをまとめた。そして、病理組織型別に画像パターンに特異性があることを報告した。さらに、平成 27 年度に行った 2008 年前後の比較検討を行い、病理組織型あるいは画像パターン別の予後についても検討した。

また、胸水の診断マーカーである SLPI（Secretory leukocyte protease inhibitor）の画像パターン別の診断意義について検討するとともにヒアルロン酸、SMRP との比較を行った。そして、良性石綿胸水と早期中皮腫との新たな鑑別マーカーとしての意義について述べた。

画像及び病理組織を用いた遠隔診断方法について、その簡便性や精度についての最終評価を行うとともに、今後の中皮腫診断に対する方向性について海外支援を含めた有用性に言及した。

胸膜中皮腫の病理学的鑑別診断のための新規免疫組織化学マーカーの探索では、上皮型中皮腫と反応性中皮細胞過形成、肉腫型中皮腫と肺肉腫様癌、低分化型上皮型中皮腫と低分化型小細胞性肺癌のマーカーとして有用なマーカーとして、各々特異性の高い抗体を推奨した。

一方、胸膜中皮腫患者における免疫能について検証するため血漿サイトカイン、免疫担当細胞のマーカーと機能について、石綿ばく露によるびまん性胸膜肥厚患者を対照として検討を行い、石綿ばく露による悪性及び良性疾患の間での免疫担当細胞に相違が認められることを明らかにし、末梢血免疫担当細胞のパターンを数式化して画像以外でも胸膜中皮腫を早期診断できるかどうかの検討を行った。

さらに、過去の厚生労働省科学研究で行った石綿健康管理手帳健診受診者における低線量 CT 検査の継続経過観察の結果、低線量 CT 施行群がレントゲン撮影群に対して肺癌による予後の改善に有用であるという結果を得ることができた。

症例収集にあたっては、本研究においても診療情報を使用することを許可していただいた2003年から2008年に中皮腫によって死亡した患者のご遺族の皆様と情報提供いただいた病院関係者の皆様及び本研究の目的に賛同していただいた労災病院等の胸膜中皮腫及びびまん性胸膜肥厚患者の皆様に深く感謝いたします。

平成 29 年 3 月 31 日

胸膜中皮腫の的確な診断方法に関する研究班
研究代表者　岸本　卓巳

胸膜中皮腫の CT 画像に関する研究

岸本　卓巳、青江　啓介、芦澤　和人、岡本　賢三、加藤　勝也

【 目　的 】

胸膜中皮腫は比較的早期診断が難しい疾病であると言われているが、胸部 CT 画像上、不整形の胸膜肥厚や腫瘤形成を示さない症例が増加傾向にある。そこで胸膜中皮腫と診断された症例が初診時にどのような画像所見を呈したかについて検討した。胸膜中皮腫であると確定された症例の初診時の胸部 CT 画像所見について検討した。また、年代別に画像パターンの相違があるかどうか、中皮腫診断に対する呼吸器内科あるいは外科医の早期診断精度があがっていなかった 2008 年までに診断された症例と、診断精度が向上してきた 2009 年以降に診断された症例に分けて検討した。さらに胸膜中皮腫の病理組織型別に画像上の特徴的所見があるかどうかを検討した。また、岡山労災病院の症例においては診断時の病期を検討し、組織型あるいは画像パターンと予後の関係についても検討した。

【 対象と方法 】

以前の厚生労働科学研究において、全国で 2003 年～2008 年までに胸膜中皮腫で死亡した症例で遺族及び死亡診断書を作成した病院での同意を得て画像等の診療情報を収集した。そのうち胸膜中皮腫の 651 例で組織型が確定している 482 例、2000 年から 2016 年までの 17 年間に岡山労災病院で胸膜中皮腫と診断された 166 例、2005 年～2016 年までの 12 年間に山口宇部医療センターで診断された 110 例及び 2006 年～2016 年までの 11 年間に札幌南三条病院で診断された 24 例を併せて検討した。

次に、これらの症例を兵庫県尼崎市の旧クボタ神崎工場周辺で石綿ばく露による中皮腫が多発し社会問題化して注目度が高くなった 2009 年前後の診断年代別に分類した。2003 年～2008 年までに全国で胸膜中皮腫と診断され、組織型が確定している 482 例と 2000 年～2008 年までに岡山労災病院、山口宇部医療センター、札幌南三条病院で胸膜中皮腫と確定診断された 112 例の計 594 例と 2009 年～2015 年までに岡山労災病院、山口宇部医療センター、札幌南三条病院で胸膜中皮腫と確定診断された 188 例の 3 グループに分けて検討した。また、各群は病理組織型別にもどのような胸部 CT 画像の特徴があるか検討した。（**表 1**）。

岡山労災病院の 166 例については IMIG 分類により病期を確認し、組織型別あるいは画像パターン別に予後について検討した。

表 1. 胸膜中皮腫の初診時 CT 画像の特徴

- １：単発胸膜腫瘤形成
- ２：環状胸膜肥厚（厚みがおおむね3mm以上）
- ３：軽度胸膜肥厚（厚みが３mm未満）
- ４：縦隔側胸膜肥厚
- ５：胸水のみ
- ６：多発性腫瘤形成（漿膜腫瘤）
- ７：特殊型 （胸壁腫瘤形成、縦隔腫瘤形成等）

これらの症例は平成 26 年度に本研究を始めた際に決定した既述の分類によって検討した。1：単発胸膜腫瘤形成、2：環状胸膜肥厚、3：軽度胸膜肥厚、4：縦隔側胸膜肥厚、5：胸水のみ、6：多発性腫瘤形成（漿膜腫瘤）、7：特殊型である（**図 1～12**）。ただし、環状胸膜肥厚の厚みについては 5mm 以上から 3mm 以上へ変更した。また、胸水の有無について中皮腫とそれ以外の疾患別に合併率を検討した。また、岡山労災病院の 166 例については IMIG 分類に従って病期の検討を行い、病期別に胸部 CT 画像の相違を比較した。そして、病期別あるいは画像パターン別の生存期間についても検討した。

図 1. 1：単発胸膜腫瘤形成

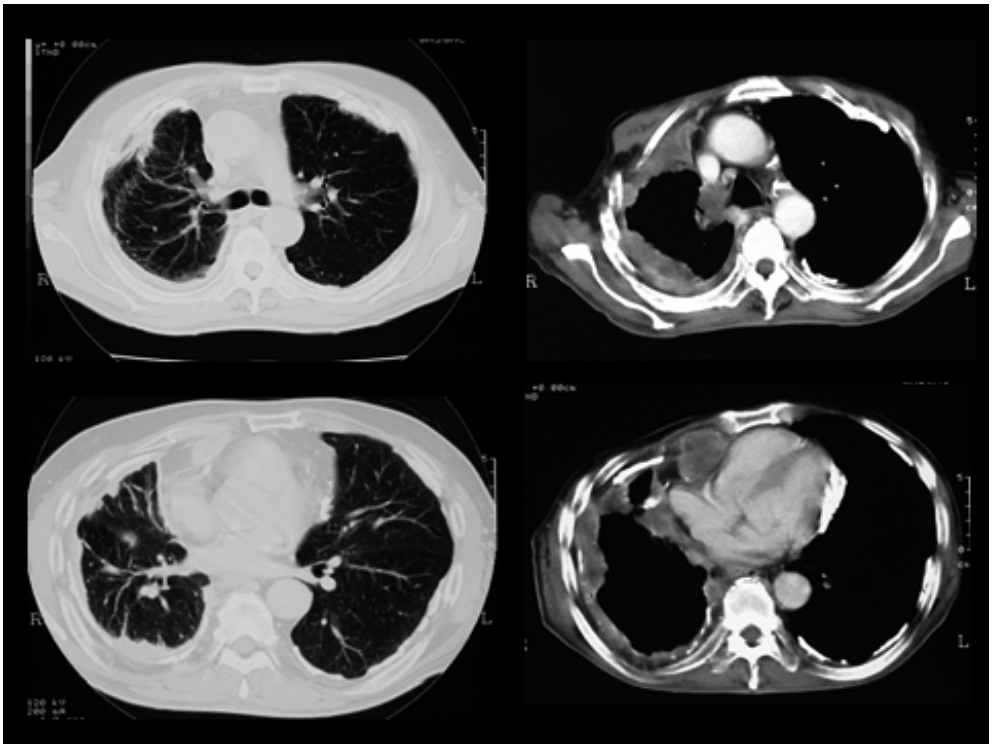

図 2. 2：環状胸膜肥厚

図 3. 2：環状胸膜肥厚

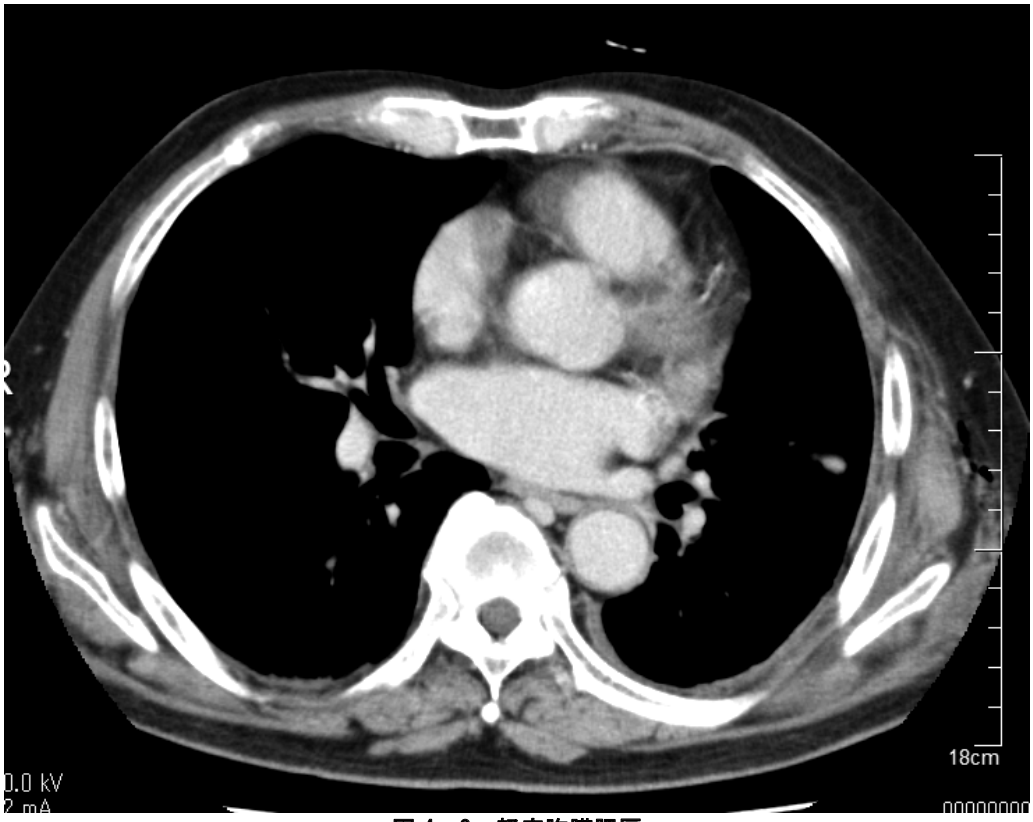

図 4. 3：軽度胸膜肥厚

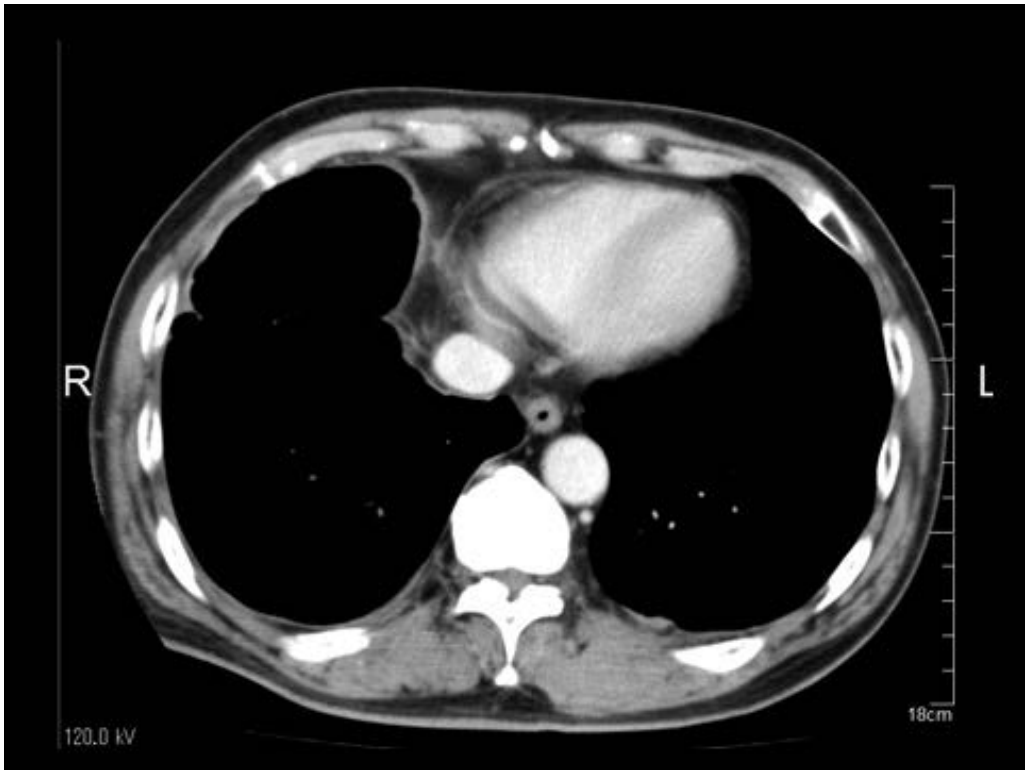

図 5. 3：軽度胸膜肥厚＋4：縦隔側胸膜肥厚

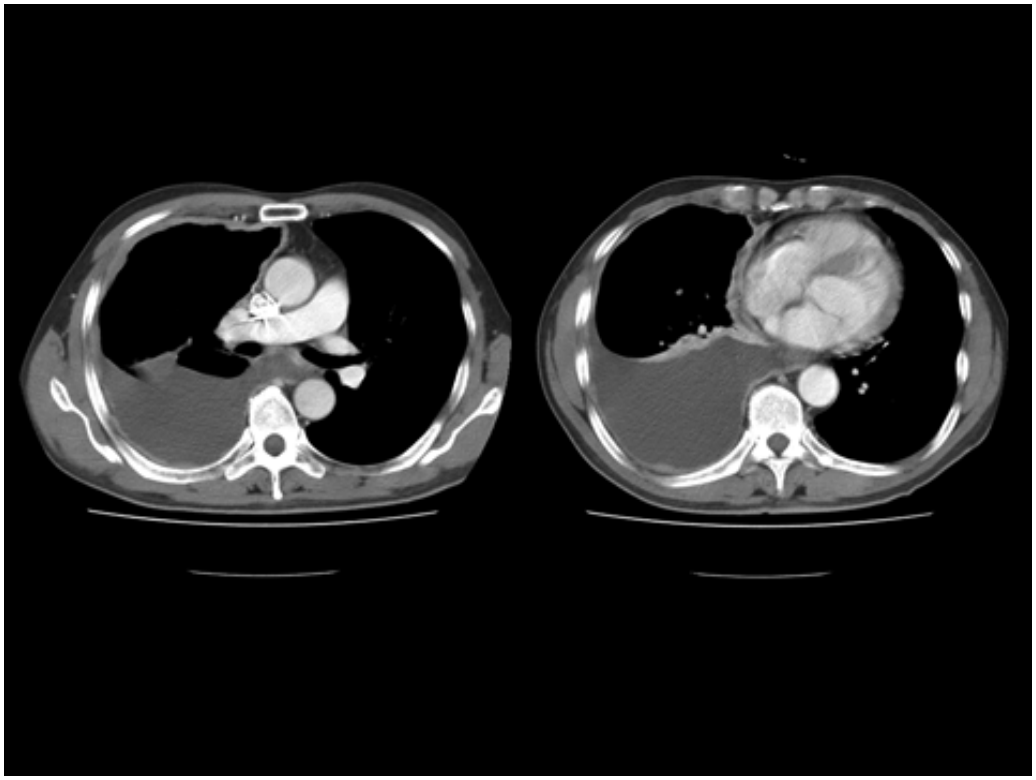

図 6．3：軽度胸膜肥厚＋4：縦隔側胸膜肥厚

図 7．5：胸水のみ

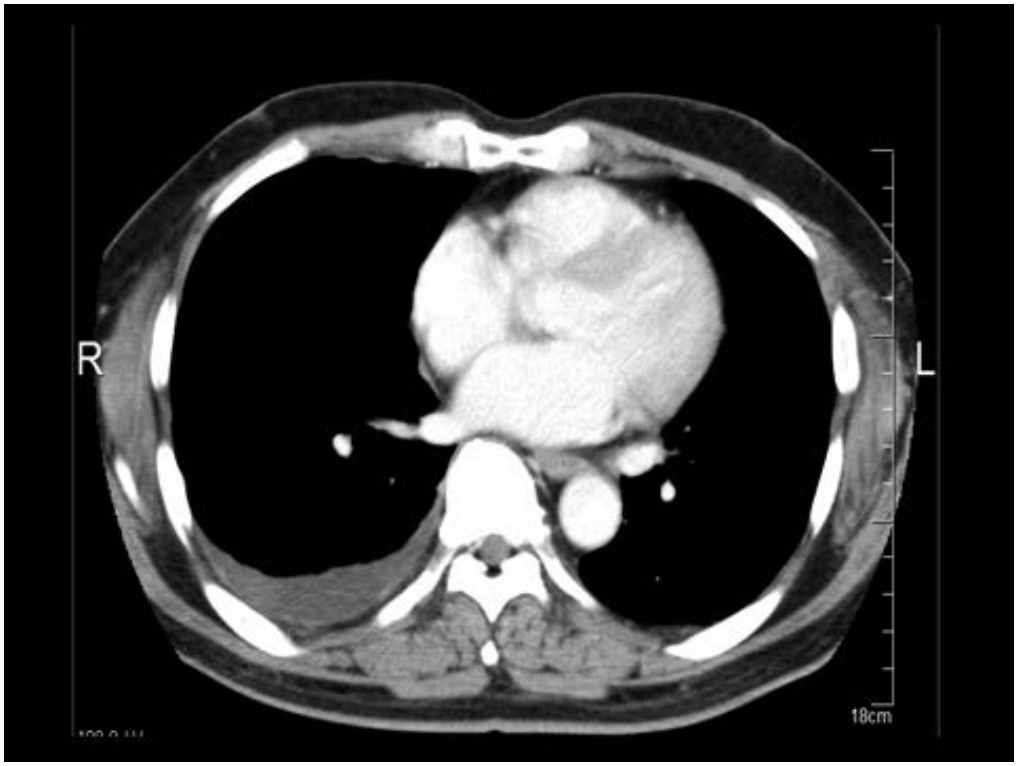

図 8. 5：胸水のみ

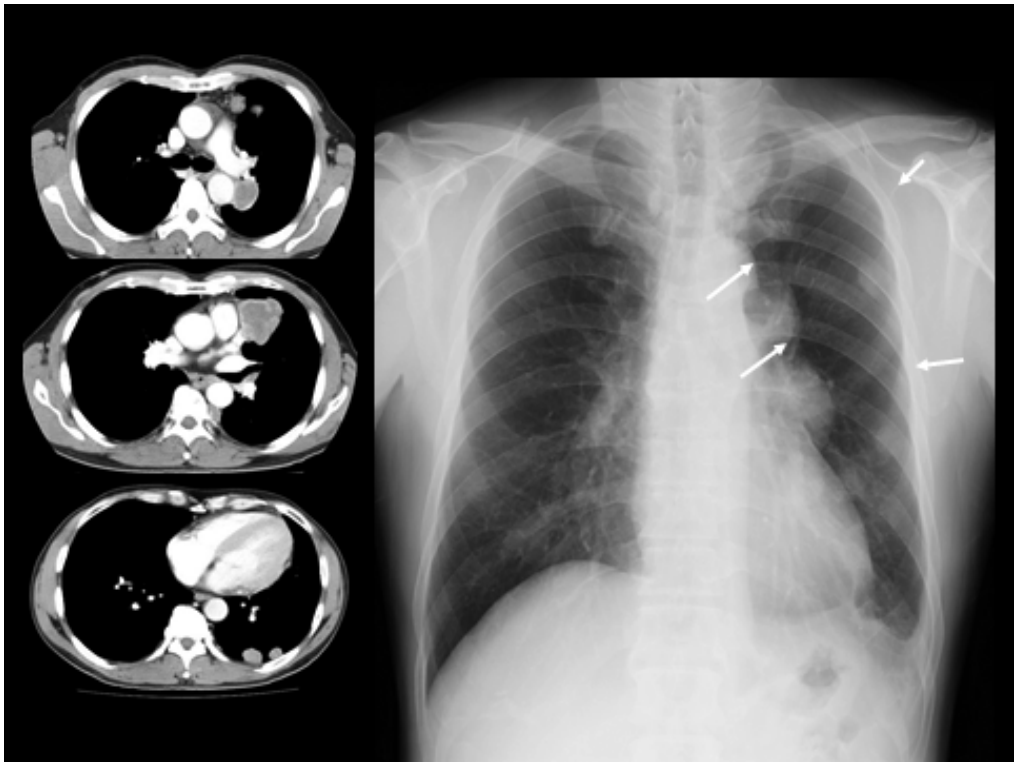

図 9. 6：多発性腫瘤形成

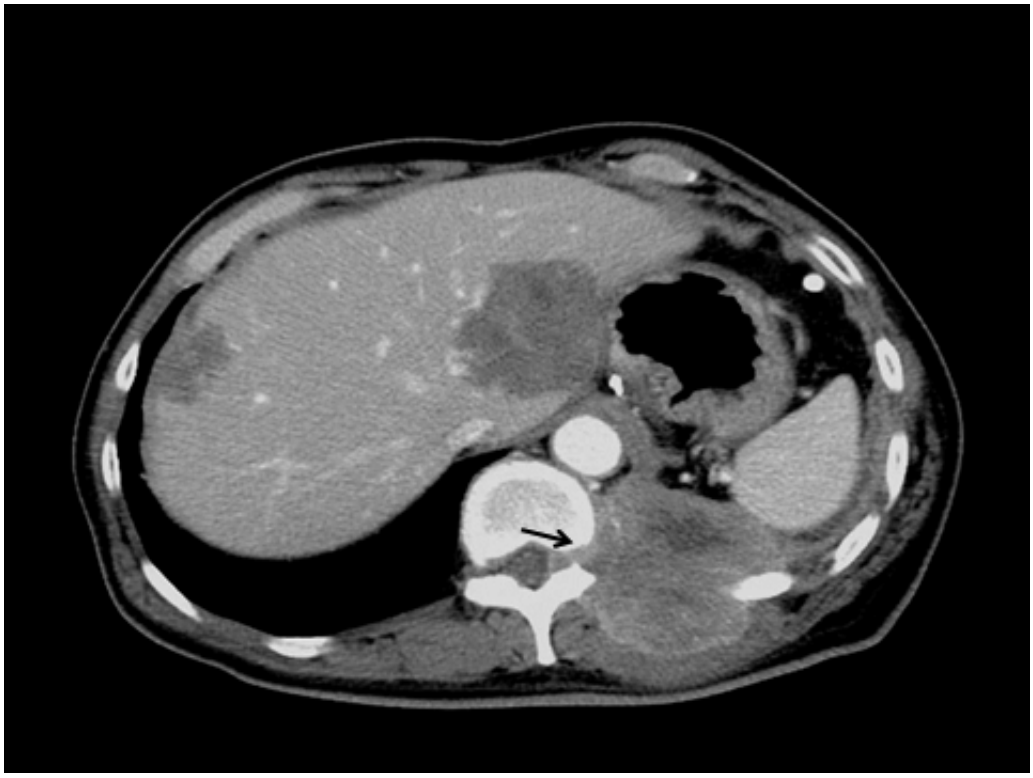

図 10. 7：特殊型（胸壁腫瘤形成）

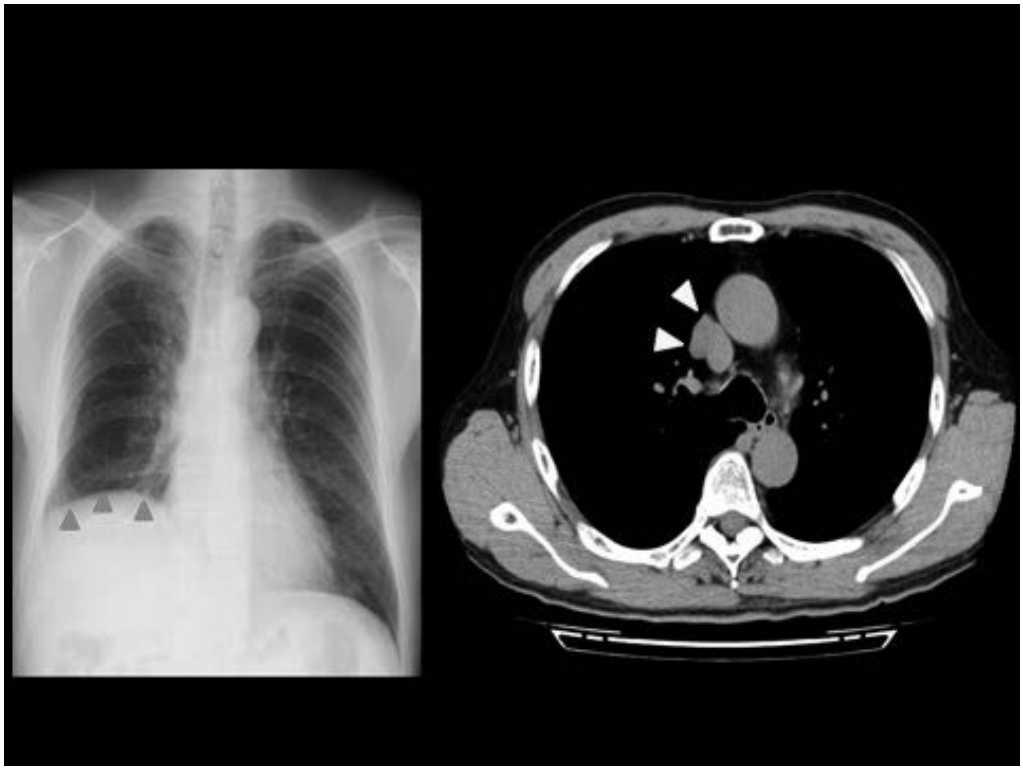

図 11. 7：特殊型（縦隔腫瘤形成）

【 結　果 】

1. 全対象者 782 例の結果

（1）組織型、胸水の有無と画像パターン

病理組織型が確定した胸膜中皮腫 482 例の全国症例、2000 年～2016 年までの 17 年間に岡山労災病院で胸膜中皮腫と診断された 166 例、山口宇部医療センターで 2005 年～2016 年までに診断された 110 例と 2006 年～2016 年までに札幌南三条病院で診断された 24 例の合計 782 症例については上皮型 59.6%、肉腫型 21.5%、二相型 18.3%、特殊型 0.6%であった（**図 12**）。そのうち、胸水を伴う症例は 89.1%であった。画像パターンでは、環状胸膜肥厚が 39.0%と最も多く、次に多発性腫瘤形成が 14.9%、縦隔側胸膜肥厚が 14.8%、軽度胸膜肥厚が 12.7%、単発胸膜腫瘤形成は 9.2%、胸水のみが 8.4%、特殊型が 1.0%であった（**図 13**）。

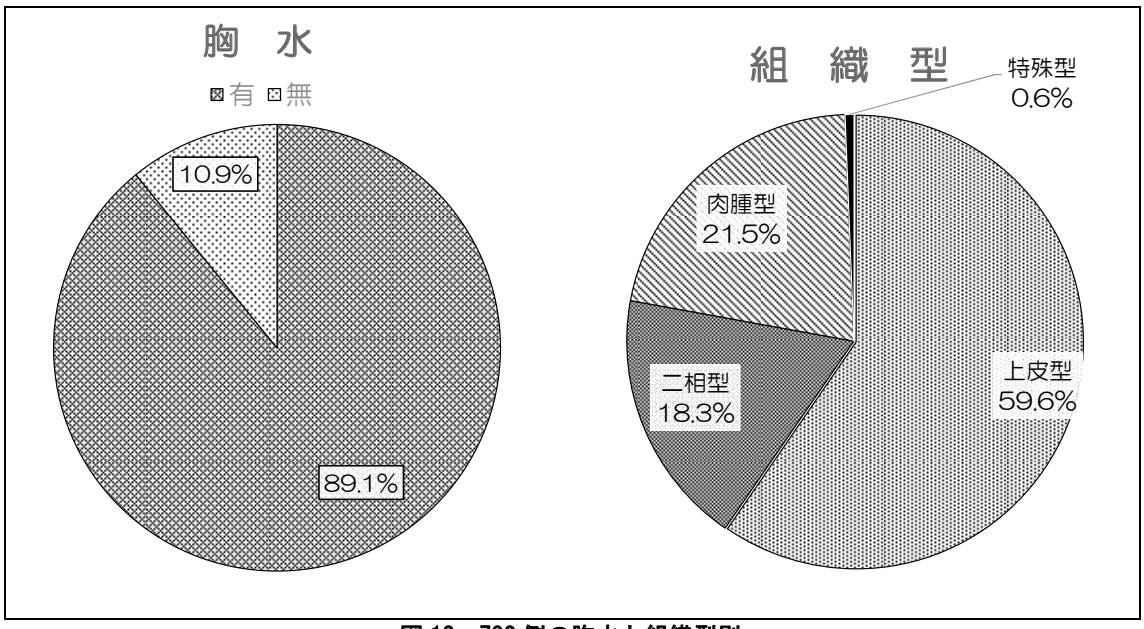

図 12. 782 例の胸水と組織型別

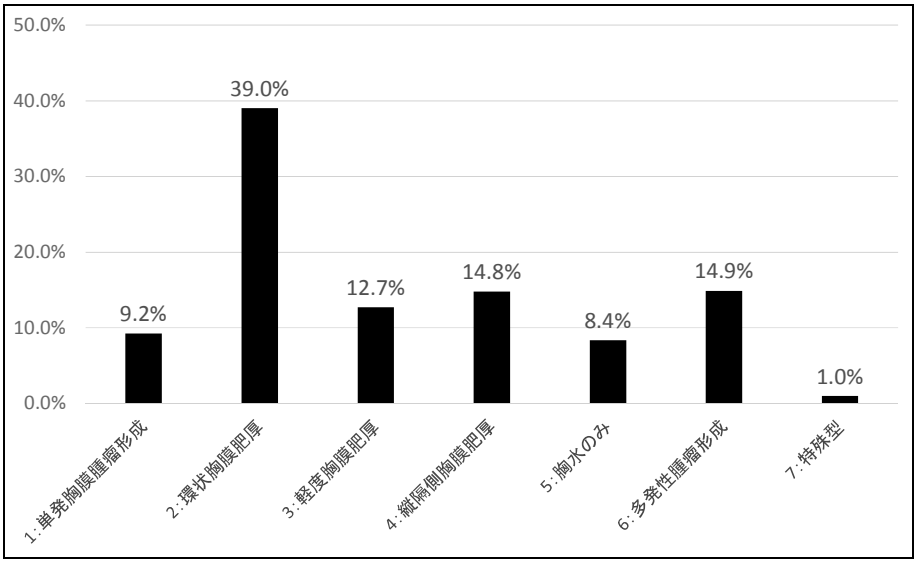

図 13. 総合 782 例

（２）組織型別画像パターン

組織型別では、上皮型 466 例（**図 14**）では環状胸膜肥厚が 35.2%と最も多く、次に、縦隔側胸膜肥厚が 16.8%、軽度胸膜肥厚が 13.8%、多発性腫瘤形成が 13.7%、胸水のみが 10.1%、単発胸膜腫瘤形成が 9.2%、特殊型が 1.2%であった。二相型 143 例（**図 15**）では環状胸膜肥厚が 42.7%、次いで縦隔側胸膜肥厚が 15.8%、多発性腫瘤形成が 14.0%、軽度胸膜肥厚が 11.7%、胸水のみが 8.8%、単発胸膜腫瘤形成は 6.4%と少なかった。また、特殊型は 0.6%であった。さらに肉腫型 168 例（**図 16**）では環状胸膜肥厚が 47.5%、多発性腫瘤形成が 19.5%、単発胸膜腫瘤形成が 11.9%であった。一方、胸水のみはわずか 2.7%で、特殊型は 0.5%であった。

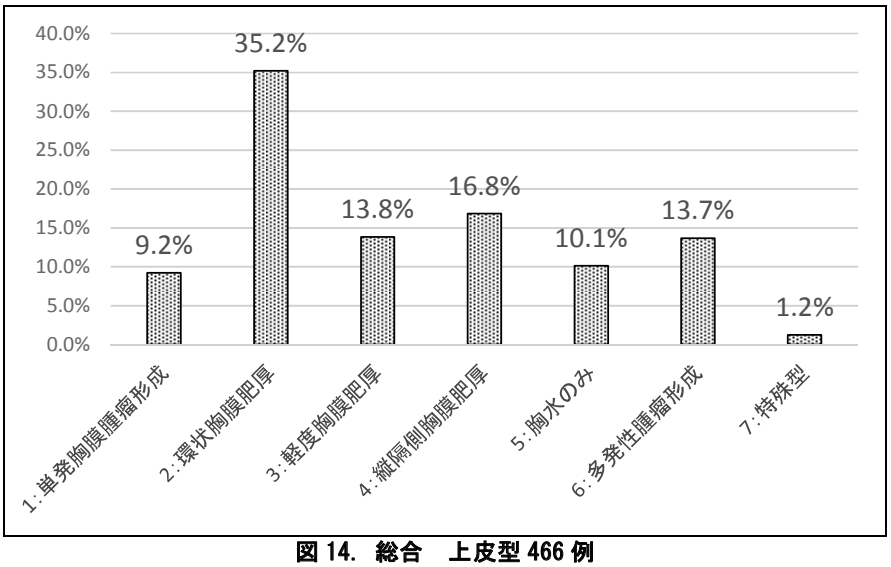

図 14. 総合　上皮型 466 例

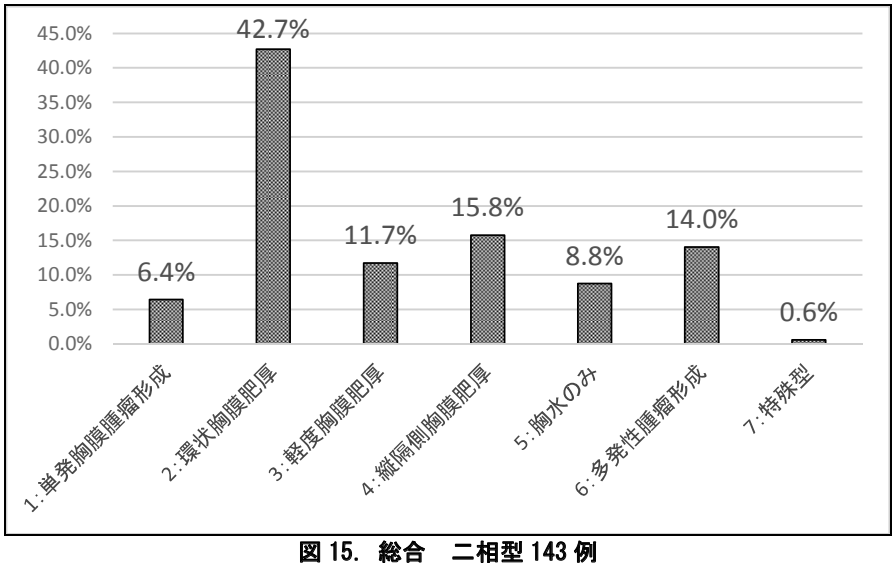

図 15. 総合　二相型 143 例

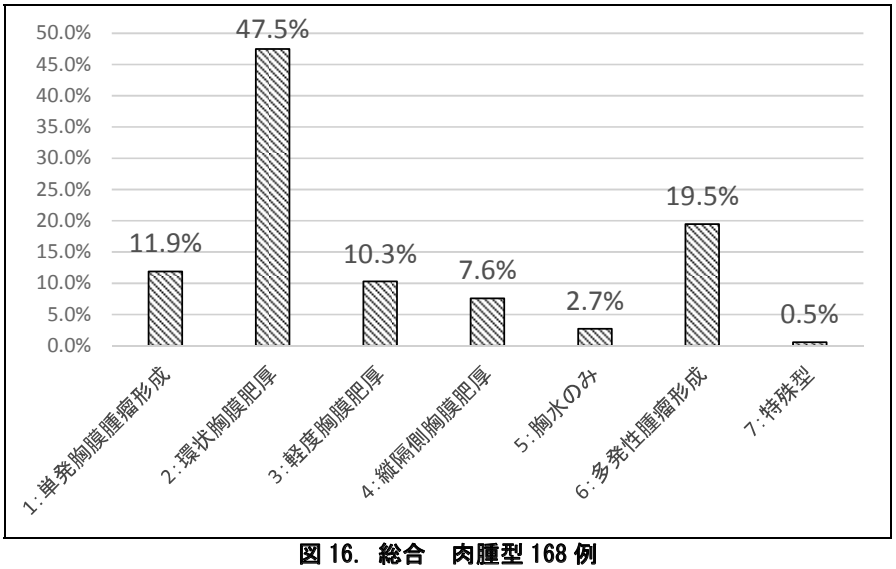

図 16. 総合　肉腫型 168 例

２．年代別画像パターン

（１）2008 年までの画像パターン

2008 年までの全国で胸膜中皮腫と診断された 482 例と、2000 年～2008 年までに岡山労災病院、山口宇部医療センター、札幌南三条病院で胸膜中皮腫と確定診断された 112 例の診断例では、環状胸膜肥厚が 41.3%、次いで多発性腫瘤形成が 16.1%、軽度胸膜肥厚が 12.4%、縦隔側胸膜肥厚が 12.0%、単発胸膜腫瘤形成が 10.1%、胸水のみが 7.5%、特殊型 0.6%であった（**図 17**）。

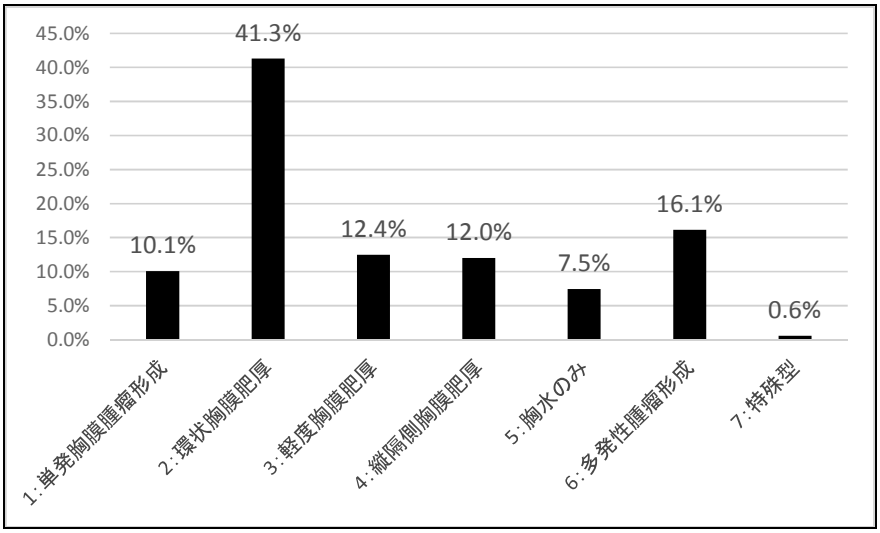

図 17. ～2008 年まで　総合

（２）2008 年までの組織型別画像パターン

このパターンを組織型別で検討すると、2008 年までの上皮型の診断例では、環状胸膜肥厚が 39.1%、多発性腫瘤形成が 14.7%、軽度胸膜肥厚と縦隔側胸膜肥厚が各 13.2%、単発胸膜腫瘤形成が 10.4%、胸水のみが 8.9%、特殊型 0.5%であった（**図 18**）。二相型の 2008 年までの診断例では、環状胸膜肥厚が 41.8%、多発性腫瘤形成が 15.5%、縦隔側胸膜肥厚が 14.0%、軽度胸膜肥厚 11.6%、胸水のみが 9.3%、単発胸膜腫瘤形成が 7.0%、特殊型 0.8%であった（**図 19**）。肉腫型の 2008 年までの診断例では、環状胸膜肥厚が 46.2%、多発性腫瘤形成が 20.0%、単発胸膜腫瘤形成が 11.9%、軽度胸膜肥厚が 11.3%、縦隔側胸膜肥厚が 7.5%、胸水のみは、わずか 2.5%であった。また、特殊型については 0.6%であった（**図 20**）。

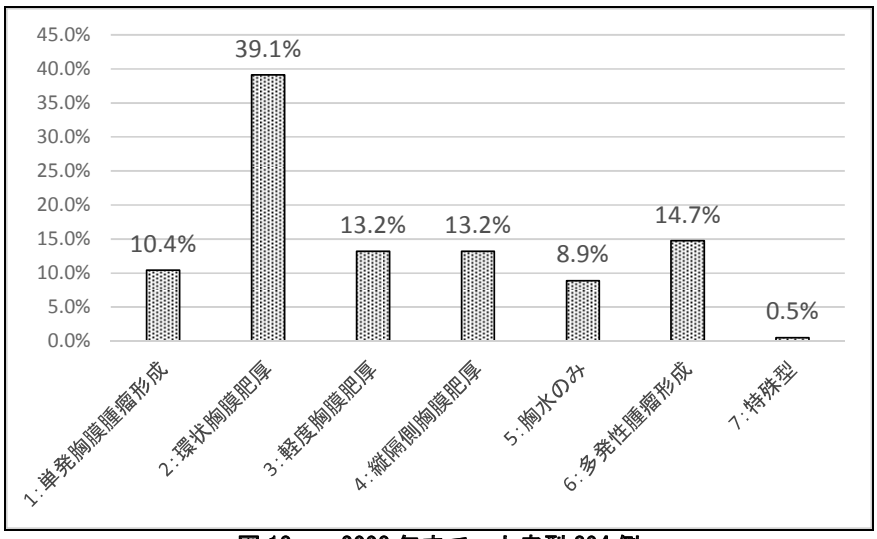

図 18. ～2008 年まで　上皮型 394 例

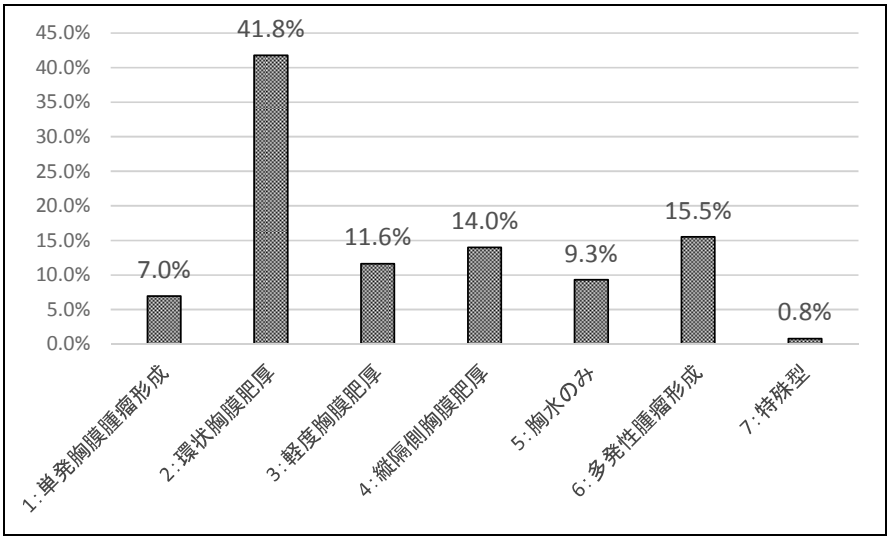

図 19. ～2008 年まで　二相型 129 例

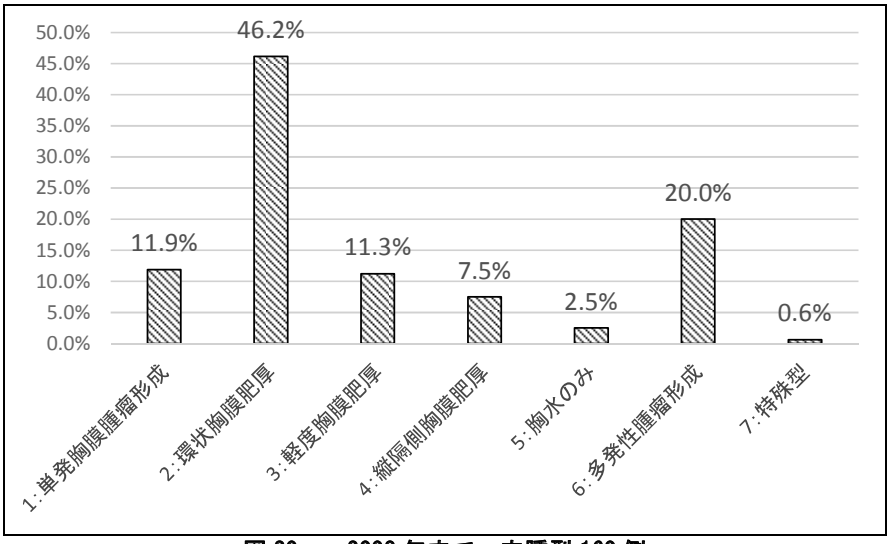

図 20. ～2008 年まで　肉腫型 160 例

（3）2009 年以降の画像パターン

2009 年以降の岡山労災病院、山口宇部医療センター、札幌南三条病院の診断例 188 例では、環状胸膜肥厚が 40.9%、縦隔側胸膜肥厚が 19.8%、多発性腫瘤形成 12.2%、胸水のみが 8.0%、単発胸膜腫瘤形成が 7.7%であった。（**図 21**）

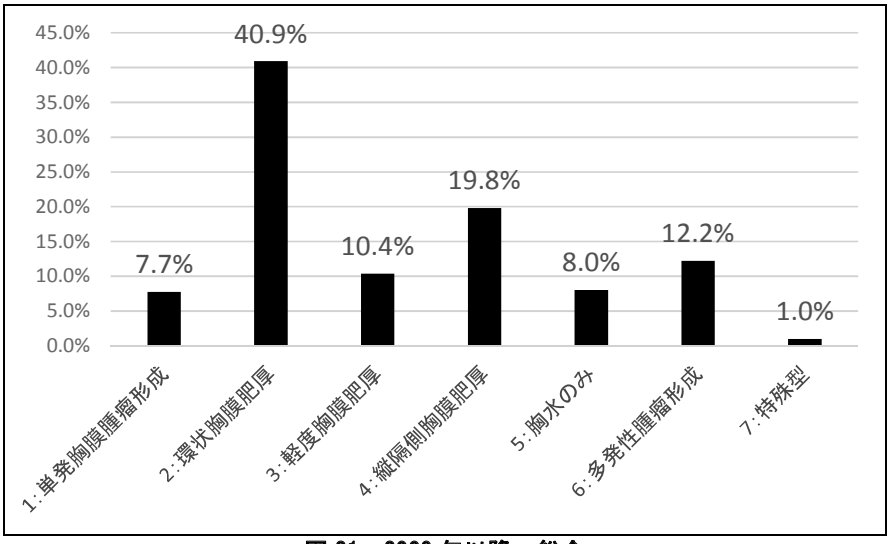

図 21. 2009 年以降　総合

（4）2009 年以降の組織型別画像パターン

2009 年以降の上皮型の診断例では、環状胸膜肥厚 25.9%、縦隔側胸膜肥厚が 25.3%、軽度胸膜肥厚が 15.3%、胸水のみが 12.9%、多発性腫瘤形成が 11.2%、単発胸膜腫瘤形成が 6.5%、特殊型が 2.9%であった（**図 22**）。二相型の 2009 年以降の診断例では、環状胸膜肥厚 40.5%、縦隔側胸膜肥厚が 26.2%、軽度胸膜肥厚が 11.9%、多発性腫瘤形成 9.5%、胸水のみが 7.1%、単発胸膜腫瘤形成が 4.8%であった。二相型では特殊型がなく、単発胸膜腫瘤形成型が最も少なかった（**図 23**）。肉腫型の 2009 年以降の診断例では、環状胸膜肥厚が 56.0%、多発性腫瘤形成 16.0%、単発胸膜腫瘤形成 12.0%、縦隔側胸膜肥厚が 8.0%、軽度胸膜肥厚と胸水のみが各 4.0%で、特殊型がなく、環状胸膜肥厚が圧倒的に多かった（**図 24**）。

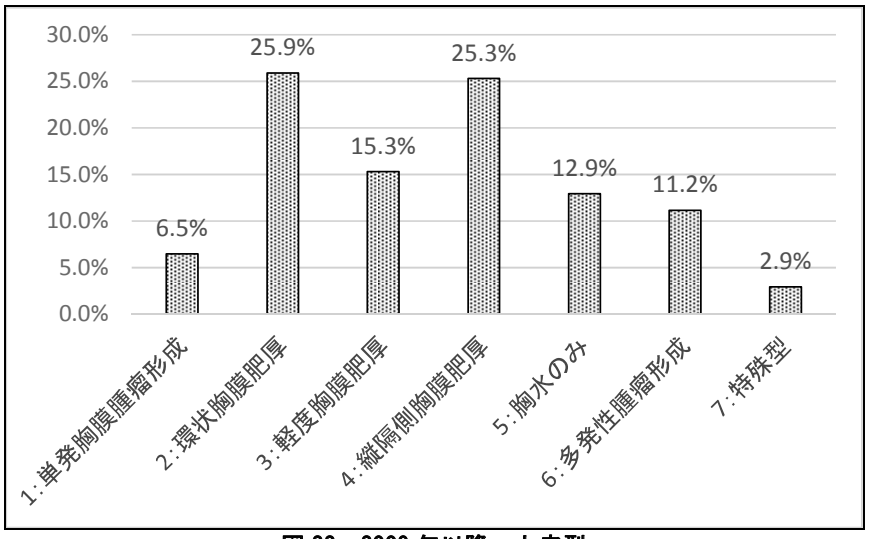

図 22. 2009 年以降　上皮型

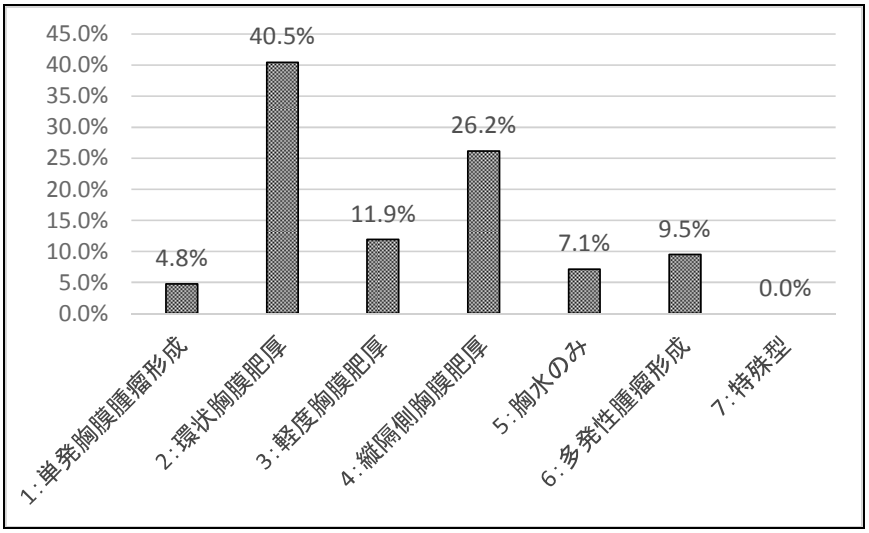

図 23. 2009 年以降　二相型

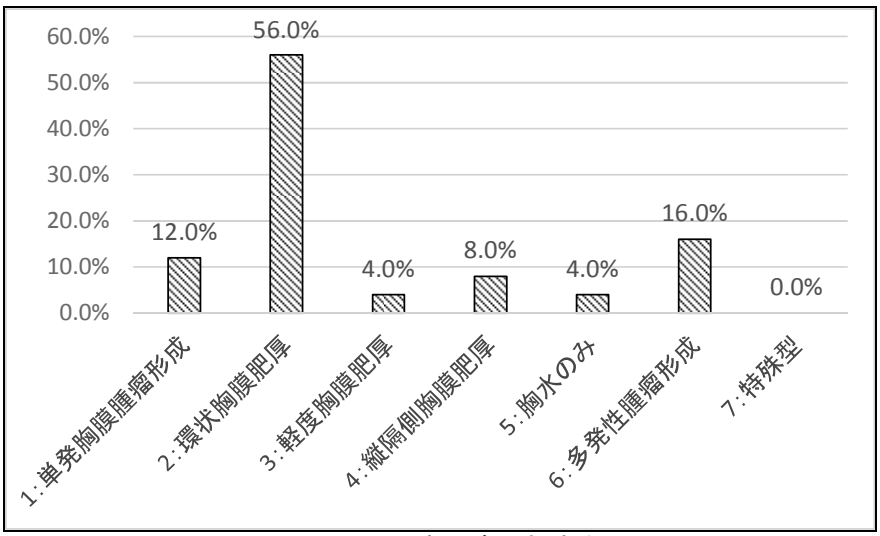

図 24. 2009 年以降　肉腫型

３．岡山労災病院症例の病期、組織型、画像パターンと生存期間

（１） 病期と組織型及び画像パターン

岡山労災病院の 166 例を IMIG 分類で病期別に検討したところ(**表 2**)、StageⅢが 36.7%と最も多かったが、StageⅠ、Ⅱも各々22.9%あり、ほぼ StageⅢと同数であった。

組織型別で検討したところ（**図 25**)、上皮型では早期病変の StageⅠ、Ⅱが合わせて 60 例と 50%を超えていた。一方肉腫型では StageⅠは 0 例で StageⅡが 5 例（17.9%）と極めて早期例が少なかった。

画像パターンでは胸水のみでは StageⅠ、Ⅱが 83.4%と大半を占めたが、環状胸膜肥厚では StageⅢ、Ⅳが 72.9%を占めた。

表 2. 岡山労災病院 166 例 IMIG 分類臨床病期の分布

	N0	N1	N2	N3
T1	38	0	0	0
T2	38	1	3	0
T3	48	4	5	0
T4	9	1	14	5

Stage Ⅰ	38
Stage Ⅱ	38
Stage Ⅲ	61
Stage Ⅳ	29

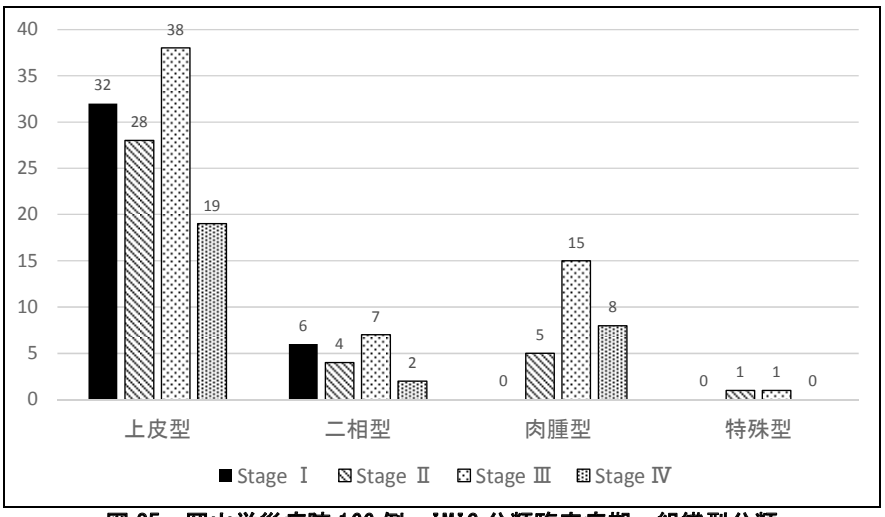

図 25. 岡山労災病院 166 例　IMIG 分類臨床病期　組織型分類

（2） 組織型と生存期間

上皮型では**図 26** のように生存期間が長く、中央値が 14.3 ヶ月であったが、肉腫型では 6.5 ヶ月と極めて予後不良であった。

（3） 画像パターンと生存期間

画像別では（**図 27**）単発胸膜腫瘤形成が最も良好で、次いで胸水のみ＋軽度胸膜肥厚であった。これに反して、環状胸膜肥厚型が最も生存期間が短かった。進行病期を示唆する環状胸膜肥厚と多発性腫瘤形成は予後不良であった。

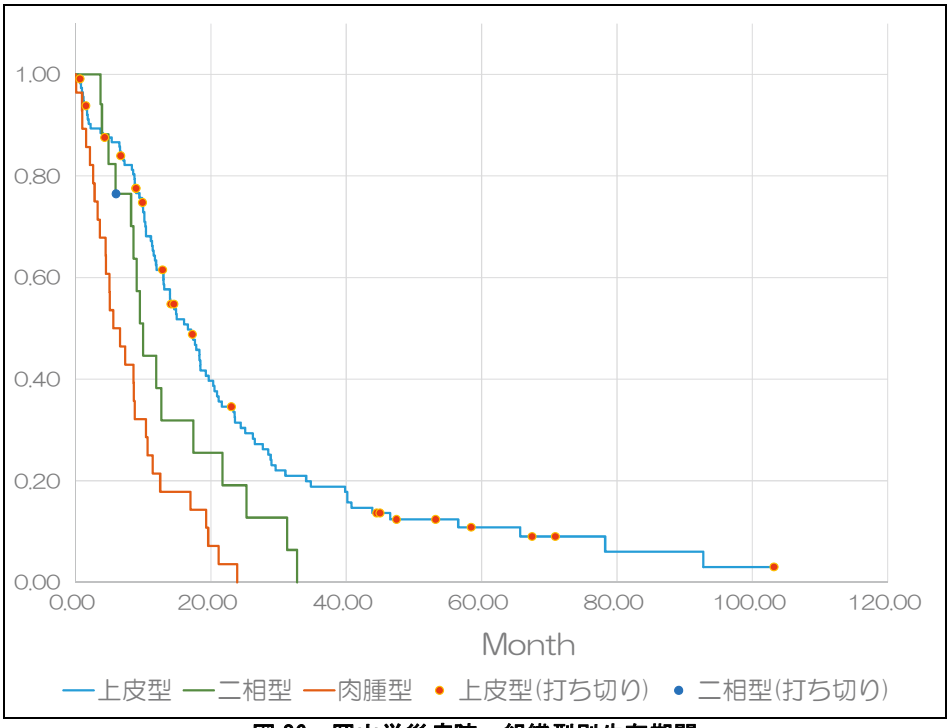

図 26. 岡山労災病院　組織型別生存期間

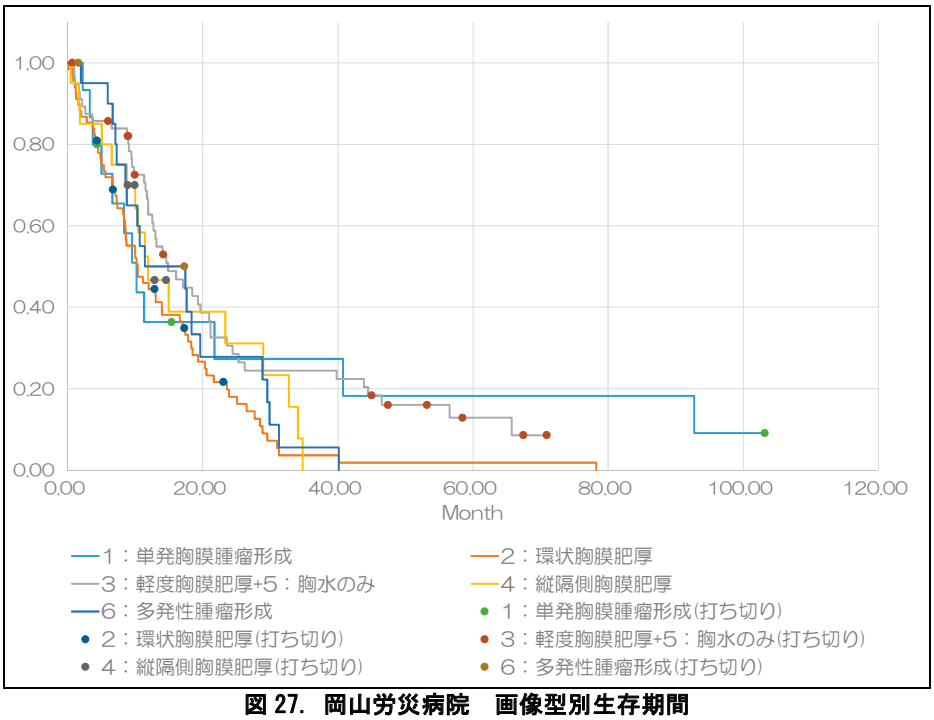

図 27. 岡山労災病院　画像型別生存期間

【 考　察 】

胸膜中皮腫 CT の典型像は壁側胸膜に発生する腫瘍が胸膜沿いに不整な肥厚像を呈して水平方向に増殖する環状胸膜肥厚（pleural rind）が最も多いと記載されている[1)-3)]。腫瘍は胸壁や肋骨浸潤を伴うこともあるが比較的まれである[3)]。今回、我々は過去の厚生労働科学研究において収集した2003年から2008年に中皮腫で死亡した症例の遺族及び病院の同意を得られた651例のうち病理組織型が確定されていた482例、岡山労災病院において確定診断された166例および山口宇部医療センターで診断された110例と札幌南三条病院で診断された24例、合計782例の胸部CT画像所見について検討した。

その結果、胸膜中皮腫の初診時の胸部CT画像では環状胸膜肥厚が最も多く、次いで多発性腫瘤形成、縦隔側胸膜肥厚、軽度胸膜肥厚、単発胸膜腫瘤形成で胸水のみの症例はわずか8.4%であった。Kato[3)]も2003年～2008年までの全国調査で収集下胸膜中皮腫の胸部CT画像の18%では、腫瘍性胸膜肥厚を示さない胸水のみあるいはわずかな胸膜肥厚のある症例であったと報告している。この傾向は病理組織診断で病型が確定している782例においてもほぼ同様のパターンを示した。また、胸膜中皮腫の組織型別でも、上皮型、二相型、肉腫型のいずれにおいても環状胸膜肥厚が最も多かった。しかし、組織型別に詳細に検討したところ、二相型では環状胸膜肥厚に次いで、縦隔側胸膜肥厚、多発性腫瘤形成が多く、単発胸膜腫瘤形成はわずか6.4%のみであった。また、肉腫型でも環状胸膜肥厚が47.5%と最も多く、次いで多発性腫瘤形成、3番目に単発胸膜腫瘤形成であったが、胸水のみは2.7%と少なかった。すなわち、組織型により画像パターンは異なり、進展度の速い肉腫型では画像上胸水のみの早期診断が極めて難しいことが判った。

この画像パターンを2008年（いわゆるクボタショックの翌年）を境として、その前後で比較したところ、2009年以降では胸水のみの症例が7.5%から8.0%へと増加しているとともに、縦隔側胸膜肥厚は12.0%から19.8%へと増加していた。その理由として、2009年以降胸水を来たす疾患の鑑別診断として胸膜中皮腫がクローズアップされ、胸水中のヒアルロン酸等の測定頻度が増加するとともに胸水細胞診における免疫染色の導入も加速化されたことが挙げられる。さらに、精密検査が必要な症例には胸腔鏡下胸膜生検が積極的に行われるようになったこと、また縦隔側胸膜肥厚を比較的早期の中皮腫病変と認識するようになったことが早期の胸膜中皮腫診断が行われる契機となったと思われる。特に岡山労災病院では2009年以降石綿ばく露歴があって胸水を来たした症例については中皮腫を除外するため、胸水ヒアルロン酸、SMRPを測定してその疑いがある症例には胸腔鏡検査を行って肉眼的に観察するとともに疑わしい部位を複数箇所生検することで胸水のみの段階での早期診断が可能となったと考えている。

画像パターン別に生存期間を検討したところ、単発胸膜腫瘤形成が胸水のみや軽度胸膜肥厚よりも予後良好の傾向があった。この型は手術による完全切除も可能で、大きな腫瘤形成で胸壁や肋骨に浸潤がある場合を除いて予後が良好であると考えられた。また、StageⅠ、Ⅱの早期病変で診断された場合には治療手段として手術や放射線療法が適応となる。

早期に診断されて複数の治療を受けることができれば予後良好と報告[4]されており、胸膜中皮腫の標準外科手術方法である Extrapleural pneumonectomy（EPP）あるいは Pleurectomy/Decortication（P/D）を行うことはそうでない場合より予後を改善すると認識されている[5]。組織型別では上皮型の生存期間がその他の型に比較して有意に長かった。その理由として、この型では胸水のみ等早期に診断される症例が多く、手術及び放射線療法のみならず化学療法に対する効果も良好であったことから予後を延長させることになったと考えられる。しかし、上述の手術療法では術後の合併症等により術後 30 日以内に死亡する症例も少なくなく、現在もなお本疾患に対する手術療法に問題が残ることも事実である[6,7]。一方、環状胸膜肥厚型や多発性腫瘤形成型は進展に伴い、急速に呼吸面積が縮小するため呼吸不全や急性肺炎の合併等が死因となることが多いことが判った。

【 結　論 】

病理組織診断で病型までが確定された 782 例の胸膜中皮腫の画像診断では環状胸膜肥厚の頻度が最も高かった。しかし、単発胸膜腫瘤形成や胸水のみの症例も各々10%程度あるため、肺癌や良性石綿胸水や感染性胸膜炎等との鑑別診断を確実に行う必要がある。また、組織型別では、画像パターンが異なり上皮型では胸水のみや軽度胸膜肥厚等早期病変の診断が可能であったが、肉腫型では極めて少なく早期診断が困難であり、環状胸膜肥厚や多発性腫瘤形成が大半で予後不良の一因となっていた。

また、年代別に検討したところ、2009 年以降岡山労災病院や山口宇部医療センターでは画像上悪性胸膜病変を呈さない胸水のみあるいは胸膜炎でも認められる軽度胸膜肥厚のような早期病変で確定診断される症例が増加していることから、胸水マーカーあるいは細胞診検査を繰り返し行って、胸膜中皮腫が疑われる場合には必ず組織診を行って診断を確定させることが必要であると思われた。また、胸水のみや軽度胸膜肥厚あるいは単発胸膜腫瘤形成は手術適応となりうることから、生存期間の延長が期待できるため過去の石綿ばく露歴のある例に胸水が出現した際には、このような画像パターンを示す症例が少なからず存在することを周知する必要がある。

参考文献

1) Robinson BWS, Lake RA. Advances in malignant mesothelioma. N Engl J Med. 353:1591-1603,2005
2) Ismail-Khan R, Robinson LA, Willians CC, Garett CR, Bepler G, Siomn GR. Malignant pleural mesothelioma a comprehensive review.Cancer .13:255-263,2006
3) Kato K, Gemba K, Fujimoto N, et al. Fatal pleural mesothelioma in Japan (2003-2008):evaluation of computed tomography findings. Jpn J Radiol,2016
4) Ho L, Sugarbaker DJ, Skarin AT. Malignant pleural mesothelioma. Cancer Treat Res. 105:327-73,2001

5) Hasegawa S. Extrapleural pneumonectomy or pleurectomy/decortication for malignant pleural mesothelioma. Gen Thorac Cardiovasc Surg. 62:516-521,2014
6) Domen A, De Laet C, Vanderbruggen W, Gielis J, Hendriks JM, Lauwers P, Janssens A, Hiddinga B, Van Meerbeeck JP, Van Schil PE. Malignant pleural mesothelioma: single-institution experience of 101 patients over a 15-year period. Acta Chir Belg. 117:157-63,2017
7) Zahid I, Sharif S, Routledge T, Scarci M. Is pleurectomy and decortication superior to palliative care in the treatment of malignant pleural mesothelioma? Interact Cardiovasc Thorac Surg. 12:812-7,2011

悪性胸膜中皮腫の診断における胸水中の Secretory leukocyte protease inhibitor（SLPI）の有用性について

藤本　伸一、岸本　卓巳

はじめに

悪性胸膜中皮腫（以下中皮腫）はその多くが石綿ばく露に起因する予後不良な悪性腫瘍であり、本邦では今後も患者数の増加が予想されている。我々はこれまでに、わが国においても中皮腫の約 8 割が石綿ばく露に起因して発生することを報告した[1)]。中皮腫の診断は病理所見に基づくものであるが多くの場合肺癌や良性石綿胸水などとの鑑別診断が非常に困難であり、診断確定までに長い時間を要することがまれではない。一般臨床で用いられる画像所見に加え、血清あるいは胸水中の分子マーカーなどを加えた正確で迅速な診断方法の確立が急務である。本研究では、近年その中皮腫での発現が報告された、いくつかの分子マーカーに着目し、まずこれまでに採取され保存されている胸水検体を用いて測定をおこなった（探索的研究）。その中で特に Secretory leukocyte protease inhibitor（SLPI）について有望な所見が得られたため、その有用性を明らかにするための validation study を企画し施行した。

I. 探索的研究（Exploratory Research）

対象・方法

まず探索的研究として、岡山労災病院において過去に診断、治療された中皮腫 52 例、胸水貯留を伴う肺癌 69 例、良性石綿胸水 50 例の胸水検体を用い、診療録から胸水中のヒアルロン酸濃度を抽出した。また ELISA キットを用いて可溶性メソテリン関連蛋白（SMRP）、Galectin-3、chemokine chemokine（C-C motif）ligand 2（CCL2）、Vascular endothelial growth factor（VEGF）および SLPI の濃度を測定した。

結果

１．　ヒアルロン酸

中皮腫、肺癌、良性石綿胸水における胸水中のヒアルロン酸濃度の中央値（標準偏差）は、それぞれ 86950（553386.7）ng/ml、 20700（22785.8）ng/ml、 31500（30068.9）ng/ml であった（**図 1**）。中皮腫におけるヒアルロン酸濃度は他疾患に比べ有意に高値であった（Kruskal Wallis 検定、P=0.000）。

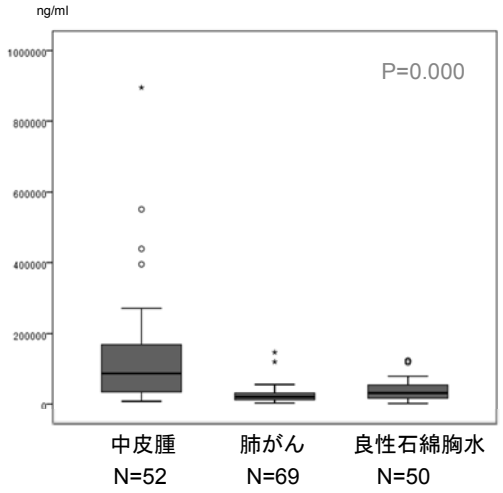

	中央値	標準偏差
中皮腫	86950.0	553386.7
肺癌	20700.0	22785.8
良性石綿胸水	31500.0	30068.9

図 1. ヒアルロン酸

２．　SMRP

中皮腫、肺癌、良性石綿胸水における胸水中の SMRP の濃度の中央値（標準偏差）は、それぞれ 15.38（46.55）ng/ml、5.70（6.79）ng/ml、7.31（3.69）ng/ml であった（**図 2**）。中皮腫における胸水中の SMRP 濃度は他疾患に比べ有意に高値であった（Kruskal Wallis 検定、P=0.000）。

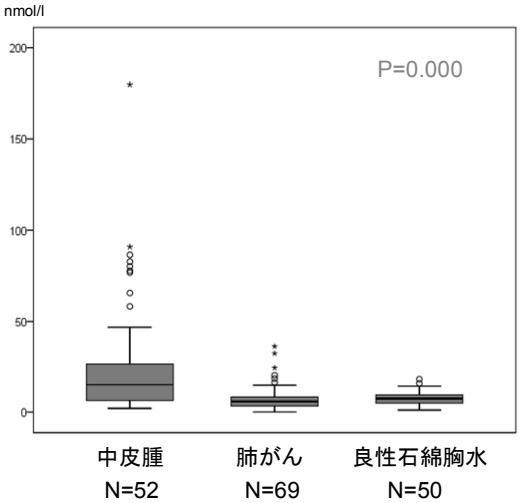

	中央値	標準偏差
中皮腫	15.38	46.55
肺癌	5.70	6.79
良性石綿胸水	7.31	3.69

図 2. SMRP

３．　Galectin-3

次に胸水中の Galectin-3 値を測定した。中皮腫、肺癌、良性石綿胸水における胸水中の Galectin-3 値の中央値（標準偏差）は、それぞれ 13.99（102.1）ng/ml、16.82（31.6）ng/ml、8.17（11.6）ng/ml であった（**図 3**）。肺癌における胸水中の Galectin-3 値は他疾患に比べ高値を示した（Kruskal Wallis 検定、P=0.000）。

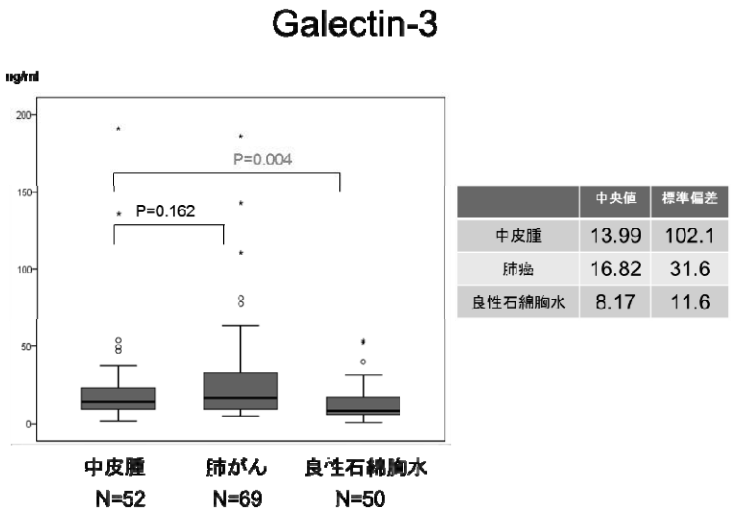

	中央値	標準偏差
中皮腫	13.99	102.1
肺癌	16.82	31.6
良性石綿胸水	8.17	11.6

図 3. Galectin-3

４．　CCL2

次に胸水中の CCL2 濃度を測定した。中皮腫、肺癌、良性石綿胸水における胸水中の CCL2 濃度の中央値（標準偏差）は、それぞれ 2592.0（5478.3）ng/ml、1723.5（2400.2）ng/ml、4520.9（6247.8）ng/ml であった（**図 4**）。胸水中の CCL2 濃度は良性石綿胸水において高値を呈した（Kruskal Wallis 検定、P=0.000）。

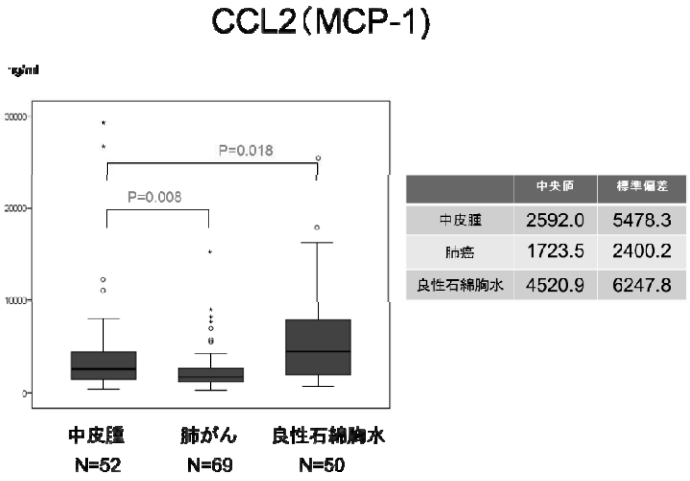

	中央値	標準偏差
中皮腫	2592.0	5478.3
肺癌	1723.5	2400.2
良性石綿胸水	4520.9	6247.8

図 4. CCL2 (MCP-1)

6． VEGF

次に胸水中の VEGF 濃度を測定した。中皮腫、肺癌、良性石綿胸水における胸水中の VEGF 濃度の中央値(標準偏差)は、それぞれ 328.3（690.2）ng/ml、367.2（489.6）ng/ml、328.6（535.3）ng/ml であった（**図 6**）。胸水中の VEGF 濃度は各疾患群において有意な差を認めなかった（Kruskal Wallis 検定、P=0.414）。

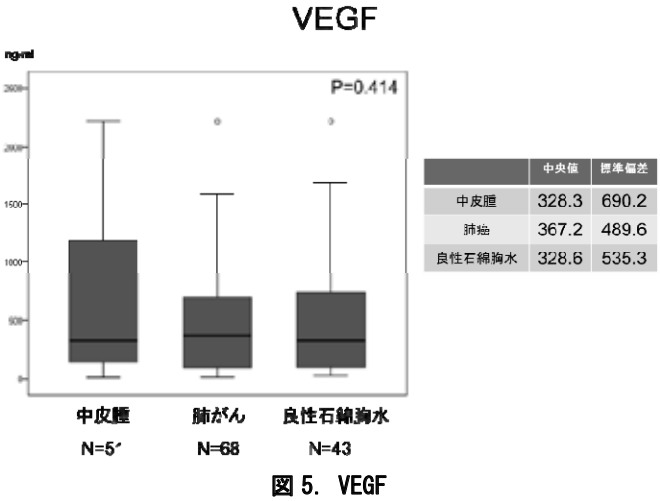

	中央値	標準偏差
中皮腫	328.3	690.2
肺癌	367.2	489.6
良性石綿胸水	328.6	535.3

図 5. VEGF

５．　SLPI

次に胸水中の SLPI 値を測定した。中皮腫、肺癌、良性石綿胸水における胸水中の SLPI 濃度の中央値（標準偏差）は、それぞれ 108.1（146.7）ng/ml、87.6（84.4）ng/ml、48.6（22.1）ng/ml であった（**図 6**）。中皮腫における胸水中の SLPI 濃度は他疾患に比べ有意に高値であった（Kruskal Wallis 検定、P=0.000）。

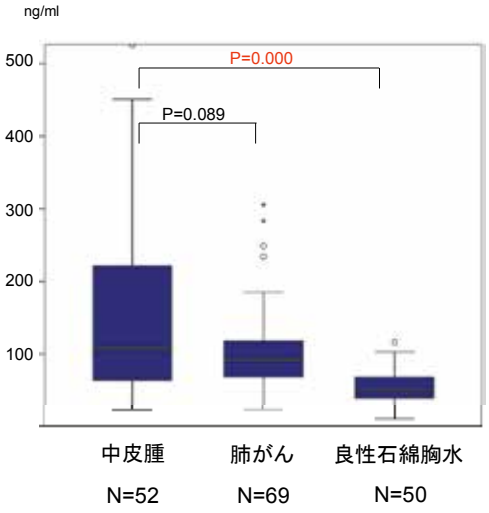

	中央値	標準偏差
中皮腫	108.1	146.7
肺癌	87.6	84.4
良性石綿胸水	48.6	22.1

図 6.　SLPI

６．　中皮腫の鑑別診断における胸水 SLPI の有用性について

胸水を用いた中皮腫の鑑別診断について検討した。肺癌、良性石綿胸水に対し有意に高値を呈した SLPI、ヒアルロン酸、SMRP を用いて、まず中皮腫とそれ以外（肺癌および良性石綿胸水）の鑑別における有用性を検討するため、ROC 曲線を作成した（**図 7**）。SLPI、ヒアルロン酸、SMRP における AUC 値はそれぞれ 0.688、0.812、0.752 であった。

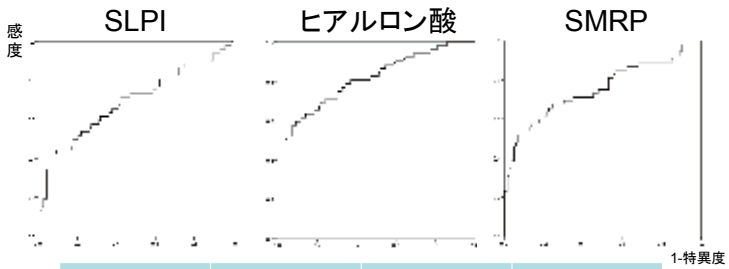

	SLPI	ヒアルロン酸	SMRP
AUC	0.688	0.812	0.752
95%信頼区間	0.594-0.782	0.738-0.886	0.664-0.840
カットオフ値	147.5 ng/ml	58500 ng/ml	14.3 nmol/l
感度（%）	42.3	59.6	53.8
特異度（%）	93.3	90.8	91.6

図 7.　中皮腫と肺癌・良性石綿胸水の鑑別

次に肺癌をのぞいて、中皮腫と良性石綿胸水の鑑別における有用性を検討するため、同様に ROC 曲線を作成した（**図 8**）。SLPI、ヒアルロン酸、SMRP における AUC 値はそれぞれ 0.823、0.760、0.743 であった。

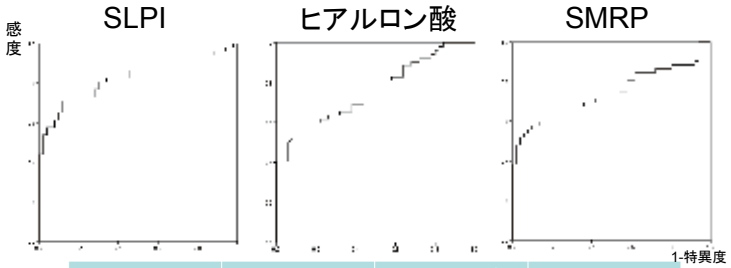

	SLPI	ヒアルロン酸	SMRP
AUC	0.823	0.760	0.743
95%信頼区間	0.739-0.907	0.668-0.852	0.664-0.843
カットオフ値	74.8 ng/ml	86950 ng/ml	15.0 nmol/l
感度（%）	71.2	50.0	51.9
特異度（%）	88.0	94.0	96.0

図 8. 中皮腫と良性石綿胸水の鑑別

中皮腫の早期診断における SLPI の有用性についてさらに検討するため、本事業において研究代表者岸本卓巳が分類している胸膜中皮腫の画像所見の分類に基づき、胸水中の SLPI を比較した（**図 9**）。この中で特に、中皮腫に特徴的な胸膜の肥厚や腫瘤形成を伴わない「胸水のみ」の症例に着目したところ、胸膜肥厚や腫瘤形成を伴う症例と比較しても有意差のない SLPI 値が得られた。

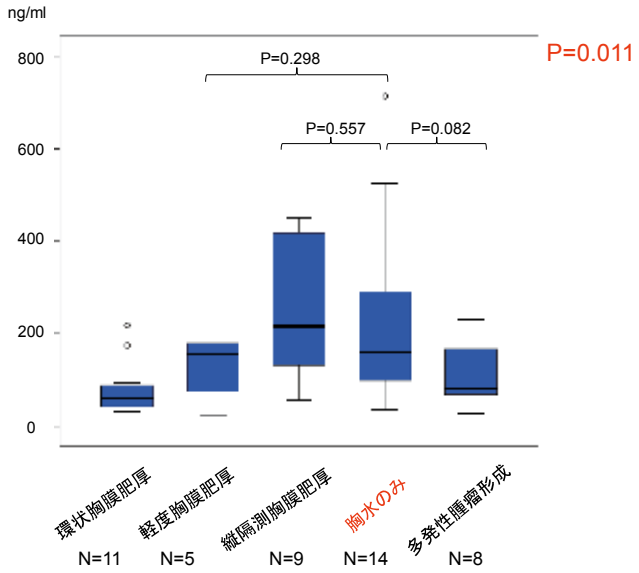

図 9. 中皮腫の画像所見と胸水 SLPI

さらにこの「胸水のみ」の中皮腫症例に着目し、胸水中の SLPI 値を良性石綿胸水群と比較したところ、「胸水のみ」の中皮腫群では良性石綿胸水に比べ有意に高値を呈した（**図 10**）。

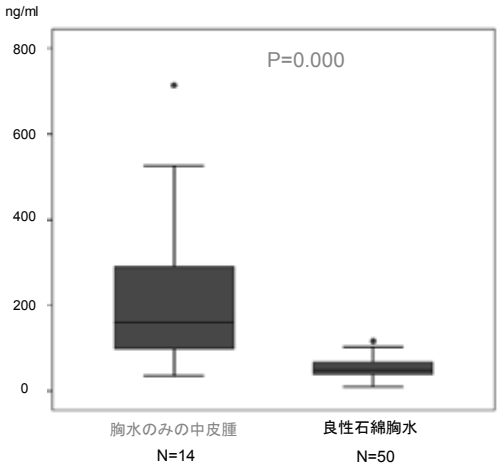

図 10. 中皮腫の画像所見と胸水 SLPI

II. 有用性を確認する研究（Validation study）

先の探索的研究において、胸水中の SLPI が中皮腫において高値を示し、特に良性石綿胸水との鑑別において有用である可能性が示唆された。この結果を検証するため、本研究期間中に集積した症例を対象として、胸水中の SLPI 値を比較検討した。

対象・方法

岡山労災病院において平成 24 年 12 月から平成 28 年 12 月の間に胸水の診断目的にて受診した患者から採取された胸水検体の残りを用い、Quantikine ELISA　Human SLPI（R&D Systems）キットを用いて胸水中の SLPI の測定をおこなった。また探索的研究と同様に、診療録から胸水中のヒアルロン酸濃度を抽出し、また ELISA キットを用いて可溶性メソテリン関連蛋白（SMRP）の濃度を測定した。

結果

この期間中に、中皮腫 16 例（上皮型 13 例、肉腫型 1 例、組織型が特定できなかったもの 2 例）、良性石綿胸水 28 例、肺癌 28 例（腺癌 21 例、小細胞癌 3 例、扁平上皮癌 1 例、神経内分泌腫瘍 2 例、組織型が特定できなかったもの 1 例）、他臓器の癌 8 例（膵臓癌 4

例、乳癌 1 例、肝臓癌 1 例、胆道癌 1 例、原発不明癌 1 例）、胸膜炎 23 例の計 103 例が集積された。

胸水中の SLPI を比較したところ、中皮腫では良性石綿胸水に比べ有意に高値であった（P=0.000）。また有意差には至らないものの、他疾患（肺癌や胸膜炎など）に比べても高値を示していた（**図 11**）。

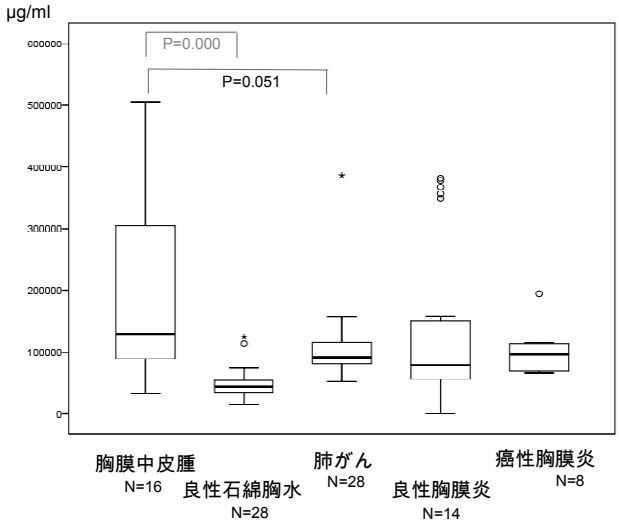

図 11. 胸水中の SLPI

また胸水中のヒアルロン酸および SMRP の濃度についても比較したが、探索的研究と同様に中皮腫では他疾患に比べ有意に高値を示した（**図 12、図 13**）。

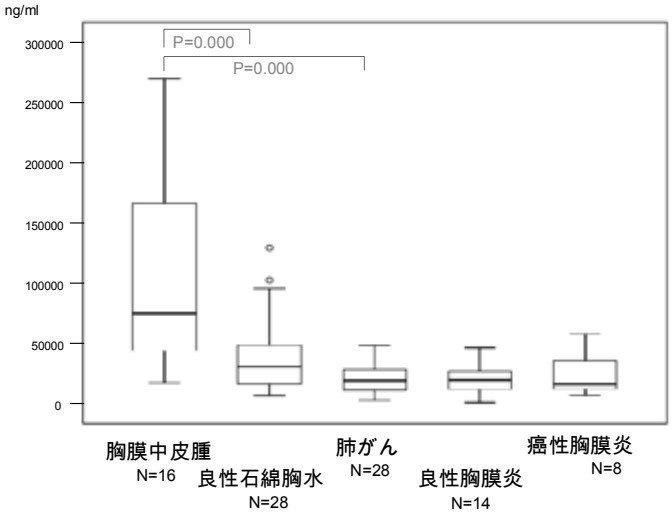

図 12. 胸水中のヒアルロン酸

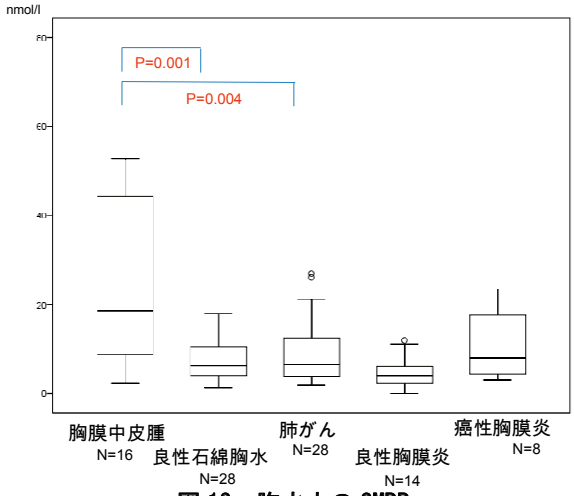

図 13. 胸水中の SMRP

探索的研究と同様に、胸水を用いた中皮腫の鑑別診断について検討した。SLPI、ヒアルロン酸、SMRP を用いて、まず中皮腫とそれ以外の疾患群との鑑別における有用性を検討するため、ROC 曲線を作成した（**図 14**）。SLPI、ヒアルロン酸、SMRP における AUC 値はそれぞれ 0.739、0.891、0.800 であった。

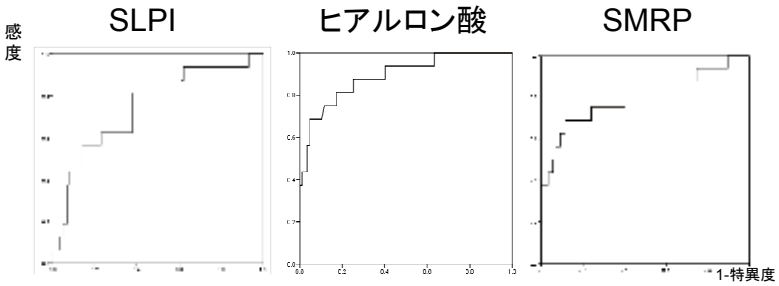

	SLPI	ヒアルロン酸	SMRP
AUC	0.739	0.891	0.800
95%信頼区間	0.602-0.877	0.801-0.982	0.658-0.942
カットオフ値	88.6 ng/ml	60700	13.78
感度（%）	81.3	68.8	68.8
特異度（%）	62.1	95.4	88.5

図 14. 中皮腫と他疾患の鑑別

次に肺癌をのぞいて、中皮腫と良性石綿胸水の鑑別における有用性を検討するため、同様に ROC 曲線を作成した（**図 15**）。SLPI、ヒアルロン酸、SMRP における AUC 値はそれぞれ 0.911、0.819、0.797 であった。

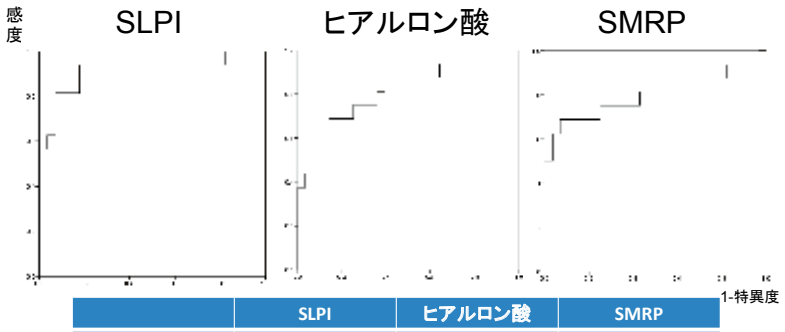

	SLPI	ヒアルロン酸	SMRP
AUC	0.911	0.819	0.797
95%信頼区間	0.805-1.000	0.688-0.951	0.635-0.959
カットオフ値	59.8 ng/ml	60700	13.54
感度(%)	93.8	68.8	68.8
特異度(%)	82.1	85.7	92.9

図 15. 中皮腫と良性石綿胸水の鑑別

さらに探索的研究と同様に、「胸水のみ」の中皮腫症例に着目した。中皮腫 16 例中 5 例が画像上「胸水のみ」と判断された。これらの症例の胸水中の SLPI 値を良性石綿胸水群と比較したところ、「胸水のみ」の中皮腫群では良性石綿胸水に比べ有意に高値を呈した（**図 16**）。

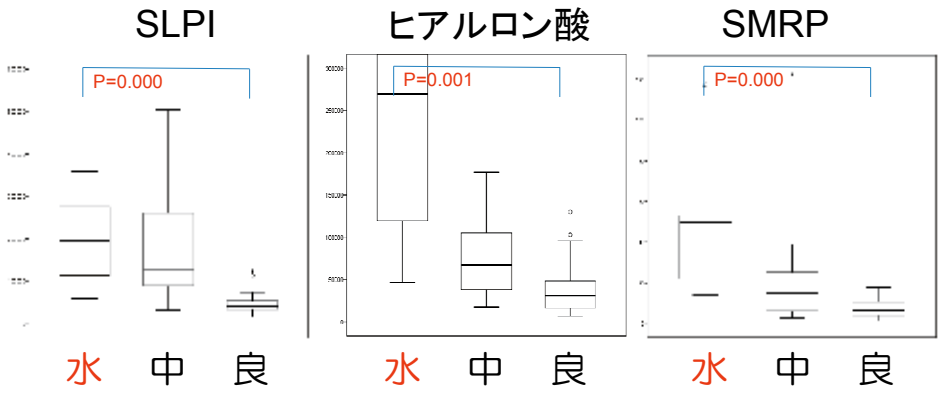

水：胸水のみの中皮腫 n=5
中：通常の中皮腫 n=11
良：良性石綿胸水 n=28

図 16. 胸水のみの中皮腫

考察

本研究では、胸水中の分子マーカーの測定を行い中皮腫の鑑別における有用性について検討した。最初に探索的研究として、岡山労災病院においてこれまでに診断、治療された中皮腫 52 例、胸水貯留を伴う肺癌 69 例、良性石綿胸水 50 例の胸水検体を用いて ELISA キットにより SMRP、SLPI、Galectin-3、CCL2 の測定をおこない、また診療録から胸水中のヒアルロン酸濃度を抽出した。中皮腫においては胸水中のヒアルロン酸濃度と SMRP 濃度が有意に高値であったほか、中皮腫における胸水中の SLPI 濃度も他疾患に比べ有意に高値であった。ヒアルロン酸、SMRP に加え、胸水中の SLPI 濃度の測定が中皮腫の診断マーカーとして有用である可能性があらためて示唆された。特に中皮腫と良性石綿胸水との鑑別に関する ROC 曲線による解析において、AUC=0.911 とヒアルロン酸、SMRP のそれを上回っており、中皮腫と良性石綿胸水の鑑別における SLPI の有用性が示唆された。

これらの結果をさらに検証するため、研究期間内に症例を蓄積し、新たに診断された症例を用いて胸水中の SLPI の測定を行ったところ、探索的研究とほぼ同様の結果が得られた。胸水中の SLPI を測定することは、特に中皮腫と良性石綿胸水の鑑別において有用であると考える。

従来中皮腫の鑑別マーカーとして、上述の胸水ヒアルロン酸[2]、SMRP[3]のほかオステオポンチン、Fiblin-3 などの有用性が報告されてきたが臨床応用には至っていない。我々が過去に行った検討でも、これらの有用性は確認できなかった。このたびの研究では、近年新しい有用なマーカーの候補として報告された CCL2、Galectin-3、及び SLPI に着目し[4][5]、これらのマーカーの測定を行った。CCL2、Galectin-3 については有用性を示唆するような所見は得られず、中皮腫の鑑別における有用性については否定的である。SLPI は SLPI 遺伝子にコードされる酵素であり、白血球エラスターゼ、トリプシン、肥満細胞キマーゼなどを阻害する。SLPI 遺伝子は中皮腫細胞において高発現していることが報告されており、胸膜中皮腫の胸水において高値を呈することが報告されている[5]。今回の我々の検討において、特に中皮腫と良性石綿胸水との間に有意差が認められたことは注目に値する。通常の臨床において胸水を呈する症例の場合、まず胸膜炎や肺癌を念頭に置くが、これらは臨床徴候や画像、血液検査などよりある程度の鑑別が可能である。しかし特に石綿ばく露歴がある方の胸水に直面する場合、しばしば中皮腫と良性石綿胸水の鑑別に苦慮する。胸水中の SLPI は実臨床において中皮腫、良性石綿胸水の鑑別に有用であり、またこれらの疾患のスムーズな労災認定にも役立つ可能性がある。

結語

中皮腫の診断マーカーの開発に取り組み、胸水中のヒアルロン酸、SMRP に加え、新たに SLPI が有用であることを明らかにした。

参考文献

1) Gemba K, Fujimoto N, Kato K, Aoe K, Takeshima Y, Inai K, Kishimoto T. National survey of malignant mesothelioma and asbestos exposure in Japan. Cancer Sci. 103: 483-90.2012
2) Fujimoto N, Gemba K, Asano M, Fuchimoto Y, Wada S, Ono K, Ozaki S, Kishimoto T. Hyaluronic acid in the pleural fluid of patients with malignant pleural mesothelioma. Respir Investig. 51:92-7.2013
3) Fujimoto N, Gemba K, Asano M, Wada S, Ono K, Ozaki S, Kishimoto T. Soluble mesothelin-related protein in pleural effusion from patients with malignant pleural mesothelioma. Exp Ther Med. 1:313-7.2010
4) Gueugnon F, Leclercq S, Blanquart C, Sagan C, Cellerin L, Padieu M, Perigaud C, Scherpereel A, Gregoire M. Identification of novel markers for the diagnosis of malignant pleural mesothelioma. Am J Pathol. 178:1033-42.2011
5) Blanquart C, Gueugnon F, Nguyen JM, Roulois D, Cellerin L, Sagan C, Perigaud C, Scherpereel A, Gregoire M. CCL2, Galectin-3, and SMRP combination improves the diagnosis of mesothelioma in pleural effusions. J Thorac Oncol. 7:883-9.2012

中皮腫の病理学的鑑別診断の為の新規免疫組織化学マーカーの探索

櫛谷　桂、Amatya V. Jeet、武島　幸男

1. 緒言

過去の大量のアスベスト輸入・使用により、日本では中皮腫は増加の一途をたどっており、疫学的にこの増加傾向は今後 10～15 年は続くとされている [1)]。

中皮腫には多くの組織亜型が存在するため、病理組織学的鑑別診断の対象となる疾患も多岐にわたるが、その鑑別が必ずしも容易でない例がある。我々は、過去の日本の中皮腫症例を再検討した結果、約 15%の例で診断が適切でなかったと報告している [2)]。

中皮腫の鑑別診断のためには、臨床情報とともに、ヘマトキシリン・エオジン（H&E）染色標本による形態学的な観察に加え、各種抗体を用いた免疫組織化学的な検討あるいは FISH 法を用いた p16 遺伝子欠失の有無の検索が必要とされているが、現在のところ 100%の精度で中皮腫と他疾患を鑑別できるマーカーあるいはマーカーパネルは確立されていない [3),4)]。

本研究では、既知の鑑別診断マーカーの有用性の再評価に加え、網羅的遺伝子発現解析による新規鑑別診断マーカーの探索を行うことにより、免疫組織化学的染色による中皮腫と他疾患の鑑別診断に有用なマーカーの選定を目的とした。

2. 材料と方法

1) 上皮型中皮腫（EM）と反応性中皮細胞過形成（RMH）の鑑別

a) 中皮腫細胞株 6 株、非腫瘍性胸膜組織の凍結組織 4 例から mRNA を抽出し、Taqman® Array Human Apoptosis Panel card（Applied Biosystems）（**図 1**）を使用して real time RT-PCR を行い、アポトーシス関連遺伝子の発現を比較した（**図 2**）。

BIRC2	BAK1	BCL3	CASP1	CASP2	CASP5	CASP7	CASP8
BCL2L13	TNFRSF21	HTRA2	TBK1	ESRRBL1	LRDD	CARD15	CARD9
BCL2L1	BCL2L2	BIK	BNIP3L	BOK	CASP3	CASP6	CASP10
BCL2L10	BCL2L11	BBC3	PYCARD	DIABLO	BIRC6	GAPDH	ACTB
CASP9	IKBKB	18S	LTB	MCL1	NFKB1	NFKB2	NFKBIB
NFKBIZ	BCL2L14	BIRC7	CARD6	BIRC8	DEDD2	APAF1	BIRC3
DAPK1	HIP1	BIRC1	NFKBIA	RELA	TNF	IKBKG	PEA15
CHUK	REL	TNFRSF1A	RIPK2	IKBKE	BCAP31	ICEBERG	TA-NFKBH
NFKBIE	PMAIP1	RELB	TNFRSF1B	TNFRSF10A	CARD4	NALP1	CASP14
BIRC4	BIRC5	FAS	FASLG	BAD	BAX	BCL2	BCL2A1
TRADD	RIPK1	HRK	TNFSF10	FADD	TNFRSF10B	CFLAR	DEDD
BID	BNIP3	CASP4	LTA	TNFRSF25	CRADD	BCL10	CASP8AP2

図 1. Taqman® Array Human Apoptosis Panel card (Applied Biosystems)
93 のアポトーシス関連遺伝子と House-keeping gene (18S、ACTB、GAPDH) がプロットされている。

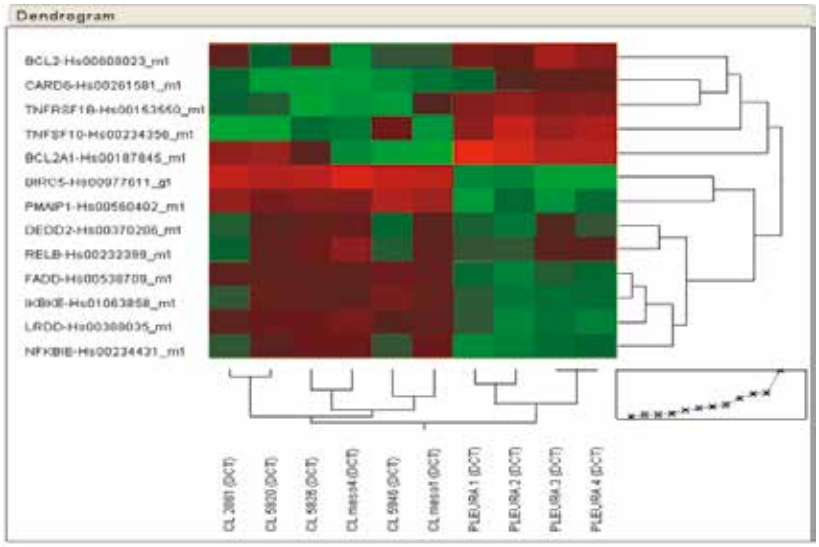

図 2. 中皮腫細胞株と非腫瘍性胸膜組織におけるアポトーシス関連遺伝子発現のクラスタリング解析
13 の遺伝子に発現の差を認め、そのうち BIRC5 (Survivin)、PMAIP1 (Noxa)に特に顕著な差がみられた。

b) Real time RT-PCR の結果、発現に最も顕著な差が認められた Noxa (PMAIP1)、Survivin (BIRC5) に加え、最近上皮型中皮腫と反応性中皮細胞過形成の鑑別に有用であると報告されている BAP1 と [5]、既知の鑑別診断マーカー7 種 (EMA、Desmin、GLUT-1、IMP3、CD146、p53、Ki-67) に対する抗体を使用し [6)-10)]、広島大学大学院医歯薬保健学研究院病理学研究室にて 2000 年から 2016 年までに経験した上皮型中皮腫 79 例、反応性中皮細胞過形成 78 例を対象として免疫組織化学的染色を行った。使用した一次抗体は**表 1** に示す如くである。

表 1. 本研究に使用した免疫組織化学マーカー

マーカー	クローン	販売元	評価対象
Noxa	Polyclonal	Anaspec	細胞質
Survivin	Polyclonal	R&D Systems	核
BAP1	C-4	Santa Cruz Biotech.	核
Desmin	D33	Dako	細胞質
EMA	E29	Dako	細胞膜
GLUT-1	Polyclonal	Spring Bioscience	細胞膜
IMP3	69.1	Dako	細胞質
CD146	N1238	Leica (Novocastra)	細胞膜
p53	DO-7	Dako	核
Ki-67	MIB-1	Dako	核
MUC4	8G7	Santa Cruz	細胞質
Calretinin	SP65	Ventana	核
Podoplanin	D2-40	Nichirei	細胞膜
WT1	6f-H2	Ventana	核
Pancytokeratin	AE1/AE3/PCK26	Ventana	細胞質
Cytokeratin	CAM5.2	Ventana	細胞質
Claudin-4	3E2C1	LifeTechnologies	細胞膜
CK5/6	D5/16 B4	Dako	細胞質
TTF-1	SP141	Ventana	核
Napsin A	MRQ-60	Ventana	細胞質
CEA	COL-1	Nichirei	細胞質
ERA	MOC31	Dako	細胞膜
p40	BC28	Biocare Medical	核
p63	DAK-p63	Dako	核
DAB2	1C8	Sigma	細胞質
Intelectin-1	3G9	IBL	細胞質

c) 染色結果は**表 1** に示す如く各種抗体の局在に注目して判定し、**表 2** に示す如く判定量的に評価した。Survivin、Ki-67 は Hot Spot（組織切片全体のうち最も標識率が高い領域）における標識率を算出し、Survivin は ROC 曲線（**図 3**）による解析から設定したカットオフ値 4.000%以上を陽性、Ki-67 は ROC 曲線（**図 4**）による解析から設定したカットオフ値 10.333%以上を陽性と判定した。Hot Spot は強拡大 1 視野とし、最低 100 個以上の細胞を評価した。強拡大 1 視野に含まれ

る対象細胞数が 100 個未満の場合、評価細胞数が 100 個を越えるまで視野を追加した。BAP1 は陽性対照と同程度ないしそれ以上の染色強度のものを「発現消失なし」、陰性のものを「発現消失あり」と定義した。

表 2. 免疫組織化学的染色の評価方法

陽性細胞の割合	染色グレード
0%	0
0%<, ≦10%	1
10%＜, ≦50%	2
50%＜	3

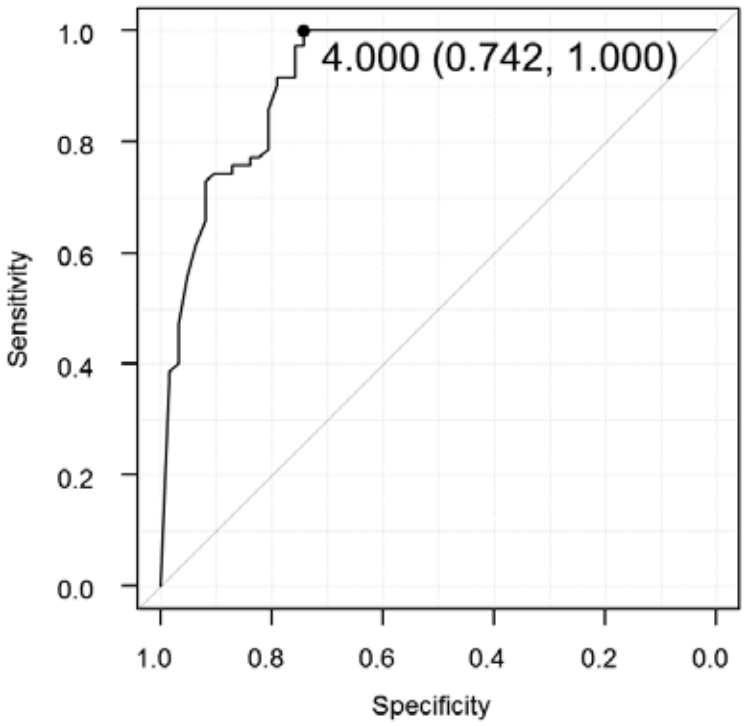

図 3. Survivin の ROC 曲線
感度と特異度の和が最大となる点（4.000）をカットオフ値とした。

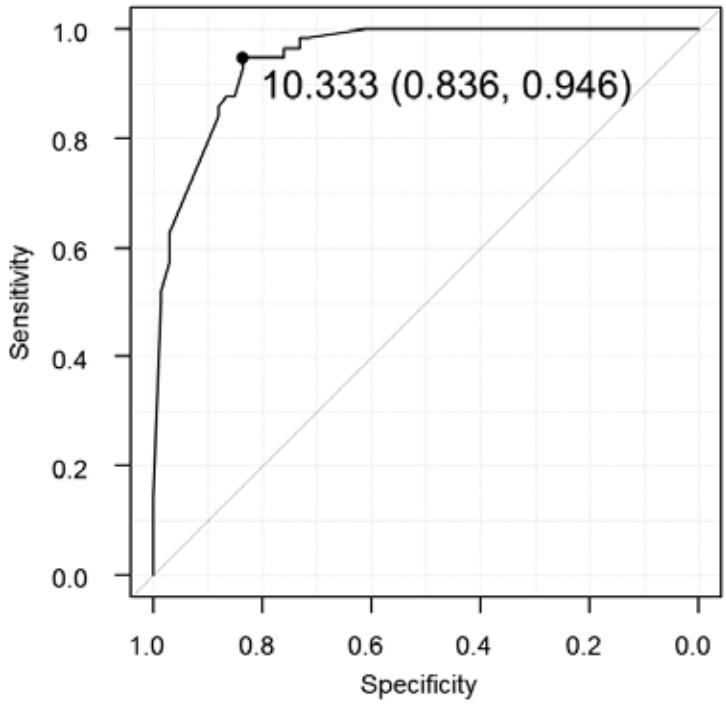

図 4. Ki-67 の ROC 曲線
感度と特異度の和が最大となる点（10.333）をカットオフ値とした。

d) 上皮型中皮腫と反応性中皮細胞過形成における Survivin、Ki-67 の標識率について EZR（Saitama Medical Center, Jichi Medical University）を使用して統計解析を行い、ROC 曲線の作成およびカットオフ値の設定を行った [11]。

e) 各抗体および複数抗体の組み合わせによる感度、特異度、正診率を計算した。

2) 肉腫型中皮腫と肺肉腫様癌の鑑別

a) 肉腫型中皮腫 6 例、肺肉腫様癌 6 例のホルマリン固定パラフィン包埋（FFPE）組織から RNA を抽出し、遺伝子発現の解析を行った（**図 5**、**図 6**）。

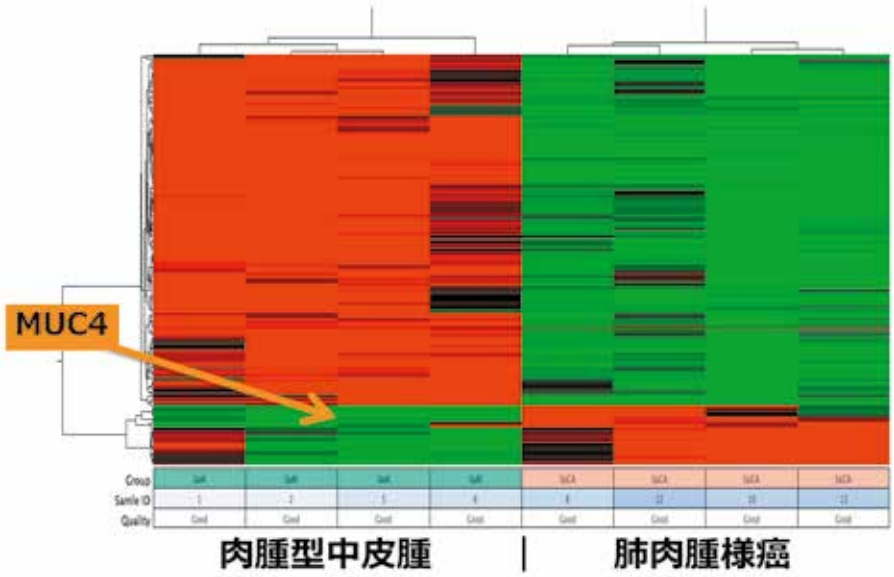

図 5. 肉腫型中皮腫と肺肉腫様癌における遺伝子発現のクラスタリング解析
肉腫型中皮腫で 156 遺伝子、肺肉腫様癌で 46 遺伝子の過剰発現を認めた。

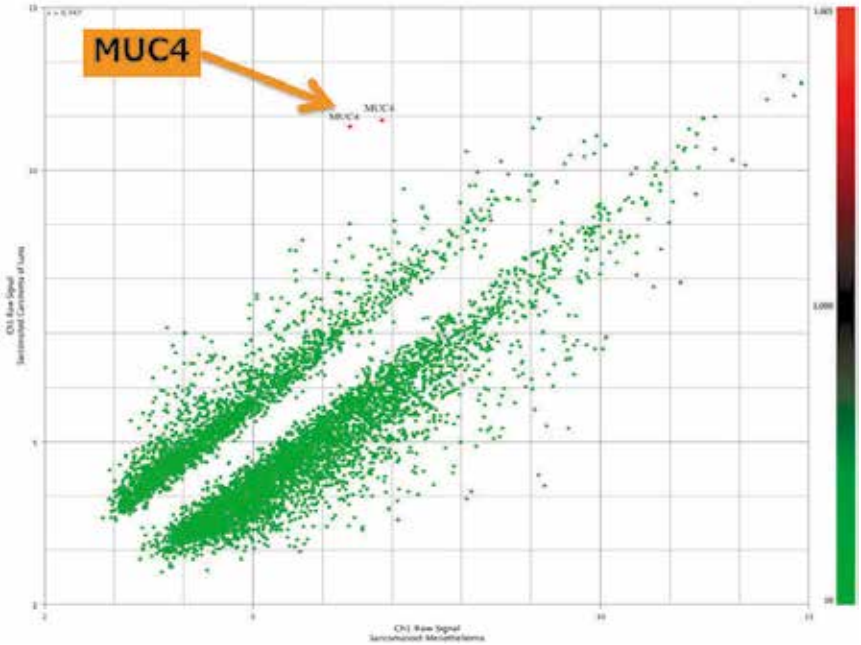

図 6. 肉腫型中皮腫と肺肉腫様癌における遺伝子発現の Scatter Plot
プロットエリアの右下方に近いほど肉腫型中皮腫で発現が強く、
左上方に近いほど肺肉腫様癌で発現が強いことを示す。

b) 遺伝子発現解析の結果、両者の間で発現に顕著な差が認められた MUC4 に加え、既知の鑑別診断マーカー8 種（Calretinin、D2-40、WT1、AE1/AE3、CAM5.2、p40、TTF-1、Claudin-4）に対する一次抗体を使用し、広島大学大学院医歯薬保

健学研究院病理学研究室にて 2005 年から 2015 年までに経験した肉腫型中皮腫 31 例、肺肉腫様癌 29 例を対象として免疫組織化学的染色を行った。使用した一次抗体は**表 1** に示す如くである。

c) 染色結果は**表 1** に示す如く各種抗体の局在に注目して判定し、腫瘍性異型紡錘形細胞の陽性割合に応じて、**表 2** に示す如く判定量的に評価した。

d) 各抗体の感度、特異度、陽性的中率、陰性的中率、正診率を算出した。

3) 低分化型（充実型）上皮型中皮腫と低分化型非小細胞性肺癌の鑑別

a) 充実性増殖パターンを示す上皮型中皮腫 36 例、低分化型肺腺癌 35 例、低分化型肺扁平上皮癌 38 例を対象とし、Calretinin、D2-40、WT1、CK5/6、TTF-1、Napsin A、CEA、MOC31、Claudin-4、p40、p63 に対する一次抗体を使用して免疫組織化学的染色を行った。使用した一次抗体は**表 1** に示す如くである。

b) 染色結果は**表 1** に示す如く各種抗体の局在に注目して判定し、**表 2** に示す如く判定量的に評価した。

c) 各抗体および 2 抗体の組み合わせによる感度、特異度を算出した。

4) 上皮型中皮腫と肺腺癌の新規鑑別診断マーカー

a) 上皮型中皮腫 5 例、肺腺癌 5 例の FFPE 組織から RNA を抽出し、遺伝子発現の解析を行った。（**図 7**、**図 8**）

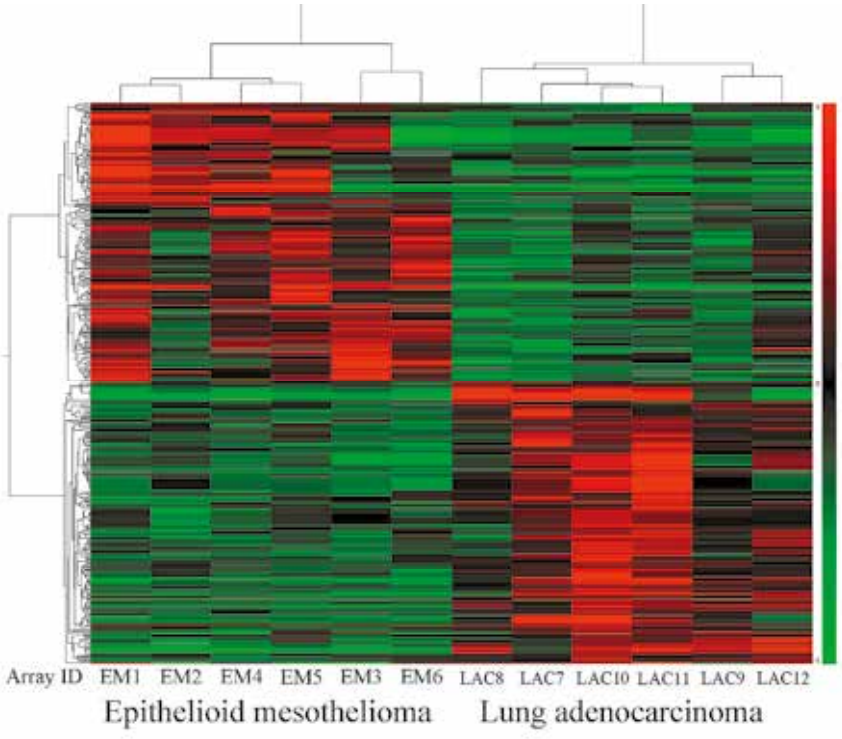

図 7. 上皮型中皮腫と肺腺癌における遺伝子発現のクラスタリング解析
上皮型中皮腫で 197 遺伝子、肺肉腫様癌で 229 遺伝子の過剰発現を認めた。

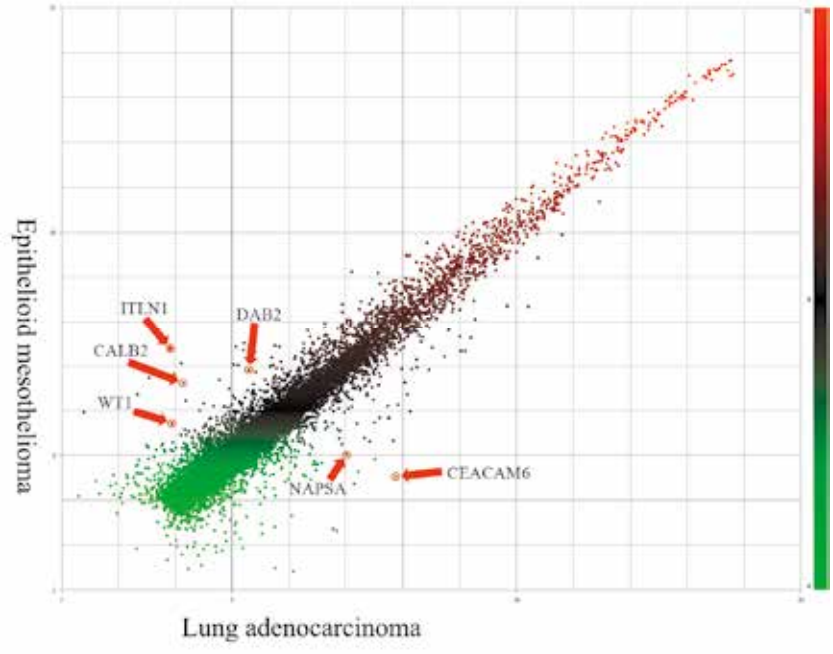

図 8. 上皮型中皮腫と肺腺癌における遺伝子発現の Scatter Plot
プロットエリアの右下方に近いほど肺腺癌で発現が強く、
左上方に近いほど上皮型中皮腫で発現が強いことを示す。

b) 遺伝子発現解析の結果、両者の間で発現に顕著な差が認められた disabled homolog 2（DAB2）、Intelectin-1 に加え、既知の鑑別診断マーカー3 種（Calretinin、D2-40、WT1）に対する一次抗体を使用し、広島大学大学院医歯薬保健学研究院病理学研究室にて 2000 年から 2016 年までに経験した上皮型中皮腫 75 例、肺腺癌 67 例を対象として免疫組織化学的染色を行った。使用した一次抗体は**表 1** に示す如くである。

c) 染色結果は**表 1** に示す如く各種抗体の局在に注目して判定し、**表 2** に示す如く判定量的に評価した。

d) 各抗体および 2 抗体の組み合わせによる感度、特異度を算出した。

3. 結果と考察

1) 上皮型中皮腫と反応性中皮細胞過形成の鑑別

代表的な症例の HE 染色および免疫組織化学的染色像を**図 9～図 13**、上皮型中皮腫、反応性中皮細胞過形成における各マーカーの陽性率を**表 3**、上皮型中皮腫と反応性中皮細胞過形成の鑑別診断における各マーカーの診断特性を**表 4** に示す。

iMig 2012, update では、上皮型中皮腫と反応性中皮細胞過形成の鑑別診断に有用なマーカーとして Desmin、EMA、p53、GLUT-1、IMP3 を挙げているが [3]、本研究では p53、IMP3 より BAP1、CD146、Survivin、Noxa の正診率が高く、これらの抗体を鑑別診断に使用することが推奨される。

複数抗体の組み合わせによる診断特性の検討では、Survivin と BAP1 の組み合わせ（Survivin 標識率 4.0%以上あるいは BAP1 発現消失のいずれかを認めた場合を陽性と判定する）が感度 93.2%、特異度 100%、正診率 96.9%で、最も高い診断精度を示した。

免疫組織化学的染色における BAP1 発現消失は、上皮型中皮腫に対して 100%の特異性を持つ所見であり、上皮型中皮腫と反応性中皮細胞の鑑別診断に有用とされるが、感度が 70%以下と低い点が問題であった [12)-15)]。しかし、本研究の結果から BAP1 に Survivin を組み合わせることにより、特異度を 100%に保ったまま感度を大幅に上昇させることが可能であることが明らかとなり、上皮型中皮腫と反応性中皮細胞過形成の鑑別診断においては BAP1 と Survivin を組み合わせた検討を行うことが推奨される。

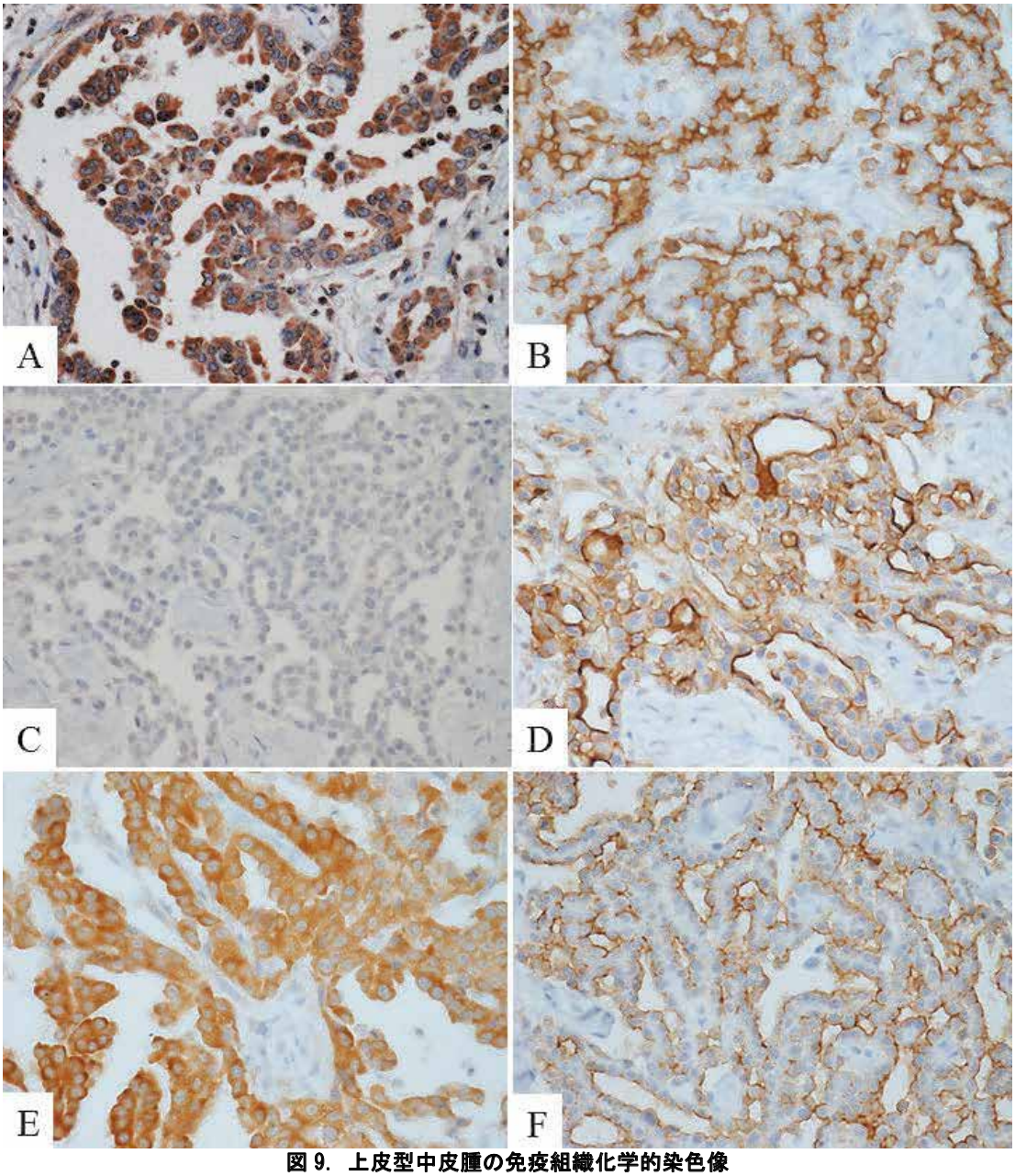

図 9. 上皮型中皮腫の免疫組織化学的染色像

A: Noxa 陽性、B: EMA 陽性、C: Desmin 陰性、
D: GLUT-1 陽性、E: IMP3 陽性、F: CD146 陽性

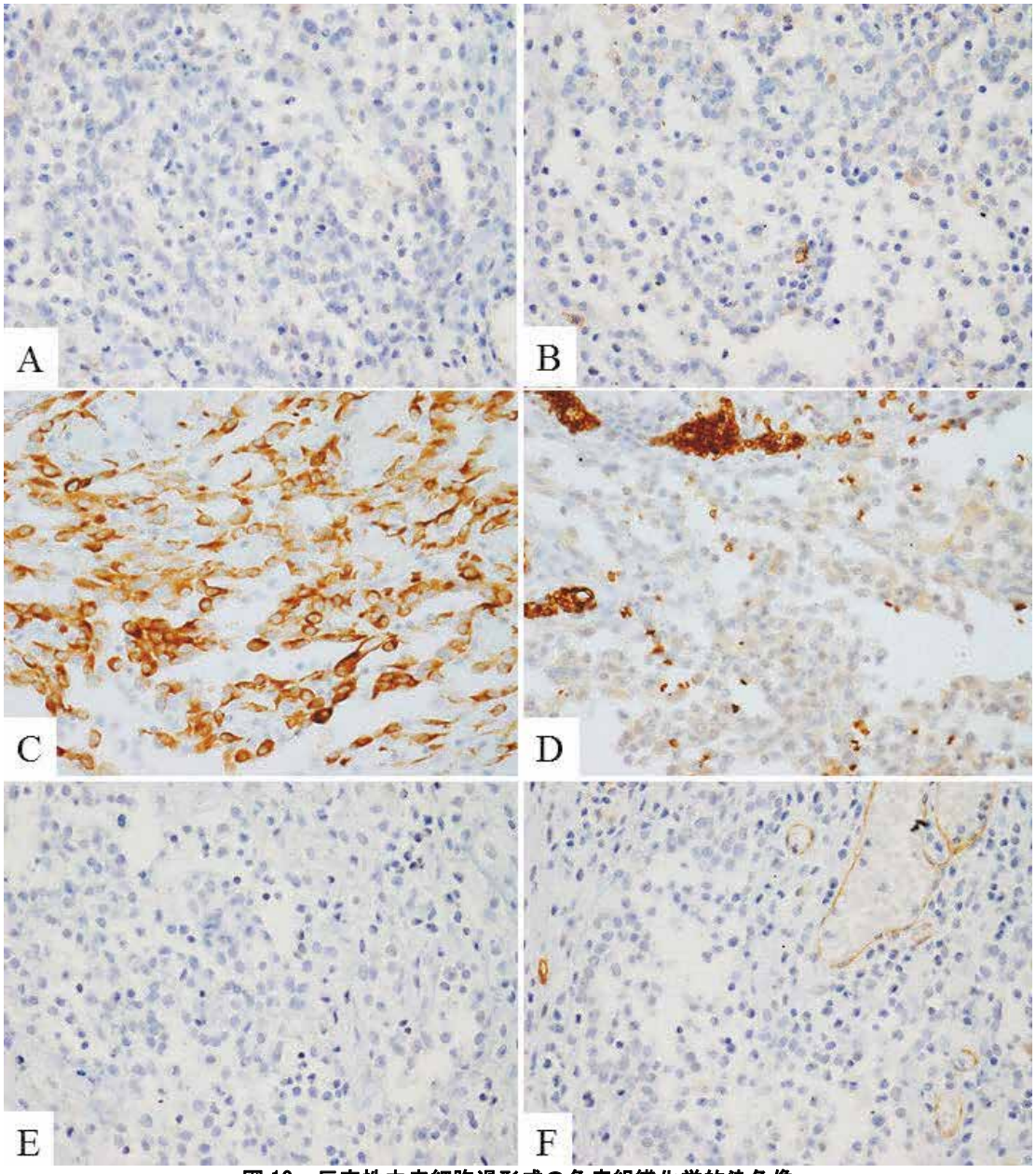

図 10. 反応性中皮細胞過形成の免疫組織化学的染色像

A: Noxa 陰性、B: EMA 陰性、C: Desmin 陽性、
D: GLUT-1 陰性、E: IMP3 陰性、F: CD146 陰性

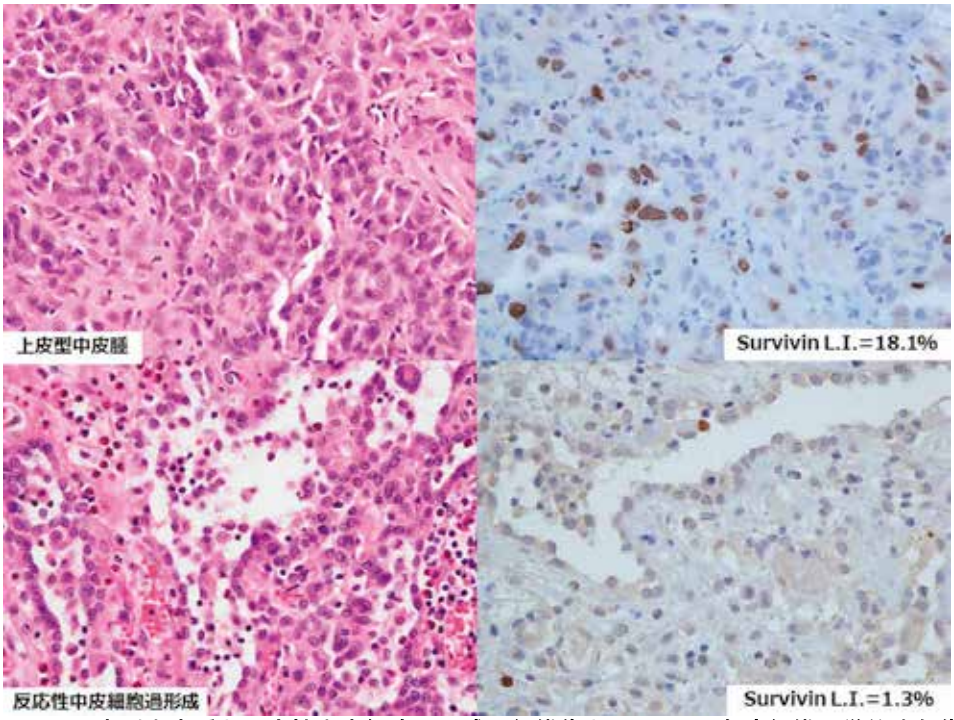

図 11. 上皮型中皮腫と反応性中皮細胞過形成の組織像と Survivin 免疫組織化学的染色像
上皮型中皮腫の Survivin 標識率は 18.1%、
反応性中皮細胞過形成の Survivin 標識率は 1.3%である。

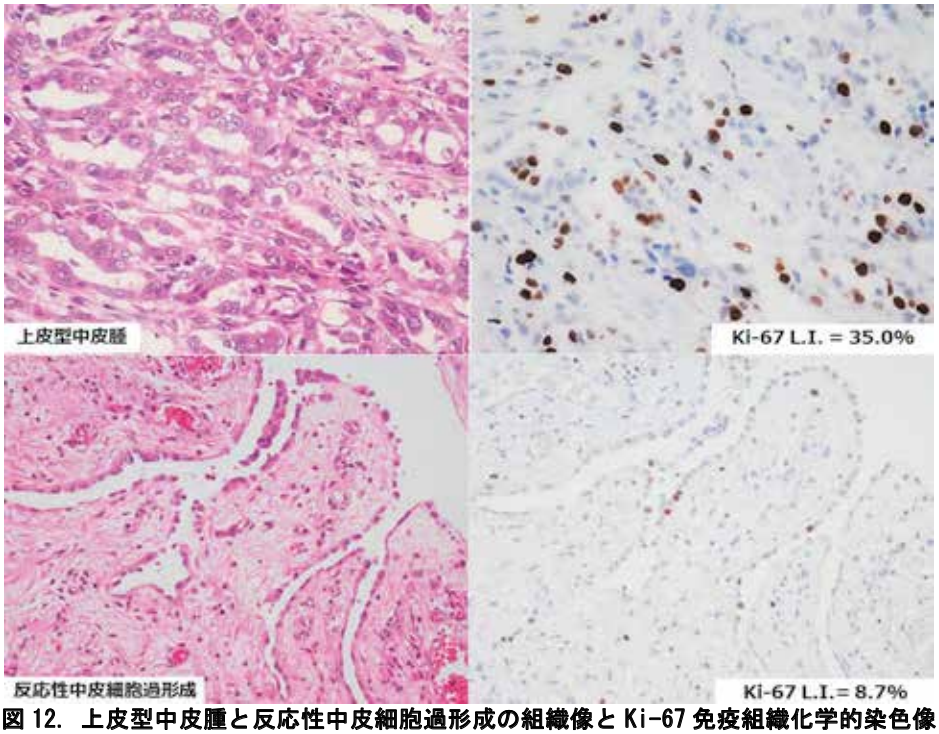

図 12. 上皮型中皮腫と反応性中皮細胞過形成の組織像と Ki-67 免疫組織化学的染色像
上皮型中皮腫の Ki-67 標識率は 35.0%、
反応性中皮細胞過形成の Ki-67 標識率は 8.7%である。

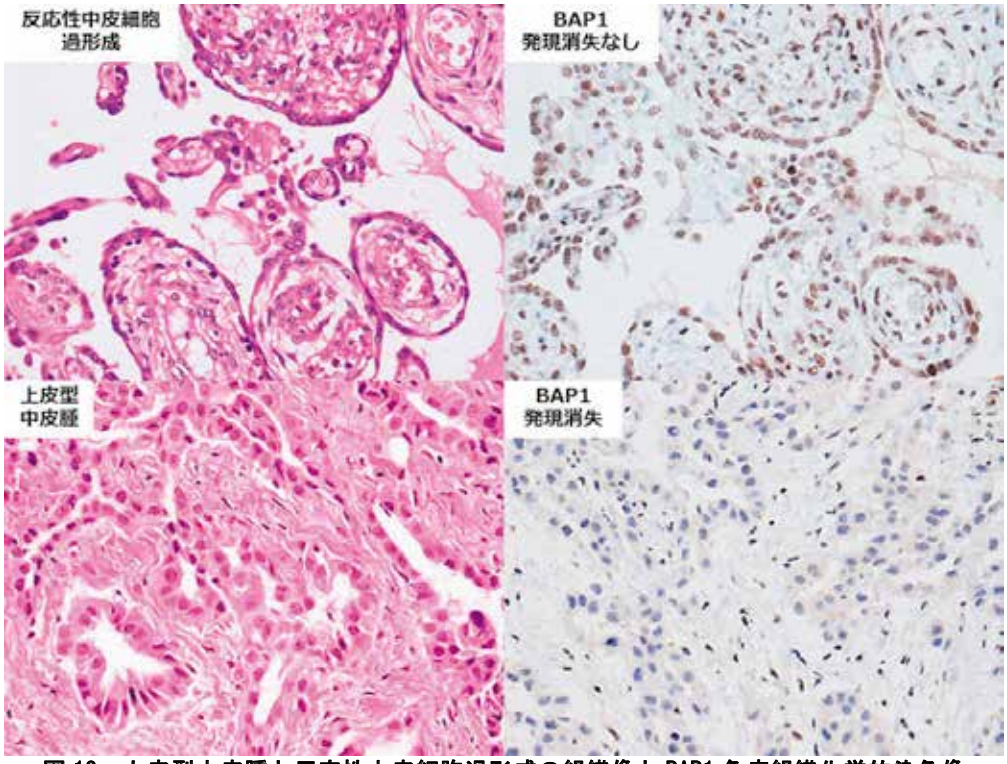

図 13. 上皮型中皮腫と反応性中皮細胞過形成の組織像と BAP1 免疫組織化学的染色像
上皮型中皮腫において BAP1 発現の消失を認める。
背景の炎症細胞、線維芽細胞、血管内皮細胞の核は BAP1 を発現している。

表 3. 上皮型中皮腫と反応性中皮細胞過形成における各マーカーの陽性率

	上皮型中皮腫			反応性中皮細胞過形成		
マーカー	n (%)	陰性	陽性	n (%)	陰性	陽性
Survivin (4.0%<)	46/62 (74.2)	16	46	0/70	70	0
BAP1-loss	49/74 (66.2)	25	49	0/78	78	0
Ki-67 (10.3%<)	56/67 (83.6)	11	56	3/56 (5.4)	53	3
		染色グレード			染色グレード	
マーカー	n (%)	0	1+	2+	n (%)	0	1+	2+
Noxa	40/58 (69.0)	18	37	3	3/47 (6.4)	44	3	0
Desmin	12/79 (15.2)	67	12	0	48/53 (90.6)	5	19	29
EMA	81/81 (100)	0	29	52	6/53 (11.3)	47	6	0
GLUT-1	60/66 (90.9)	6	45	15	10/55 (18.2)	45	7	3
IMP-3	43/64 (67.2)	21	29	14	2/45 (4.4)	43	2	0
CD146	41/48 (85.4)	7	18	23	1/26 (3.8)	25	1	0

表 4. 上皮型中皮腫と反応性中皮細胞過形成の鑑別診断における各マーカーの診断特性

マーカー	感度	特異度	正診率
Survivin (4.0%<)	74.2%	100%	87.8%
BAP1-loss	66.2%	100%	83.6%
Ki-67 (10.3%<)	83.6%	94.6%	88.6%
Noxa	69.0%	93.6%	80%
Desmin (-)	84.8%	90.6%	87.1%
EMA (+)	100%	88.6%	95.5%
GLUT-1 (+)	90.9%	81.8%	86.8%
IMP-3 (+)	67.2%	95.6%	78.9%
CD146 (+)	85.4%	96.2%	89.2%
SVV＞4% or BAP1-loss	93.2%	100.0%	96.9%
BAP1-loss or Ki-67＞10.3%	96.9%	94.4%	95.8%
SVV＞4% or Ki-67＞10.3%	91.1%	94.1%	92.5%
BAP1-loss or SVV＞4% or Ki-67＞10.3%	98.2%	94.0%	96.2%

2) 肉腫型中皮腫と肺肉腫様癌の鑑別

代表的な症例の HE 染色および免疫組織化学的染色像を**図 14**、**図 15**、肉腫型中皮腫、肺肉腫様癌における各マーカーの陽性率を**表 5**、肉腫型中皮腫と肺肉腫様癌の鑑別診断における各マーカーの診断特性を**表 6** に示す。

MUC4 は肺肉腫様癌の 72%が陽性を示したが、肉腫型中皮腫は全例陰性であり、特異性の高い中皮腫陰性マーカー（肉腫様癌マーカー）と考えられた。

MUC4 の肉腫型中皮腫と肺肉腫様癌の鑑別診断における正診率は 87%で、今回検討した全てのマーカーの中で最も優れていた。

肉腫型中皮腫と肺肉腫様癌の鑑別診断に有用な免疫組織化学マーカーは現在のところ存在せず、両者の鑑別は画像診断あるいは切除検体の病理診断によって病変の局在（肺内病変か肺外病変か）を確認することによってのみ可能であった[16),17)]。

本研究で同定された MUC4 は肉腫型中皮腫と肺肉腫様癌を高い精度で鑑別できる免疫組織化学マーカーであり、今後の両者の鑑別診断、特に生検診断への応用が期待される[18)]。

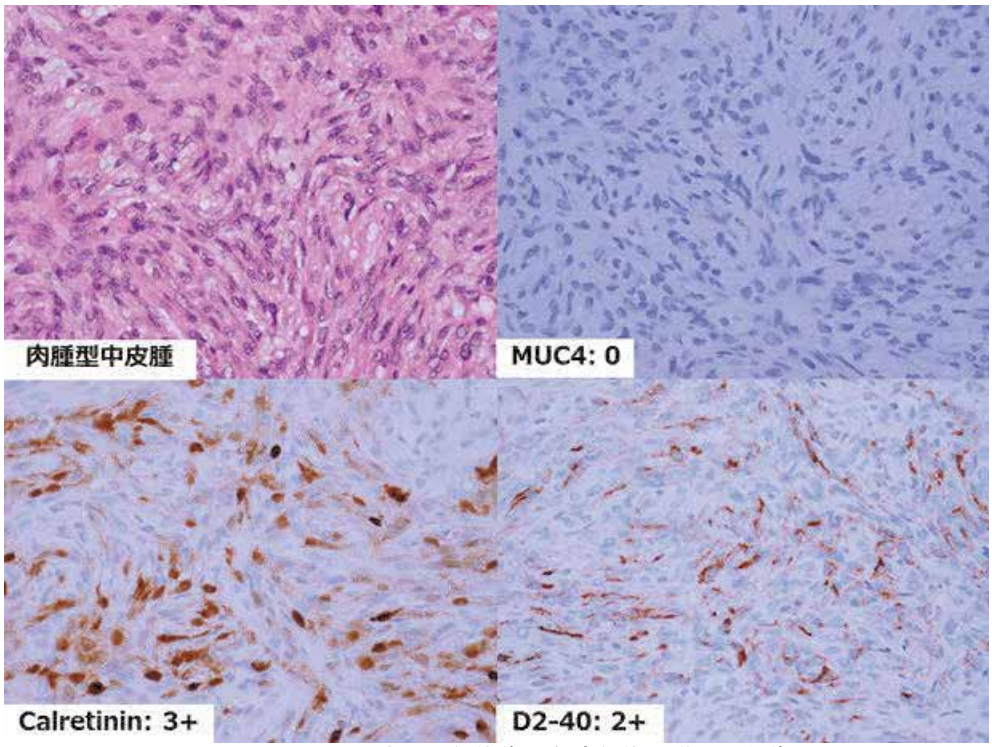

図 14. 肉腫型中皮腫の組織像と免疫組織化学的染色像
Calretinin、D2-40 が陽性、MUC4 は陰性である。

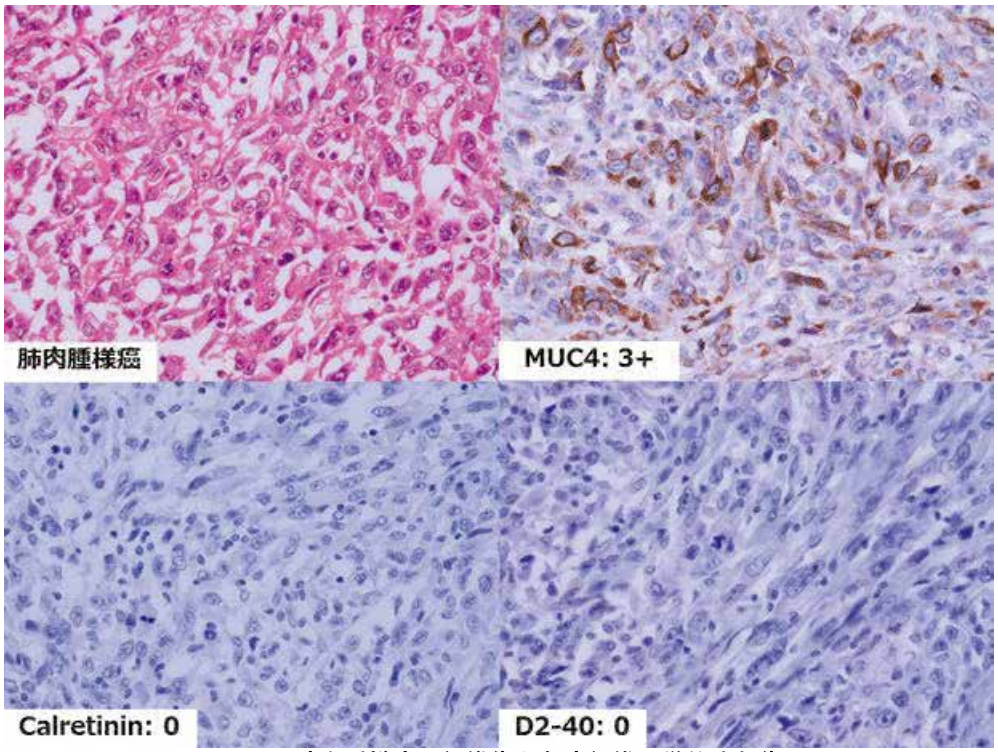

図 15. 肺肉腫様癌の組織像と免疫組織化学的染色像
MUC4 が陽性、Calretinin、D2-40 は陰性である。

表 5. 肉腫型中皮腫、肺肉腫様癌における各マーカーの陽性率

	肉腫型中皮腫						肺肉腫様癌					
			染色グレード						染色グレード			
マーカー	陽性症例	%	0	1＋	2＋	3＋	陽性症例	%	0	1＋	2＋	3＋
MUC4	0/31	0%	31	0	0	0	21/29	72%	8	9	9	3
Calretinin	23/31	74%	8	7	11	5	13/29	45%	16	5	6	2
D2-40	22/31	71%	9	9	12	1	9/29	31%	20	9	0	0
WT1	6/31	19%	25	5	1	0	1/29	3%	28	1	0	0
AE1/AE3	29/31	94%	2	2	8	19	29/29	100%	0	5	2	22
CAM5.2	28/31	90%	3	1	8	19	28/29	97%	1	6	5	17
p40	2/31	7%	29	2	0	0	6/29	21%	23	0	3	3
TTF-1	0/31	0%	31	0	0	0	15/29	52%	14	0	4	11
Claudin-4	0/31	0%	31	0	0	0	13/29	45%	16	4	5	4

表 6. 肉腫型中皮腫と肺肉腫様癌の鑑別診断における各マーカーの診断特性

所見	感度	特異度	陽性的中率	陰性的中率	正診率
MUC4 (−)	100%	72%	80%	100%	87%
Calretinin (＋)	74%	55%	64%	67%	65%
D2-40 (＋)	71%	69%	71%	69%	70%
WT1 (＋)	19%	97%	86%	53%	57%
AE1/AE3 (＋)	94%	0%	50%	0%	48%
CAM5.2 (＋)	90%	3%	50%	25%	48%
p40 (−)	94%	21%	56%	75%	58%
TTF-1 (−)	100%	52%	69%	100%	77%
Claudin-4 (−)	100%	45%	66%	100%	73%

3) 低分化型（充実型）上皮型中皮腫と低分化型非小細胞性肺癌の鑑別

代表的な症例の HE 染色および免疫組織化学的染色像を**図 16**～**図 18**、低分化型上皮型中皮腫、低分化型肺腺癌、低分化型扁平上皮癌における各マーカーの陽性率を**表 7**、**表 8**、低分化型上皮型中皮腫と低分化型肺腺癌の鑑別診断における各マーカーの診断特性を**表 9**、低分化型上皮型中皮腫と低分化型肺扁平上皮癌の鑑別診断における各マーカーの診断特性を**表 10** に示す。

低分化型上皮型中皮腫と低分化型肺腺癌の鑑別においては、陽性マーカー（いわゆる中皮細胞系マーカー）の中では D2-40 が正診率 93.0%で最も優れており、陰性マーカー（癌腫マーカー）の中では CEA が正診率 98.6%で最も優れていた。Claudin-4 の陰性マーカーとしての正診率は 97.2%と CEA とほぼ同程度で、TTF-1 の正診率

95.8%を上回った。中皮腫陽性マーカーとして、現在 Calretinin が最も強く推奨されているが[19]、低分化型上皮型中皮腫と低分化型肺腺癌の鑑別診断における Calretinin の陽性マーカーとしての正診率は 81.7%、特異度は 71.4%と低く、Calretinin の染色結果を過信すべきではないと考える。

低分化型上皮型中皮腫と非角化型肺扁平上皮癌の鑑別においては、陽性マーカーの中では WT1 が正診率 85.1%と最も優れていたが、感度が 72.2%と低い点が問題である。Calretinin、D2-40 の正診率は 75.7%、67.6%といずれも低く、特に特異度が 60.5%、39.5%と低いため、鑑別には有用でない。陰性マーカーでは CEA が正診率 95.9%、p40 が正診率 94.6%、Claudin-4 が正診率 93.2%で、感度・特異度ともに高く、いずれも優れた鑑別診断マーカーである[20]。

TTF-1、Napsin A はいずれも中皮腫の鑑別診断マーカー（陰性マーカー）として推奨されているが[19]、肺扁平上皮癌での陽性率は 13.2%、7.9%と低く、上皮型中皮腫と肺扁平上皮癌の鑑別には有用でない。そのため、TTF-1、Napsin A のみを陰性抗体として用いると、非角化型扁平上皮癌を中皮腫と誤診する可能性がある[20]。

現在推奨されている中皮腫の鑑別診断マーカー（Calretinin、D2-40、TTF-1、Napsin A）は[19]、低分化な上皮型中皮腫と低分化な非小細胞性肺癌の鑑別においては診断上の pit-fall が生じるため、注意が必要である[20]。

CEA、Claudin-4 は腺癌、扁平上皮癌ともに高率に陽性になる一方、上皮型中皮腫ではほとんどの例が陰性であるため、低分化型上皮型中皮腫と低分化型非小細胞性肺癌の鑑別にきわめて有効であり、強く推奨される[20]。

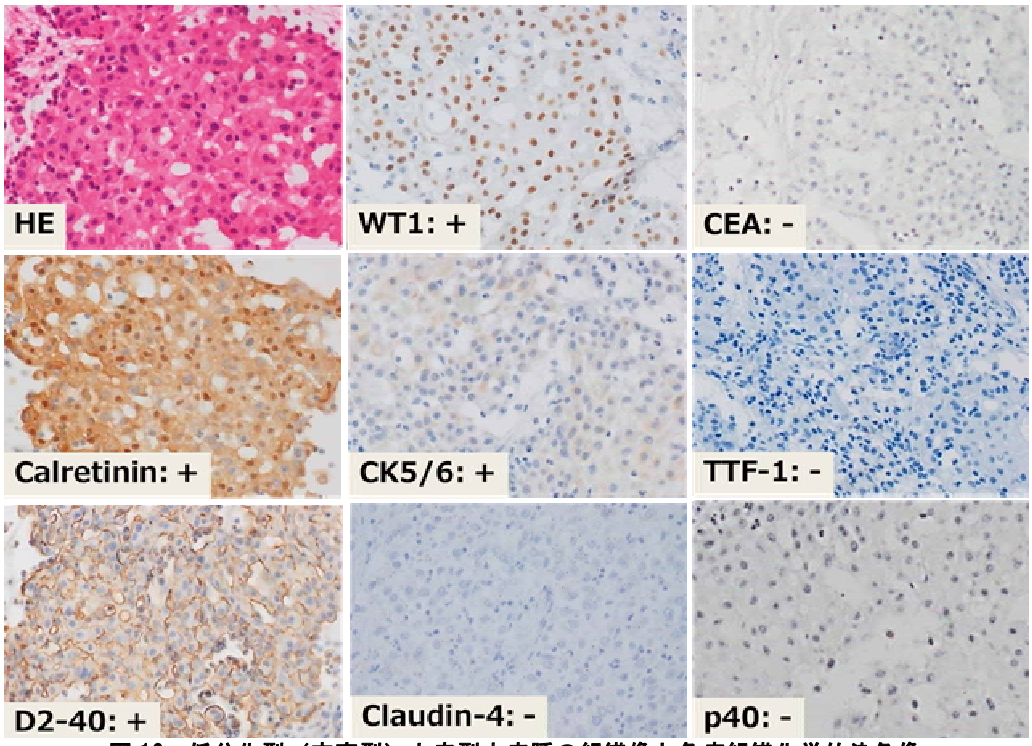

図 16. 低分化型（充実型）上皮型中皮腫の組織像と免疫組織化学的染色像
Calretinin、D2-40、WT1、CK5/6 が陽性、Claudin-4、CEA、TTF-1、p40 が陰性である。

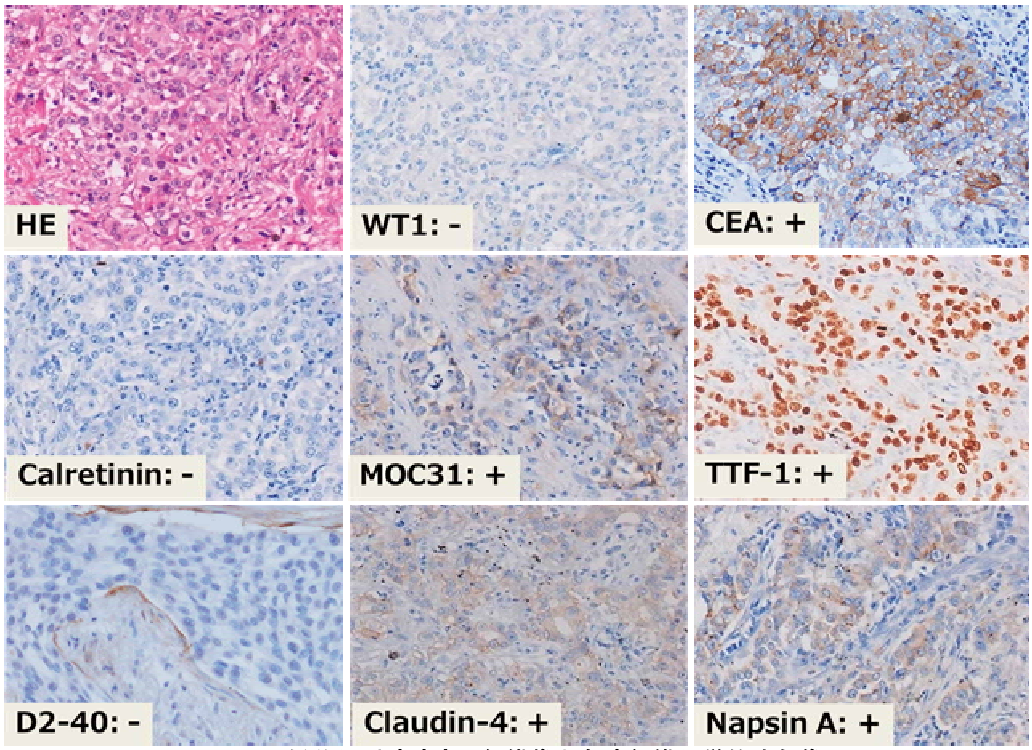

図 17. 低分化型肺腺癌の組織像と免疫組織化学的染色像
MOC31、Claudin-4、CEA、TTF-1、Napsin A が陽性、Calretinin、D2-40、WT1 が陰性である。

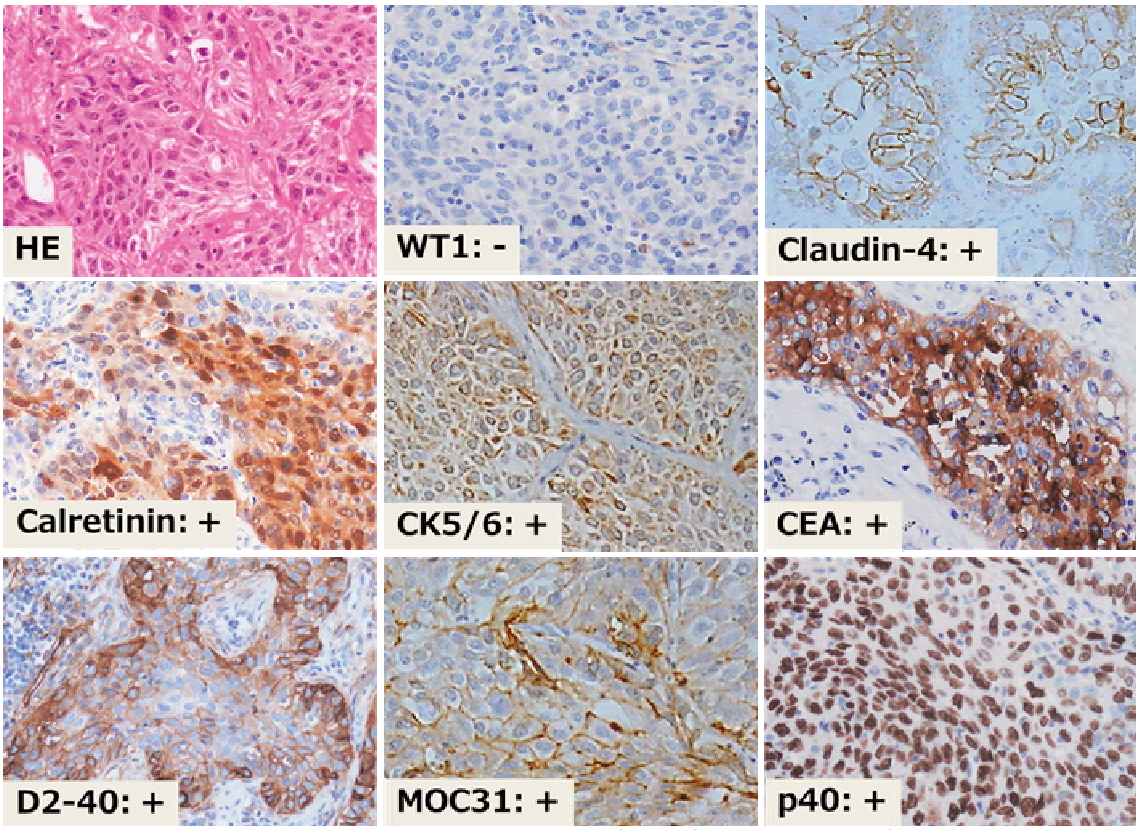

図 18. 低分化型扁平上皮癌の組織像と免疫組織化学的染色像

Calretinin、D2-40、CK5/6、MOC31、Claudin-4、CEA、p40 が陽性、WT1 が陰性である。

表 7. 低分化型（充実型）上皮型中皮腫と低分化型肺腺癌における各マーカーの陽性率

	低分化型上皮型中皮腫						低分化型肺腺癌					
			染色グレード						染色グレード			
マーカー	陽性症例	陽性率	0	1	2	3	陽性症例	陽性率	0	1	2	3
Calretinin	33/36	91.7%	3	0	2	31	10/35	28.6%	25	7	3	0
D2-40	35/36	97.2%	1	3	2	30	4/35	11.4%	31	2	2	0
WT1	26/36	72.2%	10	5	3	18	0/35	0.0%	35	0	0	0
CK5/6	26/36	72.2%	10	5	6	15	13/35	37.1%	22	6	5	2
CEA	0/36	0.0%	36	0	0	0	34/35	97.1%	1	7	7	20
Claudin 4	2/36	5.6%	34	2	0	0	35/35	100%	0	0	3	32
MOC31	12/36	33.3%	24	8	3	1	29/35	82.9%	6	9	7	13
TTF-1	0/36	0.0%	36	0	0	0	32/35	91.4%	3	2	3	27
Napsin A	0/36	0.0%	36	0	0	0	25/35	71.4%	10	6	2	17
p40	2/36	5.6%	34	2	0	0	3/35	8.6%	32	2	1	0
p63	6/36	16.7%	30	5	0	1	13/35	37.1%	22	5	3	5

表 8. 低分化型上皮型中皮腫と非角化型肺扁平上皮癌における各マーカーの陽性率

	低分化型上皮型中皮腫						非角化型扁平上皮癌					
			染色グレード						染色グレード			
マーカー	陽性症例	陽性率	0	1	2	3	陽性症例	陽性率	0	1	2	3
Calretinin	33/36	91.7%	3	0	2	31	15/38	39.5%	23	7	4	4
D2-40	35/36	97.2%	1	3	2	30	23/38	60.5%	15	5	12	6
WT1	26/36	72.2%	10	5	3	18	1/38	2.6%	37	1	0	0
CK5/6	26/36	72.2%	10	5	6	15	37/38	97.4%	1	2	6	29
p40	2/36	5.6%	34	2	0	0	36/38	94.7%	2	0	4	32
p63	6/36	16.7%	30	5	0	1	37/38	97.4%	1	1	2	34
CEA	0/36	0.0%	36	0	0	0	35/38	92.1%	3	14	13	8
MOC31	12/36	33.3%	24	8	3	1	34/38	89.5%	4	5	11	18
Claudin 4	2/36	5.6%	34	2	0	0	35/38	92.1%	3	3	17	15
TTF-1	0/36	0.0%	36	0	0	0	5/38	13.2%	33	5	0	0
Napsin A	0/36	0.0%	36	0	0	0	3/38	7.9%	35	3	0	0

表 9. 低分化型上皮型中皮腫と低分化型肺腺癌の鑑別における各種マーカーの診断特性

所見	感度	特異度	陽性的中率	陰性的中率	正診率
Calretinin (+)	91.7%	71.4%	76.7%	89.3%	81.7%
D2-40 (+)	97.2%	88.6%	89.7%	96.9%	93.0%
WT1 (+)	72.2%	100%	89.7%	76.2%	81.7%
CK5/6 (+)	72.2%	62.9%	66.7%	68.8%	67.6%
CEA (-)	100%	97.1%	97.3%	100%	98.6%
Claudin-4 (-)	94.4%	100%	100%	94.6%	97.2%
MOC31 (-)	66.7%	82.9%	80%	71%	74.6%
TTF-1 (-)	100%	91.4%	92.3%	100%	95.8%
Napsin A (-)	100%	71.4%	78.3%	100%	85.9%
p40 (-)	94.4%	8.6%	51.5%	60%	52.1%
p63 (-)	83.3%	37.1%	57.7%	68.4%	60.5%

表 10. 低分化型上皮型中皮腫と非角化型肺扁平上皮癌の鑑別における各種マーカーの診断特性

所見	感度	特異度	陽性的中率	陰性的中率	正診率
Calretinin (+)	91.7%	60.5%	68.8%	88.5%	75.7%
D2-40 (+)	97.2%	39.5%	60.3%	93.8%	67.6%
WT1 (+)	72.2%	97.4%	96.3%	78.7%	85.1%
CK5/6 (-)	27.8%	97.4%	90.9%	58.7%	63.5%
CEA (-)	100%	92.1%	92.3%	100%	95.9%
Claudin-4 (-)	94.4%	92%	92%	94.6%	93.2%
MOC31 (-)	66.7%	89.5%	86%	74%	78.4%
TTF-1 (-)	100%	13.2%	52.2%	100%	55.4%
Napsin A (-)	100%	7.9%	50.7%	100%	52.7%
p40 (-)	94.4%	94.7%	94.4%	95%	94.6%
p63 (-)	83.3%	97.4%	96.8%	86.0%	90.5%

4) 上皮型中皮腫と肺腺癌の新規鑑別診断マーカー

代表的な症例の HE 染色および免疫組織化学的染色像を**図 19**、**図 20**、上皮型中皮腫、肺腺癌における各マーカーの陽性率を**表 11**、上皮型中皮腫と肺腺癌の鑑別診断における各マーカー及び 2 抗体の組み合わせによる診断特性を**表 12** に示す。

DAB2 は上皮型中皮腫の 80%が陽性を示したが、肺腺癌は 3%しか陽性を示さなかった。また、Intelectin-1 は上皮型中皮腫の 76%が陽性を示したが、肺腺癌は全例陰性であった。これらの結果から、DAB2、Intelectin-1 はいずれも特異性の高い中皮腫陽性マーカーと考えられた。

Calretinin、D2-40 は上皮型中皮腫の 99%、95%が陽性であったが、肺腺癌における陽性率もそれぞれ 25%、10%と比較的高値であり、特異性に問題がある。

WT1 の陽性率は上皮型中皮腫で 83%、肺腺癌で 0%であり、DAB2、Intelectin-1 とほぼ同程度であった。

2 抗体の組み合わせによる検討では、Intelectin-1 と WT1 を組み合わせた（Intelectin-1 陽性あるいは WT1 陽性のいずれかを満たす場合を陽性と評価する）場合が感度 93%、特異度 100%と最も高い正診率を示した。

現在上皮型中皮腫と肺腺癌の鑑別診断における中皮腫陽性マーカーとしては Calretinin、D2-40、WT1 が推奨され、頻用されているが[3),9)]、DAB2、Intelectin-1 も WT1 と遜色ない診断精度を有するマーカーであり、抗体パネルに加えるべきである[21)]。また、Calretinin、D2-40 を上皮型中皮腫の陽性マーカーとして用いる場合には、これらが肺腺癌においても陽性になる場合がある点に留意する必要がある。

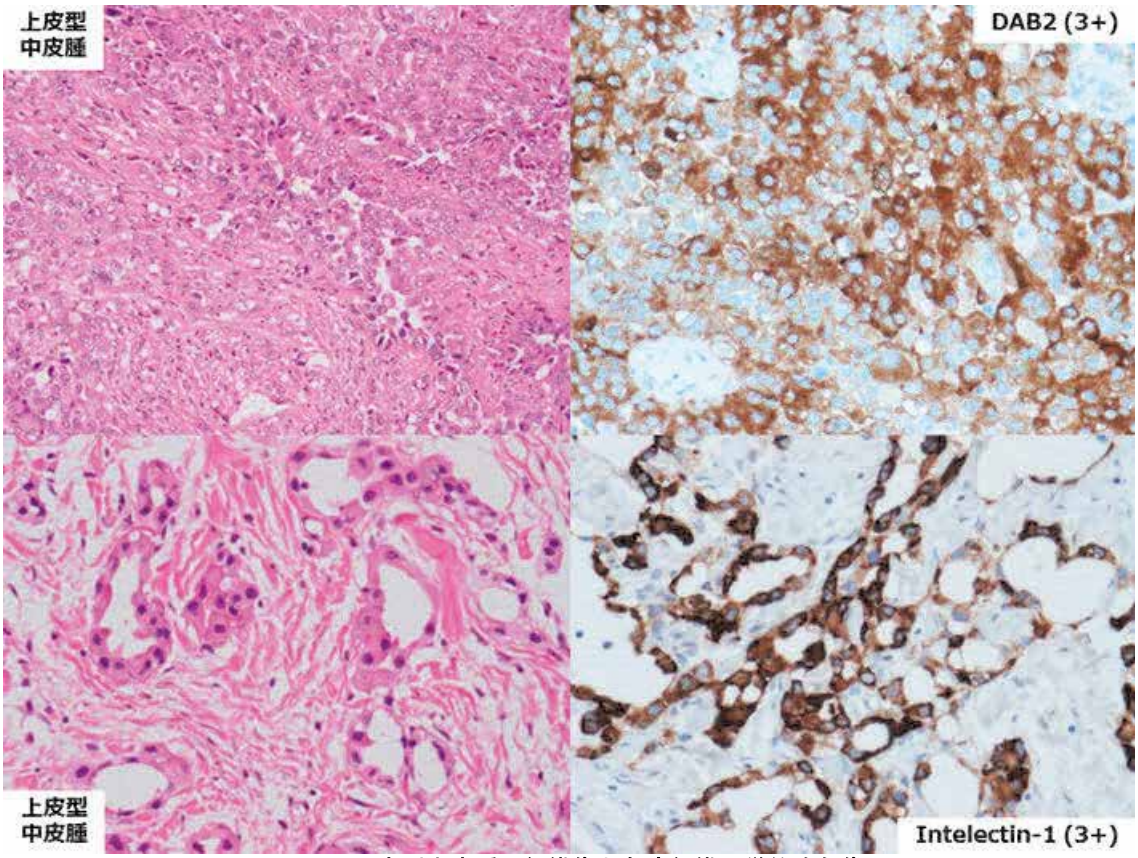

図 19. 上皮型中皮腫の組織像と免疫組織化学的染色像
DAB2、Intelectin-1 が陽性である。

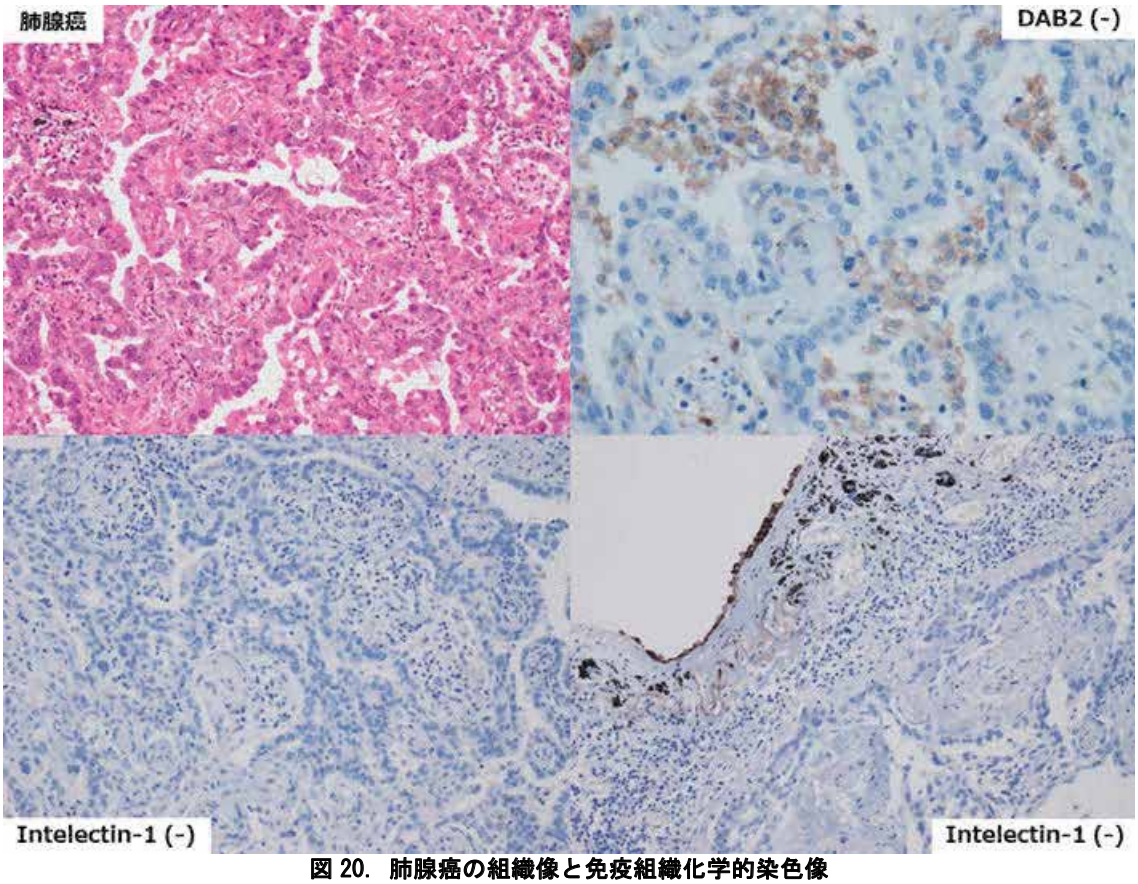

図 20. 肺腺癌の組織像と免疫組織化学的染色像

腫瘍細胞は DAB2、Intelectin-1 陰性である。肺胞マクロファージが DAB2 陽性、
臓側胸膜の中皮細胞と弾力膜が Intelectin-1 陽性を示す。

表 11. 上皮型中皮腫、肺腺癌における各マーカーの陽性率

	上皮型中皮腫						肺腺癌					
			染色グレード						染色グレード			
マーカー	陽性症例	(%)	0	1＋	2＋	3＋	陽性症例	(%)	0	1＋	2＋	3＋
DAB2	60/75	80%	15	12	18	30	2/67	3%	65	2	0	0
Intelectin-1	57/75	76%	18	17	4	36	0/67	0%	67	0	0	0
Calretinin	74/75	99%	1	7	2	65	17/67	25%	50	10	7	0
D2-40	71/75	95%	4	5	6	60	7/67	10%	60	5	2	0
WT1	62/75	83%	13	18	7	37	0/67	0%	67	0	0	0

表 12. 上皮型中皮腫と肺腺癌の鑑別診断における
各マーカー及び 2 抗体の組み合わせによる診断特性

マーカー	感度	特異度
DAB2	80%	97%
Intelectin-1	76%	100%
WT1	83%	100%
Calretinin	99%	75%
D2-40	95%	90%
Intelectin-1 or DAB2	93%	95%
Intelectin-1 and DAB2	60%	100%
Intelectin-1 or WT1	93%	100%
DAB2 or WT1	93%	95%
Intelectin-1 and Calretinin	76%	100%
Intelectin-1 or Calretinin	99%	75%
DAB2 and D2-40	75%	98%
DAB2 or D2-40	100%	86%

4. 結語

平成 26、27、28 年度研究の結果、上皮型中皮腫と反応性中皮細胞過形成の鑑別診断、肉腫型中皮腫と肺肉腫様癌の鑑別診断、低分化型（充実型）上皮型中皮腫と低分化型非小細胞性肺癌の鑑別、上皮型中皮腫と肺腺癌の鑑別診断のそれぞれにおいて、既知のマーカーの有用性の再評価および有用な新規マーカーの同定を行うことができた。

本研究から得られた中皮腫と他疾患の鑑別マーカーのまとめを**表 13** に示す。

今後更なる検討によるこれらのマーカーの有用性の確立と高い診断精度を持つマーカーの探索を継続していく必要がある。

表 13. 中皮腫と他疾患の鑑別マーカーのまとめ（下線は本研究で明らかとなったもの）

1. 上皮型中皮腫と反応性中皮細胞過形成の鑑別マーカー	
陽性マーカー:	EMA, Glut-1, IMP-3, CD146, p16 gene欠失, **Noxa, Survivin**, Ki-67
陰性マーカー:	BAP1, Desmin

2. 肉腫型中皮腫と肺肉腫様癌の鑑別マーカー	
陽性マーカー:	サイトケラチン (AE1/AE3, CAM5.2), D2-40
陰性マーカー:	p40, TTF-1, Claudin-4, **MUC4**

3. 低分化型（充実型）上皮型中皮腫と低分化型肺腺癌の鑑別マーカー	
陽性マーカー:	Calretinin, D2-40, WT1, **DAB2, Intelectin-1**
陰性マーカー:	CEA, Claudin-4, TTF-1, Napsin A

4. 低分化型（充実型）上皮型中皮腫と低分化型肺扁平上皮癌の鑑別マーカー	
陽性マーカー:	WT1, Calretinin
陰性マーカー:	CEA, Claudin-4, p40, p63

参考文献

1) Murayama T, Takahashi K, Natori Y, Kurumatani N. Estimation of future mortality from pleural malignant mesothelioma in japan based on an age-cohort model. Am J Ind Med. 49:1-7.2006
2) Takeshima Y, Inai K, Amatya VJ, Gemba K, Aoe K, Fujimoto N, Kato K, Kishimoto T. Accuracy of pathological diagnosis of mesothelioma cases in Japan: clinicopathological analysis of 382 cases. Lung Cancer. 66:191-7.2009
3) Husain AN, Colby T, Ordonez N, et al Guidelines for pathologic diagnosis of malignant mesothelioma: 2012 update of the consensus statement from the International Mesothelioma Interest Group. Arch Pathol Lab Med. 137(5):647-67.2013
4) Galateau-Salle F, Churg A, Roggli V et al. Tumours of the pleura. In Travis WD, Brambilla E, Burke AP, Marx A, Nicholson AG eds. Who classification of tumours of the lung, pleura, thymus and heart. Lyon: International Agency for Research on Cancer, 153-181.2015
5) Cigognetti M, Lonardi S, Fisogni S, et al. BAP1 (BRCA1-associated protein 1) is a highly specific marker for differentiating mesothelioma from reactive mesothelial proliferations. Mod Pathol. 28(8): 1043-57.2015
6) Hanley KZ, Facik MS, Bourne PA, et al. Utility of anti-L523S antibody in the diagnosis of benign and malignant serous effusions. Cancer. 114(1):49-56.2008

7) Kato Y, Tsuta K, Seki K, et al. Immunohistochemical detection of GLUT-1 can discriminate between reactive mesothelium and malignant mesothelioma. Mod Pathol. 20(2):215-20.2007
8) Okazaki Y, Nagai H, Chew SH, et al. CD146 and insulin-like growth factor 2 mRNA-binding protein 3 predict prognosis of asbestos-induced rat mesothelioma. Cancer Sci. 104(8):989-95.2013
9) Sato A, Torii I, Okamura Y, et al. Immunocytochemistry of CD146 is useful to discriminate between malignant pleural mesothelioma and reactive mesothelium. Mod Pathol. 23(11):1458-66.2010
10) Tsukiji H, Takeshima Y, Amatya VJ et al. Myogenic antigen expression is useful for differentiation between epithelioid mesothelioma and non-neoplastic mesothelial cells. Histopathology. 56(7):969-74.2010
11) Kanda Y. Investigation of the freely available easy-to-use software 'EZR' for medical statistics. Bone Marrow Transplant. 48(3):452-8.2013
12) Hida T, Hamasaki M, Matsumoto S et al. Bap1 immunohistochemistry and p16 fish results in combination provide higher confidence in malignant pleural mesothelioma diagnosis: Roc analysis of the two tests. Pathol Int. 66:563-570.2016
13) Hwang HC, Sheffield BS, Rodriguez S et al. Utility of bap1 immunohistochemistry and p16 (cdkn2a) fish in the diagnosis of malignant mesothelioma in effusion cytology specimens. Am J Surg Pathol. 40:120-126.2016
14) McGregor SM, Dunning R, Hyjek E, Vigneswaran W, Husain AN, Krausz T. Bap1 facilitates diagnostic objectivity, classification, and prognostication in malignant pleural mesothelioma. Hum Pathol. 46:1670-1678.2015
15) Cigognetti M, Lonardi S, Fisogni S et al. Bap1 (brca1-associated protein 1) is a highly specific marker for differentiating mesothelioma from reactive mesothelial proliferations. Mod Pathol. 28:1043-1057.2015
16) Kushitani K, Takeshima Y, Amatya VJ, Furonaka O, Sakatani A, Inai K. Differential diagnosis of sarcomatoid mesothelioma from true sarcoma and sarcomatoid carcinoma using immunohistochemistry. Pathol Int. 58:75-83.2008
17) Takeshima Y, Amatya VJ, Kushitani K, Kaneko M, Inai K. Value of immunohistochemistry in the differential diagnosis of pleural sarcomatoid mesothelioma from lung sarcomatoid carcinoma. Histopathology. 54:667-676.2009
18) Amatya VJ, Kushitani K, Mawas AS et al. Muc4, a novel immunohistochemical marker identified by gene expression profiling, differentiates pleural sarcomatoid mesothelioma from lung sarcomatoid carcinoma. Mod Pathol 2017. [Epub ahead of print]

19) 環境再生保全機構. アスベスト（石綿）健康被害の救済
https://www.erca.go.jp/asbestos/medical/index.html
20) Kushitani K, Amatya VJ, Okada Y, et al. Utility and pitfalls of immunohistochemistry in the differential diagnosis between epithelioid mesothelioma and poorly differentiated lung squamous cell carcinoma. Histopathology. 70:375-384.2017
21) Kuraoka M, Amatya VJ, Kushitani K, et al. Identification of DAB2 and Intelectin-1 as the Novel Positive Immunohistochemical Markers of Epithelioid Mesothelioma by Transcriptome Microarray Analysis for its Differentiation from Lung Adenocarcinoma. Am J Surg Pathol. 2017. In press.

胸膜中皮腫の的確な診断に資するための ICT を用いた遠隔病理及び画像診断の応用

井内　康輝、由佐　俊和

研究目的：

胸膜中皮腫の病理診断（細胞診断を含む）及び画像診断については、多くの研究の進展がみられているにも拘らず、未だ診断困難な症例が数多くみられる。特に近年、検診の普及などによって早期中皮腫を疑う例が見出されるに伴って、早期上皮型中皮腫と反応性中皮細胞過形成との鑑別､線維形成型中皮腫と線維性胸膜炎との鑑別が重要となりつつある。さらに、病理診断における免疫組織化学的染色の普及によって、的確な病理診断が下されることが多いが、肺癌や胸膜を占拠する他の悪性腫瘍との鑑別において、各例の染色結果の判断や多くの染色結果の総合的判断に意見のくい違いがみられる例の扱いが問題となることにも遭遇するようになった。

こうした診断困難例については、中皮腫診断の経験豊富な複数の病理診断医あるいは放射線画像診断医によるそれぞれの分野での合議や、病理診断と画像診断の総合判断が必要である。しかしながら、この合議や総合的判断を下す作業は容易ではない。すなわち、日時を定めて会場を設定し、診断者が一同に会することを企画すること自体が難しく、かつ診断者の参加が一定でないことから、参加者数などによって、合議の内容や判定の結果が左右されることが見受けられる。そこで、診断者（病理診断医、放射線画像診断医、呼吸器内科医、呼吸器外科医など）が、それぞれ自らの施設において病理像や放射線画像を観察でき、それぞれに診断意見を述べた上で、合議による結論を導き出すことができれば、合理的である。すなわち、常に一定の診断者が確保され、それぞれの意見が均等に評価されて結論に至れば、診断の的確さが担保され、かつ結論をうるまでの日数が節約され、同時に経費の節減にも繋がる。

本研究は、こうした観点から、インターネット回線とクラウドサービスを用いて新しい診断討議システムを構築し、実用化することを目的とする。

研究方法：

１．遠隔診断ソフト“LOOKREC”を基盤に、新たな“診断討議システム”を開発した。

２．研究班員（10 名：病理診断医 3 名、放射線画像診断医 2 名、呼吸器内科医 4 名、呼吸器外科医 1 名）の各々に Gmail アカウントを取得してもらい、クラウドへのアクセスを可能とした。

３．症例の提示から診断の決定までは、以下の手順で行った。

1) 各医療機関（研究班員の所属する施設）で中皮腫を疑った症例について、診断の根拠となった以下の材料を用意する。

① 病理検査材料（生検組織標本、細胞診材料、剖検組織材料）

② 放射線画像（X 線フィルム、CT 画像、MRI 画像）の DICOM データ材料

2) 患者の個人情報保護のルール（研究結果において詳述する）に従って、患者情報を秘匿して、各医療機関から、病理診断センターに送付する。

3) 病理診断センターでは、病理組織標本はバーチャルスライドシステム（Nanozoomer®、浜松フォトニクス）を用いデジタルデータとし、画像の DICOM データは、ポータルシステム、ビューワーシステムによって、クラウドサービスのプラットホームにあげる（**図 1**）。

4) 診断者（研究班員 10 名に委嘱する）は、それぞれの Gmail アカウントによって診断システムにアクセスし、病理画像、DICOM 画像を自施設のブラウザ（コンピューター）で観察し、その診断意見をレポートシステムによって入力して、クラウドサービスのプラットホームにあげる（**図 1**）。

5) 研究分担者（井内）は、これらの意見をまとめ、最終診断を作成し（キー画像も貼布）、診断者にフィードバックする。

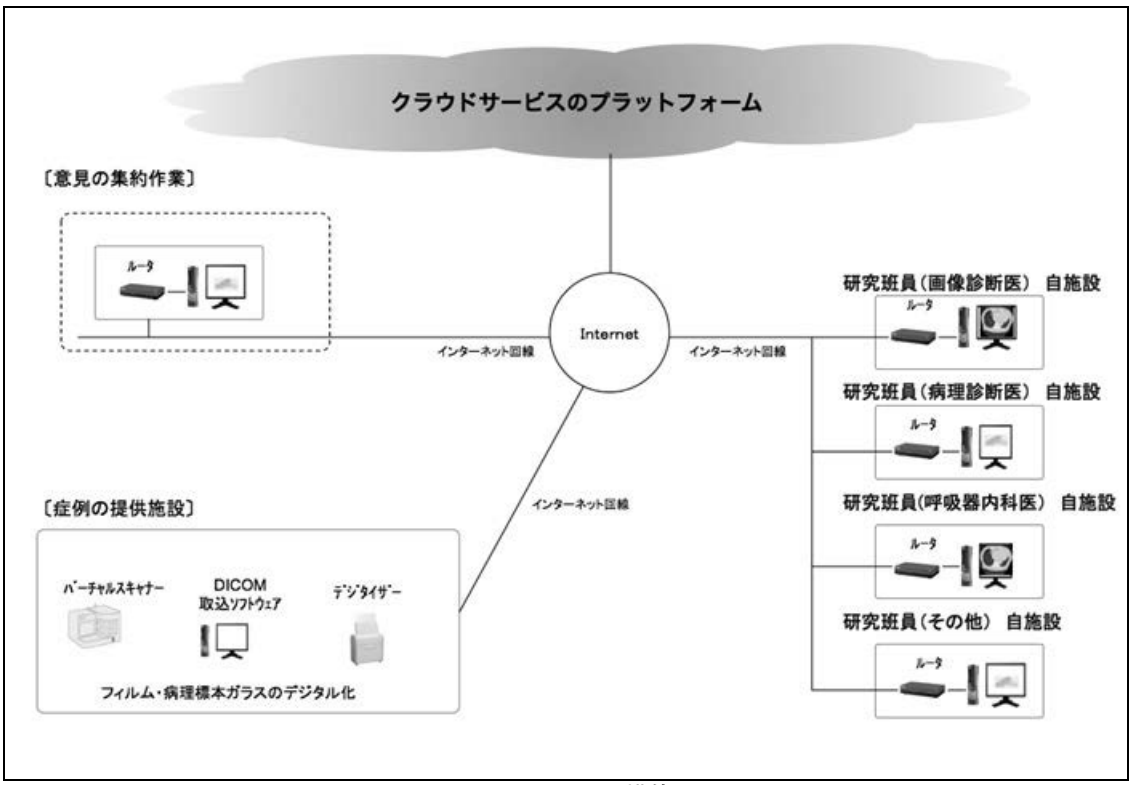

図 1. システムの構築図

研究結果：

１．個人データの院外への持ち出しに関する患者の同意のとり方と個人情報の秘匿について検討し、以下のようにすることとした。

1) 患者の同意について

本研究の実施については、患者（被験者）の検査時、入院時あるいは手術時に医療機関から提示される、画像検査あるいは病理検査を含めた包括的同意書の中に述べられる“患者から得られた材料は研究目的に使われることがある”との条文が患者によって合意されれば、研究対象とすることは可能と考えた。

なぜならば､本研究は､患者から既に手術によって切除された組織を用いるので、この研究によって患者には特別な危険あるいは不利益は生じない。中皮腫としての登録が行なわれる点については､“がん登録法”においても、公共の利益に資するためであるので、個人情報の秘匿が完全に行なわれるならば、特別な問題は生じないと考えた。

また、本研究の実施にあたっては、各医療機関および各研究施設のホームページに“本研究を行っている”旨を掲示し、周知徹底する。また、対象患者から各機関あるいは施設に対して情報開示請求があった場合は、個別に誠実に対応することとした。

なお、本研究によって得られた情報については本研究のみに使用し、情報の漏洩がないように研究責任者および研究分担者を責任者として定め、情報の管理を厳密に行うこととした。

2) 患者の個人情報の秘匿について

本研究においては、中皮腫の診断について、多くの病理診断医、放射線画像診断医、呼吸器内科医、呼吸器外科医などの個々の診断が必要であることから、診断時に必要な最低限の患者情報（年齢・性別・病変の部位など）は、インターネット通信によって情報交換した。

その際、患者（被験者）の人権擁護として、患者情報が漏洩することを防ぐために以下の方法をとることとした。

① 本研究に関して、個人情報管理者を患者情報を発信する医療機関におく。

② 各医療機関からの患者情報を受け取る病理診断センターには個人情報管理責任者として、研究分担者の井内康輝がその任を努める。

③ 個人情報管理者は、中皮腫が疑われる症例に、個人情報とは無関係の「匿名化番号」を付与する。

④ 個人のカルテ等の情報ソースと「匿名化番号」の対応表は、個人情報管理者が厳重に管理し、研究責任者、研究分担者には渡さない。この対応表は、施錠可能なキャビネット等で保管する。

⑤　本研究に関して、個人のカルテ等の情報ソースから転記する項目は、「年齢」、「性別」、「職歴」、「病理標本番号」、「病理組織診断」及び「画像検査番号」のみであり、患者の氏名、生年月日、住所等の他の個人情報は一切転記しない。

⑥　病理標本の提供にあたっては、個人情報管理者は技術職員に対して「病理標本番号」のみの情報を与え、これにもとづいて当該パラフィンブロックの薄切、染色を行う。完成した標本には、患者名の代りに「匿名化番号」のみが記載され、提供される。

⑦　検査画像の提供にあたっては、個人情報管理者は画像の保管者に対して「画像番号」のみの情報を与え、画像は、患者名の代りに「匿名化番号」のみが付記されて、提供される。

⑧　提供されたデータの全ては、研究が終了する平成 29 年 3 月 31 日より 5 年間保管する。その時点で必要性が生じた場合はさらに 5 年間延長する。その後にはクラウド上から全てのデータを消去ないし廃棄する。この消去・廃棄は、研究責任者の指示のもと、研究分担者として病理診断センターの個人情報管理責任者を努める井内康輝が行う。

２．討議会議システムを用いた検討例の結果の一覧

1)　2015 年及び 2014 年の予備的な検討症例の一覧（**表 1**）

2)　2016 年の検討症例の一覧（**表 2**）

3)　2017 年の検討症例の一覧（**表 3**）

表 1. 2015 年及び 2014 年の予備的な検討症例の一覧

登録番号	提供施設	提供材料	病理標本(枚数)	画像	最終診断
2014-001	A 病院	手術	16	CR,CT	肺がん
2014-002	〃	剖検	6	CR,CT	肺がん
2015-001	〃	生検	13	CR,CT,PT	中皮腫
2015-002	〃	生検	8	CR,CT	良性石綿肺
2015-003	〃	生検	19	CR,CT,PT	肺がん
2015-004	〃	生検	9	CT	中皮腫
2015-005	〃	生検	13	CR,CT,PT,MRI	中皮腫
2015-006	C 病院	生検(右胸膜)	13	CR,CT	胸膜炎
2015-007	A 病院	剖検	17	なし	胸膜炎
2015-008	〃	剖検	20	CR,CT	良性石綿肺

CR:Chest X-P
CT:CT
MRI:MRI
PT : PET-CT

表 2. 2016 年の検討症例の一覧

登録番号	提供施設	病理標本（枚数）	画像	最終診断
2016-001	A 施設	8	CT	中皮腫（低分化上皮型）
2016-002	〃	12	CR,CT	肺多形癌
2016-003	B 施設	9	なし	中皮腫（低分化上皮型）
2016-004	〃	12	なし	中皮腫（非浸潤上皮型）
2016-005	C 施設	14（細胞診）	なし	中皮腫（上皮型）
2016-006	D 施設	9（細胞診）	CT	中皮腫（上皮型）
2016-007	〃	8	なし	線維性胸膜炎
2016-008	〃	8	なし	中皮腫（肉腫型）
2016-009	〃	9	CT	中皮腫（二相型）
2016-010	〃	6	なし	線維性胸膜炎
2016-011	A 施設	9	CR,CT	中皮腫（腹膜、上皮型）
2016-012	〃	12	CT	肺多形癌（剖検例）
2016-013	〃	18	CR,CT	中皮腫（2016-011 と同一）
2016-014	E 施設	7	CR,CT	中皮腫（肉腫型）
2016-015	〃	7	CR,CT	中皮腫（上皮型、粘液産生）
2016-016	〃	9	CR,CT	中皮腫（肉腫型）

表 3. 2017 年の検討症例の一覧

登録番号	提供施設	提供材料	病理標本(枚数)	画像	最終診断
2017-001	C 病院	生検	7	CR, CT	中皮腫（上皮型）
2017-002	〃	生検	8	CR, CT	中皮腫（肉腫型）
2017-003	〃	生検	8	CR, CT	中皮腫（上皮型）
2017-004	D 病院	生検	15	CT	肺多形がん
2017-005	〃	手術	10	CT	中皮腫（肉腫型）
2017-006	E 病院	生検(右胸膜)	10	CR, CT	中皮腫（上皮型）
2017-007	〃	生検(右胸膜)	10	CR, CT	中皮腫（二相型）
2017-008	〃	生検(右胸膜)	10	CR, CT	中皮腫（肉腫型）
2017-009	〃	生検(右胸膜)	9	CR, CT	線維性胸膜炎
2017-010	〃	生検(右胸膜)	8	CT	線維性胸膜炎
2017-011	〃	生検(右胸膜)	12	CR, CT	中皮腫（二相型）

3．2017 年症例のうち、診断者の意見が分れた例を 3 例表示する。それらは、2017-004（**図 2**、**3**）、2017-009（**図 4**、**5**）、2017-010（**図 6**、**7**）である。

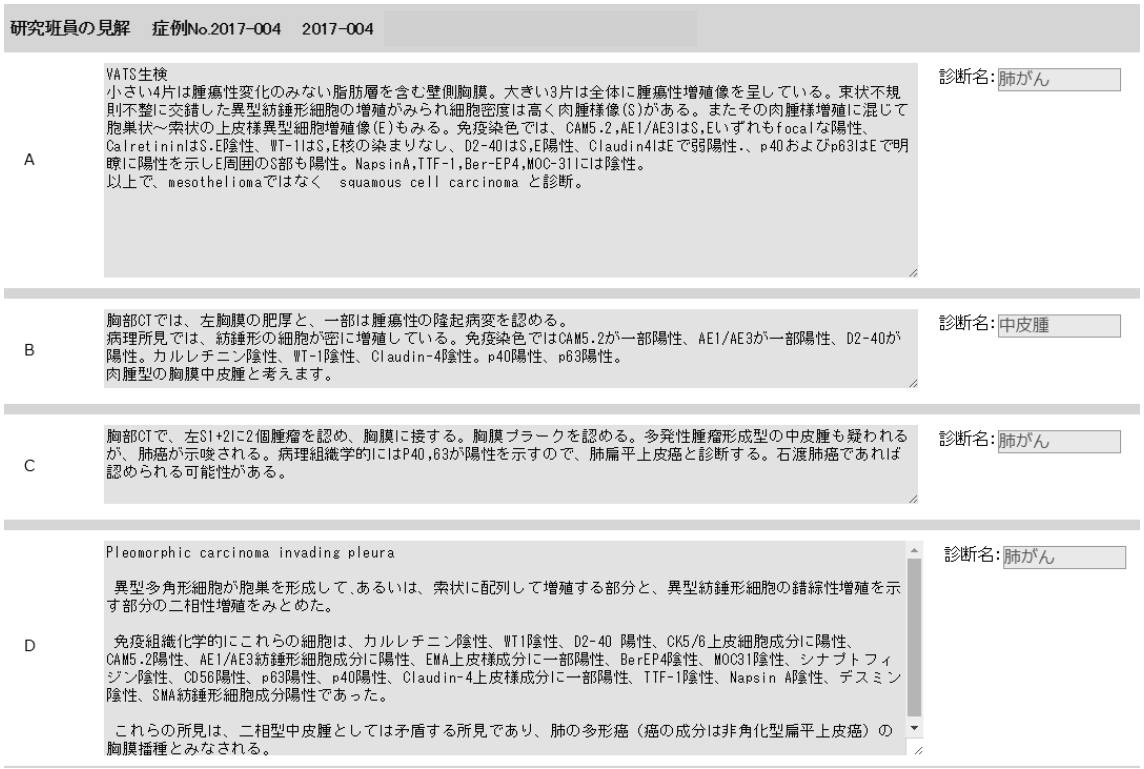

図 2. 2017-004


最終診断名:
肺がん
所見
画像では、胸膜に限局性の結節性病変を認めますが、中皮腫より肺癌の可能性が高いとみなされます。
病理像では、異型性の強い紡錘形細胞の増殖が主体を占める腫瘍ですが、低分化な癌腫が示唆される上皮様細胞が一部に混在します。
免疫染色では、サイトケラチンは上皮様部分を中心に陽性、D2-40も陽性ですが、calretininおよびWT-1は陰性です。Desminは陰性です。肺癌マーカーは全て陰性ですが、p40，p63は上皮様部分に陽性です。Claudin-4は上皮様部分の一部で弱陽性です。
これらの所見からは、中皮腫と診断することは困難で、肺原発の多形癌(pleomorphic carcinoma)と診断されます。上皮様部分は低分化型の扁平上皮癌(squamous cell carcinoma)とみなされます。
臨床医1名は中皮腫(肉腫型）、1名は肺がんの診断です。病理医2名はいずれも肺多形癌で上皮様部分は低分化扁平上皮癌との診断です。
付記
報告症例No:
キー画像
番号
検査日
書き込み

図 3. 2017-004

研究班員の見解　症例No.2017-009　2017-009

A	右胸水(+)で厚い胸膜肥厚(+)、不整像は軽度です。縦隔側胸膜肥厚は目立たず、右下肺に円形無気肺所見(+)、一見びまん性胸膜肥厚も考えますが、胸膜プラーク(-)、右胸郭容量低下高度で中皮腫をより疑います。	診断名:中皮腫
B	右胸郭の縮小化と腫瘍性胸膜肥厚があり、粘膜下の腫瘍細胞は上皮成分を含む腫瘍性増殖をしているので中皮腫に矛盾しない	診断名:中皮腫
C	VATS下右壁側胸膜生検 胸腔側面にフィブリン層、深層に脂肪層・胸内筋膜・横紋筋をみ、脂肪層と壁側胸膜の境界はリンパ濾胞の目立つ小円形細胞の炎症細胞浸潤が目立つ。壁側胸膜は硝子化した強い線維性肥厚を呈し、その線維性増殖は胸膜に平行な方向を示し不規則不整な配列像に乏しい。また、炎症細胞の随伴が目立つ。脂肪層への浸潤像や圧排増殖像はみない。免疫染色では線維性肥厚部の紡錘形細胞はCAM5.2,AE1/AE3に強陽性、Calretinin,D2-40に陽性、SMA陽性、Desmin陽性。 以上で、肥厚した壁側胸膜は、配列の乱れが乏しく、深部浸潤像明らかでなく、Desmin陽性像がみられ、採取された標本内ではfibrous pleuritisと診断する。	診断名:その他
D	右胸水と胸膜肥厚を認め、胸腔内に気腔が見られる。CTでは肥厚した胸膜に接して円形無気肺と思われる腫瘤陰影を認める。両側肺とも気腫性変化が目立つ。 病理所見では、異型細胞が増殖しているように見えますが、その部位では免疫染色ではいずれも陰性と思われます。 画像所見を重視し、胸膜炎と診断させていただきます。	診断名:良性石綿肺
E	Diffuse pleural thickening (pleuritis), pleura, biopsy Non-Atypical spindle cells proliferation in parallel fashion along pleural cavity. In deep region, marked chronic inflammation is noted. No obvious stromal invasion Vague zonation (+) CAM5.2: 3+ AE1/AE3: 2+ Calretinin: 1+ WT-1: - D2-40: 2+ Desmin: 1+ Surface only SMA: 3+ CD34: -	診断名:その他

図 4.　2017-009

図 5.　2017-009

研究班員の見解　症例No.2017-010　2017-010

A	左側の胸郭の容積減少あり。被包化胸水があり、左下葉の無気肺を伴っています。壁側胸膜の平滑な肥厚がみられ、肥厚は軽度ですが、中皮腫で矛盾しない所見です。	診断名:中皮腫
B	左胸水(+)で肺尖部主体に縦隔側胸膜肥厚を伴っています。胸膜不整は軽度ですが、中皮腫をより疑います。 胸膜プラーク(-) 肺癌を疑う腫瘤形成(-) 有意サイズのリンパ節腫大(-)	診断名:中皮腫
C	左胸郭の縮小化と胸膜肥厚有、HE染色でも腫瘍細胞が密度高く存在するので、desmoplastic mesotheliomaと診断する	診断名:中皮腫
D	左壁側胸膜生検 胸腔側面は出血およびフィブリン層が、深層には脂肪層・胸内筋膜が含まれた肥厚した壁側胸膜。その肥厚した壁側胸膜は硝子化した強い線維の増生で、胸膜に平行な方向性を示し不規則不整な配列に乏しい。炎症細胞の随伴がやや目立っている。脂肪層は薄いが浸潤像や圧排増殖像はみない。免疫染色では、CAM5.2,AE1/AE3に強陽性を示す紡錘形細胞は浅層～中層部に分布し、深層部にはみない。Calretinin,D2-40,WT-1に陽性、SMA陽性、Desminに明瞭な陽性。 以上で、肥厚した壁側胸膜の配列の乱れが乏しく、浸潤像明らかでなく、CK陽性増殖細胞は深層部には認めず、またDesminに明瞭な陽性像がみられる。採取された標本内ではfibrous pleuritisと診断する。	診断名:その他
E	画像上は、左胸水を認め、おそらく一部は器質化している。不整な胸膜肥厚は認めない。 病理所見でも、悪性病変を疑うような異型細胞は認めないように思います。	診断名:良性石綿肺
F	Diffuse pleural thickening (pleuritis), pleura, biopsy Non-Atypical spindle cells proliferation in parallel along pleural cavity. In deep region, marked chronic inflammation is noted. No obvious stromal invasion Vague zonation (+) CAM5.2: 3+ AE1/AE3: 2+ Calretinin: 2+ WT-1: - D2-40: 2+ Desmin: 2+ SMA: 3+	診断名:その他

図 6.　2017-010

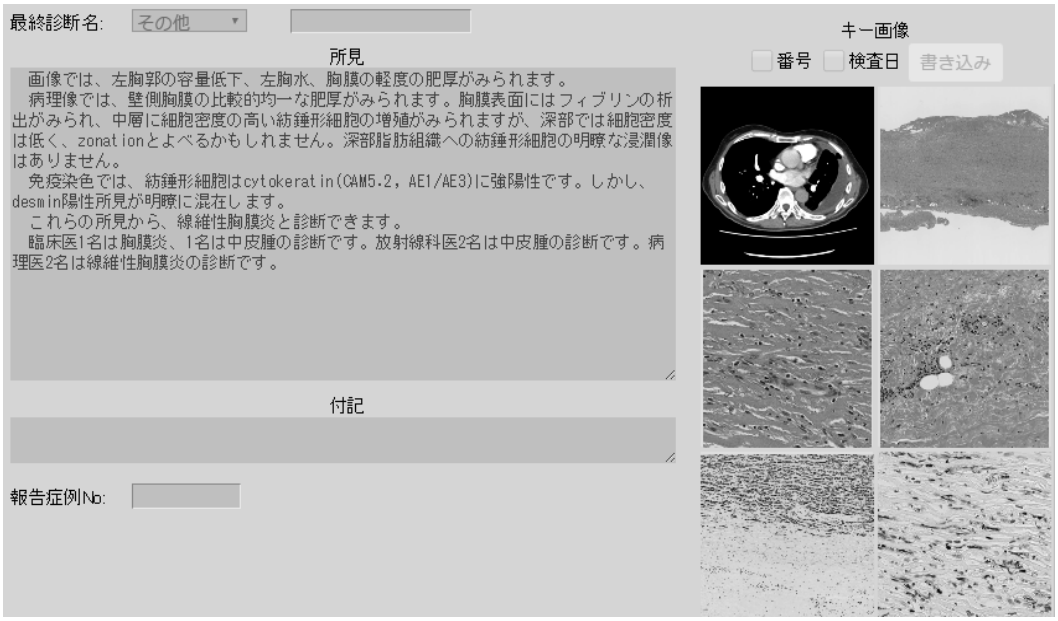

図 7.　2017-010

考察：

診断討議システムの構築にあたっては、いくつか問題となった点があった。

ひとつは、このシステムの中では、各医療機関から個人情報に相当する症例の年齢、性別、病変の部位などの診断に際して必要な基本的情報が、診断者に与えられていないことである。そこでクラウドシステムにあげる情報の中には含めないとしても、各診断者と診断のとりまとめ役との間の E-mail を用いて、必要最低限の情報を共有することで代用した。具体的には、以下のような内容を診断者に送付することとした。

1)　年齢：10 歳毎の年齢階層で表現

2)　性別：男女

3)　病変部位：胸膜、腹膜、心膜、精巣鞘膜など

この情報交換については、症例を提出する各医療機関における個人情報の秘匿を厳守することと、いかに整合性をはかるかについて検討した。患者の同意については、検査時、入院時あるいは手術時に患者からえられる包括的同意書の範囲内で許容される診断行為であること、このシステムの運用によって患者に特別な危険あるいは不利益は生じないことを前提に、このシステムにおいて情報管理を徹底することで対応できると考えた。本システムは、正しい診断をつけることで患者の利益をはかり、かつ石綿ばく露による健康被害者を把握するという公共の利益に資するところが大きいと判断される点も、最低限の個人情報が利用されることは許容できる根拠となると考えた。

次に、システム自体は、各診断者にとって扱いやすく、負担の少ないことを重視することが、実現したか、の点である。診断者が自施設において、ビューワーを用いて、放射線画像あるいは病理画像をみて診断意見を下していく際に、画像のダウンロードのスピードが早いことが求められる。各施設におけるインターネットの使用容量に差があることから改良することに限界はあるが、システム開発者の手によって、画像のダウンロードスピードや画像がスムーズに展開されるための工夫が加えられつつあり、より完成度の高いものになると考えられる。

このシステムは、研究分担者（井内）も加わって（株）エムネスが開発した医療支援クラウドサービス“LOOKREC” を診断会議用に改良したものである。“LOOKREC”を用いた遠隔画像及び病理診断については、アジア諸国において、医療の質の向上のために普及がはかられようとしている。ひとつは、2016 年 5 月に始ったカンボジアにおける“女性乳がん検診の導入”において、乳腺超音波画像の診断支援に用いられている。2017 年 4 月からは、モンゴルにおいてじん肺や石綿肺などの呼吸器疾患の早期診断のために導入される予定である。こうした利用はまず、各症例の診断を下す際の、日本の専門医の現地医師へのアドバイスを“LOOKREC”を用いて行うが、その上で今回開発した診断討議システムを使って、現地の医師との間でコミュニケーションをとり、彼らの診断能力の向上をはかることができると考える。

さらに、このシステムを用いた正しい診断を下された症例を蓄積することによって、一定地域あるいは国レベルでの症例登録が可能となり、貴重なデータベースの構築につながる。日本においても、環境再生保全機構によって“中皮腫登録”が行なわれているが、紙ベースであり、新しいシステムを用いることで、より効率的に登録を行い、再利用の利便性を高めることが求められる。また、労災保険制度のもとでの石綿ばく露関連疾患の診断については、全国各地の労働局単位で判定が行なわれているが、その精度に問題がないとはいえない。このシステムの導入によってより精度の高い診断作業と効率的な労災疾病の認定が行なわれていくことを期待したい。

中皮腫の症例において他疾患との鑑別が困難な症例の収集、的確な鑑別診断の方法に関する研究、及び胸水の症例において石綿によるものと他の原因によるものとの鑑別が困難な症例の収集、的確な鑑別診断の方法に関する研究

大槻　剛巳

１．研究分担者らのこれまでの研究について

研究分担者・大槻の所属する川崎医科大学衛生学では、従来繊維・粒子状物質の生体影響、なかでも免疫担当細胞に対する影響を観察してきた。繊維・粒子状物質としては、アスベスト繊維ならびに珪酸粒子を中心に研究を進めてきている。

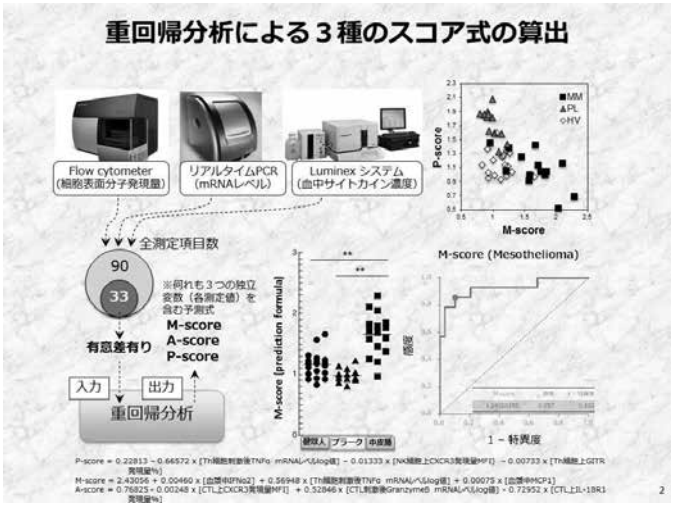

２．本研究班の中での検討項目

本研究班の中では、中皮腫の診断の中で特にハイリスクグループのポピュレーションの中でのスクリーニングに適した採血によるデバイスの開発を担当し、その応用として胸水症例などにも適応させることを目的としている。

昨年度までに凝固剤入の末梢血 20ml の採取により、血漿成分をルミネックス法による 29 種類のサイトカイン測定、血球成分についてはフローサイトメトリーを用いて大きさ（FSC）と内部構造（SSC）により単球、およびリンパ球からは CD4 陽性のヘルパーT 細胞、CD8 陽性の細胞傷害性 T 細胞、および CD56 陽性のナチュラルキラー（NK）細胞を分画し､それらの中で新鮮な状況での膜表面発現分子､および遺伝子発現の測定を行った。さらに、血球成分についてはソート後、PMA/イオノマイシンにて一晩刺激後の遺伝子発

現も合わせて検討し、これは免疫担当細胞としての潜在能力を示し、アスベストばく露や中皮腫担癌によって修飾させられている可能性があることによる測定である。

検体の群は健常人、胸膜プラーク症例（アスベストばく露有、担癌無)、悪性中皮腫症例（アスベストばく露・担癌ともに有）であった。

全測定項目 99 のうち 3 群の中で、なんらかの有意差が検出された 33 項目について、重回帰分析を実施し、それぞれの群のみを示唆する公式の検出（最重要な 3 つの独立変数を用いる）を試みた結果、M-score（中皮腫群を検出)、A-score（健常人群と他の 2 群＝アスベストばく露群を判別)、および P-score（胸膜プラーク群を他の 2 群と判別）という 3 つの予測式を構築することができていた。

ちなみに P-score と M-score でプロットすると 3 群は異なった領域に分布し、有用性が明らかになった。

またそれぞれのスコアの ROC 曲線は、感度・1-特異度ともに 0.9 前後となり、これも有用性を示唆する結果であった。

なお、カットオフ値で検討すると、ROC 曲線からも想定できるように、10&内外の偽陽性あるいは偽陰性が生じており、これは検体数を増やしていかなければならないところである。

カットオフ値で陰性／陽性を判定した時の
石綿曝露・悪性中皮腫・胸膜プラークの予測能

		Healthy	Plaque	Mesothelioma
A-score (for asbestos exposure) Cutoff value=1.5876022	A-	88.20%[a] (15/17)	**8.30%[b] (1/12)**	**16.70%[b] (2/12)**
	A+	11.80%[a] (2/17)	**91.70%[b] (11/12)**	**83.30%[b] (10/12)**
M-score (for mesothelioma) Cutoff value=1.2492035	M-	82.40%[a] (14/17)	100.00%[a] (12/12)	**8.30%[b] (1/12)**
	M+	17.60%[a] (3/17)	0.00%[a] (0/12)	**91.70%[b] (11/12)**
P-score (for plaque, no tumor) Cutoff value=1.4253498	P-	94.10%[a] (16/17)	**8.30%[b] (1/12)**	91.70%[a] (11/12)
	P+	5.90%[a] (1/17)	**91.70%[b] (11/12)**	8.30%[a] (1/12)
A-score M-score	others	94.10%[a] (16/17)	100.00%[a] (12/12)	**25.00%[b] (3/12)**
	A+,M+	5.90%[a] (1/17)	0.00%[a] (0/12)	**75.00%[b] (9/12)**

Each subscript character shows no statistical difference with $p<0.05$, analyzed by SPSS software with Z test.

19

３．平成 28 年度の試み

１）検体収集

上記の検討から、平成 27 年度には、石綿ばく露関連非腫瘍性疾患と悪性中皮腫との免疫学的差異の解析と、スコアの有効性の確認とその改良ということを目標として、びまん性胸膜肥厚（DP)、良性石綿胸水および悪性中皮腫症例の検体収集と測定を実施した。

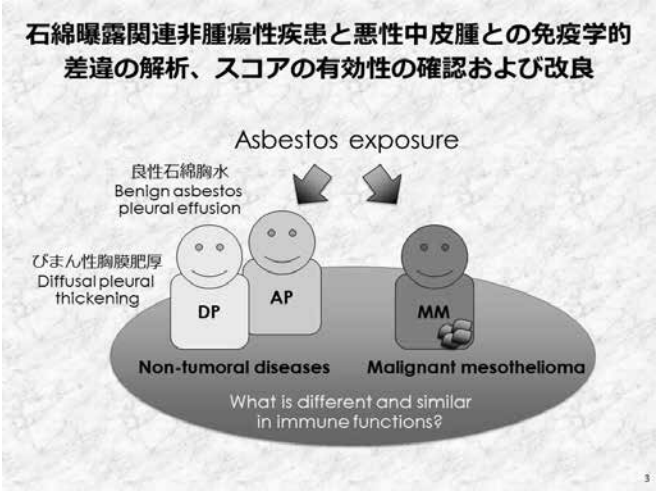

これまでの検討では、当日採血の上、輸送し解析に供与するまでが数時間以内のものを用いていたが、今回の班研究では、さらに将来的に全国的に有用なデバイスとするためには、一晩の輸送期間を寛容しなければならないため、今回は、その対応も検討することとした。

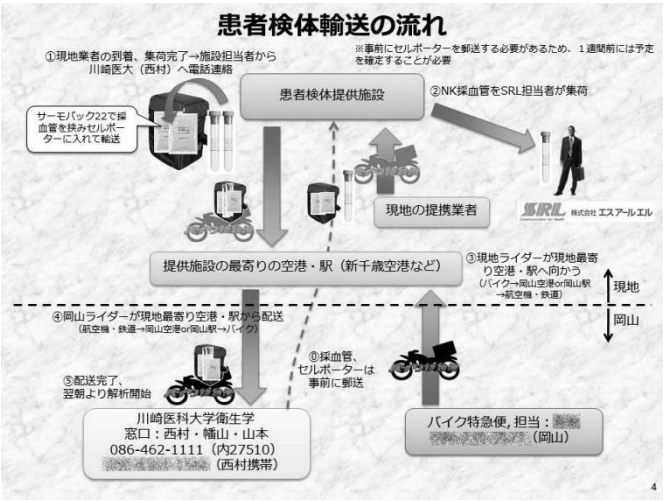

すなわち、患者提供施設での採血の後に、NK 活性については、株式会社エスアールエルへの検体の提供、またサーモパックにて川崎医科大学への輸送をするにあたって、セルポーターに入れた後に、提携するバイク便などで最寄りの空港あるいは JR 等の駅に移送し、その後、交通機関の便として取り扱った後に、岡山でのバイク便での回収と、川崎医科大学への移送というステップが必要になってくる。

また今後の調整のためにセルポーター内の温度記録装置「おんどとり」によって、そのモニターも実施することとした。

２）検体測定

測定については、上記のごとく、サイトカイン濃度の測定、各細胞集団上の細胞の表面分子発現量の測定、さらに各細胞集団をソート収集して新鮮な状態とともに、一晩、PMA/イオノマイシンで刺激した後の遺伝子発現を解析した。

３）症例一覧

現在の症例の一覧を示す。

現在までに、びまん性胸膜肥厚（DO）13 例、悪性中皮腫（MM）11 例の試料保存・一部解析を完了（※MM-9 の FACS データは状態が悪いため解析不可）した。

改めて膜表面マーカーの解析について、項目を図示する。

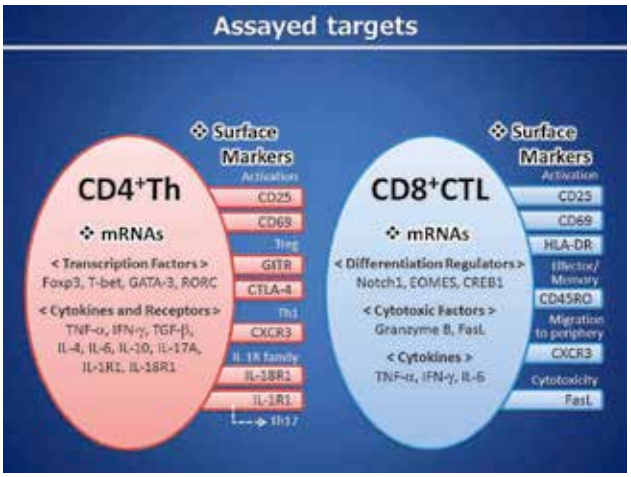

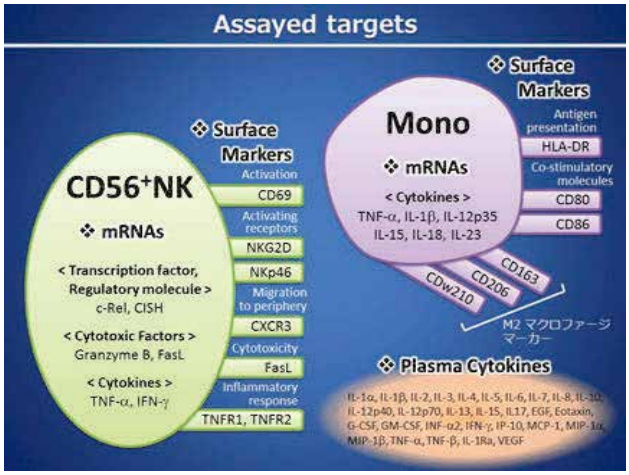

ならびに、上図の下段には、サイトカインについて表示する。

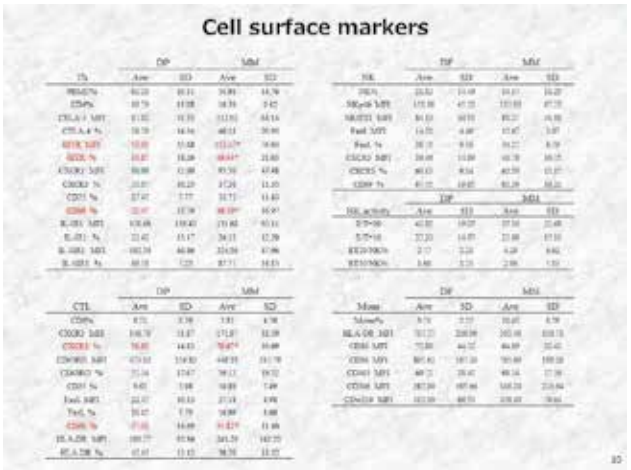

細胞表面マーカーについて、DP 群と MM 群で、有意な差が認められたものは、Th 細

胞群における GITR と CD69、CTL における CXCR3、および CD69 であった。NK 細胞あるいは単球（MONO）では、明らかな違いが認められたものはなかった。

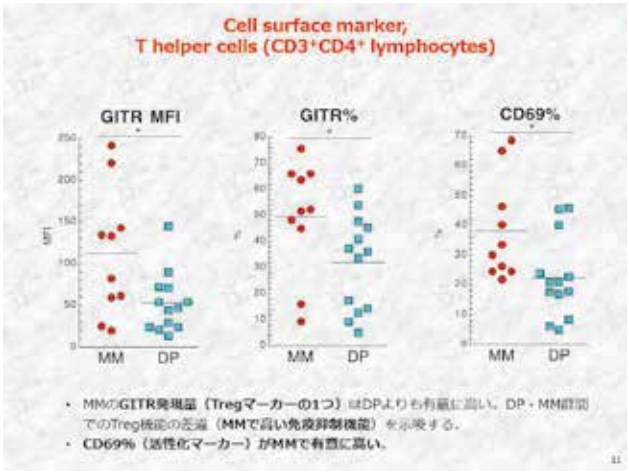

上図では、Th 細胞の GITR の平均蛍光強度あるいは陽性細胞数の率による差、ならびに CD69 の陽性細胞比率を示す。

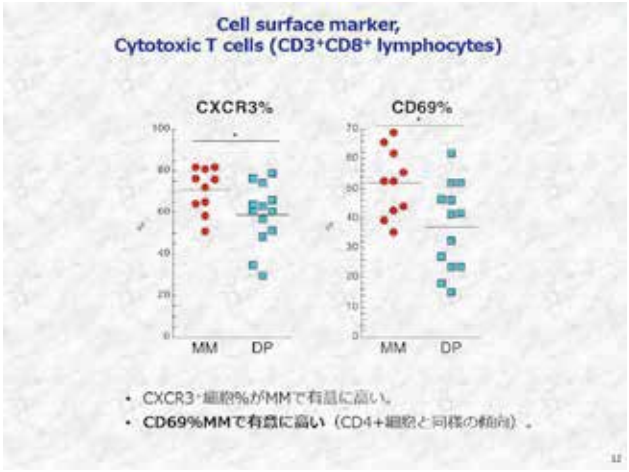

また次の図では、CTL 細胞の CXCR3 の陽性細胞数の率による差、ならびに CD69 の陽性細胞比率を示す。

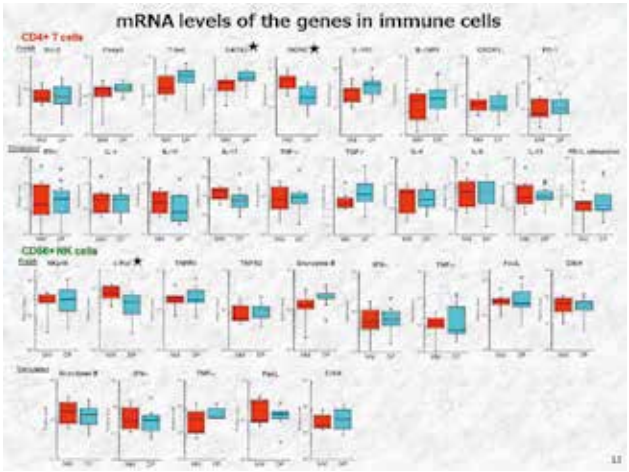

遺伝子発現については、検索した遺伝子群の DP 群と MM 群についての総括的な結果を上の図に示す。

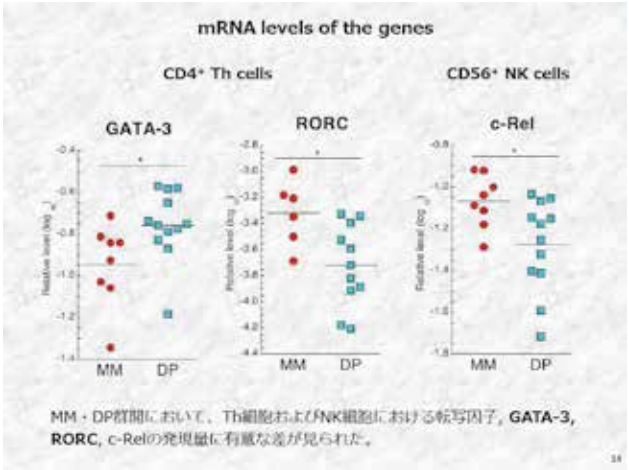

明らかな違いがあったのは CD4 陽性細胞における GATA3 および RORC、NK 細胞における c-Rel であった。

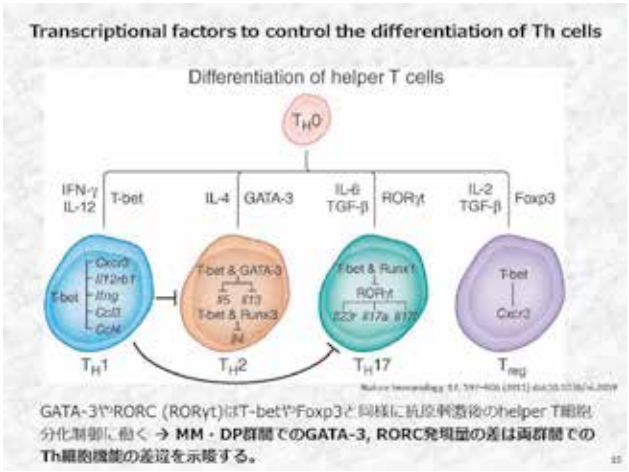

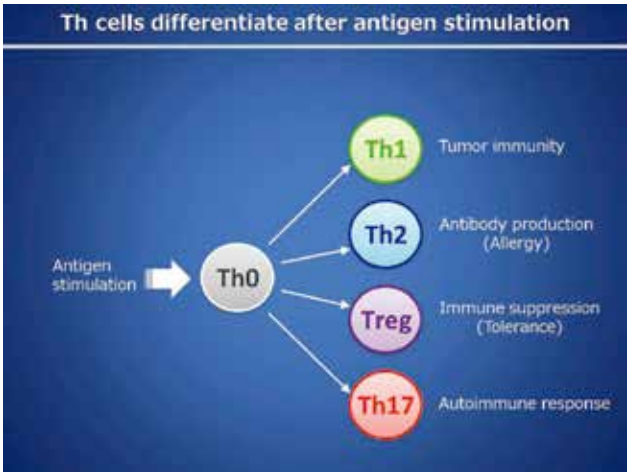

特に GATA3 や RORC については、CD4 陽性のヘルパーT 細胞における亜集団への分化に必須の転写因子でありアスベストばく露とともに、その病態形成に、亜集団への分化に関わる転写因子の発現の違いが生じていることが想定され、興味深い結果となった。

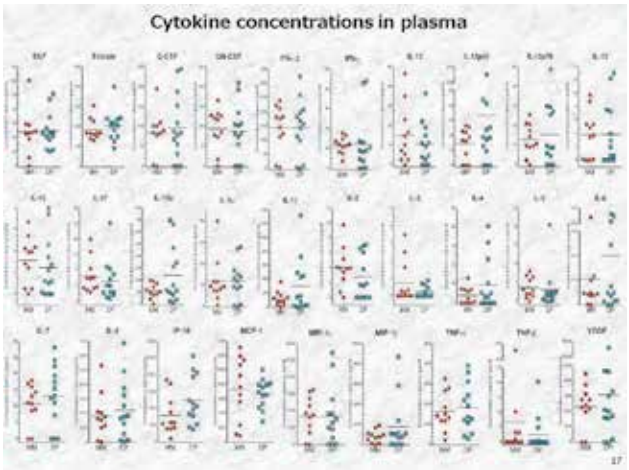

サイトカインについては、現状では明らかな差は認められなかった。
そこで、重回帰分析を用いて、DP 群と MM 群を判別する公式の構築を試みた。

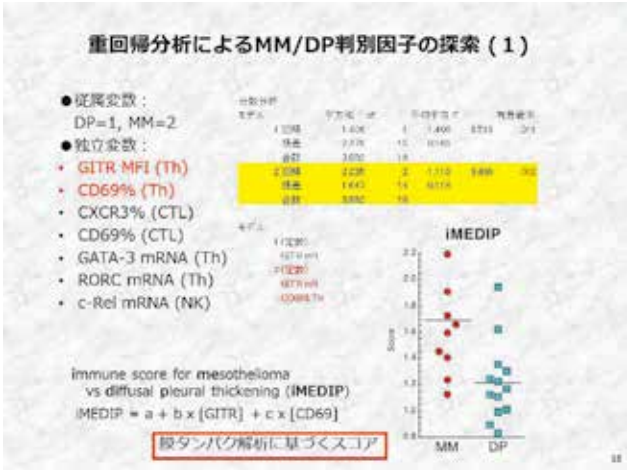

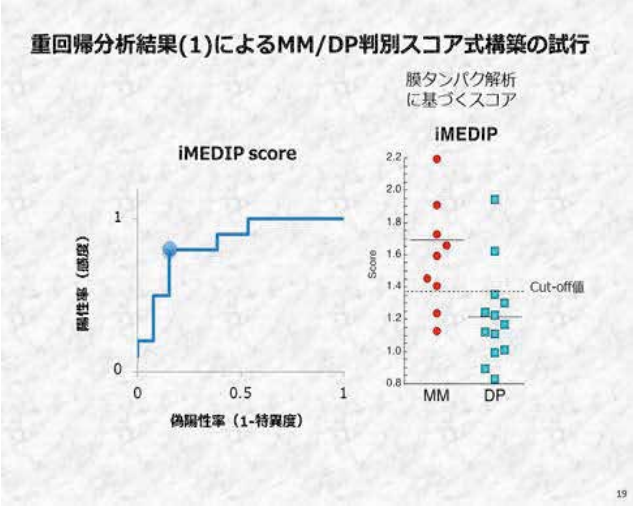

一つは、Th 細胞の GITR と CD69 の発現度による公式である。

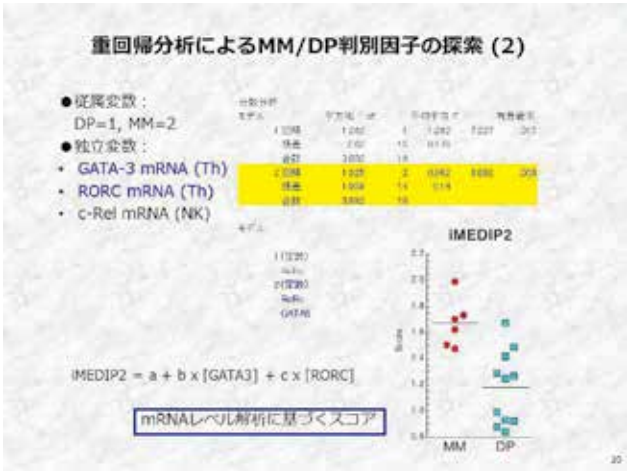

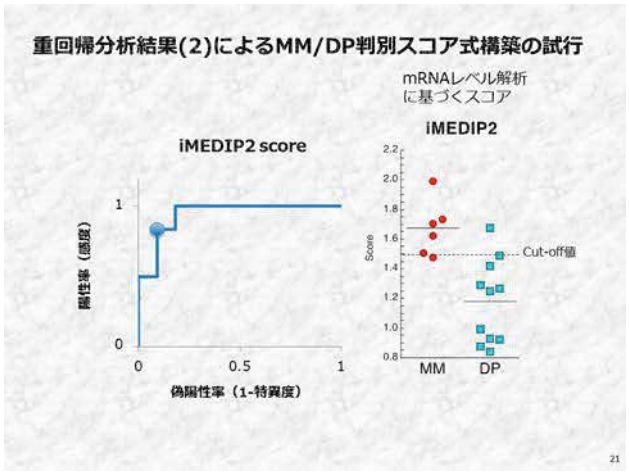

また他の一つは Th 細胞における GATA3 と RORC の遺伝子発現の度合いを用いたものである。

いずれも ROC 曲線では、まだ十分なところに至っていないものの、ある程度判別可能と考えられる。また今年度で、班研究は終了となるが、今後も症例を集積することで、明らかな違いを表出することが可能になると思われた。

まとめとして

- びまん性胸膜肥厚（DP）と悪性中皮腫（MM）の $CD4^+$T（Th）細胞において制御性 T 細胞マーカー値に差が見られ、MM における GITR 発現量は DP よりも有意に高かった。
- MM・DP 群間では $CD4^+$T（Th）細胞では GATA-3、RORC の、NK 細胞では c-Rel の mRNA レベルに差が見られた。
- GATA-3、RORC は Th 細胞分化のマスター遺伝子であり、MM および DP の疾患

背景における免疫動態との関連が示唆される。

- 有意差が見られた因子を独立変数とする重回帰分析を行い MM・DP 判別因子の探索およびスコア式の構築を試行し、膜タンパク発現量または mRNA レベル解析に基づく 2 式を導いた。
- 後者の独立変数は、上述のように helper T 細胞機能のマスター遺伝子であり、従って、算出される数式で免疫動態を測ることは免疫学的にも充分説明可能であり、非常に魅力的である。胸水貯留がみられる石綿ばく露歴患者などへのスクリーニングデバイスとしての応用の可能性が示唆される。

という内容が、平成 28 年度の検討結果となった。

こういった＜胸膜中皮腫の的確な診断方法に関する研究＞として、特に三カ年で DP と MM 群の鑑別に重要な免疫学的指標を同定していく努力を行ってきたが、それに加えて、この三カ年で、将来、このプロジェクトから発展する MM の診断に免疫学的に寄与貢献可能な論文の公表が可能であった。

① Ying C, Maeda M, Nishimura Y, Kumagai-Takei N, Hayashi H, Matsuzaki H, Lee S, Yoshitome K, Yamamoto S, Hatayama T, Otsuki T. Enhancement of regulatory T cell-like suppressive function in MT-2 by long-term and low-dose exposure to asbestos. Toxicology 338, 2015, 86–94

この論文では、アスベスト繊維に継続ばく露されたヒト T 細胞株において、当該細胞株が制御性 T 細胞の機能を有しており、その機能について、親株（即ち、アスベストばく露を受けていない株）と継続ばく露株（継続的に低濃度のアスベストにばく露され続けてきた亜株）での比較を行った所、継続ばく露亜株では制御性 T 細胞の機能が細胞間接着においても、また制御性 T 細胞としての代表的な可溶性作用分子である IL-10 や TGF-β の産生においても亢進しており、これは制御性 T 細胞機能の亢進すなわち抗腫瘍免疫の減衰に至っていると考えられる結果であった。

② Matsuzaki H, Lee S, Maeda M, Kumagai-Takei N, Nishimura Y, Otsuki T. FoxO1 Regulates Apoptosis Induced by Asbestos in the MT-2 Human T-Cell Line. J Immunotoxicol.2016; 13(5): 620-7 doi. 10.3109/1547691X.2016.1143539

本論文では､アスベスト継続ばく露亜株における転写因子 FoxO1 の発現減弱に着目し、こういった継続ばく露株ではアスベスト繊維による一過性ばく露の際に生じるアスベスト起因性アポトーシスに対して抵抗性を有するようになっているが、その要因として、以前に報告した IL-10 の過剰産生からオートクリンでの利用で STAT3 のリン酸化、そしてその下流にある Bcl-2 の過剰発現があることに加えて、FoxO1 によって制御されるいくつか

の好アポトーシス分子（Bim や Puma、あるいは Fas ligand）の発現が低値となっており、これらもアスベスト起因性のアポトーシスに抵抗性を有するようになることの要因であることが判明した。

③ Kumagai-Takei N, Nishimura Y, Matsuzaki H, Lee S, Yoshitome K, Hayashi H,Otsuki T. The suppressed induction of human mature cytotoxic T lymphocytes caused by asbestos is not due to Interleukin-2 insufficiency. J Immunol Res. vol. 2016, Article ID 7484872, 10 pages, 2016. doi:10.1155/2016/7484872

この論文では、CD8 陽性の細胞傷害性 T 細胞（CTL）に着目し、混合リンパ球培養法で CTL の分化増殖が、アスベスト繊維との混合培養では減弱扠せられることの以前の報告の際に（これは、アスベストばく露によって抗腫瘍免疫の減衰が生じることの別の照明でもあるが）、その回復をもたらす因子として IL-2 の存在が示唆されたことを検証するものであった。検証の結果、IL-2 の過剰添加によって検討して、若干の回復は細胞傷害性顆粒において認められるものの、十分ではないことが判明し、アスベストばく露免疫担当細胞による抗腫瘍免疫の減衰が、単独サイトカインでは回復しないこと、さらにこういった指標もまた、抽出されてきた DP と MM 群との差異の中で、CTL の CD69 や CXCR3 など、抗腫瘍免疫あるいは細胞の慢性活性化に関連する分子が表出されてきていることとの関連を示唆するものであった。

④ Lee S, Mastuzaki H, Maeda M, Yamamoto S, Kumagai-Takei N, Hatayama T, Ikeda M, Yoshitome K, Nishimura Y, Otsuki T. Accelerated cell cycle progression of human regulatory T cell-like cell line caused by continuous exposure to asbestos fibers. Int J Oncol 50: 66-74, 2016

本論文では、上記①の論文で、制御性 T 細胞機能の亢進を示したが、②で示した FoxO1 転写因子では、細胞周期に関連する遺伝子発現を FoxO1 が制御し、その減衰によって細胞周期を加速化する分子群の発現亢進、細胞周期を抑制する分子群の発現減弱がもたらされる可能性があることから、アスベスト長期ばく露株において、その検討を行った結果、予測通りにアスベスト継続ばく露株では細胞周期の加速化が増強されており、それは FoxO1 転写因子に制御されていることが判明した。この事は、アスベストにばく露された制御性 T 細胞では、機能の増強もさることながら、細胞周期の加速化に伴い数＝量としても増強がもたらされていることが判明した。

本研究班開始前の我々の検討に加えて、今回の三カ年で得られた結果も踏まえて、アスベスト繊維の免疫担当細胞へのばく露と抗腫瘍免疫の減衰についてまとめる図を文末に示す。

これらの検討は、川崎医科大学衛生学教室の教室員―准教授・西村泰光、助教・武井直

子、松﨑秀紀、李順姫および研究補助員、幡山圭代、山本祥子による検討の総和としての成果報告であり、報告書誌上ではあるが、改めて彼らの協力と多大な尽力に深謝の意を表するところである。

上記の原著論文も含めて、アスベスト関連の研究班活動期間内における総説論文やテキストのチャプターでの公表について以下に示す。

1) Maeda M, Chen Y, Hayashi H, Kumagai-Takei N, Matsuzaki H, Lee S, Nishimura Y, Otsuki T. Chronic exposure to asbestos enhances TGF-β1 production in the human adult T cell leukemia virus-immortalized T cell line MT-2. Int J Oncol 2014 Dec;45(6):2522-32. doi: 10.3892/ijo.2014.2682. Epub 2014 Sep 29.

2) Kumagai-Takei N, Nishimura Y, Maeda M, Hayashi H, Matsuzaki H, Lee S, Kishimoto T, Fukuoka K, Nakano T, Otsuki T. Functional properties of CD8+ lymphocytes in patients with pleural plaque and malignant mesothelioma. J Immunol Res Volume 2014 (2014), Article ID 670140, http://dx.doi.org/10.1155/2014/670140

3) Ying C, Maeda M, Nishimura Y, Kumagai-Takei N, Hayashi H, Matsuzaki H, Lee S, Yoshitome K, yamamoto S, Hatayama T, Otsuki T. Enhancement of regulatory T cell-like suppressive function in MT-2 by long-term and low-dose exposure to asbestos. Toxicology. 338, 2015, 86–94

4) Nishimura Y, Takahashi K, Mase A, Kotani M, Ami K, Maeda M, Shirahama T, Lee S, Matsuzaki H, Kumagai-Takei N, Yoshitome K, Otsuki T. Enhancement of NK Cell Cytotoxicity Induced by Long-Term Living in Negatively Charged-Particle Dominant Indoor Air-Conditions. PlosOne. Published: July 14, 2015DOI: 10.1371/journal.pone.0132373

5) Nishimura Y, Takahashi K, Masae A, Kotani M, Ami K, Maeda M, Shirahama T, Lee S, Matsuzaki H, Kumagai-Takei N, Yoshitome K, Otsuki T. Exposure to negaively-charged particle domitant air-conditions on human lymphocytes in vitro activates immunological responses. Immunobiology Immunobiology. Vol220, Issue 12, 1359–1368 2015 Jul 17. pii: S0171-2985(15)30025-5. doi: 10.1016/j.imbio.2015.07.006.

6) Maeda M, Yamamoto S, Hatayama T, Mastuzaki H, Lee S, Kumagai-Takei N, Yoshitome K, Nishimura Y, Kimura Ym Otsuki T. T Cell Alteration Caused by Exposure to Asbestos. In: Biological Effects of Fibrous and Particulate Substances, (Series Title: Current Topics in Environmental Health and

Preventive Medicine) (Otsuki T, Holian A, Yoshioka Y. eds), Springer Japan, Tokyo, pp195-210, 2015

7) Kumagai-Takei N, Nishimura Y, Matsuzaki H, Maeda M, Lee S, Yoshitome K, Otsuki T. Effects of Asbestos Fibers on Human Cytotoxic T Cells In: Biological Effects of Fibrous and Particulate Substances, (Series Title: Current Topics in Environmental Health and Preventive Medicine) (Otsuki T, Holian A, Yoshioka Y. eds), Springer Tokyo, pp211-221, 2015

8) Kumagai-Takei N, Nishimura Y, Matsuzaki H, Lee S, Yoshitome K, Otsuki T. The suppressed induction of human mature cytotoxic T lymphocytes caused by asbestos is not due to Interleukin-2 insufficiency. J Immunol Res. vol. 2016, Article ID 7484872, 10 pages, 2016. doi:10.1155/2016/7484872 ※

9) Matsuzaki H, Lee S, Maeda M, Kumagai-Takei N, Nishimura Y, Otsuki T. FoxO1 Regulates Apoptosis Induced by Asbestos in the MT-2 Human T-Cell Line. J Immunotoxicol.2016; 13(5):1-8 doi. 10.3109/1547691X.2016.1143539

10) Otsuki T, Matsuzaki H, Lee S, Kumagai-Takei N, Yamamoto S, Hatayama T, Yoshitome K, Nishimura Y. Environmental factors and human health: fibrous and particulate substance-induced immunological disorders and construction of a health-promoting living environment. Environ Heallth Prev Med 2016; 21(2), 71-81 DOI:10.1007/s12199-015-0499-6

11) Maki Y, Nishimura Y, Toyooka S, Soh J, Tsukuda K, Shien K, furukawa M, Muraoka T, Ueno T, Tanaka N, Yamamoto H, Asano H, Maeda M, Kumagai-Takei N, Lee S, Matsuzaki H, Otsuki T, Miyoshi S. The proliferative effects of asbestos-exposed peripheral blood mononuclear cells on mesothelial cells. Oncol Lett. 2016 May;11(5):3308-3316. Epub 2016 Apr 5

12) Kumagai-Takei N, Nishimura Y, Matsuzaki H, Lee S, Yoshitome K, Yamamoto S, Hatayama T, Maeda M, Otsuki T. Reduction of anti-tumor immunity caused by asbestos exposure. In. Asbestos: Risk Assessment, Health Implications and Impacts on the Environment. Edited by Dean L. Simmons. NOVA Scientific Publishers, INC. Hauppauge, NY, 2016, pp45-62.

13) Matsuzaki H, Lee S, Kumagai-Takei N, Yamamoto S, Hatayama T, Yoshitome K, Hayashi H, Maeda M, Nishimura Y, Otsuki T. Immunological risks caused by fibrous and particulate substances. In. Environmental Health Risks. (Marcelo Larramendy, Sonia Soloneski. Editors), ISBN 978-953-51-4706-0. InTech Publisher, Rijeka, Croatia, 2016 DOI: 10.5772/62749 Open Access

14) Nishimura Y, Kumagai-Takei N, Maeda M, Matsuzaki H, Lee S, Yamamoto S, Hatayama T, Yoshitome K, Otsuki T. Suppressive effects of asbestos exposure on

the human immune surveillance system. In: Allergy and Immunotoxicology in Occupational Health, (Series Title: Current Topics in Environmental Health and Preventive Medicine) (Otsuki T, Di Gioacchino M, Petrarca C. eds), Springer Japan, Tokyo. 2016. pp. 1-14.

15) Lee S,Hayashi H, Matsuzaki H, Kumagai-Takei N, Maeda M, Yoshitome K, Yamamoto S, Hatayama T, Nishimura Y, Otsuki T. Silica-induced immunotoxicity: chronic and aberrant activation of immune cells In: Allergy and Immunotoxicology in Occupational Health, (Series Title: Current Topics in Environmental Health and Preventive Medicine) (Otsuki T, Di Gioacchino M, Petrarca C. eds), Springer Japan, Tokyo. 2016. pp. 15-26.

16) Lee S, Mastuzaki H, Maeda M, Yamamoto S, Kumagai-Takei N, Hatayama T, Ikeda M, Yoshitome K, Nishimura Y, Otsuki T. Accelerated cell-cycle progression of human regulatory T cell-like cell line caused by continuous exposure to asbestos fibers. Int J Oncol 50: 66-74, 2017

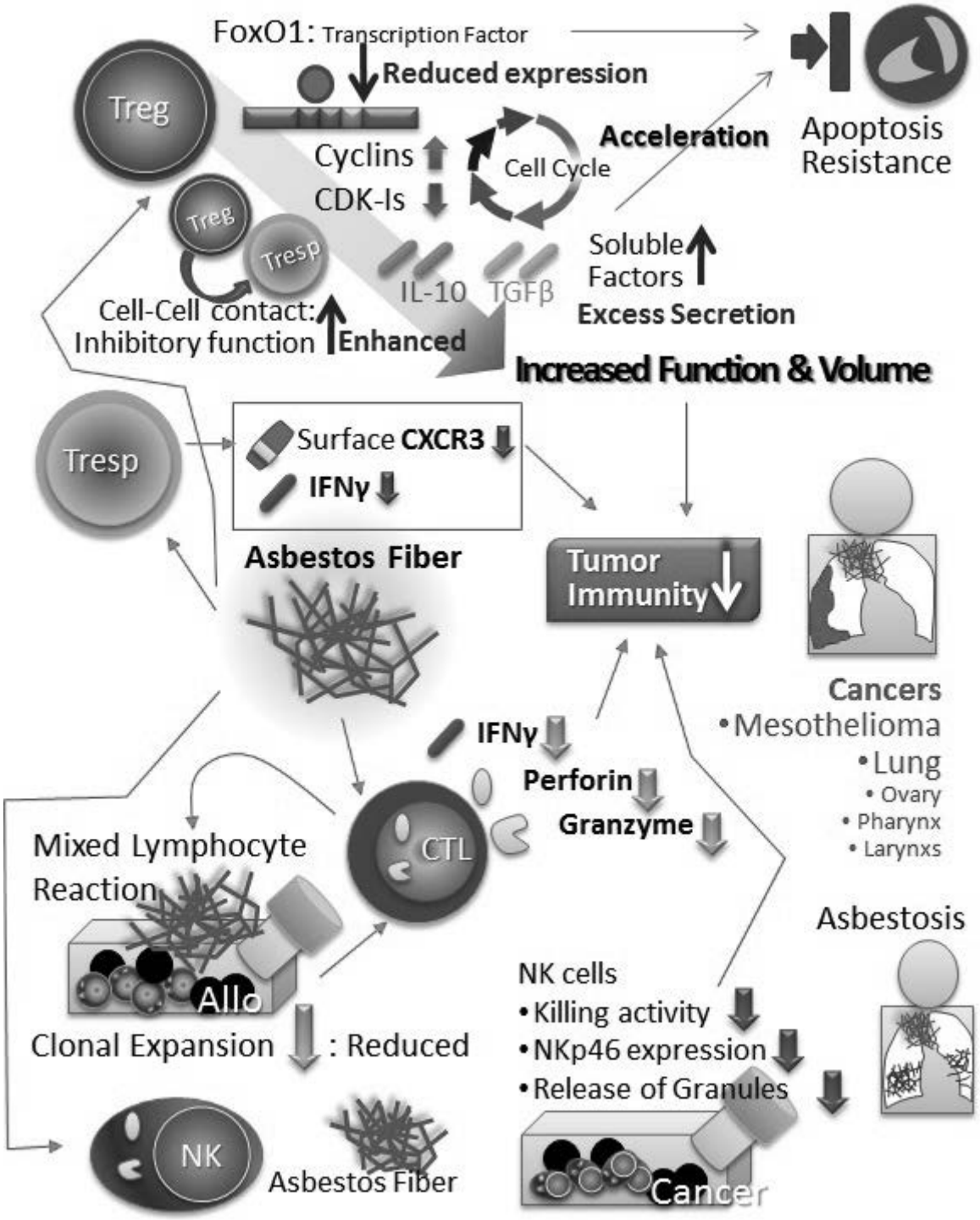
FoxO1: Transcription Factor
Reduced expression
Treg
Cyclins
CDK-Is
Cell Cycle
Acceleration
Apoptosis Resistance
Treg
Tresp
Soluble Factors
IL-10
TGFβ
Excess Secretion
Cell-Cell contact: Inhibitory function
Enhanced
Increased Function & Volume
Tresp
Surface CXCR3
IFNγ
Asbestos Fiber
Tumor Immunity
Cancers
• Mesothelioma
• Lung
• Ovary
• Pharynx
• Larynxs
IFNγ
Perforin
Granzyme
CTL
Mixed Lymphocyte Reaction
Allo
Clonal Expansion : Reduced
Asbestosis
NK cells
• Killing activity
• NKp46 expression
• Release of Granules
NK
Asbestos Fiber
Cancer

石綿健康管理手帳健診受診者を対象とした低線量 CT についての検討
-長期経過観察後の解析-

玄馬　顕一、加藤　勝也、芦澤　和人、由佐　俊和、岸本　卓巳

【 背　景 】

石綿取扱い等の業務に従事した労働者は、離職の際または離職の後に都道府県労働局長に申請し、審査を経た上で石綿に関する健康管理手帳の交付を受ける。そして、健康管理手帳が交付されると、指定された医療機関で年 2 回の健康診断を受けることが出来る。健康診断の項目は、一次健診が自他覚症状・既往歴の聴取と胸部 X 線撮影であり、医師が必要と認めた場合には二次健診として CT 等特殊な X 線撮影・喀痰細胞診・気管支鏡検査等を行うと定められている。一方、わが国における肺癌検診は胸部 X 線および喀痰細胞診で行われているが、低線量 CT を用いた肺癌検診を行うことでより早期で小型の肺癌が発見されるようになったと報告されている[1)-3)]。更に肺癌発症リスクの高い重喫煙者を対象としてアメリカで行われた低線量 CT 検診と胸部 X 線検診の無作為化比較試験である NLST（National Lung Screening Trial）では、CT 検診により肺癌死亡率を約 20%減少させることが報告された[4)]。肺癌の高危険群である石綿ばく露者に対する肺癌検診として、今後低線量 CT 検診を導入するか否についての検討が必要となっている。そこで、我々は平成 23～25 年度厚生労働科学研究として「石綿関連疾患の診断基準及び手法に関する調査研究」を行った。石綿健康管理手帳健診受診者を対象として低線量 CT を撮影し、胸膜プラークや CT 上の線維化所見等との関連性について検討したが、石綿ばく露者の中から高危険群を抽出することは出来なかった。しかし、CT 受診者の中から新たな肺癌症例が発見されていたことから、昨年長期経過観察後の検討を行った。その結果、背景肺にすりガラス状陰影、蜂窩肺、肺気腫・肺嚢胞が指摘された症例では有意に高頻度に肺癌が発症していた。しかし、低線量 CT を撮影した肺癌症例と通常の手帳健診のみを受診した肺癌症例との比較では、研究への登録を開始日とした生存期間には有意な差が認められなかった。最終の低線量 CT 撮影から 5 年間が経過したため、最終の解析を行った。

【 目　的 】

CT 検診を行うに当たって、放射線被ばくの問題および費用対効果の問題を避けて通れない。そこで、職業性石綿ばく露者の中から肺癌の高危険群を抽出し、今後 CT 検診を受診すべき症例群を明らかにすることが今回の検討の目的である。また、低線量 CT を受診した肺癌症例と通常の手帳健診のみを受診した肺癌症例を比較することにより、石綿ばく露者を対象とした CT 検診の有用性についての検討も行った。

【 対象と方法 】

対象は、岡山労災病院、富山労災病院、千葉労災病院、香川労災病院、北海道中央労災病院、玉野三井病院、近畿中央胸部疾患センター、山口宇部医療センターの 8 施設における石綿健康管理手帳健診受診者および石綿ばく露歴を有する現役労働者のうち低線量 CT 撮影に文書で同意した者である。

CT は、肺内の軽微な間質性を評価するために腹臥位で、被ばくを最小限とするために 30mAs 以下の線量で各施設の機器を用いて、年 1 回撮影した。画像データは 5mm 厚 5mm 間隔の肺野条件・縦隔条件、元データから再構成した 2mm 厚 5mm ギャップの thin-section CT であり、DICOM 形式で保存したデータを用いてモニター診断を行った。なお、読影は、5 名の放射線専門医のうち 2 名が独立して二重読影を行った。

CT 所見として、肺癌または中皮腫疑い以外に**図 1** に示したような間質性変化所見を中心に subpleural curvilinear shadow（SCLS）/ subpleural dots（DOTS）、すりガラス状陰影～小葉内網状影、牽引性気管支・細気管支拡張、蜂窩肺、parenchymal band、肺気腫・肺嚢胞、胸水、びまん性胸膜肥厚、円形無気肺、胸膜プラークおよびその石灰化の有無について記載した。

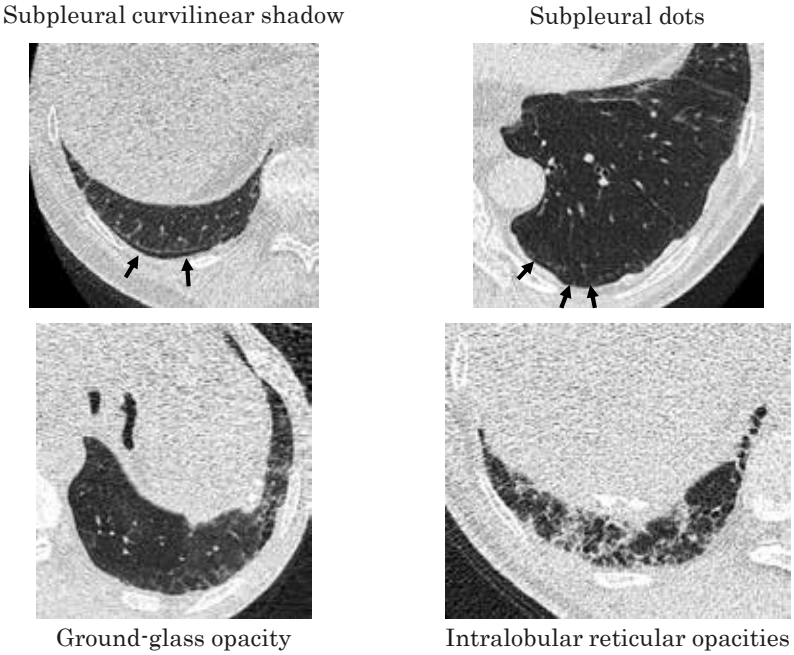

図 1. CT 上の間質性変化所見

なお、間質性変化については、**図 2** 左に示した領域（左右を 3 領域づつ計 6 領域に分割）毎に評価（病変が最も高度な撮像断面での病変の拡がりを 0～3 点に点数化）し、その合計を間質性変化スコア（IP スコア）とした。**図 2** 右に示した症例では、2+1+3+0+1+2=9 で

あり、IP スコア 9 点となる。また、胸膜プラークに関して、その範囲を最も高度な断面で評価し、**図 3** のように 0～4 点に点数化（plaque score）し、厚さについては 5mm 未満と 5mm 以上に分けて評価した。

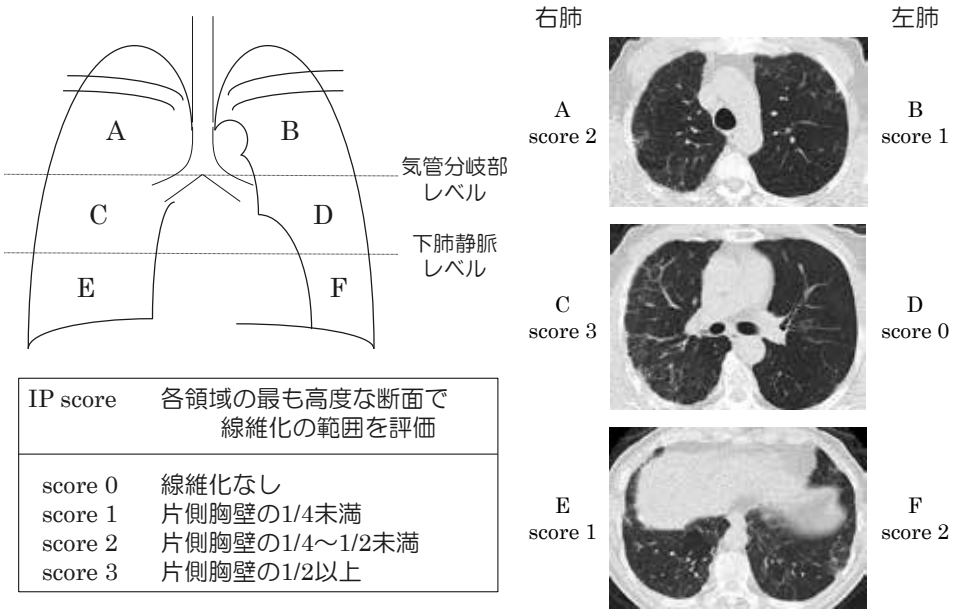

IP score	各領域の最も高度な断面で線維化の範囲を評価
score 0	線維化なし
score 1	片側胸壁の1/4未満
score 2	片側胸壁の1/4～1/2未満
score 3	片側胸壁の1/2以上

図 2. 間質性変化スコア（IP スコア）

Plaque Score	プラークが最も高度な断面で評価
Score 1	片側胸壁の1/4未満
Score 2	片側胸壁の1/4～1/2未満
Score 3	片側胸壁の1/2～3/4未満
Score 4	片側胸壁の3/4以上

Score 1　　Score 2　　Score 3

図 3. 胸膜プラークの拡がり（Plaque Score）

CT 受診者のうち、生検・切除標本等で組織診または細胞診で病理学的に原発性肺癌と確定診断された症例を肺癌群とし、それ以外の症例を対照群として初回 CT 受診時の年齢・性別・喫煙歴・石綿ばく露の作業歴・上記の CT 所見について比較検討した。なお、作業歴から石綿ばく露濃度を推測し下記の 3 群に分類した。石綿製品製造業、石綿吹付け、保温・断熱作業、解体作業のいずれかの作業歴を有していた症例を高濃度ばく露群、前述の作業歴を有していない症例のうち造船所内の作業、電気工事業、配管作業、発電所内の作業のいずれかの作業歴を有していた症例を中等度ばく露群とし、高濃度および中等度ばく露に該当する作業歴がない症例を低濃度ばく露群とした。

次に CT 受診者の肺癌症例（CT 群）と通常の石綿健康管理手帳健診のみを受診した肺癌症例（通常群）について、治療法・生存期間等の臨床的特徴について比較検討を行った。通常群は、岡山労災病院、富山労災病院、千葉労災病院、香川労災病院、玉野三井病院、山口宇部医療センター、福山医療センターの 7 施設での健康管理手帳健診の受診者のうち組織診または細胞診で病理学的に原発性肺癌と確定診断された症例である。なお、両群の生存期間は、リードタイムバイアスを避けるために本研究への登録日を起点として算出した。

【 結　果 】

平成 22 年から平成 24 年の間に低線量 CT を撮影した症例は 2,130 例であり、施設別の症例数は、岡山労災病院 501 例、千葉労災病院 392 例、玉野三井病院 370 例、近畿中央胸部疾患センター313 例、香川労災病院 214 例、富山労災病院 195 例、山口宇部医療センター96 例、北海道中央労災病院 49 例であった。

低線量 CT を撮影した 2,130 例のうち平成 28 年 12 月までに計 62 例（2.9%）が肺癌の診断が確定した。確定診断日が判明した 58 例について、**図 4** に初回の低線量 CT 撮影から肺癌の確定診断までの期間別の頻度について示した。CT 撮影から 1 年未満が 17 例(29.3%)と最も多く、1 年以上 2 年未満、2 年以上 3 年未満と減少しているが、初回 CT 撮影から 3 年以上経てから肺癌と確定診断された症例も 26 例（44.8%）存在した。

性別・年齢階層別の肺癌発症率を**表 1** に示した。男性では 2,048 人中 60 人（2.9%）に肺癌が発症しており、女性でも 82 人中 2 人（2.4%）に発症しており、男女間に差は認められなかった（p=0.796、χ^2 検定）。初回 CT 撮影時の年齢については、肺癌群では平均 72.0 歳と対照群 70.7 歳よりも有意に高齢であった（p=0.010、t 検定）。しかし、60 歳、65 歳、70 歳、75 歳を cut-off 値とした年齢階層別の肺癌発症率についての検討では、いずれの検討においても高齢者群に肺癌が高率に発症していたが、2 群間に有意な差は認められなかった。

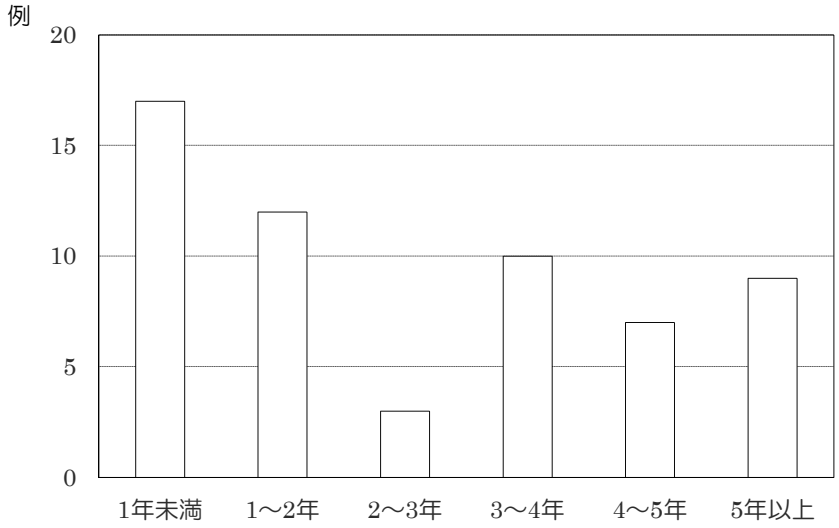

図 4. 初回低線量 CT 撮影から肺癌診断までの期間

表 1. CT 受診者 2130 例における性・年齢と肺癌発症率の関連性

		CT受診者	肺癌群(%)	対照群	p値
性別	男性	2048	60 (2.9%)	1988	0.796
	女性	82	2 (2.4%)	80	
年齢	60歳未満	73	1 (1.4%)	72	0.425
	60歳以上	2057	61 (3.0%)	1996	
	65歳未満	350	7 (2.0%)	343	0.268
	65歳以上	1780	55 (3.1%)	1725	
	70歳未満	959	21 (2.2%)	938	0.073
	70歳以上	1171	41 (3.5%)	1130	
	75歳未満	1545	41 (2.7%)	1504	0.251
	75歳以上	585	21 (3.6%)	564	

CT 受診者の喫煙歴と肺癌発症率の関連性についての検討を**表 2** に示した。現喫煙・既喫煙を合わせた喫煙歴ありの 1,651 例の中から 57 例（3.5%）に肺癌が発症しており、非喫煙者の 444 例中 5 例（1.1%）に比べて有意に高率に肺癌が発症していた（$p=0.010$、χ^2 検定）。また、喫煙指数についての検討でも、肺癌群は対照群に比べ有意に喫煙指数が高値であった（$p<0.001$、Mann-Whitney の U 検定）。次に喫煙指数 200、300、400、500、600、800 本・年をそれぞれ cut-off 値として肺癌発症率の検討を行った。いずれの検討において

も喫煙指数が高い症例の方が肺癌発症率は有意に高かった。喫煙歴のある CT 受診者のみを対象とした検討でも、**表 3** に示したように喫煙指数が高い群の方が肺癌発生率は高く、cut-off 値を 400、500、800 本・年とした解析では、χ^2 検定で 2 群間に有意な差が認められた（**表 3**）。

表 2. CT 受診者における喫煙歴と肺癌発症率との関連性

		CT受診者	肺癌群(%)	対照群	p値
喫煙歴	あり	1651	57 (3.5%)	1594	0.010
	なし	444	5 (1.1%)	439	
喫煙指数（本・年）	≦200	654	9 (1.4%)	645	0.004
	＞200	1309	49 (3.7%)	1260	
	≦300	767	12 (1.6%)	755	0.004
	＞300	1196	46 (3.8%)	1150	
	≦400	898	12 (1.3%)	886	<0.001
	＞400	1065	46 (4.3%)	1019	
	≦500	1014	16 (1.6%)	998	<0.001
	＞500	949	42 (4.4%)	907	
	≦600	1172	24 (2.0%)	1148	0.004
	＞600	791	34 (4.3%)	757	
	≦800	1484	33 (2.2%)	1451	0.001
	＞800	479	25 (5.2%)	454	

表 3. 喫煙歴のある CT 受診者における喫煙指数と肺癌発症率との関連性

		CT受診者	肺癌群(%)	対照群	p値
喫煙指数（本・年）	≦200	209	4 (1.9%)	205	0.181
	＞200	1309	49 (3.7%)	1260	
	≦300	322	7 (2.2%)	315	0.147
	＞300	1196	46 (3.8%)	1150	
	≦400	453	7 (1.5%)	446	0.007
	＞400	1065	46 (4.3%)	1019	
	≦500	569	11 (1.9%)	558	0.010
	＞500	949	42 (4.4%)	907	
	≦600	727	19 (2.6%)	708	0.074
	＞600	791	34 (4.3%)	757	
	≦800	1039	28 (2.7%)	1011	0.013
	＞800	479	25 (5.2%)	454	

CT 受診者 2,130 例の主な石綿ばく露歴について**図 5** に示した。造船所内の作業が 612 例（28.7%）と最も多く、化学製品製造業 260 例（12.2%）、石綿製品製造業 259 例（12.2%）、建設業 245 例（11.5%）の順であった。石綿ばく露期間についての検討したところ、肺癌群（平均ばく露年数 30.4 年）では、対照群（平均 28.5 年）と比較して有意に長期間に渡りばく露していた（p=0.014、t 検定）。また、**表 4** に示したようにばく露期間を 10 年毎に区分した検討では、ばく露歴 10 年以下の 293 例からは 3 例（1.0%）しか肺癌が発症していなかったのに対し、10 年を越えていた 1,662 例では 53 例（3.2%）と有意に高率に肺癌が発症していた（p=0.041、χ^2 検定）。「対象と方法」の項に記した方法で石綿ばく露濃度の推測を行った。高濃度ばく露・中等度ばく露・低濃度ばく露の 3 群に分類したところ、**表 4** に示したように低濃度・中等度・高濃度ばく露の各群における肺癌発症率はそれぞれ 1.9%、3.4%、2.8%であり、ばく露濃度と肺癌発生率との間に関連性は認められなかった。そこで、ばく露濃度とばく露期間の双方を反映する指標としてばく露指数を算出した。低濃度ばく露群に比べて中等度度ばく露群では 2 倍のばく露濃度があり、中等度ばく露群に比べて高濃度度ばく露群では 2 倍のばく露濃度があったと仮定した。すなわち、低濃度ばく露群ではばく露年数×1、中等度ばく露群ではばく露年数×2、高濃度ばく露群ではばく露年数×4 をばく露指数とした。ばく露指数と肺癌発症率との関連について検討したところ（**表 4**）、ばく露指数の cut-off 値を 10 および 40 とした場合、ばく露指数が高い症例では低い症例に比べて有意に高率に肺癌が発症していた（p=0.044、p=0.023、χ^2 検定）。

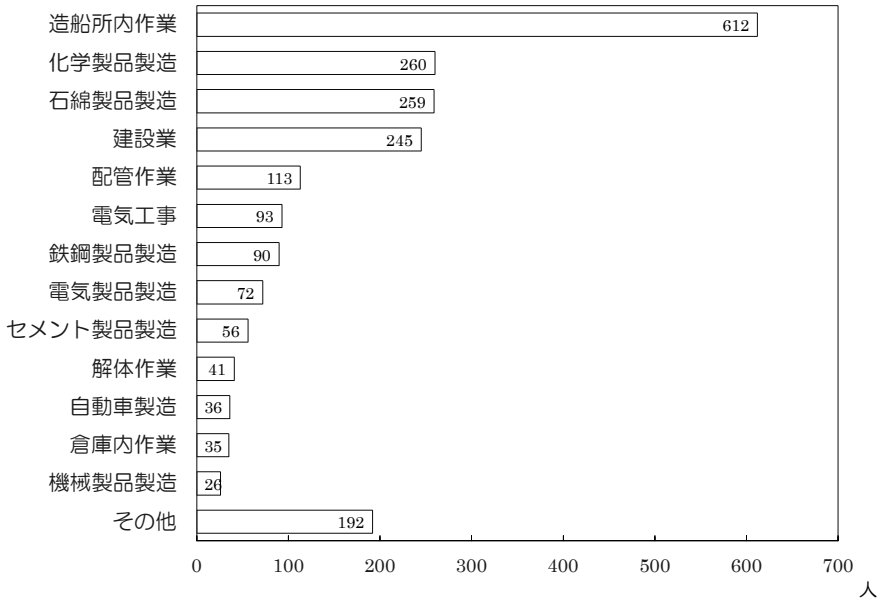

図 5. CT 受診者 2,130 例における主な石綿ばく露の作業歴

表 4. CT 受診者における石綿ばく露歴と肺癌発症率との関連性

		CT受診者	肺癌群(%)	対照群	p値
ばく露期間（年）	≦10	293	3 (1.0%)	290	0.041
	＞10	1662	53 (3.2%)	1609	
	≦20	623	13 (2.1%)	610	0.159
	＞20	1332	43 (3.2%)	1289	
	≦30	987	27 (2.7%)	960	0.730
	＞30	968	29 (3.0%)	939	
ばく露濃度	低濃度	317	6 (1.9%)	311	
	中等度	825	28 (3.4%)	797	
	高濃度	988	28 (2.8%)	960	
ばく露指数	≦10	188	1 (0.5%)	187	0.044
	＞10	1767	55 (3.1%)	1712	
	≦20	438	11 (2.5%)	427	0.615
	＞20	1517	45 (3.0%)	1472	
	≦40	921	18 (2.0%)	903	0.023
	＞40	1034	38 (3.7%)	996	

間質性変化を示す CT 所見の有無と肺癌発症率との関連性について検討した結果を**表 5** に示した。すりガラス状陰影～小葉内網状影が認められた 482 例では 23 例（4.8%）と同所見が認められなかった症例の 2.4%より有意に高率に肺癌が発症していた（p=0.006、χ^2 検定)。牽引性気管支・細気管支拡張症についても、所見が認められた症例では、認められなかった症例に比べ有意に高率の肺癌が発症しており（5.4% vs 2.7%、p=0.036)、蜂窩肺についても、所見が認められた症例からは 9.5%もの肺癌が発症しており、所見が認められなかった症例の 2.8%に比べて有意に高率であった（p=0.010、χ^2 検定)。一方、SCLS / DOTS については、所見が認められた症例の方が認められなかった症例よりも肺癌発症率が高かったもののその差は有意ではなかった。低線量 CT にて間質性変化である SCLS / DOTS、すりガラス状陰影～小葉内網状影、牽引性気管支・細気管支拡張、蜂窩肺の 4 所見のうち 1 つ以上の所見が認められた 565 例では 27 例（4.8%）に肺癌が発症しており、何れも認められなかった 1,565 例からの発症 35 例（2.2%）に比して、肺癌発症率が有意に高率であった（p=0.002、χ^2 検定)。

また、間質性変化の拡がりを示す IP score は、肺癌群では対照群に比べは有意に高値を示していた（p=0.001、Mann-Whitney の U 検定)。**表 6** に示したように 1.0 点、1.5 点、2.0 点、2.5 点、3.0 点、3.5 点を cut-off 値として IP スコアの高い群と低い群の肺癌発症率を比較したところ、いずれの検討 IP score が高い群の肺癌発症率は低い群に比較して有意に高かった（χ^2 検定)。

表 5. CT 上の間質性変化と肺癌発症率との関連性

		CT受診者	肺癌群(%)	対照群	p値
SCLS/DOTS	あり	297	13 (4.4%)	284	0.105
	なし	1833	49 (2.7%)	1784	
GGO	あり	482	23 (4.8%)	459	0.006
・小葉内網状影	なし	1648	39 (2.4%)	1609	
牽引性気管支	あり	186	10 (5.4%)	176	0.036
・細気管支拡張	なし	1944	52 (2.7%)	1892	
蜂窩肺	あり	42	4 (9.5%)	38	0.010
	なし	2088	58 (2.8%)	2030	
間質性変化	あり	565	27 (4.8%)	538	0.002
	なし	1565	35 (2.2%)	1530	

表 6. CT 上の間質性変化の拡がりと肺癌発症率との関連性

IP score	CT受診者	肺癌群(%)	対照群	p値
0～0.5	1565	35 (2.2%)	1530	0.002
1.0～	565	27 (4.8%)	538	
0～1.0	1602	36 (2.2%)	1566	0.002
1.5～	528	26 (4.9%)	502	
0～1.5	1628	38 (2.3%)	1590	0.004
2.0～	502	24 (4.8%)	478	
0～2.0	1845	42 (2.3%)	1803	<0.001
2.5～	285	20 (7.0%)	265	
0～2.5	1883	46 (2.4%)	1837	<0.001
3.0～	247	16 (6.5%)	231	
0～3.0	1951	51 (2.6%)	1900	0.007
3.5～	179	11 (6.1%)	168	

低線量 CT で指摘された胸膜プラーク所見と肺癌発症との関連性について**表 7** に示した。CT 受診者 2,130 例の大部分が健康管理手帳健診受診者であるため、1,904 例（89.4%）に胸膜プラークが認められた。胸膜プラークが認められた症例での肺癌発生率は 2.8%であり、認められなかった症例（4.0%）よりも低いという結果であった（p=0.311、χ^2 検定）。胸膜プラークが認められた 1,904 例におけるプラークの石灰化の有無についての検討でも、石

灰化を認めない胸膜プラークを有する症例の肺癌発症率は 3.2%であり、石灰化プラーク症例の 2.8%とほぼ同じであった（p=0.951、χ^2 検定）。また、5mm を cut-off としたプラークの厚みについての検討でも、5mm 以上の群と 5mm 未満の群の間に肺癌発症率に有意な差はなく（p=0.158、χ^2 検定）、プラークの範囲を点数化した plaque score についても、肺癌発生率に一定の傾向は認められず、肺癌群と対照群の plaque score には有意な差は認められなかった（p=0.696、Mann-Whitney の U 検定）。

表 7. CT 上の胸膜プラーク所見と肺癌発症率との関連性

		CT受診者	肺癌群(%)	対照群	p値
胸膜プラーク	あり	1904	53 (2.8%)	1851	0.311
	なし	226	9 (4.0%)	217	
石灰化プラーク	あり	1408	39 (2.8%)	1369	0.589
	なし	722	23 (3.2%)	699	
胸膜プラークの厚み	＜5mm	790	16 (2.0%)	773	0.158
	≧5mm	1114	36 (3.2%)	1078	
胸膜プラークの拡がり*	0.5～1	1187	29 (2.4%)	1158	
	1.5～2	537	20 (3.7%)	517	
	2.5～	180	4 (2.2%)	176	

*：Plaque Score

表 8 は、その他の CT 所見と肺癌発症率の関連性について示したものである。肺気腫・肺嚢胞所見が認められた 978 例の肺癌発症率は 4.0%であり、認められなかった 1,152 例の 2.0%よりも有意に高率であった（p=0.006、χ^2 検定）。また、肺気腫・肺嚢胞所見が認められた 978 例中 328 例（33.5%）に前述の間質性変化が認められ、肺気腫・肺嚢胞所見がない 1,152 例中の 237 例（20.6%）に比べると有意に高率であった（p<0.001、χ^2 検定）。そして、肺気腫・肺嚢胞所見および間質性変化の双方が認められた 328 例では 23 例（7.0%）もの肺癌が発症しており、それ以外の症例の 2.2%と比較して有意に高率であった（p<0.001、χ^2 検定）。

表 8. その他の CT 所見と肺癌発症率との関連性

		CT受診者	肺癌群(%)	対照群	p値
Parenchymal band	あり	287	7 (2.4%)	280	0.609
	なし	1843	55 (3.0%)	1788	
肺気腫・肺嚢胞	あり	978	39 (4.0%)	939	0.006
	なし	1152	23 (2.0%)	1129	
胸水	あり	44	6 (13.6%)	38	<0.001
	なし	2086	56 (2.7%)	2030	
びまん性胸膜肥厚	あり	292	7 (2.4%)	285	0.574
	なし	1838	55 (3.0%)	1783	
円形無気肺	あり	70	0 (0%)	70	0.141
	なし	2060	62 (3.0%)	1998	

胸水貯留が指摘された 44 例中 6 例（13.6%）に肺癌が発症しており、胸水なしの 2.7%よりも有意に高率であった（$p<0.001$、χ^2 検定）。胸水貯留が認められた 6 例の肺癌の組織型は 4 例が腺癌、2 例が扁平上皮癌であり、腺癌の 2 例では診断時に癌性胸膜炎を併発していた。腺癌 2 例と扁平上皮癌 1 例に対しては切除が行われていたことより、肺癌に起因しない胸水貯留と考えられるが、扁平上皮癌 1 例の胸水については詳細不明である。なお、parenchymal band、びまん性胸膜肥厚および円形無気肺の所見の有無と肺癌発症率の間には関連性は認められなかった。

現行の石綿健康管理手帳健診のみを受診した症例は、岡山労災病院 582 例、玉野三井病院 406 例、香川労災病院 324 例、富山労災病院 101 例、福山医療センター30 例、山口宇部医療センター20 例、千葉労災病院 15 例の計 1,478 例であった。38 例（2.6%）が原発性肺癌と確定診断されていた。**図 6** に肺癌発症率の経年的な推移を示した。平成 24 年度の報告書の際の検討では、CT 受診者では 1.8%に肺癌が発症していたのに対し、手帳健診のみの受診者からの肺癌発症は 0.5%に過ぎなかった。平成 25 年度、平成 27 年度と解析の度に両群の肺癌発症率の差は縮まり、今回の検討では CT 受診者での肺癌発症率は 2.91%、手帳健診のみの症例では 2.57%とほぼ同等となっていた。

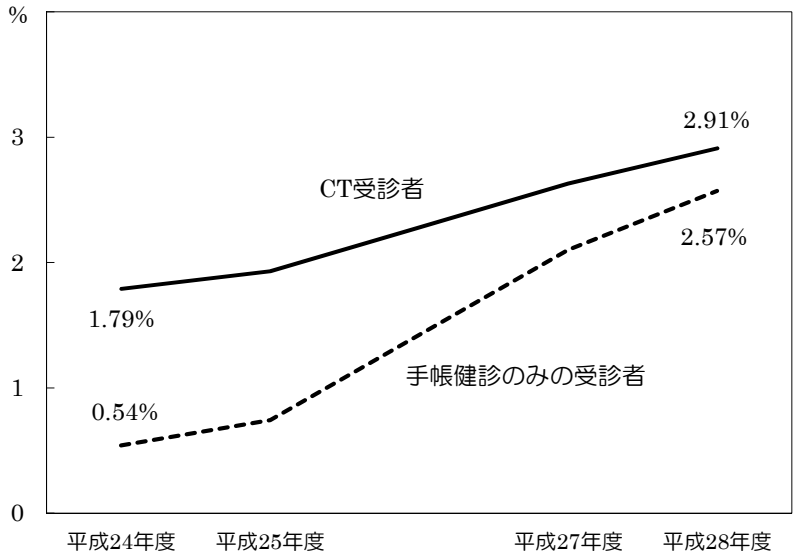

図 6. 肺癌発症率の推移　-CT 受診者と手帳健診のみの受診者の比較 -

CT 検診を受診していた肺癌症例 62 例を CT 群、現行の健康管理手帳健診のみを受診していた肺癌症例 38 例を通常群として、両群の比較検討を行った。**表 9** に示したように女性の肺癌症例は CT 群の 2 例のみであった。登録時の平均年齢は、CT 群 72.8 歳、通常群 71.8 歳であり、両群間に有意差は認められなかった（p=0.635、t 検定）。組織型は、両群ともに腺癌が最も多く、CT 群では 39 例（62.9%）と通常群の 19 例（50.0%）と両群間に有意差は認められなかった（p=0.204、χ^2 検定）。臨床病期が判明した症例の検討では、CT 群では 58 例中 35 例（60.3%）が I 期であり、通常群の 37 例中 19 例（51.4%）と比べ I 期の割合がやや多かったが、両群間に有意差は認められなかった（p=0.388、χ^2 検定）。治療として切除が行われた症例も、CT 群では 42 例（67.7%）と通常群では 20 例（52.6%）に比べて切除率が高かったが、有意な差は認められなかった（p=0.105、χ^2 検定）。

表 9. CT 群と通常群の比較

	CT群	通常群
受診者	2130	1478
肺癌症例	62 (2.9%)	38 (2.6%)
年齢中央値	72	74
（範囲）	51～87	61～86
性別：男性	60 (96.8%)	38 (100%)
女性	2 (3.2%)	0 (0%)
組織型：腺癌	39 (62.9%)	19 (50.0%)
扁平上皮癌	15 (24.2%)	12 (31.6%)
小細胞癌	7 (11.3%)	4 (10.5%)
その他	1 (1.6%)	3 (7.9%)
臨床病期：I 期	35 (60.3%)	19 (51.4%)
II～IV 期	23 (39.7%)	18 (48.6%)
不明	4	1
切除	42 (67.7%)	20 (52.6%)

両群の I 期腺癌症例について CT 画像の検討を行ったところ、CT 群では 24 例中 8 例がすりガラス型を呈していたが、通常群で同様の画像所見は 7 例中 1 例のみであった。

肺癌診断の発見動機について検討したところ、両群ともに検診発見が最も多かったが、CT 群では 56 例（90.3%）、通常群では 25 例（65.8%）との両群間に有意な差が認められた（p=0.016、χ^2 検定）。また、他疾患治療中に CT を撮影した際に発見された等の偶然発見された症例は、CT 群 3 例（4.8%）に対し、通常群では 6 例（15.8%）と有意に高頻度であった（p=0.045、χ^2 検定）。本研究への登録日を起点とした両群の生存期間を Kaplan-Meier 法で示した（**図 7**）。5 年生存率は、CT 群で 77.4%、通常群では 60.3%であり、CT 群では通常群に比べて有意な生存期間の延長が得られていた（p=0.028、Log Rank test）。また、両群の Hazard 比は 0.476（95%信頼区間 0.241～0.939、p=0.032）であり、低線量 CT を行うことにより肺癌による死亡を 52%低下させることが示唆された。

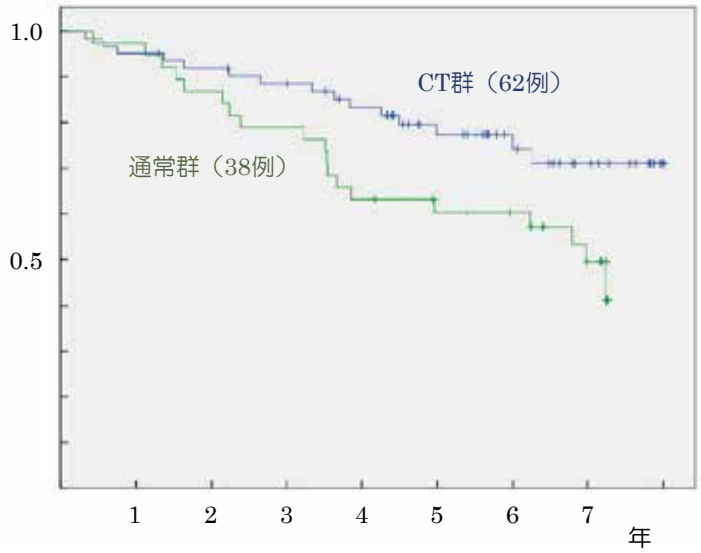

図 7. CT 群および通常群の生存曲線

【 考　察 】

石綿健康管理手帳健診受診者の中から肺癌の高危険群を抽出することを目的に 2,130 例の石綿ばく露者を対象とした低線量腹臥位 CT 撮影を行った。これまでの低線量 CT 検診では肺癌発見率が 0.3～0.85%と報告されていた[1)-3)]のに対し、CT 受診者の肺癌発症率は 2.9%と高率であった。また、通常の健康管理手帳健診のみを受診した症例からも 2.6%もの肺癌が発症していた。これらの結果から石綿健康管理手帳健診受診者全体が肺癌発症の高危険群であることが確認できたと考えられる。

石綿ばく露と肺癌発生との間には、ばく露量が多いほど肺癌発生頻度が高くなるとする量-反応関係が知られている。そこで、今回の対象者を石綿ばく露の作業歴からばく露濃度を高濃度・中濃度・低濃度ばく露群に分類して検討したが、ばく露濃度と肺癌発症率との関連は認められなかった。しかし、ばく露期間と肺癌発症についての検討では、10 年よりも長期間のばく露歴を有する症例では、10 年以下の症例よりも高率に肺癌が発症していた。この結果は、胸膜プラークが認められる症例では 10 年以上職業性石綿ばく露歴が確認されれば石綿肺癌として認定されるという労災の認定基準に合致していた。また、ばく露濃度と作業従事期間からばく露指数を算出してみたが、ばく露指数と肺癌発症の間にも有意な相関が認められた。

石綿ばく露者の中から重喫煙者を抽出すると 4.28%と高率に肺癌が発症すると報告されている[5)]。今回の検討でも、非喫煙者に比べ現喫煙・既喫煙者では有意に高率に肺癌を発症していた。更に喫煙者を喫煙指数で分割して検討してみたが、重喫煙者と軽喫煙者の肺癌発症率には有意な差が認められなかった。肺癌に対する高危険群を抽出するという観点から喫煙歴を有する症例に限定して低線量 CT 検診を行うという方法がある。しかし、石綿ばく露と喫煙は、互いに独立して肺癌死亡を相乗的に増加させること[6)]を考えると、石綿ばく

露者に対する低線量 CT 検診は非喫煙者をも対象に含めるべきであるとも考えられる。

今回の検討では、肺内特に下肺野背側の微細な線維化を検出するために腹臥位での撮影を行った。現在、胸部 X 線で 1 型以上の石綿肺を認めるのは極限られた症例のみである。しかし、CT でしか検出できないような微細な線維化を有する症例は存在し、しかも、線維化を有する症例では、線維化が認められない症例よりも石綿ばく露量が多いことを想定した。石綿ばく露と肺癌発生に量-反応関係が成り立つのであれば、CT で検出される間質性変化、特に石綿肺に比較的特異的な所見とされる SCLS / DOTS 等[6),7)]が認められる症例での肺癌発症率が高くなるという仮説の下に、CT 所見と肺癌発症率の関連性について検討した。胸膜プラークについては、CT 所見の有無・範囲・厚み・石灰化の有無と肺癌発症率との間にはいずれも有意な相関は認められなかった。しかし、すりガラス状陰影～小葉内網状影、牽引性気管支・細気管支拡張および蜂窩肺については、CT 所見を有する症例では所見が認められなかった症例に比べいずれも有意に高率に肺癌が発症しており、1 つ以上の間質性変化が認められた症例では 4.8%もの肺癌が発症していた。また、間質性変化の拡がりを示す IP score に関する検討でも、肺癌症例では肺癌を発症していない対照群と比較して有意に IP score が高値を示しており、IP score が高い群と低い群との比較でも、高い群では低い群に比べて肺癌発症率が有意に高率であった。胸部 X 線における線維化所見が認められる症例については肺癌のリスクが増加するとの報告があるものの[8),9)]、CT での線維化所見が肺癌発症の危険因子となるか否かという検討は報告されていない。今回の検討では、腹臥位 CT のみで指摘し得る軽微な間質性変化の存在と肺癌発症率の有意な関連性を示すことが出来たという点において有意義であったと考える。CT 上の間質性変化が石綿ばく露に起因するものか否かの検証は出来ていないが、IP score が高い群での肺癌発症率が高率であったことから、間質性変化と肺癌発症には正の相関が示唆される。従って、石綿ばく露者に対し低線量腹臥位 CT 撮影を行えば、微細な間質性変化が認められた症例を肺癌発症の高危険群として抽出することが出来る。

間質性変化所見以外にも肺気腫・肺嚢胞所見および胸水貯留が認められた症例において肺癌発症率が有意に高率であった。慢性閉塞性肺疾患患者の約 90%に喫煙歴がある[10)]ことからも解るように肺気腫・肺嚢胞所見には喫煙の関与が強く疑われる。今回の検討においても、肺気腫・肺嚢胞所見が認められ喫煙歴が確認できた 960 例のうち 89.8%が喫煙者であり、62.7%が喫煙指数 600 本・年以上の重喫煙者であった。従って、肺気腫・肺嚢胞の有所見における肺癌発症は、喫煙による肺癌と考えられる。また、CT にて胸水貯留が認められた症例でも有意に肺癌発症率が高かったが、胸水貯留が認められた症例は 44 例(2.1%)に過ぎず、危険群というより肺癌に伴う癌性胸膜炎の所見であった症例も含まれていた。従って、肺癌の高危険群を抽出するという観点からすると胸水貯留を選択条件とすることは不適切である。

石綿健康管理手帳健診受診者を対象として低線量 CT を撮影することにより高頻度に肺癌を発見することが出来ることを報告してきた。しかし、長期間の経過観察を行ったとこ

ろ、通常の石綿健康管理手帳健診のみの受診者からも多数の肺癌が発症してきた。手帳健診受診者という共通の母集団から抽出された症例であるため当然ではあるが、手帳健診受診者が肺癌の高危険群であることを示す結果であるといえる。

肺癌と確定診断された症例は、CT 群と通常群の比較では、CT 群の方が通常群よりも I 期症例が占める割合や肺癌切除率が高かったが、その差は有意なものではなかった。一方、CT 撮影によるリードタイムバイアスを除くために研究登録日を起点とした生存期間についての解析では、CT 群での有意な生存期間の延長が示された。2017 年 1 月に改訂された「肺癌取り扱い規約　第 8 版」では、画像診断指針として、原発巣を高分解能 CT の吸収値により、すりガラス型・部分充実型・充実型に分類することとなっている。TNM 分類においても、肺野型の場合、充実性成分 0 cm かつ病変全体径 3 cm 以下の T 因子を Tis とし、TisN0M0 を 0 期とされる。旧分類で I 期とされる症例の割合は両群間に差がなかったものの、I 期腺癌症例の中ですりガラス型を呈した症例は、通常群に比べ CT 群の方が多かった。この結果より、低線量 CT を撮影することで、より早期の肺癌を発見する出来るため、リードタイムバイアスを除外しても生存期間を延長できたものと考える。

石綿健康管理手帳健診における CT 検診の導入を考えた際に、高危険群である CT 上の間質性変化を有する症例はその対象となると考えられる。しかし、今回の検討において CT 受診者である肺癌 62 例のうち間質性変化の有所見者は 27 例（43.5%）に過ぎない。対象者の大多数（今回の検討では 77.5%）が喫煙歴を有すること、石綿ばく露と喫煙が肺癌発症において相乗効果を示すこと[8]を鑑みると、間質性変化の有無に関わらず石綿健康管理手帳受診者を生存期間延長に繋がる CT 検診の対象者とすべきであると考える。

【 結　語 】

石綿健康管理手帳健診受診者、特に喫煙歴を有する者は肺癌発症の高危険群と考えられるので、低線量 CT 検診の導入が望まれる。

参考文献

1) Sone S, et al. Mass screening for lung cancer with mobile spiral computed tomography scanner. Lancet.351:1242-1245,1998
2) Kaneko M, Eguchi K, Ohmatstu H,et al. Peripheral lung cancer: screening and detection with low-dose spiral CT versus radiography. Radiology 201: 798-802, 1996
3) Henschke CI, et al. Early Lung Cancer Action Project: overall design and findings from baseline screening. Lancet.354: 99-105,1999
4) The National Lung Screening Trial Research Team. Reduced lung-cancer mortality with low-dose computed tomographic screening. N Engl J Med 365: 395-409, 2011.
5) Das M, Muhlenbruch G, Mahnken AH, et al. Asbestos Surveillance Program Aachen

(ASPA): Initial results from baseline screening for lung cancer in asbestos-exposed high-risk individuals using low-dose multidetector-row CT. Eur Radiol. 17: 1193-1199, 2007.

6) Akira M, Yamamoto S, Inoue Y, Sakatani M. High-resolution CT of asbestosis and idiopathic pulmonary fibrosis. American Journal of Roentgenology. 181(1): 163-169, 2003

7) Akira M, Yokoyama K, Yamamoto S, et al. Early asbestosis: evaluation with high-resolution CT. Radiology. 178(2): 409-416, 1991

8) Hammond EC, Selikoff IJ, Seidman H. Asbestos exposure, cigarette smoking and death rates. Ann NY Acad Sci 330: 473-490, 1970.

9) Consensus Report. Asbestos, Asbestosis, and Cancer: the Helsinki Criteria for diagnosis and attribution, Scand J Work Environ Health. 23: 311-316, 1997.

10) Snider GL. Chronic obstructive pulmonary disease: risk factors, pathophysiology and pathogenesis. Annu Rev Med 40: 411-429, 1989

11) 国立がん研究センターがん対策情報センター. 地域がん登録全国推計によるがん罹患データ（1975年～2008年）http://ganjoho.jp/professional/statistics/statistics.html

12) 飯沼武. 検診における安全性の担保 ～原発事故から学ぶ放射線の安全性確保～. 日本がん検診・診断学会 19: 188-194, 2011

研究成果の刊行に関する一覧表

【雑　誌】

発表者氏名	論文タイトル名	発表誌名	巻号	ページ	出版年
Kuraoka M, Amatya VJ, Kushitani K, Mawas AS, Miyata Y, Okada M, Kishimoto T, Inai K, Nishisaka T, Sueda T, Takeshima Y.	Identification of DAB2 and Intelectin-1 as Novel Positive Immunohistochemical Markers of Epithelioid Mesothelioma by Transcriptome Microarray Analysis for its Differentiation From Pulmonary Adenocarcinoma.	Am J Surg Pathol.			in press
Amatya VJ, Kushitani K, Mawas AS, Miyata Y, Okada M, Kishimoto T, Inai K, Takeshima Y.	MUC4, a novel immunohistochemical marker identified by gene expression profiling, differentiates pleural sarcomatoid mesothelioma from lung sarcomatoid carcinoma.	Mod Pathol		1-10	2017
Matsuzaki H, Lee S, Maeda M, Kumagai-Takei N, Nishimura Y, Otsuki T.	FoxO1 Regulates Apoptosis Induced by Asbestos in the MT-2 Human T-Cell Line.	J Immunotoxicol	13(5)	620-627	2016
Kumagai-Takei N, Nishimura Y, Matsuzaki H, Lee S, Yoshitome K, Hayashi H,Otsuki T.	The suppressed induction of human mature cytotoxic T lymphocytes caused by asbestos is not due to Interleukin-2 insufficiency.	J Immunol Res.			2016

Lee S, Mastuzaki H, Maeda M, Yamamoto S, Kumagai-Takei N, Hatayama T, Ikeda M, Yoshitome K, Nishimura Y, Otsuki T.	Accelerated cell cycle progression of human regulatory T cell-like cell line caused by continuous exposure to asbestos fibers.	Int J Oncol	50	66-74	2016
Ying C, Maeda M, Nishimura Y, Kumagai-Takei N, Hayashi H, Matsuzaki H, Lee S, Yoshitome K, Yamamoto S, Hatayama T, Otsuki T.	Enhancement of regulatory T cell-like suppressive function in MT-2 by long-term and low-dose exposure to asbestos.	Toxicology	338	86–94	2015

研究成果の刊行物・別刷

Identification of DAB2 and Intelectin-1 as Novel Positive Immunohistochemical Markers of Epithelioid Mesothelioma by Transcriptome Microarray Analysis for its Differentiation From Pulmonary Adenocarcinoma

Masatsugu Kuraoka, MD,†‡ Vishwa J. Amatya, MBBS, PhD,* Kei Kushitani, MD, PhD,* Amany S. Mawas, MVSc,*§ Yoshihiro Miyata, MD, PhD,‖ Morihito Okada, MD, PhD,‖ Takumi Kishimoto, MD, PhD,¶ Kouki Inai, MD, PhD,*# Takashi Nishisaka, MD, PhD,† Taijiro Sueda, MD, PhD,‡ and Yukio Takeshima, MD, PhD**

Abstract: As there are currently no absolute immunohistochemical positive markers for the definite diagnosis of malignant epithelioid mesothelioma, the identification of additional "positive" markers that may facilitate this diagnosis becomes of clinical importance. Therefore, the aim of this study was to identify novel positive markers of malignant mesothelioma. Whole genome gene expression analysis was performed using RNA extracted from formalin-fixed paraffin-embedded tissue sections of epithelioid mesothelioma and pulmonary adenocarcinoma. Gene expression analysis revealed that disabled homolog 2 (DAB2) and Intelectin-1 had significantly higher expression in epithelioid mesothelioma compared with that in pulmonary adenocarcinoma. The increased mRNA expression of DAB2 and Intelectin-1 was validated by reverse transcriptase polymerase chain reaction of RNA from tumor tissue and protein expression was validated by Western blotting of 5 mesothelioma cell lines. The utility of DAB2 and Intelectin-1 in the differential diagnosis of epithelioid mesothelioma and pulmonary adenocarcinoma was examined by an immunohistochemical study of 75 cases of epithelioid mesothelioma and 67 cases of pulmonary adenocarcinoma. The positive rates of DAB2 and Intelectin-1 expression in epithelioid mesothelioma were 80.0% and 76.0%, respectively, and 3.0% and 0%, respectively, in pulmonary adenocarcinoma. Immunohistochemically, the sensitivity and specificity of DAB2 was 80% and 97% and those of Intelectin-1 were 76% and 100% for differentiation of epithelioid mesothelioma from pulmonary adenocarcinoma. In conclusion, DAB2 and Intelectin-1 are newly identified positive markers of mesothelioma and have potential to be included in future immunohistochemical marker panels for differentiation of epithelioid mesothelioma from pulmonary adenocarcinoma.

Key Words: DAB2, Intelectin-1, gene expression analysis, immunohistochemistry, epithelioid mesothelioma, pulmonary adenocarcinoma

(*Am J Surg Pathol* 2017;00:000–000)

Malignant mesothelioma is a rare and fatal malignant tumor.[1] In Japan, the mesothelioma death rate is increasing, approaching 1500 deaths in 2015, increased from 500 in 1995 according to Vital Statistics data published by the Ministry of Health, Labour and Welfare, Japan.[2] Similarly, the death rate due to mesothelioma is increasing globally, including the UK and Ireland,[3] the United States and other developing countries.[4] Asbestos exposure is the main risk factor for malignant pleural mesothelioma, including both occupational and environmental exposure. The time interval between first exposure to asbestos and diagnosis of mesothelioma is speculated to range from 20 to 50 years. Apart from the relatively long time it takes for asbestos to cause disease, delayed onset of symptoms can contribute to late-stage diagnosis and by then, the cancer spreads into the thoracic cavity and is more difficult to treat. Therefore, accurate diagnosis of mesothelioma is essential for its correct management.

A common site of origin of malignant mesothelioma is the pleura followed by other tissues including the peritoneum, pericardium, and tunica vaginalis. Malignant

From the Departments of *Pathology; ‡Surgery, Institute of Biomedical and Health Sciences; ‖Department of Surgical Oncology, Research Institute for Radiation Biology and Medicine, Hiroshima University; †Department of Clinical Research and Laboratory, Hiroshima Prefectural Hospital; #Pathologic Diagnostic Center Inc., Hiroshima, Japan; ¶Department of Internal Medicine, Okayama Rosai Hospital, Okayama, Japan; and §Department of Pathology and Clinical Pathology, South Valley University, Qena, Egypt.

Part of this study was performed at the Analysis Center of Life Science, Hiroshima University.

Conflicts of Interest and Source of Funding: T.K., K.I., and Y.T. has received grant from the Japanese Ministry of Health, Labour and Welfare Organization. The authors have disclosed that they have no significant relationships with, or financial interest in, any commercial companies pertaining to this article.

Correspondence: Yukio Takeshima, MD, PhD, Department of Pathology, Hiroshima University Institute of Biomedical and Health Sciences, Hiroshima University, 1-2-3 Kasumi, Minami-ku, Hiroshima 734-8551, Japan (e-mail: ykotake@hiroshima-u.ac.jp).

Supplemental Digital Content is available for this article. Direct URL citations appear in the printed text and are provided in the HTML and PDF versions of this article on the journal's Website, www.ajsp.com.

mesothelioma is classified into 3 major histologic subtypes: epithelioid, sarcomatoid, and biphasic as described in the 2015 World Health Organization (WHO) histologic classification of tumors of lung and pleura, 2015.[5] Epithelioid mesothelioma, which constitutes more than 60% of all mesothelioma, is the most common histologic subtype, and has a relatively better prognosis than sarcomatoid or biphasic mesothelioma. Epithelioid mesothelioma shows various histologic patterns including tubulopapillary, micropapillary, acinar, adenomatoid, and solid. As epithelioid mesothelioma closely resembles other malignant tumors showing pseudomesotheliomatous growth patterns, such as those of primarily lung carcinoma, breast carcinoma, and cancer that affects the lining of internal organs, the diagnosis of malignant mesothelioma is challenging, both histopathologically and clinically. Currently, the final diagnosis of malignant mesothelioma requires thorough reviewing of clinico-radiologic and pathologic findings (gross examination and histologic findings in tissue samples) with adequate immunohistochemical and/or genetic analyses. As an immunohistochemical marker with absolute sensitivity and specificity is not yet available, the search for additional novel immunohistochemical markers is critical.

The aim of this study was to identify novel positive immunohistochemical markers by analysis of whole gene expression data using microarray gene chips. We performed gene expression analysis on epithelioid cells dissected from formalin-fixed paraffin-embedded (FFPE) tissue of epithelioid mesothelioma and pulmonary adenocarcinoma and identified several novel genes that are differentially expressed between epithelioid mesothelioma and pulmonary adenocarcinoma. Of these, we identified disabled homolog 2 (DAB2) and Intelectin-1 as potential novel positive immunohistochemical markers of epithelioid mesothelioma for differentiation from pulmonary adenocarcinoma.

MATERIALS AND METHODS

Patients and Histologic Samples

The materials included in this study were obtained from the archives of the Department of Pathology, Hiroshima University. The study group consisted of 75 patients with epithelioid mesothelioma who had undergone thoracoscopic pleural biopsy, pleurectomy/decortication, extrapleural pneumonectomy, or autopsy between 2000 and 2016. Between 2005 and 2016, 67 pulmonary adenocarcinoma cases were also obtained by thoracoscopic surgical segmentectomy or lobectomy of lung harboring adenocarcinoma. All microscopic slides were reviewed and reclassified using the current WHO histologic classification of tumors of lung and pleura, 2015[6] by 4 pathologists (M.K., K.K., V.J.A., and Y.T.). Pathologic diagnosis of each case was confirmed by histologic findings and an immunohistochemical marker panel recommended by Guidelines for Pathologic Diagnosis of Malignant Mesothelioma: 2012 Update of the Consensus Statement from the International Mesothelioma Interest Group (IMIG)[7] and current 2015 WHO histologic classification of tumors of the lung, pleura, thymus, and heart.[6]

Anonymized tissue samples were provided by the Department of Pathology for gene expression and immunohistochemical analysis. This study was carried out in accordance with the Ethics Guidelines for Human Genome/Gene Research enacted by the Japanese Government for the collection of tissue specimens and was approved by the institutional ethics review committee (Hiroshima University E-974).

Gene Expression Analysis

Identification of Genes With Marked Difference Between Epithelioid Mesothelioma and Pulmonary Adenocarcinoma

FFPE sections from 6 epithelioid mesothelioma cases and 6 pulmonary adenocarcinoma cases were used for gene expression analysis. RNA extraction for gene expression analysis was performed from papillary or solid growth of tumor cells in each specimen. Five 10 μm thick FFPE tumor tissue sections, each approximately 1 cm in diameter, were processed for total RNA extraction using the Maxwell RSC RNA FFPE Kit (Promega KK, Tokyo, Japan) according to the manufacturer's protocol. Briefly, after deparaffinization and lysis with proteinase K, the samples were treated with DNase I for 15 minutes at room temperature. Following this, RNA purification was carried out according to the manufacturer's protocol using a Maxwell RSC automation instrument (Promega KK). RNA quality check and quantification was performed as described previously[8] and RNA with an absorbance ratio of ≥ 1.9 between 260 and 280 nm was used for microarray analysis. The Human Transcriptome 2.0 GeneChip Array (Affymetrix, Santa Clara, CA) containing gene transcript sets of 44,699 protein coding and 22,829 nonprotein coding clusters was used to analyze gene expression profiles. Total RNA was amplified and labeled with a 3′ IVT Labeling Kit (Affymetrix) before hybridization onto the GeneChip. Briefly, 100 ng total RNA was amplified with GeneChip 3′ IVT Pico kit (Affymetrix) to generate 30 μg of SenseRNA according to the manufacturer's protocol. SenseRNA (25 μg) was labeled with a 3′ IVT Labeling Kit (Affymetrix) and hybridized to a Human Transcriptome 2.0 GeneChip (Affymetrix) as described previously.[8] The data were analyzed using the Gene Expression Console Software (Affymetrix), and further statistical analyses were performed using the Subio Software Platform (Subio, Amami-shi, Japan) to plot graphs and for fold change of expression and hierarchical clustering.

Validation of Gene Expression Analysis

Real-time Reverse Transcriptase Polymerase Chain Reaction

The same 6 cases of epithelioid mesothelioma and pulmonary adenocarcinoma that were analyzed for gene expression profiling were used to validate the microarray

expression data by mRNA expression. The relative mRNA expression of DAB2 and Intelectin-1 was assessed with SYBR Green-based real-time reverse transcriptase polymerase chain reaction (RT-PCR) using GAPDH as a control. A total of 100 ng of RNA was used for mRNA expression with a VeryQuest SYBR Green 1-step RT-PCR Master Mix (Affymetrix) using a Stratagene Mx3000P qPCR System (Agilent Technologies, Santa Clara, CA). The primer pairs used for amplification of DAB2 and Intelectin-1 were DAB2-F: GTA GAA ACA AGT GCA ACC AAT GG, DAB2-R: GCC TTT GAA CCT TGC TAA GAG A, ITLN1-F: ACG TGC CCA ATA AGT CCC C, ITLN1-R: CCG TTG TCA GTC CAA CAC TTT C. Primers for GAPDH were GAPDH-F: ACA ACT TTG GTA TCG TGG AAG G, GAPDH-R: GCC ATC ACG CCA CAG TTT C. Data analysis was performed using the δδCT method for relative quantification. Briefly, threshold cycles (CT) for GAPDH (control) and DAB2 and Intelectin-1 (samples) were determined in triplicate. The relative expression (r_I) was calculated using the formula: $r_I = 2^{-(\text{CT sample} - \text{CT normal})}$.

Western Blotting

Total proteins were extracted from 5 commercially available mesothelioma cell lines (ACC-MESO-1, CRL-5915, ACC-MESO-4, CRL-5946, HMMME) using cell lysis protein extraction reagent (Cell-LyEX1 kit, TOYO B-Net, Tokyo, Japan). Approximately 25 μg of protein was subjected to electrophoresis on a Novex 10% Bis-Tris gel using a Bolt mini gel tank (Thermo Fisher Scientific, Yokohama, Japan). The proteins were then transferred to a Hybond-P PVDF membrane (GE Healthcare, Buckinghamshire, UK) using a Mini Blot Module (Thermo Fisher Scientific). After treating with blocking buffer, the transfer membrane was incubated with anti-DAB2 antibody (1:2000 rabbit polyclonal, catalog #HPA028888; Sigma-Aldrich, St. Louis, MO), anti-Human Intelectin-1 (1:2000, mouse monoclonal 3G9; Immuno-Biological Laboratories, Gunma, Japan) overnight at 4°C. This was followed by streptavidin-labeled anti-mouse or anti-rabbit secondary antibodies (Cell Signaling Technology, Tokyo, Japan) and Immunostar LD (Wako Pure Chemicals, Tokyo, Japan) as a chemiluminescent detection reagent. Anti-GAPDH antibody (rabbit polyclonal, Santa Cruz Biotechnology, CA) was used as control. The blot membrane was captured by scanning with C-DiGit Blot Scanner (LI-COR) for detection of proteins of interest.

Immunohistochemical Procedures and Evaluation of Expression of DAB2 and Intelectin-1

Immunohistochemistry was performed using 3 μm tissue sections prepared from the best representative FFPE blocks of epithelioid mesothelioma and pulmonary adenocarcinoma cases. Immunohistochemical staining was performed using the Ventana Benchmark GX automated immunohistochemical station (Roche Diagnostics, Tokyo, Japan). Cell Condition buffer #1 at 95°C for 32 minutes (Roche Diagnostics) was used for antigen retrieval. The sections were then incubated with primary antibodies to calretinin (rabbit monoclonal, SP65, prediluted; Roche Diagnostics), podoplanin (mouse monoclonal, D2-40, Prediluted; Nichirei Bioscience, Tokyo, Japan), Wilms' tumor gene product (WT1) (mouse monoclonal, 6F-H12, 1:25; Dako, Glostrup, Denmark), DAB2 (rabbit polyclonal, catalog #HPA028888, 1:200; Sigma-Aldrich), and Intelectin-1 (mouse monoclonal, 3G9, 1:1000; Immuno-Biological Laboratories). Incubation with the secondary antibody and detection was performed with Ventana ultraView Universal DAB Detection Kit.

Immunoreactivity was scored as either negative (no immunostaining) or positive. Cells showing nuclear staining for calretinin and WT1, cytoplasmic staining for DAB2 and Intelectin-1, or membranous staining for podoplanin (clone: D2-40) were recorded as "positive." Positive immunoreactivity was further scored as 1+ for up to 10% of tumor cells showing positive immunostaining, 2+ for 10% to 50% positive tumor cells, and 3+ for >50% positive tumor cells. Statistical analyses were performed using the Fisher exact test. Sensitivity, specificity, positive predictive value, negative predictive value, and accuracy rate were calculated using a simple 2 × 2 table.

RESULTS

Differential Gene Expression and Validation in Epithelioid Mesothelioma and Pulmonary Adenocarcinoma

Of the 44,699 protein coding and 22,829 nonprotein coding transcripts on the Human Transcriptome 2.0 GeneChip Array, 902 statistically significant mRNA transcripts were differentially expressed, with a greater than 1.3-fold difference, between epithelioid mesothelioma and pulmonary adenocarcinoma (Fig. 1). Hierarchical clustering of 426 protein coding mRNA transcripts revealed 197 upregulated mRNA transcripts in epithelioid mesothelioma, including CALB2, WT1, DAB2, and Intelectin-1, and 229 upregulated mRNA transcripts in pulmonary adenocarcinoma, including CEACAM6 and NAPSA (Fig. 2; Supplementary Table S1, Supplemental Digital Content 1, http://links.lww.com/PAS/A504).

Real-time RT-PCR showed relative mRNA expression of DAB2 and Intelectin-1 was significantly higher in epithelioid mesothelioma than that in pulmonary adenocarcinoma (data not shown). Western blot analysis showed DAB2 and Intelectin-1 protein expression in all 5 commercially available mesothelioma cells lines with an electrophoretic band of 80 kDa with DAB2 and 1 or 2 electrophoretic bands in the range of 30 to 40 kDa with the Intelectin-1 antibody (Fig. 3).

Immunohistochemical Expression Profiles in Epithelioid Mesothelioma and Pulmonary Adenocarcinoma

The expression of positive mesothelioma markers are summarized in Table 1 and the representative images for DAB2 and Intelectin-1 expression in epithelioid mesothelioma and pulmonary adenocarcinoma are pre-

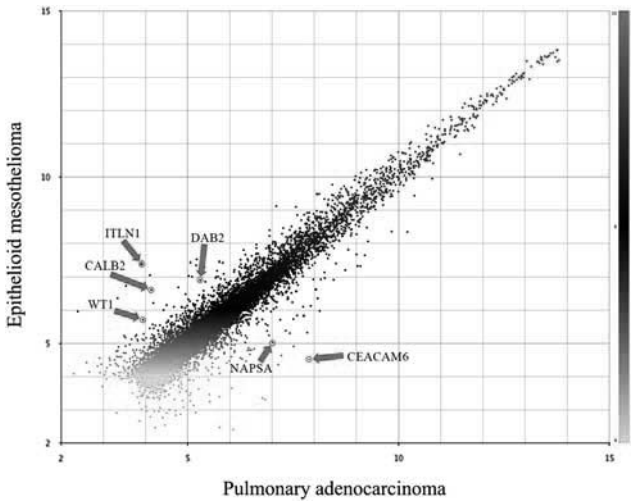

FIGURE 1. Scatter plot diagram showing differential expression of various genes between epithelioid mesothelioma and pulmonary adenocarcinoma. Note, DAB2 and Intelectin-1 locate toward the epithelioid mesothelioma, in addition to previously known mesothelioma positive markers, CALB2 (calretinin) and WT1, while NAPSA (Napsin-A) and CEACAM6 (major gene for CEA), positive pulmonary adenocarcinoma markers, locate towards pulmonary adenocarcinoma.

sented in Figures 4 and 5, respectively. The staining pattern for each marker in 2 tumor types is described in the following sections.

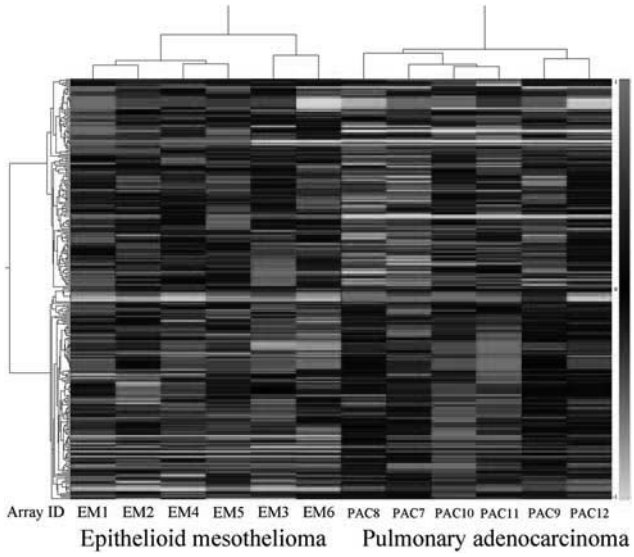

FIGURE 2. Supervised hierarchical clustering of differentially expressed genes between epithelioid mesothelioma and pulmonary adenocarcinoma. The hierarchical clustering of 426 protein coding mRNA transcripts revealed 197 upregulated mRNA transcripts in epithelioid mesothelioma and 229 upregulated mRNA transcripts in pulmonary adenocarcinoma. See detailed data in Supplementary Table S1 (Supplemental Digital Content 1, http://links.lww.com/PAS/A504).

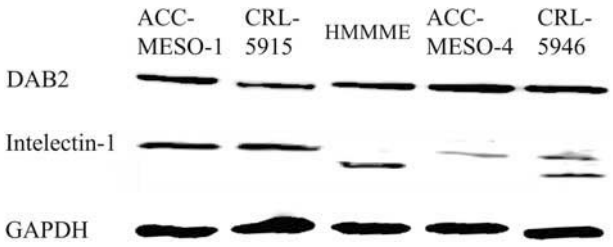

FIGURE 3. Western blot showing DAB2 and Intelectin-1 expression in mesothelioma cell lines. DAB2 expression is present in all 5 mesothelioma cell lines as a single band; however, Intelectin-1 expression is present as either a single or double band.

DAB2 and Intelectin-1 Expression

The expression of DAB2 and Intelectin-1 was localized in the cytoplasm of tumor cells in epithelioid mesothelioma cases. Positive DAB2 expression was observed in 60 of 75 epithelioid mesotheliomas (80.0%) and 2 of 67 pulmonary adenocarcinomas (3.0%). In half of epithelioid mesotheliomas, DAB2 immunoreactivity was generally strong and diffuse (score 3+). In contrast, pulmonary adenocarcinomas showing DAB2 expression was focal (score 1+). In addition, DAB2 expression in alveolar macrophages in pulmonary adenocarcinomas was a helpful internal positive control. Positive Intelectin-1 expression was observed in 57 of 75 epithelioid mesotheliomas (76.0%), with most of them showing score 3+, whereas none of the 67 pulmonary adenocarcinomas were positive for Intelectin-1.

Calretinin, D2-40, and WT1 Expression

Positive calretinin expression was recorded for 74 of 75 epithelioid mesotheliomas (98.7%) and 17 of 67 pulmonary adenocarcinomas (25.4%). In epithelioid mesotheliomas, immunoreactivity was generally strong and diffuse (score 3+). In contrast, staining score in pulmonary adenocarcinomas was 1+ and 2+. There were no score 3+ cases in pulmonary adenocarcinomas. Positive D2-40 expression was observed in 71 of 75 epithelioid mesotheliomas (94.7%), with most of them showing score 3+, whereas only 7 pulmonary adenocarcinomas (10.4%) were focally positive (score 1+ and 2+) for D2-40. Positive WT1 expression was recorded in 62 of 75 epithelioid mesotheliomas (82.7%), whereas none of 67 pulmonary adenocarcinomas (0%) were positive for WT1.

Sensitivity and Specificity of Each Marker for Differential Diagnosis of Epithelioid Mesothelioma and Pulmonary Adenocarcinoma

The sensitivity and specificity of each marker for the differential diagnosis between epithelioid mesothelioma and pulmonary adenocarcinoma are shown in Table 2. Sensitivity of Intelectin-1 (76%) was lowest among 5 positive markers; however, its specificity (100%) was absolute. Sensitivity (80.0%) and specificity (97.0%) of

TABLE 1. Immunohistochemical Findings for Epithelioid Mesothelioma and Pulmonary Adenocarcinoma

	Epithelioid Mesothelioma					Pulmonary Adenocarcinoma				
		Immunoreactivity Score*					Immunoreactivity Score*			
Marker	n/N (%)	0	1+	2+	3+	n/N (%)	0	1+	2+	3+
DAB2	60/75 (80.0)	15	12	18	30	2/67 (3.0)	65	2	0	0
Intelectin-1	57/75 (76.0)	18	17	4	36	0/67 (0)	67	0	0	0
Calretinin	74/75 (98.7)	1	7	2	65	17/67 (25.4)	50	10	7	0
Podoplanin (D2-40)	71/75 (94.7)	4	5	6	60	7/67 (10.4)	60	5	2	0
WT1	62/75 (82.7)	13	18	7	37	0/67 (0)	67	0	0	0

*0, negative; 1+, <10% positive; 2+, 10% to 50% positive; 3+, 50% < positive.

DAB2 were nearly those of WT1. Specificity of calretinin (74.6%) was lowest among 5 markers.

DISCUSSION

Pathologically, the role of immunohistochemistry in distinguishing pleural epithelioid mesothelioma from pulmonary adenocarcinoma has received much attention especially in the last 20 years. Currently, there are many immunohistochemical markers available for distinguishing epithelioid mesothelioma from pulmonary adenocarcinoma. Among these, calretinin, cytokeratin 5/6, podoplanin (D2-40), and WT1 are the preferred positive markers for epithelioid mesothelioma. Carcinoembryonic antigen (CEA), MOC31 (epithelial-related antigen), Ber-EP4, BG-8, thyroid transcription factor-1, claudin-4, and napsin-A are the preferred positive markers for pulmonary adenocarcinoma. The IMIG 2012 guidelines recommended the consideration of 2 mesothelial and 2 carcinoma markers, based on morphology at initial observation.[7] In practice, immunohistochemical examination, most laboratories use calretinin, D2-40, and WT1 for diagnosis of epithelioid mesothelioma. However, pathologists must interpret the results of staining by these markers carefully, as specificity of calretinin (74.6% in this study, 90% to 95% in IMIG 2012 guidelines) and D2-40 (88.9% in this study, up to 85% in IMIG 2012 guidelines) is not absolute; additionally, WT1 shows low sensitivity (82.7% in this study, approximately 90% to 100% in IMIG 2012 guidelines). Therefore, novel positive immunohistochemical markers, other than calretinin, D2-40, or WT1, are necessary for increasing the accuracy of epithelioid mesothelioma diagnosis.

Recent development of molecular techniques enabled gene expression analysis from RNA extracted from archival FFPE tumor tissues using GeneChip technology. This method is very useful to find new diagnostic markers, especially in rare tumors, including malignant mesothelioma. We have recently reported the identification of a novel marker, MUC4, for differentiating pleural sarcomatoid mesothelioma from pulmonary sarcomatoid carcinoma by analyzing gene expression data from a gene chip microarray.[8] In this study, we performed gene expression microarray analysis of 6 cases of mesothelioma and 6 cases of pulmonary adenocarcinoma to identify differentially expressed gene products in epithelioid mesothelioma and pulmonary adenocarcinoma. We found that the expression of DAB2 and Intelectin-1 in epithelioid mesothelioma was significantly higher than that in pulmonary adenocarcinoma and this was validated by real-time RT-PCR analysis of mRNA extracted from the same tissue source and Western blot analysis of proteins extracted from mesothelioma cell lines. Immunohistochemical analysis showed that expression of DAB2 and Intelectin-1 in epithelioid mesotheliomas was significantly higher than that in pulmonary adenocarcinomas. These novel positive mesothelial markers, DAB2 and/or Intelectin-1, contribute in accurate mesothelioma diagnosis, in addition to known positive markers (calretinin, D2-40, and WT1). In the present study, we analyzed gene expression analysis of only 6 cases of epithelioid mesothelioma and 6 cases of pulmonary adenocarcinoma, and found many differentially expressed genes mentioned in Supplementary Table S1 (Supplemental Digital Content 1, http://links.lww.com/PAS/A504). As the analysis of substantially larger number will make these findings more credible, we plan to include more cases in the future.

DAB2, a mitogen-responsive phosphoprotein, is expressed in normal ovarian epithelial cells, but is downregulated or absent from ovarian carcinoma cell lines, suggesting its role as a tumor suppressor.[9] Decreased DAB2 expression has been reported in various human cancers, including esophageal,[10] lung,[11] ovarian,[9] prostate,[12] and breast[13] cancers. DAB2 downregulation in these cancers were reported partly due to miRNA targeting DAB2[10,14] or promoter hypermethylation.[13,15] However, the biological significance or expression of DAB2 has not yet been reported in malignant mesothelioma. In the present study, we found increased expression of DAB2 in epithelioid mesothelioma compared with that in pulmonary adenocarcinoma by gene expression microarray analysis. We also confirmed this increased expression of DAB2 in epithelioid mesothelioma by real-time RT-PCR and western blot. From the differential analysis of DAB2 expression between epithelioid mesothelioma and pulmonary adenocarcinoma by immunohistochemical study, we found higher sensitivity and specificity in epithelioid mesothelioma of >80%. In 2 of the 67 cases of pulmonary adenocarcinoma, DAB2 expression was identified in tumor cells but with a low immunoreactivity score. DAB2 expression in pulmonary adenocarcinomas was present in inflammatory cell infiltration, mainly macrophages; therefore, precaution must be taken by the physician

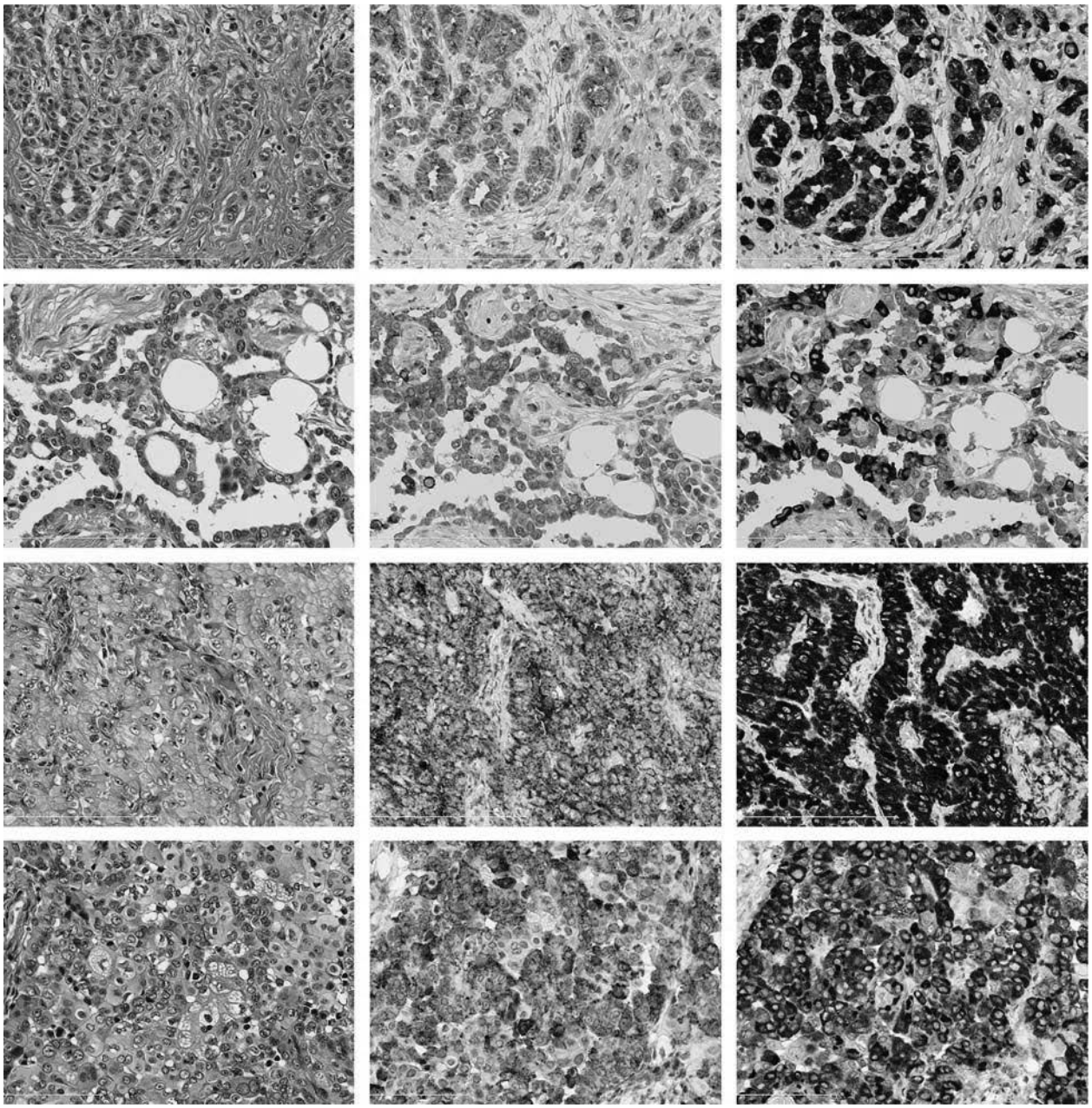

FIGURE 4. DAB2 and Intelectin-1 expression in epithelioid mesothelioma. Various histomorphologic patterns of epithelioid mesothelioma showing prominent expression of DAB2 (middle column) and Intelectin-1 (right column). Each row shows epithelioid mesothelioma with corresponding DAB2 and Intelectin-1 immunohistochemistry.

when interpreting pulmonary adenocarcinoma results for DAB2 expression.

Human Intelectin-1, also known as omentin, is a galactose-binding lectin that is usually expressed in the heart and small intestine as a host defense lectin that binds to bacterial galactofuranose.[16] Intelectin-1 is mainly expressed in the intestinal goblet cells and omentum, and occasionally in the thymus, bronchus, heart, liver, kidney collecting tubule cells, bladder umbrella, and mesothelial cells.[17] Recently, the overexpression of Intelectin-1 in human malignant pleural mesothelioma and its secretion into pleural effusions indicated toward it being a potential biomarker.[17,18] It was reported that Intelectin-1 was not expressed in various cancers, except in some mucus-producing adenocarcinomas.[19] In the present study, we observed high expression of Intelectin-1 mRNA in epithelioid mesothelioma, definite expression of Intelectin-1 in mesothelioma cell lines by western blot analysis, and in 57 of 75 mesothelioma tissue samples by immunohistochemical analysis. In addition, we also found Intelectin-1 expression in non-neoplastic mesothelial lining cells and goblet cells in bronchi and bronchioles

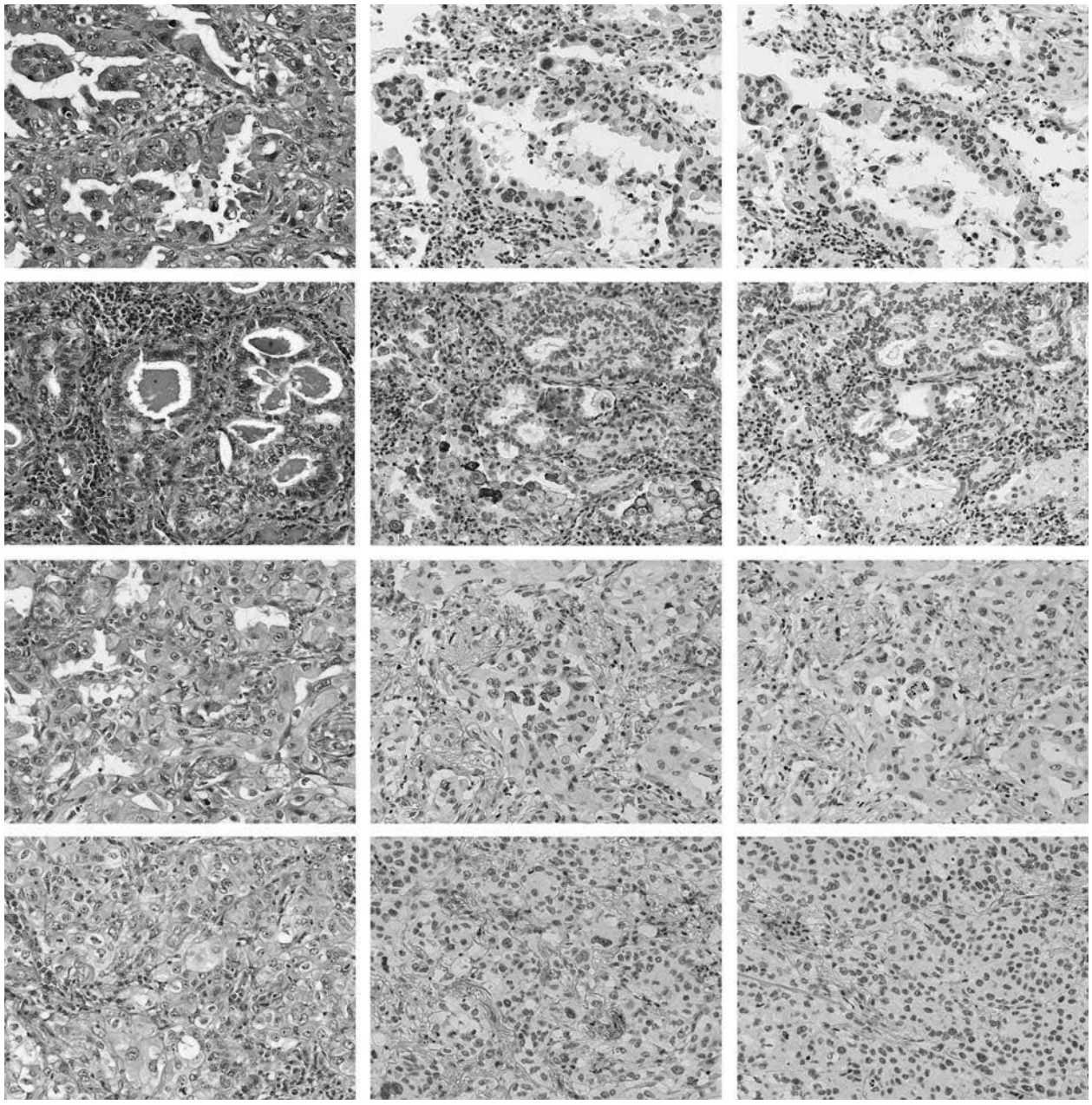

FIGURE 5. DAB2 and Intelectin-1 expression in pulmonary adenocarcinoma. Various histomorphologic patterns of pulmonary adenocarcinoma showing no expression of DAB2 (middle column) and Intelectin-1 (right column). Each row shows pulmonary adenocarcinoma with corresponding DAB2 and Intelectin-1 immunohistochemistry. There is focal reactivity of DAB2 in alveolar macrophages and lymphocytes, which need to interpreted with care.

TABLE 2. Sensitivity and Specificity of Immunohistochemical Positive Markers for Differential Diagnosis of Epithelioid Mesothelioma from Pulmonary Adenocarcinoma

Immunohistochemical Markers	Sensitivity (%)	Specificity
INT-1 +	76.0	100
DAB2 +	80.0	97.0
Calretinin +	98.7	74.6
D2-40 +	94.7	89.6
WT-1 +	82.7	100

(data not shown). No Intelectin-1 expression was recorded in any pulmonary adenocarcinoma cases, confirming its potential as a novel positive mesothelial marker. The functional roles of DAB2 and Intelectin-1 expression in epithelioid mesothelioma need further analysis, which is beyond the scope of this study.

In conclusion, we identified 2 novel positive markers of epithelioid mesothelioma, DAB2 and Intelectin-1, by using gene expression microarray analysis and confirmed their utility to differentiate epithelioid mesothelioma from

pulmonary adenocarcinoma by immunohistochemical study. Further validation of immunohistochemical staining of these markers by other institutes is warranted.

ACKNOWLEDGMENTS

The authors thank Ms Yukari Go of the Technical Center in Hiroshima University for excellent technical assistance and Ms Naomi Fukuhara for editorial assistance.

REFERENCES

1. Robinson BW, Lake RA. Advances in malignant mesothelioma. *N Engl J Med*. 2005;353:1591–1603.
2. Mortality rate due to mesothelioma in Japan: Ministry of Health, Labor & Welfare. Available at: www.mhlw.go.jp/toukei/saikin/hw/jinkou/tokusyu/chuuhisyu15/dl/chuuhisyu.pdf. Accessed January 6, 2017.
3. Mesothelioma statistics: cancer research, UK. 2015. Available at: www.cancerresearchuk.org/health-professional/cancer-statistics/statistics-by-cancer-type/mesothelioma. Accessed January 6, 2017.
4. Delgermaa V, Takahashi K, Park EK, et al. Global mesothelioma deaths reported to the World Health Organization between 1994 and 2008. *Bull World Health Organ*. 2011;89:716–724. 724A–724C.
5. Travis WD, Noguchi M, Yatabe Y, et al. Epithelioid mesothelioma. In: Travis WD, Brambilla E, Burke AP, et al, eds. *WHO Classification of Tumours of the Lung, Pleura, Thymus and Heart*. Lyon: IARC; 2015:156–164.
6. Travis WD, Noguchi M, Yatabe Y, et al. Adenocarcinoma. In: Travis WD, Brambilla E, Burke AP, et al, eds. *WHO Classification of Tumours of the Lung, Pleura, Thymus and Heart*. Lyon: IARC; 2015:26–37.
7. Husain AN, Colby T, Ordonez N, et al. Guidelines for pathologic diagnosis of malignant mesothelioma: 2012 update of the consensus statement from the International Mesothelioma Interest Group. *Arch Pathol Lab Med*. 2013;137:647–667.
8. Amatya VJ, Kushitani K, Mawas AS, et al. MUC4, a novel immunohistochemical marker identified by gene expression profiling, differentiates pleural sarcomatoid mesothelioma from lung sarcomatoid carcinoma. *Mod Pathol*. 2017. Doi:10.1038/modpathol.2016.181.
9. Mok SC, Chan WY, Wong KK, et al. DOC-2, a candidate tumor suppressor gene in human epithelial ovarian cancer. *Oncogene*. 1998;16:2381–2387.
10. Li C, Ding C, Chen T, et al. Micro ribonucleic acid-93 promotes proliferation and migration of esophageal squamous cell carcinoma by targeting disabled 2. *Thorac Cancer*. 2015;6:524–533.
11. Du L, Zhao Z, Ma X, et al. miR-93-directed downregulation of DAB2 defines a novel oncogenic pathway in lung cancer. *Oncogene*. 2014;33:4307–4315.
12. Zhoul J, Hernandez G, Tu SW, et al. The role of DOC-2/DAB2 in modulating androgen receptor-mediated cell growth via the non-genomic c-Src-mediated pathway in normal prostatic epithelium and cancer. *Cancer Res*. 2005;65:9906–9913.
13. Bagadi SA, Prasad CP, Srivastava A, et al. Frequent loss of DAB2 protein and infrequent promoter hypermethylation in breast cancer. *Breast Cancer Res Treat*. 2007;104:277–286.
14. Chao A, Lin CY, Lee YS, et al. Regulation of ovarian cancer progression by microRNA-187 through targeting disabled homolog-2. *Oncogene*. 2012;31:764–775.
15. Li C, Chen J, Chen T, et al. Aberrant hypermethylation at sites 86 to 226 of DAB2 gene in non-small cell lung cancer. *Am J Med Sci*. 2015;349:425–431.
16. Tsuji S, Uehori J, Matsumoto M, et al. Human intelectin is a novel soluble lectin that recognizes galactofuranose in carbohydrate chains of bacterial cell wall. *J Biol Chem*. 2001;276:23456–23463.
17. Washimi K, Yokose T, Yamashita M, et al. Specific expression of human intelectin-1 in malignant pleural mesothelioma and gastrointestinal goblet cells. *PLoS One*. 2012;7:e39889.
18. Tsuji S, Tsuura Y, Morohoshi T, et al. Secretion of intelectin-1 from malignant pleural mesothelioma into pleural effusion. *Br J Cancer*. 2010;103:517–523.
19. Zheng L, Weng M, Qi M, et al. Aberrant expression of intelectin-1 in gastric cancer: its relationship with clinicopathological features and prognosis. *J Cancer Res Clin Oncol*. 2012;138:163–172.

Modern Pathology (2017), 1–10

MUC4, a novel immunohistochemical marker identified by gene expression profiling, differentiates pleural sarcomatoid mesothelioma from lung sarcomatoid carcinoma

Vishwa Jeet Amatya[1], Kei Kushitani[1], Amany Sayed Mawas[1,2], Yoshihiro Miyata[3], Morihito Okada[3], Takumi Kishimoto[4], Kouki Inai[1,5] and Yukio Takeshima[1]

[1]Department of Pathology, Hiroshima University Graduate School of Biomedical and Health Sciences, Hiroshima, Japan; [2]Department of Pathology and Clinical Pathology, South Valley University, Qena, Egypt; [3]Department of Surgical Oncology, Research Institute for Radiation Biology and Medicine, Hiroshima University, Hiroshima, Japan; [4]Department of Internal Medicine, Okayama Rosai Hospital, Okayama, Japan and [5]Pathologic Diagnostic Center, Inc., Hiroshima, Japan

Sarcomatoid mesothelioma, a histological subtype of malignant pleural mesothelioma, is a very aggressive tumor with a poor prognosis. Histological diagnosis of sarcomatoid mesothelioma largely depends on the histomorphological feature of spindled tumor cells with immunohistochemical reactivity to cytokeratins. Diagnosis also requires clinico-radiological and/or macroscopic evidence of an extrapulmonary location to differentiate it from lung sarcomatoid carcinoma. Although there are promising immunohistochemical antibody panels to differentiate mesothelioma from lung carcinoma, a consensus on the immunohistochemical markers that distinguish sarcomatoid mesothelioma from lung sarcomatoid carcinoma has not been reached and requires further study. We performed whole gene expression analysis of formalin-fixed paraffin-embedded tissue from sarcomatoid mesothelioma and lung sarcomatoid carcinoma and observed significant differences in the expression of MUC4 and other genes between sarcomatoid mesothelioma and lung sarcomatoid carcinoma. Immunohistochemistry demonstrated that MUC4 was expressed in the spindled tumor cells of lung sarcomatoid carcinoma (21/29, 72%) but was not expressed in any sarcomatoid mesothelioma (0/31, 0%). To differentiate sarcomatoid mesothelioma from lung sarcomatoid carcinoma, negative MUC4 expression showed 100% sensitivity and 72% specificity and accuracy rate of 87%, which is higher than immunohistochemical markers such as calretinin, D2-40 and Claudin-4. Therefore, we recommend to include MUC4 as a novel and useful negative immunohistochemical marker for differentiating sarcomatoid mesothelioma from lung sarcomatoid carcinoma.
Modern Pathology advance online publication, 27 January 2017; doi:10.1038/modpathol.2016.181

Malignant pleural mesothelioma, a highly aggressive tumor with a poor prognosis, is strongly associated with asbestos exposure; its incidence is increasing in Japan and Western countries and is expected to increase in developing countries.[1] It is histologically classified into three subtypes: epithelioid, biphasic, and sarcomatoid mesothelioma.[2] The International Mesothelioma Interest Group (IMIG) has published guidelines for the differential diagnosis of epithelioid mesothelioma from lung adenocarcinoma and squamous cell carcinoma using immunohistochemical antibody panels of mesothelioma markers (calretinin, D2-40, WT1, cytokeratin 5/6), lung adenocarcinoma markers (CEA, TTF-1, Napsin-A, MOC-31, BerEP4, BG8, B72.3) and lung squamous carcinoma markers (p63, p40, MOC-31, Ber-EP4, cytokeratin 5/6).[3]

However, a consensus on the immunohistochemical markers that differentiate sarcomatoid mesothelioma from lung sarcomatoid carcinoma

Correspondence: Dr Y Takeshima, MD, PhD, Department of Pathology, Hiroshima University Graduate School of Biomedical and Health Sciences, 1-2-3 Kasumi, Minami-ku, Hiroshima 734-8551, Japan.
E-mail: ykotake@hiroshima-u.ac.jp
Received 15 June 2016; revised 3 September 2016; accepted 6 September 2016; published online 26 January 2017

has not been reached and requires further study. The histological diagnosis of sarcomatoid mesothelioma largely depends on the histomorphological feature of spindled tumor cells supported by immunohistochemical cytokeratin reactivity; it also requires clinico-radiological and/or macroscopic evidence of an extrapulmonary location. The immunohistochemical markers for lung adenocarcinoma and squamous carcinoma are not useful for diagnosing lung sarcomatoid carcinoma. To date, D2-40 and calretinin are two commonly used positive mesothelial markers expressed in sarcomatoid mesothelioma.[4–7] However, without convincing calretinin and D2-40 positivity, it is difficult to differentiate sarcomatoid mesothelioma from sarcomatoid carcinoma. In previous reports, including ours, high D2-40 sensitivity has been reported to differentiate sarcomatoid mesothelioma from lung sarcomatoid carcinoma; however, D2-40 specificity is not perfect.[6,7] Therefore, the clinico-radiological identification of tumor location at the extrapulmonary site remains essential to differentiate between these two diseases.

In recent decades, gene expression profiling has been used in many cancers to identify the pathways involved in malignant transformation and to identify novel candidate diagnostic and prognostic markers. We have recently reported the application of gene expression analysis to identify novel markers differentiating epithelioid mesothelioma from reactive mesothelial hyperplasia by PCR array.[8] Although gene expression analysis requires specimens with a high proportion of tumor cells containing good quality RNA, we successfully analyzed the RNA extracted from formalin-fixed paraffin-embedded samples.

The aim of this study was to perform gene expression analysis on spindled tumor cells dissected from formalin-fixed paraffin-embedded tissue of sarcomatoid mesothelioma and lung sarcomatoid carcinoma. Our gene expression microarray data identified several novel genes that are differentially expressed between sarcomatoid mesothelioma and lung sarcomatoid carcinoma, and of these, we validated MUC4 as a novel and useful negative immunohistochemical marker differentiating sarcomatoid mesothelioma from lung sarcomatoid carcinoma.

Materials and methods

Formalin-Fixed Paraffin-Embedded Tissue Samples

Sarcomatoid mesothelioma and lung sarcomatoid carcinoma cases were retrieved from surgical pathology archives of our department during 2005–2014. The clinical details were also reviewed from the patient record files. The location of tumor was confirmed by reviewing clinical information (especially chest computed tomography findings to confirm the tumor localization), gross findings and reviewing histological sections stained with H&E and Elastica van Gieson. All lung sarcomatoid carcinoma cases in this study were located in the pulmonary parenchyma, which was confirmed by radiological, thoracoscopic and operative findings. None of the lung sarcomatoid carcinoma showed diffuse pleurotropic growth pattern described as 'pseudomesotheliomatous growth'. Sarcomatoid mesothelioma was located in extrapulmonary site showing dominant pleurotrophic growth pattern without obvious tumor mass in lung parenchyma. Pathological diagnosis of each case was confirmed by histological findings and immunohistochemical marker panel recommended by Guidelines for Pathologic Diagnosis of Malignant Mesothelioma-2012 Update of the Consensus Statement from the International Mesothelioma Interest Group[3] and current 2015 WHO histological classification of tumours of the lung, pleura, thymus and heart.[9] Sarcomatoid mesothelioma is characterized by a proliferation of spindle cells arranged in fascicles or having a haphazard distribution involving adjacent adipose tissue, parietal pleura or lung parenchyma.[9] Lung sarcomatoid carcinoma is a poorly differentiated non-small cell lung carcinoma that contains a component of sarcoma or sarcoma-like (spindle and/or giant cell) differentiation. Lung sarcomatoid carcinoma is a group of five types of carcinomas based on specific histological criteria and described as giant cell carcinoma, pleomorphic carcinoma, carcinosarcoma, spindle cell carcinoma and pulmonary blastoma. Of these, spindle cell carcinoma and pleomorphic carcinoma with predominant spindle cell component requires the differentiation from sarcomatoid mesothelioma. The number of patients who were diagnosed as sarcomatoid mesothelioma and lung sarcomatoid carcinoma after surgical resection and/or autopsy examination in Hiroshima University Hospital during 2005–2014 were 35 and 34 respectively, suggesting similar frequencies of their incidence. Localization of four cases of sarcomatoid mesothelioma and five cases of lung sarcomoid carcinoma could not be confirmed and thus were excluded from this study. Finally, 31 cases of sarcomatoid mesothelioma and 29 cases of lung sarcomatoid carcinoma were analyzed in the present study. Sarcomatoid mesothelioma included 25 cases of pure sarcomatoid growth (pure sarcomatoid mesothelioma) and 6 cases of biphasic mesothelioma showing predominantly sarcomatoid growth. Lung sarcomatoid carcinoma included 5 cases of spindle cell carcinoma and 24 of pleomorphic carcinoma with predominant spindle cell carcinoma component. Minor foci of squamous cell carcinoma and adenocarcinoma component were present in 5 and 19 cases of pleomorphic carcinoma. Carcinosarcoma, giant cell carcinoma and pulmonary blastema were not included in this study.

The anonymized (unlinkable) tissue samples were provided by the Department of Pathology for gene expression analysis and immunohistochemical

study. This study is in accordance with the Ethics Guidelines for Human Genome/Gene Research enacted by the Japanese Government for the collection of tissue specimens and was approved by the institutional ethics review committee (Hiroshima University E-48).

Gene Expression Analysis

Formalin-fixed paraffin-embedded sections from six cases of sarcomatoid mesothelioma and six cases of lung sarcomatoid carcinoma were used for gene expression analysis. RNA extraction for gene expression analysis was performed from the spindled tumor cells of these cases. Five 10-μm-thick formalin-fixed paraffin-embedded tissue sections containing >90% spindled tumor tissue were processed for total RNA extraction using the Maxwell 16 LEV RNA FFPE Purification Kit (Promega, Tokyo, Japan) according to the manufacturer's protocol. After deparaffinization and lysis with proteinase K treatment, the samples were treated with a DNase cocktail for 15 min at room temperature, followed by RNA purification using a MAXWELL 16 instrument according to the manufacturer's protocol (Promega).

RNA quality was analyzed with an RNA StdSens Analysis kit using an Experion automated electrophoresis system (Bio-Rad Laboratories, Hercules, CA, USA). RNA quantity was estimated with a Qubit RNA HS Kit using a Qubit Fluorometer 2.0 (Molecular Probes/Life Technologies, Carlsbad, CA, USA). The Almac Xcel Array GeneChip (Affymetrix, Santa Clara, CA, USA) contains probe sets of >97 000 transcripts and was used to analyze gene expression profiles. Total RNA was amplified and labeled with a 3′ IVT Labeling Kit (Affymetrix) before hybridization onto the GeneChip. Briefly, 100 ng total RNA was amplified with a SensationPlus FFPE Amplification Kit (Affymetrix) to generate 30 μg of SenseRNA according to the manufacturer's protocol. Twenty-five micrograms of SenseRNA was labeled with a 3′ IVT Labeling Kit (Affymetrix) and hybridized to a Almac Xcel Array GeneChip (Affymetrix) at 45 °C for 16 h using a GeneChip Hybridization Oven 645 (Affymetrix). The hybridized GeneChip was washed, stained using GeneChip Fluidic Station 450 (Affymetrix) and scanned with a GeneChip Scanner 3000 7G (Affymetrix) using the GeneChip Operating Software (Affymetrix). The data were analyzed using the Gene Expression Console Software (Affymetrix), and further statistical analyses were performed using the Subio Software Platform (Subio, Amami-shi, Japan) to calculate plot graphs, fold change of expression and hierarchical clustering.

Validation of Gene Expression Analysis

The same 12 cases of sarcomatoid mesothelioma and lung sarcomatoid carcinoma that were analyzed for gene expression profiling were used to validate the microarray expression data. The relative mRNA expression of *MUC4*, a highly expressed gene in lung sarcomatoid carcinoma, and *IGF2*, highly expressed in sarcomatoid mesothelioma, was assessed with SYBR Green-based real-time RT-PCR using GAPDH as a control. A total of 100 ng RNA was used for mRNA expression with a one-step SYBR Green RT-PCR Kit (Takara-Bio, Tokyo, Japan) using a MX3000P real-time PCR thermal cycler (Stratagene, Agilent Technologies, Tokyo, Japan). The primer pairs used were *MUC4*-F: CAGGCCACCAACTTCA TCG; *MUC4*-R: ACACGGATTGCGTCGTGAG; *IGF2*-F: GTGGCATCGTTGAGGAGTG; *IGF2*-R: CACGTCC CTCTCGGACTTG; *GAPDH*-F: ACAACTTTGGTATC GTGGAAGG; and *GAPDH*-R: GCCATCACGCCA CAGTTTC. Data analysis was performed using the δδCT method for relative quantification. Briefly, threshold cycles (CT) for *GAPDH* (reference) and *MUC4*, *IGF2* (samples) were determined in triplicate. The relative expression (rI) was calculated using the formula: $rI = 2^{-(CT\ sample - CT\ normal)}$.

Immunohistochemistry

Immunohistochemistry was performed using 3-μm tissue sections from the best representative formalin-fixed paraffin-embedded sarcomatoid mesothelioma and lung sarcomatoid carcinoma tissue blocks. All of the immunohistochemical staining was performed with a Benchmark GX automated immunohistochemical station (Ventana, Roche Diagnostics, Tokyo, Japan) using the ultraView Universal DAB Detection Kit (Ventana, Roche Diagnostic, Tokyo, Japan). The antigen retrieval methods and antibodies used in this study are summarized in Table 1. Immunoreactivity was scored as negative (0, no immunostaining) or positive. Positive immunoreactivity was graded as +1 for up to 10% of tumor cells showing positive immunostaining, +2 for >10–50% of the tumor cells, and +3 for >50% of the tumor cells. Only spindled tumor cells from sarcomatoid mesothelioma and lung sarcomatoid carcinoma were evaluated for the immunoreactivity of various markers. Statistical analyses were performed using Fisher's exact test. Sensitivity, specificity, positive predictive value, negative predictive value and accuracy rate were calculated using a simple 2 × 2 table.

Results

Differential Gene Expression and Validation in Sarcomatoid Mesothelioma and Lung Sarcomatoid Carcinoma

Out of the 97 000 analyzable transcripts on the Almac Xcel Array GeneChip, 2099 statistically significant mRNA transcripts were differentially expressed between sarcomatoid mesothelioma and lung sarcomatoid carcinoma by a more than a two-fold difference (Figure 1, plot graph). The

Table 1 List of antibodies with their clone, commercial source and reaction conditions

Antibody to	*Clone*	*Provider*	*Dilution*	*Antigen retrieval*
MUC4	8G7	Santa Cruz Biotechnology	×25	CC1, 60 min
Calretinin	SP65	Ventana	Prediluted	CC1, 30 min
Podoplanin	D2-40	Nichirei	Prediluted	CC1, 60 min
WT1	6F-H2	Dako	×25	CC1, 60 min
Pancytokeratin	AE1/AE3	Ventana	Prediluted	Protease 8 min
Cytokeratin	CAM5.2	Ventana	Prediluted	Protease 8 min
p40	BC28	Biocare Medical	×50	CC1, 60 min
TTF-1	SP141	Ventana	Prediluted	CC1, 60 min
Claudin-4	3E2C1	Life Technologies	×50	CC1, 60 min

Abbreviation: CC1, cell conditioning buffer 1 (Tris-based buffer, pH 8.5 from Ventana).

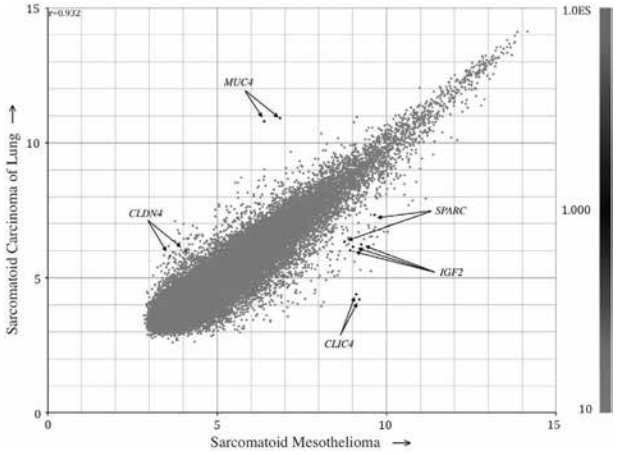

Figure 1 Scatter plot of raw data from the microarray experiments demonstrating MUC4 and CLDN4 with lower expression and IGF2, CLIC4 and SPARC4 with higher expression in sarcomatoid mesothelioma compared with that of lung sarcomatoid carcinoma.

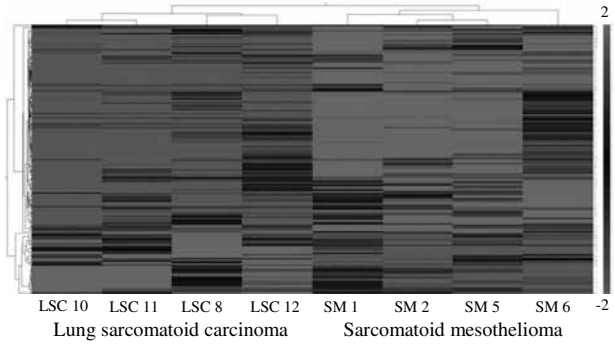

Figure 2 The hierarchical clustering of RNA transcripts with more than five-fold differential expression between sarcomatoid mesothelioma and lung sarcomatoid carcinoma revealed 156 upregulated mRNA transcripts, including *IGF2*, *MEG3*, *CLIC4* and *SPARC*, in sarcomatoid mesothelioma and 46 upregulated mRNA transcripts, including *MUC4* and *Claudin4*, in lung sarcomatoid carcinoma.

hierarchical clustering of mRNAs with more than a five-fold difference in expression revealed 156 upregulated mRNA transcripts, including *IGF2*, *MEG3*, *CLIC4* and *SPARC*, in sarcomatoid mesothelioma and 46 upregulated mRNA transcripts, including *MUC4* and *Claudin4*, in lung sarcomatoid carcinoma (Figure 2, hierarchical clustering; Supplementary Table S1). The mRNA expression hits were validated by real-time RT-PCR of *MUC4* and *IGF2*. *MUC4* mRNA expression was negligible in all six sarcomatoid mesothelioma, and the expression was observed in five of the six lung sarcomatoid carcinoma samples. *IGF2* mRNA was expressed in all of the sarcomatoid mesothelioma samples, although it was also expressed in three of the six lung sarcomatoid carcinoma samples (detailed data not shown).

Immunohistochemical Profiles of Sarcomatoid Mesothelioma and Lung Sarcomatoid Carcinoma

The percentage of positivity and immunohistochemical score for MUC4, mesothelioma markers (calretinin, D2-40, WT1) and lung carcinoma markers (TTF-1, p40, Claudin-4) along with the cytokeratins AE1/AE3 and CAM5.2 are shown in Table 2.

MUC4 Expression

MUC4 expression was observed in the cytoplasm of tumor cells, and the positivity of spindled tumor cells alone was evaluated. MUC4 was also observed in the surrounding normal lung tissue, particularly in bronchial tissue, and was considered an internal positive marker. It was expressed in spindled tumor cells of 21 lung sarcomatoid carcinoma (21/29, 72%; Figure 3b) but none in sarcomatoid mesothelioma (0/31, 0%; Figure 4b). In addition to spindled tumor cells of lung sarcomatoid carcinoma, MUC4 was also expressed in the non-small cell carcinoma component consisting of adenocarcinoma or squamous cell carcinoma in pleomorphic carcinoma. Among lung sarcomatoid carcinoma, 3 cases showed expression in $>50\%$ of tumor cells, 9 cases in 10–50% of tumor cells and 9 cases in $<10\%$ of tumor cells. Out of the 21 lung sarcomatoid carcinoma cases with MUC4

Table 2 Potential immunohistochemical markers for sarcomatoid mesothelioma and lung sarcomatoid carcinoma

	Sarcomatoid mesothelioma						*Lung sarcomatoid carcinoma*							
			Immunohistochemical score[a]						*Immunohistochemical score*[a]					
Antibody	*Positive cases*	*(%)*	*0*	*1+*	*2+*	*3+*	*Positive cases*	*(%)*	*0*	*1+*	*2+*	*3+*	P-*value*[b]	P-*value*[c]
MUC4	0/31	0	31	0	0	0	21/29	72	8	9	9	3	< 0.01	< 0.01
Calretinin	23/31	74	8	7	11	5	13/29	45	16	5	6	2	< 0.05	< 0.05
D2-40	22/31	71	9	9	12	1	9/29	31	20	9	0	0	< 0.01	< 0.01
WT1	6/31	19	25	5	1	0	1/29	3	28	1	0	0	NS	NS
AE1/AE3	29/31	94	2	2	8	19	29/29	100	0	5	2	22	NS	NS
CAM5.2	28/31	90	3	1	8	19	28/29	97	1	6	5	17	NS	NS
TTF-1	0/31	0	31	0	0	0	15/29	52	14	0	4	11	< 0.01	< 0.01
p40	2/31	7	29	2	0	0	6/29	21	23	0	3	3	NS	NS
Claudin-4	0/31	0	31	0	0	0	13/29	45	16	4	5	4	< 0.01	< 0.01

Abbreviations: NA, not available; NS, not significant; TTF-1, thyroid transcription factor; WT1, Wilms' tumor gene product.
[a]Calculated by Fisher's exact test of the positive rate between two groups.
[b]Calculated by the Mann–Whitney *U*-test of reactivity scores of the markers between two groups.
[c]Immunohistochemical score was semiquantified as follows: 0: 0%; 1+: 1–10%; 2+: 11–50%; 3+: >51% of spindled tumor cells.

expression, p40 expression was observed only in 3 cases, TTF-1 in 12 cases and Claudin-4 in 10 cases. Of the nine lung sarcomatoid carcinoma cases without MUC4 expression, p40 expression was observed in three cases, TTF-1 in three cases and Claudin-4 in three cases.

Calretinin, D2-40 and WT1

Calretinin was expressed in the nucleus and cytoplasm of spindled tumor cells of 23 (74%) sarcomatoid mesothelioma and 13 (45%) lung sarcomatoid carcinoma samples, and D2-40 was expressed in the spindled tumor cells of 21 (71%) sarcomatoid mesothelioma and 9 (31%) lung sarcomatoid carcinoma. The immunohistochemical scoring pattern for calretinin expression was not different between sarcomatoid mesothelioma and lung sarcomatoid carcinoma. However, the immunohistochemical scoring pattern for D2-40 expression showed a higher score in sarcomatoid mesothelioma than in lung sarcomatoid carcinoma. WT1 nuclear expression was present in only 6 (19%) sarcomatoid mesothelioma and 1 (3%) lung sarcomatoid carcinoma, revealing it to be a poor immunohistochemical marker to differentiate sarcomatoid mesothelioma from lung sarcomatoid carcinoma.

TTF-1, p40, Claudin-4

Nuclear expression of TTF-1 and P40 was observed in 15 (52%) and 6 (21%) cases of lung sarcomatoid carcinoma, respectively. TTF-1 expression was not observed in sarcomatoid mesothelioma, but p40 expression was observed in 2 (7%) sarcomatoid mesothelioma cases. TTF-1 and/or p40 immunoreactivity was present in 19 of the 29 (66%) cases of lung sarcomatoid carcinoma and 2 of the 31 (7%) cases of sarcomatoid mesothelioma. Claudin-4 and/or TTF-1/p40 immunoreactivity was present in 25 of the 29 (86%) of lung sarcomatoid carcinoma and 2 of the 31 (7%) cases of sarcomatoid mesothelioma. However, p40 expression in sarcomatoid mesothelioma was focal and heterogeneous with an immunohistochemical score of 1.

Cytokeratins, AE1/AE3, CAM5.2

Cytokeratin AE1/AE3 and CAM5.2 expression was present in >90% of both lung sarcomatoid carcinoma and sarcomatoid mesothelioma samples. The majority of sarcomatoid mesothelioma and lung sarcomatoid carcinoma cases showed the expression of both cytokeratins, and the remaining two lung sarcomatoid carcinoma cases and one sarcomatoid mesothelioma case expressed at least one of the two cytokeratins.

Sensitivity and Specificity of Each Marker to Differentially Diagnose Sarcomatoid Mesothelioma and Lung Sarcomatoid Carcinoma

The sensitivity, specificity, positive predictive value, negative predictive value and accuracy rate of each marker differentiating sarcomatoid mesothelioma from lung sarcomatoid carcinoma are shown in Table 3. The negative expression of the carcinoma markers TTF-1 and Claudin-4 showed 100% sensitivity, whereas p40 showed 94%; however, their specificity was restricted around or below 50%. The positive expression of calretinin showed 74% sensitivity and 55% specificity, and D2-40 showed 71% sensitivity and 69% specificity. Although WT1 showed the highest specificity of 97%, its sensitivity

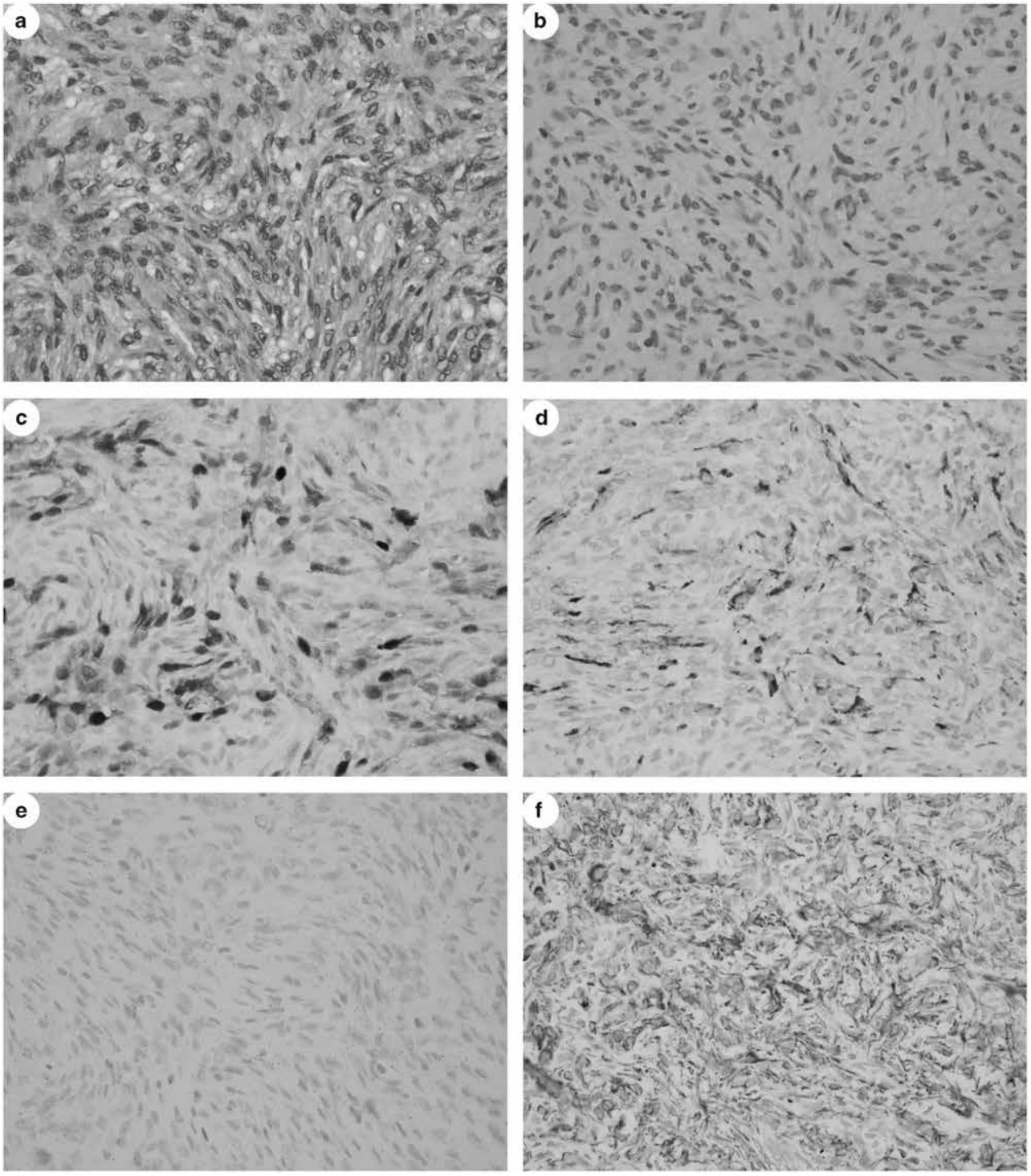

Figure 3 Representative pictures of immunohistochemical expression of MUC4 (**b**), Calretinin (**c**), D2-40 (**d**), Claudin-4 (**e**) and AE1/AE3 (**f**) from sarcomatoid mesothelioma (**a**). None of the sarcomatoid mesotheliomas showed immunohistochemical MUC4 expression.

was $< 20\%$. AE1/AE3 and CAM5.2 showed high 94 and 90% sensitivities and near 0% specificity. In comparison to all of these known immunohistochemical markers, negative expression of MUC4 showed 100% sensitivity and 72% specificity, making the accuracy rate of 87%, the highest among these immunohistochemical markers.

Value of Immunohistochemical Marker Panel to Differentially Diagnosis Sarcomatoid Mesothelioma and Lung Sarcomatoid Carcinoma

MUC4 showed the highest sensitivity and specificity among the immunohistochemical markers for differentiation of sarcomatoid mesothelioma from lung

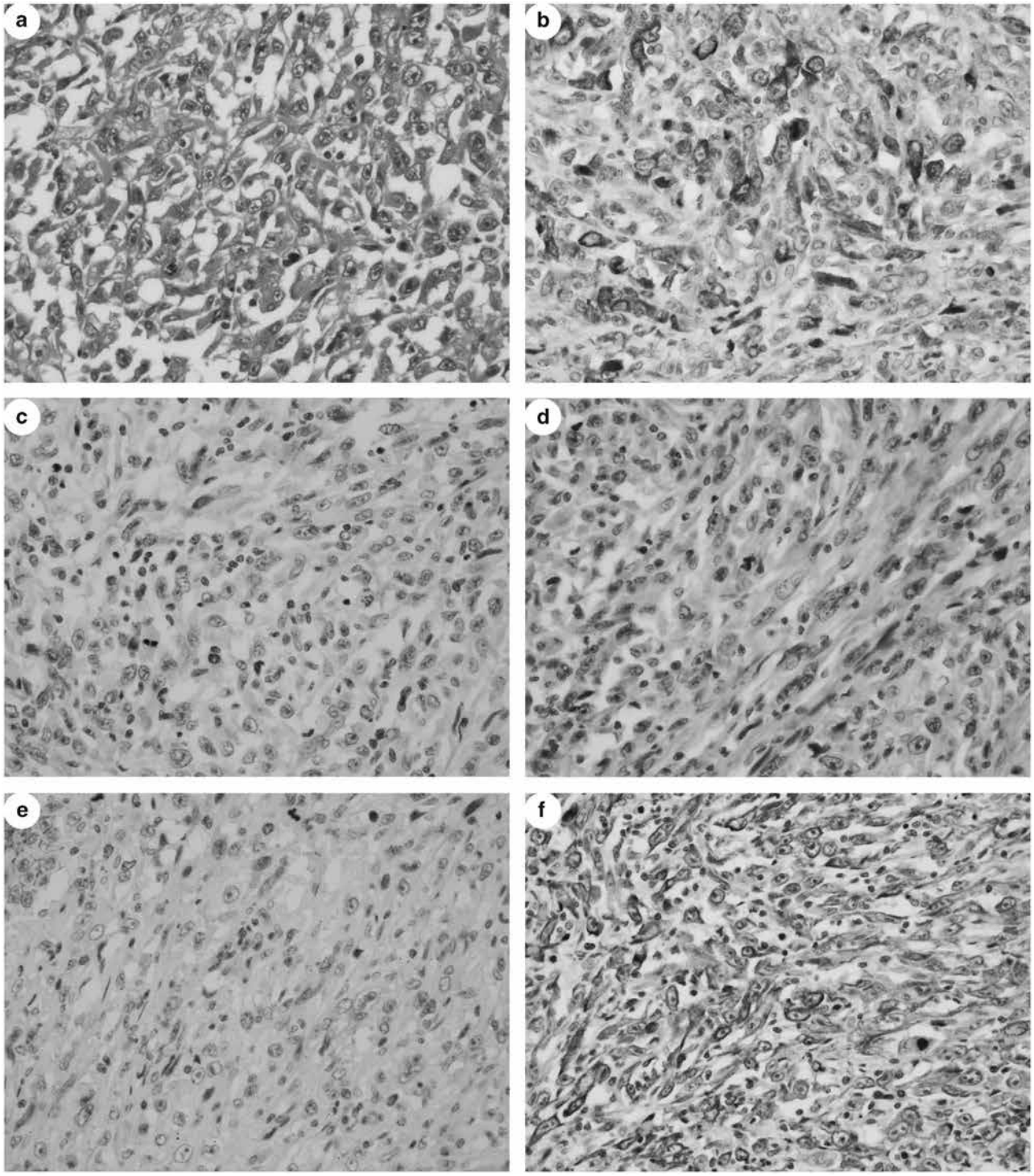

Figure 4 Representative pictures of immunohistochemical MUC4 expression (**b**), Calretinin (**c**), D2-40 (**d**), Claudin-4 (**e**) and AE1/AE3 (**f**) of lung sarcomatoid carcinoma (**a**). Twenty-one of the 29 (72%) lung sarcomatoid carcinomas exhibited cytoplasmic expression of MUC4.

sarcomatoid carcinoma. However, the specificity was 72%. Therefore, a combination of various markers was considered. Various combinations of immunohistochemical markers are shown in Table 4. Among the negative immunohistochemical markers, combination of MUC4, TTF-1 and p40 was observed in 26 of the 29 lung sarcomatoid carcinoma cases (90% specificity) and 2 of the 31sarcomatoid mesothelioma cases (93% sensitivity). Combination of MUC4 and Claudin-4 expression was found in 24 of the 29 lung sarcomatoid carcinoma cases (83% specificity) and none of the sarcomatoid

Table 3 Sensitivity, specificity, PPV, NPV and accuracy rate of each antibody to differentially diagnose sarcomatoid mesothelioma from lung sarcomatoid carcinoma

Findings	*Sensitivity (%)*	*Specificity (%)*	*PPV (%)*	*NPV (%)*	*Accuracy rate (%)*	P-*value*
MUC4 (−)	100	72	80	100	87	< 0.01
Calretinin (+)	74	55	64	67	65	< 0.05
D2-40 (+)	71	69	71	69	70	< 0.01
WT1 (+)	19	97	86	53	57	NS
AE1/AE3 (+)	94	0	50	0	48	NS
CAM5.2 (+)	90	3	50	25	48	NS
TTF-1 (−)	100	52	69	100	77	< 0.01
p40 (−)	94	21	56	75	58	NS
Claudin-4 (−)	100	45	66	100	73	< 0.01

Abbreviations: NPV, negative predictive value; NS, not significant; PPV, positive predictive value.

Table 4 Sensitivity, specificity, PPV, NPV and accuracy rate of two or more markers to differentially diagnose sarcomatoid mesothelioma from lung sarcomatoid carcinoma

Immunohistochemical markers	*Sensitivity (%)*	*Specificity (%)*	*PPV (%)*	*NPV (%)*	*Accuracy rate (%)*	P-*value*
p40 (−)/TTF-1 (−)	94	66	74	91	80	< 0.01
Claudin-4 (−)/TTF-1 (−)/p40 (−)	94	90	91	93	92	< 0.01
Claudin-4 (−)/TTF-1 (−)	100	83	86	100	92	< 0.01
MUC4 (−)/TTF-1 (−)/p40 (−)	94	93	94	93	93	< 0.01
MUC4 (−)/Claudin-4 (−)	100	83	86	100	92	< 0.01
MUC4 (−)/TTF-1 (−)/Claudin-4 (−)	100	90	91	100	95	< 0.01
MUC4 (−)/TTF-1 (−)/p40 (−)/Claudin-4 (−)	94	97	97	93	95	< 0.01

Abbreviations: NPV, negative predictive value; PPV, positive predictive value.

mesothelioma cases (100% sensitivity). The combination of MUC4, TTF-1 and Claudin-4 was observed in 26 of the 29 lung sarcomatoid carcinoma cases (90% specificity) and 0 of the 31 sarcomatoid mesothelioma cases (100% sensitivity).

Discussion

Sarcomatoid mesothelioma has the histomorphological feature of spindled tumor cells and resembles many tumors with spindled cells, including true sarcoma or sarcomatoid carcinomas. The immunohistochemical reactivity to cytokeratin remains critical to differentiate it from true sarcomas. However, differentiating sarcomatoid mesothelioma from lung sarcomatoid carcinoma is challenging, as the histomorphological and immunohistochemical characteristics are extremely similar. For this reason, clinical and/or gross evidence of an extrapulmonary location is indispensable for its diagnosis. Although the mesothelioma markers calretinin and D2-40 have been utilized to differentiate sarcomatoid mesothelioma from lung sarcomatoid carcinoma, they are not absolute, as their sensitivity and specificity are not sufficiently high. Although we previously reported the sensitivity of calretinin (78%) and D2-40 (87%), specificity was not high for calretinin (41%) and D2-40 (74%).[7] Our past and present data on calretinin and D2-40 were similar to reports by Ordonez *et al*[4] and Padgett *et al*.[6] Considering the low specificity of calretinin, D2-40 is considered the single most important immunohistochemical marker for its differentiation. However, in our practical experience, it is still very difficult to interpret the reactivity of D2-40 in these tumors, particularly in cases showing prominent fibro-collagenous proliferation.

TTF-1, a lung adenocarcinoma marker, and p40, a squamous cell carcinoma marker, have emerged as useful markers for non-small cell lung carcinoma[10,11] and are thus supposed to be expressed in pleomorphic lung carcinoma. TTF-1 might be identified as a novel marker differentiating pleomorphic carcinoma from sarcomatoid mesothelioma because of its low expression in sarcomatoid mesothelioma. However, in this study, despite their specificity of 100 or 94%, the sensitivity of TTF-1 (51%) and p40 (21%) are not good to distinguish sarcomatoid mesothelioma and lung sarcomatoid carcinoma. Though p40 expression is good marker of squamous cell carcinoma, it has been also reported in a few mesothelioma cases.[12] In this study too, we observed p40 expression in two sarcomatoid mesothelioma cases but very focal and heterogeneous, unlike its expression in squamous cell carcinoma. Claudin-4, which is reported to be a very reliable universal carcinoma marker differentiating epithelioid mesothelioma from various carcinomas,[13,14] showed limited value in lung sarcomatoid carcinoma cases. In this study, only half of lung sarcomatoid

carcinoma expressed Claudin-4, and its punctate expression in the cytoplasm of spindled cells of lung sarcomatoid carcinoma resembled that of the punctate expression in the cytoplasm of sarcomatoid mesothelioma. TTF-1, p40 and Claudin-4 expression can be reliable markers for pleomorphic carcinomas with a prominent carcinoma component, such as adenocarcinoma or squamous cell carcinoma.

In this study, we analyzed all of the genes expressed in sarcomatoid mesothelioma and lung sarcomatoid carcinoma with the aim of identifying novel markers for their differential diagnosis. Although frozen tissue yields better and less degradable RNA for gene expression analysis, we preferred formalin-fixed paraffin-embedded tissue samples because they included the microscopically identifiable spindle cell tumor tissue. For this analysis, we have to amplify the small amount of RNA extracted from the formalin-fixed paraffin-embedded tissue before hybridization to the GeneChip. The Almac Xcel GeneChip from Affymetrix, which we used here, has been reported to produce identical results to the GeneChip using RNA derived from frozen tissue samples. In addition, it contains proprietary Almac-sequenced data and filtered public data for biomarker discovery and the validation of oncogene-related transcripts for a much higher detection rate in degraded samples.

From the differential expression analysis, a more than five-fold expression change in *IGF2*, *CLIC4* and *SPARC* was observed in sarcomatoid mesothelioma, and IGF2 expression was validated by real-time RT-PCR. We did not uncover significant differential expression of IGF2 between sarcomatoid mesothelioma and lung sarcomatoid carcinoma (data not shown). The discrepancy between the microarray data and real-time RT-PCR data can be explained because *IGF2* mRNA expression on a microarray chip is the relative expression between both lung sarcomatoid carcinoma and sarcomatoid mesothelioma but in a different quantity. We later investigated the immunohistochemical expression IGF2, CLIC4 and SPARC proteins in sarcomatoid mesothelioma and lung sarcomatoid carcinoma. However, there was no significant differential expression of these proteins between lung sarcomatoid carcinoma and sarcomatoid mesothelioma, limiting their applicability as an immunohistochemical positive marker of sarcomatoid mesothelioma.

In contrast, microarray gene expression analysis showed increased expression of *MUC4* in lung sarcomatoid carcinoma compared with that of sarcomatoid mesothelioma, and we found negligible *MUC4* mRNA expression in sarcomatoid mesothelioma at the mRNA level. MUC4 stands for member of mucin protein of high molecular weight glycoprotein.[15] It is expressed in various normal epithelium of the respiratory tract, particularly in the trachea and bronchi[16] and in the epithelium of the digestive and urogenital tracts.[17] MUC4 expression has been reported in various human carcinomas, including pancreatic,[18] breast[19] and lung adenocarcinoma.[20] Llinares *et al*[21] reported the diagnostic value of MUC4 expression in distinguishing epithelioid mesothelioma and lung adenocarcinoma. They found that MUC4 was expressed in 0 of the 41 epithelioid mesotheliomas and in 32 of the 35 (91%) lung adenocarcinoma. To our knowledge, this report has not been validated by other laboratories, as the antibody to MUC4 was not commercially available in the past. We observed MUC4 expression in lung adenocarcinoma and lung squamous cell carcinoma and observed no expression in epithelioid mesothelioma using a commercially available anti-MUC4 antibody. The current study is the first report to describe MUC4 expression in lung sarcomatoid carcinoma and no MUC4 expression in sarcomatoid mesothelioma. We observed a high specificity (72%) and absolute sensitivity (100%) for negative MUC4 expression to differentiate sarcomatoid mesothelioma from lung sarcomatoid carcinoma, with an accuracy rate of 87%. These values are far better than any previously identified immunohistochemical markers differentiating sarcomatoid mesothelioma from lung sarcomatoid carcinoma.

The sensitivity of MUC4 expression as a negative marker was the highest of the immunohistochemical markers in this study. Lung sarcomatoid carcinoma cases showing MUC4 expression (21 cases) also demonstrated co-expression of TTF-1 in 12 cases, Claudin-4 in 10 cases and p40 in 3 cases. Furthermore, lung sarcomatoid carcinoma cases without MUC4 expression showed TTF-1 expression in three cases, p40 in three cases and Claudin-4 in three cases. Therefore, MUC4 expression has better additional value of the immunohistochemical markers for the differential diagnosis of sarcomatoid mesothelioma from lung sarcomatoid carcinoma. The sensitivity of these markers can be improved by combining two or more, and the addition of TTF-1 and Claudin-4 to MUC4 expression improved the accuracy rate up to 95% for the differential diagnosis of sarcomatoid mesothelioma from lung sarcomatoid carcinoma.

In conclusion, we identified a novel immunohistochemical marker MUC4 that differentiates sarcomatoid mesothelioma from lung sarcomatoid carcinoma by applying whole gene expression analysis. The combination of MUC4 with TTF-1/p40 and Claudin-4 improved the sensitivity and specificity for differential diagnosis. Therefore, we propose including MUC4 as an additional negative marker to the immunohistochemical marker panel to differentiate sarcomatoid mesothelioma from lung sarcomatoid carcinoma.

Acknowledgments

We thank Ms Naomi Fukuhara for her administrative assistance. This work was supported in part by the

Japan Society for the Promotion of Science, Grants-in-Aid Scientific Research No. JP26460452 (YT) from the Ministry of Education, Science, Sports and Culture. Part of this study was performed at the Analysis Center of Life Science, Hiroshima University.

Disclosure/conflict of interest

The authors declare no conflict of interest.

References

1 Delgermaa V, Takahashi K, Park EK, *et al.* Global mesothelioma deaths reported to the World Health Organization between 1994 and 2008. Bull World Health Organ 2011;89:716–724, 24A–24C.
2 Roggli V, Churg A, Chirieac LR, *et al.* Sarcomatoid, desmoplastic, and biphasic mesothelioma. In: Travis WD, Brambilla E, Burke S, *et al.* (eds). WHO Classification of Tumours of the Lung, Pleura, Thymus, and Heart. IARC: Lyon, France, 2015, pp 165–168.
3 Husain AN, Colby T, Ordonez N, *et al.* Guidelines for pathologic diagnosis of malignant mesothelioma: 2012 update of the consensus statement from the International Mesothelioma Interest Group. Arch Pathol Lab Med 2013;137:647–667.
4 Ordonez NG. D2-40 and podoplanin are highly specific and sensitive immunohistochemical markers of epithelioid malignant mesothelioma. Hum Pathol 2005;36:372–380.
5 Chu AY, Litzky LA, Pasha TL, *et al.* Utility of D2-40, a novel mesothelial marker, in the diagnosis of malignant mesothelioma. Mod Pathol 2005;18:105–110.
6 Padgett DM, Cathro HP, Wick MR, *et al.* Podoplanin is a better immunohistochemical marker for sarcomatoid mesothelioma than calretinin. Am J Surg Pathol 2008;32:123–127.
7 Takeshima Y, Amatya VJ, Kushitani K, *et al.* Value of immunohistochemistry in the differential diagnosis of pleural sarcomatoid mesothelioma from lung sarcomatoid carcinoma. Histopathology 2009;54:667–676.
8 Kushitani K, Amatya VJ, Mawas AS, *et al.* Use of anti-Noxa antibody for differential diagnosis between epithelioid mesothelioma and reactive mesothelial hyperplasia. Pathobiology 2016;83:33–40.
9 Kerr KM, Pelosi G, Austin JHM, *et al.* Pleomorphic, spindle cell, and giant cell carcinoma. In: Travis WD, Brambilla E, Burke AP, *et al.* (eds). WHO Classification of Tumours of the Lung, Pleura, Thymus and Heart, 4th edn. IARC: Lyon, France, 2015, pp 88–90.
10 Travis WD, Noguchi M, Yatabe Y, *et al.* Adenocarcinomal. In: Travis WD, Brambilla E, Burke AP, *et al.* (eds). WHO Classification of Tumours of the Lung, Pleura, Thymus and Heart, 4th edn. IARC: Lyon, France, 2015, pp 26–37.
11 Tsao M-S, Brambilla E, Nicholson AG, *et al.* Squamous cell carcinoma. In: Travis WD, Brambilla E, Burke AP, *et al.* (eds). WHO Classification of Tumours of the Lung, Pleura, Thymus and Heart, 4th edn. IARC: Lyon, France, 2015, pp 51–55.
12 Tatsumori T, Tsuta K, Masai K, *et al.* p40 is the best marker for diagnosing pulmonary squamous cell carcinoma: comparison with p63, cytokeratin 5/6, desmocollin-3, and sox2. Appl Immunohistochem Mol Morphol 2014;22:377–382.
13 Ordonez NG. Value of claudin-4 immunostaining in the diagnosis of mesothelioma. Am J Clin Pathol 2013;139:611–619.
14 Facchetti F, Lonardi S, Gentili F, *et al.* Claudin 4 identifies a wide spectrum of epithelial neoplasms and represents a very useful marker for carcinoma versus mesothelioma diagnosis in pleural and peritoneal biopsies and effusions. Virchows Arch 2007;451:669–680.
15 Chaturvedi P, Singh AP, Batra SK. Structure, evolution, and biology of the MUC4 mucin. FASEB J 2008;22:966–981.
16 Copin MC, Devisme L, Buisine MP, *et al.* From normal respiratory mucosa to epidermoid carcinoma: expression of human mucin genes. Int J Cancer 2000;86:162–168.
17 Audie JP, Janin A, Porchet N, *et al.* Expression of human mucin genes in respiratory, digestive, and reproductive tracts ascertained by in situ hybridization. J Histochem Cytochem 1993;41:1479–1485.
18 Moniaux N, Chaturvedi P, Varshney GC, *et al.* Human MUC4 mucin induces ultra-structural changes and tumorigenicity in pancreatic cancer cells. Br J Cancer 2007;97:345–357.
19 Rakha EA, Boyce RW, Abd El-Rehim D, *et al.* Expression of mucins (MUC1, MUC2, MUC3, MUC4, MUC5AC and MUC6) and their prognostic significance in human breast cancer. Mod Pathol 2005;18:1295–1304.
20 Kwon KY, Ro JY, Singhal N, *et al.* MUC4 expression in non-small cell lung carcinomas: relationship to tumor histology and patient survival. Arch Pathol Lab Med 2007;131:593–598.
21 Llinares K, Escande F, Aubert S, *et al.* Diagnostic value of MUC4 immunostaining in distinguishing epithelial mesothelioma and lung adenocarcinoma. Mod Pathol 2004;17:150–157.

Supplementary Information accompanies the paper on Modern Pathology website (http://www.nature.com/modpathol)

JOURNAL OF IMMUNOTOXICOLOGY, 2016
VOL. 13, NO. 5, 620–627
http://dx.doi.org/10.3109/1547691X.2016.1143539

Taylor & Francis
Taylor & Francis Group

RESEARCH ARTICLE

FoxO1 regulates apoptosis induced by asbestos in the MT-2 human T-cell line

Hidenori Matsuzaki[a], Suni Lee[a], Megumi Maeda[b], Naoko Kumagai-Takei[a], Yasumitsu Nishimura[a] and Takemi Otsuki[a]

[a]Department of Hygiene, Kawasaki Medical School, Kurashiki, Japan; [b]Department of Biofunctional Chemistry, Division of Bioscience, Okayama University Graduate School of Natural Science and Technology, Okayama, Japan

ABSTRACT

Asbestos is known to cause malignant mesothelioma and lung cancer. Recent studies implicate tumor immunity in the development of various tumors, including malignant mesothelioma. In order to establish an *in vitro* T-cell model to clarify the effects of long-term exposure of asbestos on tumor immunity, in this study, human T-cell line MT-2 cells were cultured with asbestos for longer than 8 months and the resultant cells (MT-2Rst) were assessed for the expression of forkhead transcription factor FoxO1. Gene expression analysis revealed that the amount of *FoxO1* mRNA decreased after long-term exposure of the MT-2 cells to asbestos. In accordance with this reduction in FoxO1, pro-apoptotic Foxo1 target genes *Puma*, *Fas ligand* and *Bim* were also seen to be down-regulated in MT-2Rst cells. Furthermore, shRNA-mediated knock-down of FoxO1 reduced the number of apoptotic parental MT-2 cells after treatment with asbestos. On the other hand, over-expression of FoxO1 did not affect asbestos-induced apoptosis in MT-2Rst cells. These results suggested that FoxO1 played an important role in regulating asbestos-induced apoptosis and confirmed the presence of multiple pathways regulating resistance to asbestos in MT-2Rst cells.

ARTICLE HISTORY
Received 29 October 2015
Revised 13 January 2016
Accepted 14 January 2016
Published online 31 March 2016

KEYWORDS
Asbestos; apoptosis; regulatory T-cell; transcription factor; FoxO1

Introduction

Asbestos is a set of natural fibrous silicate minerals that includes chrysotile, crocidolite and amosite and has been used in a wide range of industrial applications for its physical properties such as resistance to fires, heat and chemical damage. It has been clearly shown that prolonged inhalation of asbestos fibers causes serious diseases in pulmonary tissues, malignant pleural mesothelioma (MPM), lung cancer, asbestos-related pleural plaque (PP) and pulmonary fibrosis in humans (Lemen et al. 2006; Craighead et al. 2008). While trade involving asbestos is now restricted or banned in many countries, there are still risks with existing buildings whose structures include asbestos.

MPM is the most serious of the asbestos-related diseases because it is a highly aggressive tumor and resistant to currently available therapies (Roggli et al. 2004; Robinson et al. 2005). Many studies have and still are attempting to clarify mechanisms of MPM development caused by asbestos. For example, it was an important finding that the reactive oxygen species (ROS) produced from iron found in asbestos fibers (such as crocidolite and amosite) caused DNA damage in alveolar epithelial and mesothelial cells (Toyokuni 2009; Huang et al. 2011). Recent investigations have also implicated tumor immunity in the onset/development of various tumors, including MPM (Schreiber et al. 2011; Izzi et al. 2012). Asbestos fibers have also been shown to cause reduced expression of NKp46 activating receptor and the release of cell-killing granules containing perforin and granzyme B in natural killer (NK) cells (Nishimura et al. 2009a,b). With cytotoxic T-cells (CTL), asbestos repressed differentiation of naïve CTL to effector/memory CTL as well as their ability to proliferate (Maeda et al. 2010; Kumagai-Takei et al. 2013). Taking this and other earlier information together, we hypothesized that asbestos affected immunological systems in addition to impacting on epithelial and mesothelial cells in pulmonary tissues and that this inactivated host responses against any induced tumor cells.

In our earlier studies, MT-2 – a polyclonal T-cell line immortalized with human adult leukemia virus-1 – was cultured with a low concentration of chrysotile A, chrysotile B or crocidolite for >8 months (Miura et al. 2006; Maeda et al. 2011, 2012). The resultant seven independent sub-lines were designated CA (chrysotile A) 1–3, CB (chrysotile B) 1–3 and CR (crocidolite). These cell lines are useful to investigate the effect of continuous exposure of asbestos on T-cells since elevations in levels of anti-apoptotic factor Bcl-2 or interleukin (IL)-10 were

CONTACT Hidenori Matsuzaki hmatsuzaki@med.kawasaki-m.ac.jp Department of Hygiene, Kawasaki Medical School, 577 Matsushima, Kurashiki, Okayama 7010192, Japan

observed both in MT-2 cells and in $CD4^+$ T-cells purified from PP or MPM patients (Miura et al. 2006). These sub-lines also showed resistance to asbestos-induced apoptosis, even though exposure to asbestos induced apoptosis in the original MT-2 cells. Those investigations also reported that tyrosine kinase Src was active in MT-2CA1 cells and was implicated in resistance against the effects of asbestos. Activation of Src leads to the production of IL-10 that, in turn, induces over-expression of anti-apoptotic factor Bcl-2 in a process mediated by signal transducer and activator transcription factor 3 (STAT3). Nevertheless, it remains unclear whether activation of the Src/Bcl-2 pathway was the sole mechanism preventing apoptosis induced by asbestos.

Our laboratory has previously performed gene expression analysis of MT-2CA1–3 and of CB1–3 and compared findings against those in parental MT-2 cells (Maeda et al. 2011). That analysis revealed that forkhead transcription factor class O1 (FoxO1) was down-regulated after long-term exposure of the cells to asbestos. FoxO1 and its related molecules FoxO3 and FoxO4 belong to the winged-helix transcription factor family (Accili & Arden 2004; Eijkelenboom & Burgering 2013). Each is activated by ROS or by depletion of growth factors via prost-translational modifications such as phosphorylation, acetylation and ubiquitination. Activated FoxO family members regulate a wide range of cellular processes such as apoptosis, cell cycle arrest and various metabolic processes. Many genes have been identified as targets of FoxO family members, including pro-apoptotic genes such as Bcl-2 interacting mediator (Bim), p53 up-regulated modulator of apoptosis (Puma), Fas ligand and TRAIL.

In the study reported here, FoxO1 signaling in MT-2CA1 cells was analyzed and whether down-regulation of FoxO1 was implicated in resistance to asbestos-induced apoptosis in MT-2CA1 cells – in addition to up-regulation of the Src/Bcl-2 survival pathway – was also investigated.

Materials and methods

Reagents

Chrysotile A, chrysotile B and crocidolite were Union for International Cancer Control standard samples and obtained from the Japan Asbestos Association (Kohyama et al. 1996). Anti-FoxO1 antibody was obtained from Cell Signaling Technology (Danvers, MA). Anti-β-actin and anti-GAPDH antibodies were purchased from Santa Cruz Biotechnology (Santa Cruz, CA). TaqMan Assay probes for FoxO1, Bim, Puma, Fas ligand and GAPDH were purchased from Applied Biosystems (Foster City, CA). All culture media and supplements were bought from Sigma (St. Louis, MO). MT-2 immortalized human T-cells cells were obtained from the JCRB cell bank (Osaka, Japan). Human embryonic kidney 293T (HEK293T) cells were purchased from ATCC (Manassas, VA).

Cell culture

MT-2 cells were cultured in RPMI 1640 supplemented with 10% fetal bovine serum (FBS) and antibiotics at 37 °C in a 5% CO_2 incubator. The MT-2 sub-lines to be generated – comprising CA1–3, CB1–3 and CR – were cultured with, respectively, 10 μg/ml chrysotile A, 10 μg/ml chrysotile B or 25 μg/ml crocidolite (Maeda et al. 2012). HEK293T cells were maintained in Dulbecco's modified eagle medium supplemented with 10% FBS and antibiotics at 37 °C in a 5% CO_2 incubator.

Plasmids

Human FoxO1 cDNA was isolated from a human heart cDNA library (Clontech, Mountain View, CA) by polymerase chain reaction (PCR), according to the registered sequence (GenBankNM_002015.3). The cDNA fragments corresponding to the FLAG epitope-tagged FoxO1 were generated with PCR and cloned into pMXs-puro retrovirus plasmid vector (Kitamura et al. 2003). The resultant plasmid was designated pMXs-FLAG-FoxO1. The sequence of the construct was confirmed by a di-deoxynucleotide chain-termination method using a DNA sequencing system 3100-Avant (Applied Biosystems). Lentivirus plasmid vectors pLKO.1-puro-Control and pLKO.1-puro containing shRNA targeting human FoxO1 (TRCN0000039579 and TRCN0000039580) were purchased from Sigma.

Western blot analysis

MT-2 cells were lysed in 20 mM Tris-HCl (pH 7.5) containing 1 mM EDTA, 1 mM EGTA, 10 mM 2-mercaptoethanol, 1% Triton X-100, 1% sodium deoxycholate, 0.1% sodium lauryl sulfate, 150 mM NaCl and 1% protease inhibitor cocktail (Sigma) and briefly sonicated. After centrifugation at 18 000 × g for 10 min, the supernatant was collected and measured using a BCA protein assay kit (Pierce, Rockford, IL). Cell lysate containing 50 μg protein was boiled in SDS-sample buffer and then subjected to SDS-PAGE separation. The resolved proteins were subsequently electrotransferred onto Immobilon P membranes (Millipore, Bedford, MA). After initial blocking with Tris-buffered saline containing 0.2% Tween 20 (TBS-T) supplemented with 5% BSA,

membranes were then incubated with each primary antibody in TBS-T containing 1% BSA at dilutions recommended by the manufacturers for 1–2 h at room temperature (RT). Thereafter, the membrane was gently rinsed with TBS-T and then incubated with horseradish peroxidase-conjugated anti-mouse or anti-rabbit antibody secondary antibody in TBS-T at dilutions recommended by the manufacturers for 1 h at RT. After a final set of rinsing with TBS-T, the presence of the proteins of interest was evaluated using a chemiluminescence reaction mediated by an ECL Plus chemiluminescence detection kit (GE Healthcare, Little Chalfont, UK) and each was then visualized with Chemi-Stage (Toyobo, Osaka, Japan).

FoxO1 knockdown cell lines

Recombinant lentivirus was produced by transfection of lentivirus constructs with packaging plasmids pLP1, pLP2 and pLP/VSVG from a Block-it Lentiviral RNAi Expression System (Invitrogen, Carlsbad, CA) into HEK293T cells using Effectene transfection reagent (Qiagen, Hilden, Germany). Culture supernatants containing recombinant lentivirus were then harvested after 48–72 h. Growing MT-2 cells were infected with each recombinant lentivirus and the cells were then selected by culturing in the presence of 1 μg/ml puromycin (Sigma) for > 2 weeks at 37 °C. Resultant cell lines were designated Org-Ctrl (Scramble), Org-KD#1(TRCN0000039579) or Org-KD#2(TRCN0000039580).

Stable cell line expressing recombinant FoxO1

Recombinant retroviruses were produced by transfection of the retroviral constructs, pMXs-FLAG-FoxO1 or empty pMXs-puro, with packaging plasmids pCMV-VSV-G and pCMV-gag/pol into HEK293T cells using Effectene (Qiagen) transfection reagent. Culture supernatants containing recombinant retrovirus were harvested after 48–72 h. Growing MT-2CA1 cells were incubated with each recombinant retrovirus for 24 h and infected cells then selected by culture in the presence of 1 μg/ml puromycin for > 2 weeks at 37 °C. The established cells were then named CA1FoxO1 and CA1Empty, respectively.

Real-time RT-PCR analysis

Total RNA was isolated from growing MT-2 cells with an RNA purification Kit (Qiagen) and cDNA synthesized using a PrimeScript II 1st strand cDNA synthesis kit with an oligo-dT primer (Takara, Shiga, Japan). Real-time PCR analysis was performed with TaqMan probes and Brilliant III Ultra Fast QPCR master mix (Agilent Technologies, Palo Alto, CA) using a Mx3000P QPCR System (Agilent Technologies), according to manufacturer protocols.

Apoptosis assay

MT-2 cells were treated with chrysotile A for 24 h at 37 °C, then washed with ice-cold PBS and fixed in 70% ethanol. After staining with 40 μg/ml propidium iodide and treatment with 10 μg/ml RNase, the DNA content of cells was analyzed with a FACSCanto II (Becton Dickenson, Franklin Lakes, NJ) flow cytometer and FlowJo software (FlowJo, Ashland, OR). Apoptotic cells were quantified as the population of cells with subG$_1$-DNA content. A minimum of 20 000 events/sample was acquired.

Statistical analyses

All experiments were performed in triplicate. Data were expressed as mean ± SD. Differences in *FoxO1* mRNA levels in MT-2 org and MT-2 sub-lines were analyzed using a one-way analysis of variance (ANOVA) with a Dunnett's multiple comparison test. Differences between two samples in expression of FoxO1 target genes or in the population of apoptotic cells were evaluated using a Student's *t*-test. All analyses were performed with IBM SPSS 20 software (IBM, Armonk, NY). Statistical significance was defined at $p < 0.05$.

Results

Expression of FoxO1 mRNA and FoxO1 protein

The MT-2 cell sub-lines CA1–3, CB1–3 and CR were established after continuous exposure to three kinds of asbestos, namely, chrysotile A, chrysotile B or crocidolite, respectively (Hyodoh et al. 2005; Miura et al. 2006; Maeda et al. 2011, 2012). Those established sub-lines exhibited reduced apoptotic fractions when exposed to CA, CB or CR at a high concentration. Microarray gene expression analysis of MT-2CA1–3, CB1–3 and MT-2Org cells revealed 84 genes were up-regulated and 55 genes down-regulated in the MT-2 sub-lines exposed to asbestos. The current study focused on FoxO1 – a protein whose transcriptional activity is induced by reactive oxygen species and that regulates apoptosis in various cells (Accili & Arden 2004; Eijkelenboom & Burgering 2013) – which was reduced in MT-2 cells after continuous exposure to asbestos. The study initially examined expression of *FoxO1* mRNA in cells

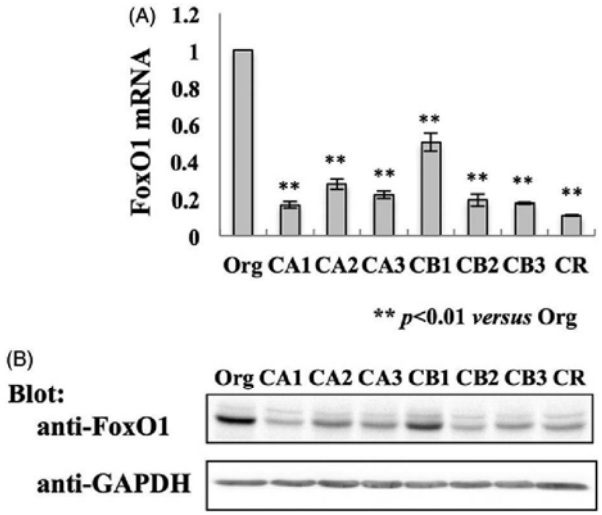

Figure 1. Expression of FoxO1 in MT-2Org and MT-2Rst cells. (A) Total RNA was isolated from MT-2Org and MT-2Rst cells and amount of *FoxO1* mRNA measured by real-time RT-PCR. The amount of FoxO1 mRNA in MT-2Org is shown as 100%. Data shown are means ± SD of three independent experiments. (B) Cell extracts of MT-2Org and MT-2Rst were analyzed by immunoblotting using anti-FoxO1 or anti-GAPDH antibodies. Data are representative of three independent experiments. Differences between MT-2Org and MT-2Rst sub-lines were analyzed using a Dunnett's test.

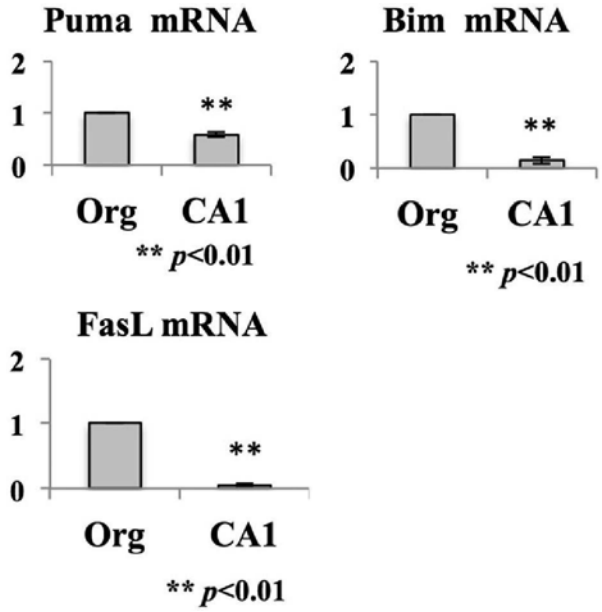

Figure 2. Expression of FoxO1 target genes. Total RNA was prepared from MT-2Org and MT-2CA1 cells and the amounts of *Bim*, *Puma* and *Fas-ligand* mRNA measured by real-time RT-PCR. Amounts shown are relative to those in MT-2Org cells. Data shown are means ± SD of three independent experiments. Differences between MT-2Org and MT-2CA1 were compared with using a Student's *t*-test.

using real-time RT-PCR (Figure 1A). The data showed that the amount of *FoxO1* mRNA in all the MT-2 sub-lines exposed to asbestos was 20–30% that in MT-2Org cells and was in agreement with the results of the microarray analysis. Consistent with the expression of *FoxO1* mRNA, the presence of the FoxO1 protein was down-regulated in MT-2 cells exposed to asbestos (Figure 1B).

Down-regulation of FoxO1 target genes

This study also analyzed mRNA expression of FoxO1 target genes related to induction of apoptosis (Figure 2). Puma and Bim – members of the Bcl-2 superfamily – have a pro-apoptotic function through binding to anti-apoptotic protein Bcl-2 or Bcl-xL (Puthalakath & Strasser 2002). Fas-ligand – a member of the TNF superfamily of cytokines – induces receptor-mediated apoptosis through binding to its receptor Fas (Nagata 1997). These genes have a FoxO1 binding sequence (i.e. Daf-16 binding element) on their promoter regions (Furuyama et al. 2000). In accordance with the reduction of FoxO1 in the MT-2Rst cells, the mRNA levels of these molecules were also decreased in the CA1 cells. These findings suggested that death signaling mediated by FoxO1 was suppressed in MT-2CA1 cells.

Knockdown of FoxO1 in MT-2Org cells

To investigate the effect of down-regulation of FoxO1 in MT-2 cells, FoxO1 knockdown cells were established by introducing lentivirus vector expressing shRNA targeting human FoxO1. The non-specific effects associated with RNA interference are well known; therefore, this study employed two different shRNA sequences targeting human FoxO1 as well as a scramble shRNA sequence as a control for knockdown of the FoxO1. As shown in Figure 3A, both of the shRNA targeting FoxO1 reduced the amount of FoxO1 protein in MT-2Org cells. To investigate the role of FoxO1 in regulation of apoptosis induced by chrysotile A, cells were treated with various concentrations of chrysotile A for 24 h. Knockdown of FoxO1 reduced the number of apoptotic cells after treatment with chrysotile A (25 μg/ml) to 50–70% of MT-2OrgCtrl cells; shRNA did not affect basal apoptotic levels. These results suggested FoxO1 played a role in regulation of apoptosis induced by chrysotile A in MT-2 cells.

Expression of FoxO1 in MT-2 CA1 cells

To investigate the effect of recovery of FoxO1 expression in MT-2CA1 cells, MT-2CA1 cells were infected with retrovirus vector expressing FLAG-epitope tagged human FoxO1. The resultant cells express FLAG-FoxO1

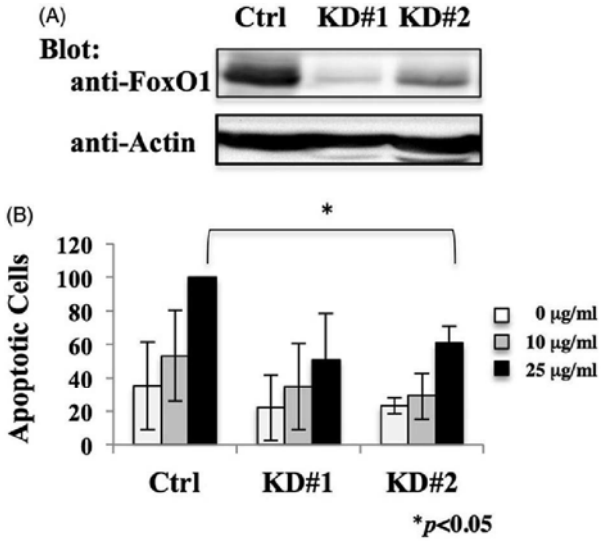

Figure 3. Effect of FoxO1 knock-down on MT-2Org cells. (A) Extracts from MT-2OrgCtrl, MT-2OrgKD#1 and MT-2OrgKD#2 cells were analyzed by immunoblotting using anti-FoxO1 and anti-actin antibodies. Data are representative of three independent experiments. (B) MT-2OrgCtrl and MT-2KD cells were treated with 10 (grey bars) or 25 (black bars) μg/ml chrysotile A for 24 h. Apoptotic cells were measured using flow cytometry. Values shown are relative to those of apoptotic cells of MT-2Ctrl treated with 25 μg/ml chrysotile A. Data shown are means ± SD of three independent experiments. Differences between Ctrl and KD#1 or Ctrl and KD#2 cells treated with 25 μg/ml chrysotile A were analyzed using a Student's *t*-test.

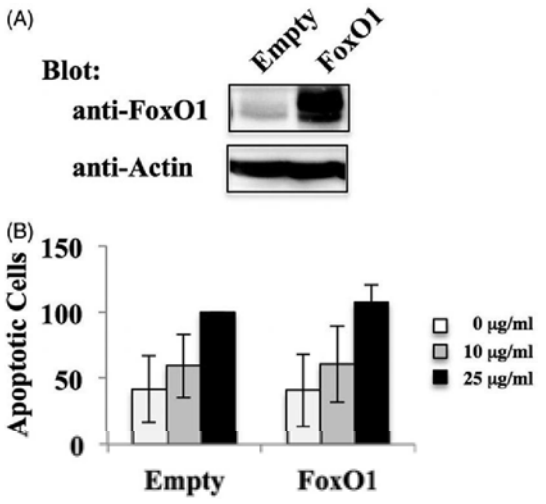

Figure 4. Effect of FoxO1 over-expression on MT-2CA1 cells. (A) Extracts of MT-CA1Empty and MT-2CA1FoxO1 cells were analyzed by immunoblotting using anti-FoxO1 and anti-actin antibodies. Data shown are representative of three independent experiments. (B) MT-CA1Empty and MT-2CA1FoxO1 cells were treated with 10 (grey bars) or 25 (black bars) μg/ml chrysotile A for 24 h. Control cells without treatment are shown as open bars. Apoptotic cells were measured using flow cytometry. Values shown are relative to those of apoptotic cells of MT-2Ctrl with 10 (grey bars) and 25 (black bars) μg/ml chrysotile A.

protein (Figure 4A) at a level above that of control MT-2CA1Empty cells. MT-2CA1FoxO1 cells express an amount of FoxO1 comparable to that of MT-2Org cells (data not shown). These cells were exposed to various concentrations of chrysotile A (Figure 4B). Expression of recombinant FoxO1 protein did not enhance the number of apoptotic cells or affect the basal level of apoptosis after treatments with chrysotile A at $\leq$ 25 μg/ml. This indicated that recovery of FoxO1 was not sufficient to cancel resistance to asbestos in MT-2CA1 cells. Therefore, expression of pro-apoptotic factor Puma, a target of FoxO1, was analyzed (Figure 5). Expression of *Puma* mRNA increased in cells expressing recombinant FoxO1 above that in the MT-2CA1Empty cells, indicating FLAG-FoxO1 could function to induce target gene expression in MT-2CA1 cells. However, expression of anti-apoptotic factor Bcl-2 was not affected by FoxO1 expression. We previously reported that Bcl-2 was up-regulated in CA1 in a STAT3-dependent manner (Miura et al. 2006; Maeda et al. 2012). The findings here indicated that expression of Bcl-2 was independent of FoxO1, and that survival signaling via Bcl-2 could overcome death signaling induced by expression of FoxO1.

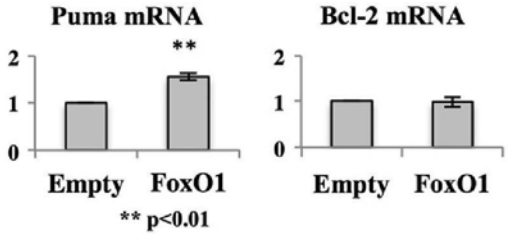

Figure 5. Expression of anti- or pro-apoptotic factors in MT-2CA1FoxO1. Total RNA was isolated from MT-2CA1Empty and MT-2CA1FoxO1 cells and the amount of *Puma* or *Bcl-2* measured using real-time RT-PCR. Values shown are relative to the amount in MT-2CA1Empty cells. Differences between MT-2CA1Empty and MT-2CA1FoxO1 cells were analyzed using a Student's *t*-test.

Discussion

It is well known that exposure to asbestos causes various diseases of the respiratory system including pulmonary fibrosis, asbestos-related pleural plaque (PP), lung cancer, and malignant pleural mesothelioma (MPM) (Lemen et al. 2006; Craighead et al. 2008). Mechanisms proposed for the cellular transformations caused by asbestos involve (1) iron-including asbestos fibers such as crocidolite and amosite causing ROS production in cells around the fibers, as well as apoptosis of alveolar macrophages following insufficient destruction of phagocytized fibers – all of which result in DNA damage in cells surrounding the fibers – and (2) physical DNA

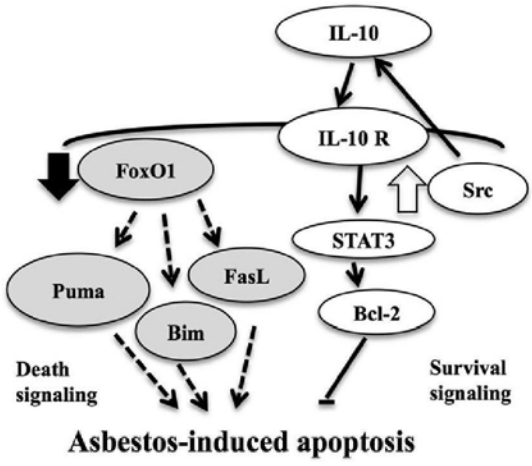

Figure 6. Schematic representation of proposed effect of asbestos on FoxO1 signaling pathway.

damage caused by the direct action of the incorporated fibers on chromatin. It was reported recently that chrysotile that does not include iron also induces iron overload in a rat model (Jiang et al. 2012). Furthermore, molecular analysis of MPM cells revealed several molecules implicated in the development of MPM. In particular, inactivation of the NF2/merlin signaling pathway caused by loss of NF2/merlin, LATS2 (Murakami et al. 2011) or up-regulation of YAP1 (Mizuno et al. 2012) in MPM cells. In addition, inactivation of p16/ink4a, inactivation of tumor suppressor PTEN, and somatic mutations of BRCA 1-associated protein-1 (BAP1) were also reported in MPM cells (Kratzke et al. 1995; Opitz et al. 2008; Bott et al. 2011; Testa et al. 2011). We have focused on the immunological effects of asbestos; our studies have shown that asbestos fibers suppressed NK and CTL cell functions (Nishimura et al. 2009a,b; Matsuzaki et al. 2012; Kumagai-Takei et al. 2013).

MT-2 cells have been used as a CD4 T-cell model for chronic and continuous exposure to a low concentration of asbestos in human respiratory tissue. Studies with MT-2 cells revealed that asbestos fibers modified the characters of MT-2 cells, such as over-expression of Bcl-2, expression of cytokine production, reduction of chemokine C-X-C receptor-3 (CXCR3) and alteration of cytoskeletal molecules. In particular, over-expression of Bcl-2 was also found in CD4 T-cells isolated from PP or MPM patients (Miura et al. 2006). CXCR3 and interferon (IFN)-γ are basically expressed in activated T-helper (T_H)-1-type cells, playing an important role in host-defense during immune surveillance against malignant cells (Rotondi et al. 2007). Similar results were obtained with *ex vivo* and *in vivo* analyses. Continuous exposure to asbestos reduced the expression of cell surface CXCR3 and IFNγ in CD4 T-cells freshly prepared from healthy donors. CD4 T-cells from PP or MPM patients express a lower amount of CXCR3 and IFNγ compared with those from healthy donors. These results supported the claim that the MT-2 cell is a good model for analyzing the effect of asbestos on human CD4 T-cells. On the other hand, it was reported that MT-2 cells express FoxP3, known as a master gene of the regulatory T (T_{reg}) cell (Yagi et al. 2004; Ohkura et al. 2013).

T_{reg} cells are designated as $CD4^+CD25^+FoxP3^+$ T-cells that inactivate immune responses in part through the suppressive cytokines transforming growth factor (TGF)-β and IL-10. T_{reg} cells are also thought to be involved in the development/progression of tumors, including MPM (Nishikawa & Sakaguchi 2010; Ireland et al. 2012). In particular, T_{reg} cells are found in MPM tissues (Hegmans et al. 2006; Anraku et al. 2008; Shimizu et al. 2009); depletion of T_{reg} cells with a neutralizing antibody induces rejection of malignant mesothelioma in mice (Hegmans et al. 2006). We previously reported that MT-2 cells produced TGFβ and IL-10 and inhibit the proliferation of effector cells *in vitro* (Maeda et al. 2008). Furthermore, it was shown that MT-2 sub-lines continuously exposed to asbestos produced more TGFβ and IL-10 than did parental cells. In agreement with those observations, the concentrations of TGFβ and IL-10 in the blood of PP or MPM patients was shown to be higher than in that of healthy donors (Maeda et al. 2008). It is possible exposure to asbestos enhanced production of suppressive cytokines by T_{reg} cells *in vivo*.

The present study clearly showed that transcription factor FoxO1 was down-regulated in the MT-2Rst sub-lines (Figure 6). Further, expression of pro-apoptotic factors regulated by FoxO1, i.e. Fas-ligand, Puma and Bim, were also suppressed in MT-2CA1 and that this outcome was consistent with reductions in cell levels of FoxO1 protein. Moreover, death signaling mediated by FoxO1 was suppressed by continuous exposure to asbestos in MT-2 cells and knockdown of FoxO1 in MT-2Org cells reduced the number of apoptotic cells induced by chrysotile A. It is known that FoxO1 regulates multiple target genes that control various cellular processes, such as apoptosis, metabolism and cell cycle progression (Eijkelenboom & Burgering 2013). Therefore, it is plausible that multiple FoxO1 target molecules and signaling pathways implicated in apoptosis were affected by knockdown or down-regulation of FoxO1 in the MT-2 cells. These results suggested to us that down-regulation of FoxO1 played an important role in the escape from apoptosis induced by asbestos in the MT-2 cells. On the other hand, over-expression of FoxO1 in MT-2CA1 cells did not alter expression of Bcl-2 or the number of apoptotic cells, indicating that expression of Bcl-2 was

independent of FoxO1. These results suggested that both suppression of FoxO1 and over-expression of Bcl-2 contributed to MT-2CA1 cell resistance against asbestos-induced apoptosis. It is also possible down-regulation of FoxO1 affected various cellular processes – including cell cycle progression and metabolism – in addition to suppressing apoptosis. Further analysis is required to more fully evaluate the role of FoxO1 down-regulation induced by asbestos to gain a more complete understanding of mechanisms of effects of asbestos on T-cells.

Both FoxO1 and Bcl-2 are implicated in the general processes of apoptosis. Thus, MT-2 cells exposed to asbestos may have resistance to other natural apoptotic stimuli. Furthermore, asbestos fibers may induce ectopic viability to increase the number of T_{reg} cells around the asbestos fibers. In addition to the findings in this study, FoxO1 is thought to suppress cell cycle progression (Eijkelenboom & Burgering 2013). Thus, it is possible that a loss of FoxO1 accelerated proliferation of MT-2 and T_{reg} cells *in vitro* and *in vivo*.

The overall results here indicated that asbestos might activate T_{reg} cell function through multiple pathways, ectopic viability, proliferation and cytokine production, as well as suppress tumor immunity. Further analyses are clearly needed required to characterize the overall chronic effect of asbestos on the immune system.

Conclusions

Our laboratory previously reported long-term exposure to asbestos altered immune cells *in vivo* and *in vitro*. Specifically, the human T-cell line MT-2 acquired resistance to a high concentration of asbestos after continuous exposure to low concentrations of asbestos *in vitro*. The present study clearly showed the effects of long-term exposure to asbestos on transcription factor FoxO1 in MT-2 cells. Namely, continuous exposure to asbestos reduced the expression of FoxO1 and its downstream pro-apoptotic factors Bim, Puma and Fas ligand. Furthermore, knock-down of FoxO1 suppressed asbestos-induced apoptosis in the MT-2 cells. These results indicated FoxO1 regulated apoptosis induced by asbestos in MT-2 cells and down-regulation of FoxO1 signaling was implicated in the acquisition of resistance to asbestos after continuous exposure to asbestos in these cells. These findings might help to increase our understanding of the effect of asbestos on tumor immunity during the progression of malignant mesothelioma.

Acknowledgments

The authors thank Ms. Tamayo Hatayama and Shoko Yamamoto for their technical support. This study was supported by JSPS KAKENHI Grant Number 23890237 and 25860471 and Kawasaki Medical School Project Grants 23-6, 24-4 and 25-67.

Disclosure statement

The authors report no conflicts of interests. The authors alone are responsible for the content and writing of the paper.

References

Accili D, Arden KC. 2004. FoxOs at the crossroads of cellular metabolism, differentiation, and transformation. Cell. 117:421–426.

Anraku M, Cunningham KS, Yun Z, Tsao MS, Zhang L, Keshavjee S, Johnston MR, De Perrot M. 2008. Impact of tumor-infiltrating T-cells on survival in patients with malignant pleural mesothelioma. J Thoracic Cardiovasc Surg. 135:823–829.

Bott M, Brevet M, Taylor BS, Shimizu S, Ito T, Wang L, Creaney J, Lake RA, Zakowski MF, Reva B, et al. 2011. The nuclear deubiquitinase BAP1 is commonly inactivated by somatic mutations and 3p21.1 losses in malignant pleural mesothelioma. Nat Genet. 43:668–672.

Craighead JE, Craighead J, Gibbs A, Editors. 2008. Diseases associated with asbestos industrial products and environmental exposure. New York: Oxford University Press.

Eijkelenboom A, Burgering BM. 2013. FOXOs: Signalling integrators for homeostasis maintenance. Nat Rev Mol Cell Biol. 14:83–97.

Furuyama T, Nakazawa T, Nakano I, Mori N. 2000. Identification of the differential distribution patterns of mRNAs and consensus binding sequences for mouse DA-16 homologues. Biochem J. 349:629–634.

Hegmans JP, Hemmes A, Hammad H, Boon L, Hoogsteden HC, Lambrecht BN. 2006. Mesothelioma environment comprises cytokines and T-regulatory cells that suppress immune responses. Eur Respir J. 27:1086–1095.

Huang SX, Jaurand MC, Kamp DW, Whysner J, Hei TK. 2011. Role of mutagenicity in asbestos fiber-induced carcinogenicity and other diseases. J Toxicol Environ Health. 14:179–245.

Hyodoh F, Takata-Tomokuni A, Miura Y, Sakaguchi H, Hatayama T, Hatada S, Katsuyama H, Matsuo Y, Otsuki T. 2005. Inhibitory effects of anti-oxidants on apoptosis of a human polyclonal T-cell line, MT-2, induced by an asbestos, chrysotile A. Scand J Immunol. 61:442–448.

Ireland DJ, Kissick HT, Beilharz MW. 2012. The role of regulatory T-cells in meso-thelioma. Cancer Microenviron. 5:165–172.

Izzi V, Masuelli L, Tresoldi I, Foti C, Modesti A, Bei R. 2012. Immunity and malignant mesothelioma: from mesothelial cell damage to tumor development and immune response-based therapies. Cancer Lett. 322:18–34.

Jiang L, Akatsuka S, Nagai H, Chew SH, Ohara H, Okazaki Y, Yamashita Y, Yoshikawa Y, Yasui H, Ikuta K, et al. 2012. Iron overload signature in chrysotile-induced malignant mesothelioma. J Pathol. 228:366–377.

Kitamura T, Koshino Y, Shibata F, Oki T, Nakajima H, Nosaka T, Kumagai H. 2003. Retrovirus-mediated gene transfer and

expression cloning: Powerful tools in functional genomics. Exp Hematol. 31:1007–1014.
Kohyama N, Shinohara Y, Suzuki Y. 1996. Mineral phases and some re-examined characteristics of the International Union Against Cancer standard asbestos samples. Am J Indust Med. 30:515–528.
Kratzke RA, Otterson GA, Lincoln CE, Ewing S, Oie H, Geradts J, Kaye FJ. 1995. Immunohistochemical analysis of the p16INK4 cyclin-dependent kinase inhibitor in malignant mesothelioma. J Natl Cancer Inst. 87:1870–1875.
Kumagai-Takei N, Nishimura Y, Maeda M, Hayashi H, Matsuzaki H, Lee S, Hiratsuka J, Otsuki T. 2013. Effect of asbestos exposure on differentiation of cytotoxic T-lymphocytes in mixed lymphocyte reaction of human peripheral blood mononuclear cells. Am J Respir Cell Mol Biol. 49:28–36.
Lemen RA, Dodson R, Hammar S, editors. 2006. Epidemiology of asbestos-related diseases and the knowledge that led to what is known today. Boca Raton (FL): CRC Press.
Maeda M, Miura Y, Nishimura Y, Murakami S, Hayashi H, Kumagai N, Hatayama T, Katoh M, Miyahara N, Yamamoto S, et al. 2008. Immunological changes in mesothelioma patients and their experimental detection. Clin Med Circ Respir Pulm Med. 2:11–17.
Maeda M, Nishimura Y, Hayashi H, Kumagai N, Chen Y, Murakami S, Miura Y, Hiratsuka J, Kishimoto T, Otsuki T. 2011. Reduction of CXC chemokine receptor 3 in an *in vitro* model of continuous exposure to asbestos in a human T-cell line, MT-2. Am J Respir Cell Mol Biol. 45:470–479.
Maeda M, Nishimura Y, Kumagai N, Hayashi H, Hatayama T, Katoh M, Miyahara N, Yamamoto S, Hirastuka J, Otsuki T. 2010. Dysregulation of the immune system caused by silica and asbestos. J Immunotoxicol. 7:268–278.
Maeda M, Yamamoto S, Chen Y, Kumagai-Takei N, Hayashi H, Matsuzaki H, Lee S, Hatayama T, Miyahara N, Katoh M, et al. 2012. Resistance to asbestos-induced apoptosis with continuous exposure to crocidolite on a human T-cell. Sci Total Environ. 429:174–182.
Matsuzaki H, Maeda M, Lee S, Nishimura Y, Kumagai-Takei N, Hayashi H, Yamamoto S, Hatayama T, Kojima Y, Tabata R, et al. 2012. Asbestos-induced cellular and molecular alteration of immunocompetent cells and their relationship with chronic inflammation and carcinogenesis. J Biomed Biotechnol. 2012:492608.
Miura Y, Nishimura Y, Katsuyama H, Maeda M, Hayashi H, Dong M, Hyodoh F, Tomita M, Matsuo Y, Uesaka A, et al. 2006. Involvement of IL-10 and Bcl-2 in resistance against an asbestos-induced apoptosis of T-cells. Apoptosis. 11:1825–1835.
Mizuno T, Murakami H, Fujii M, Ishiguro F, Tanaka I, Kondo Y, Akatsuka S, Toyokuni S, Yokoi K, Osada H, et al. 2012. YAP induces malignant mesothelioma cell proliferation by upregulating transcription of cell cycle-promoting genes. Oncogene. 31:5117–5122.
Murakami H, Mizuno T, Taniguchi T, Fujii M, Ishiguro F, Fukui T, Akatsuka S, Horio Y, Hida T, Kondo Y, et al. 2011. LATS2 is a tumor suppressor gene of malignant mesothelioma. Cancer Res. 71:873–883.
Nagata, S. 1997. Apoptosis by death factor. Cell. 88:355–365.
Nishikawa H, Sakaguchi S. 2010. Regulatory T-cells in tumor immunity. Intl J Cancer. 127:759–767.
Nishimura Y, Maeda M, Kumagai N, Hayashi H, Miura Y, Otsuki T. 2009a. Decrease in phosphorylation of ERK following decreased expression of NK cell-activating receptors in human NK cell line exposed to asbestos. Intl J Immunopathol Pharmacol. 22:879–888.
Nishimura Y, Miura Y, Maeda M, Kumagai N, Murakami S, Hayashi H, Fukuoka K, Nakano T, Otsuki T. 2009b. Impairment in cytotoxicity and expression of NK cell-activating receptors on human NK cells following exposure to asbestos fibers. Intl J Immunopathol Pharmacol. 22:579–590.
Ohkura N, Kitagawa Y, Sakaguchi S. 2013. Development and maintenance of regulatory T-cells. Immunity. 38:414–423.
Opitz I, Soltermann A, Abaecherli M, Hinterberger M, Probst-Hensch N, Stahel R, Moch H, Weder W. 2008. PTEN expression is a strong predictor of survival in mesothelioma patients. Eur J Cardiothorac Surg. 33:502–506.
Puthalakath H, Strasser A. 2002. Keeping killers on a tight leash: Transcriptional and post-translational control of the pro-apoptotic activity of BH3-only proteins. Cell Death Differ. 9:505–512.
Robinson BW, Musk AW, Lake RA. 2005. Malignant mesothelioma. Lancet. 366:397–408.
Roggli VL, Oury TD, Sporn TA, editors. 2004. Pathology of asbestos-associated diseases. New York: Springer Verlag.
Rotondi M, Chiovato L, Romagnani S, Serio M, Romagnani P. 2007. Role of chemokines in endocrine autoimmune diseases. Endocr Rev. 28:492–520.
Schreiber RD, Old LJ, Smyth MJ. 2011. Cancer immunoediting: integrating immunity's roles in cancer suppression and promotion. Science. 331:1565–1570.
Shimizu Y, Dobashi K, Imai H, Sunaga N, Ono A, Sano T, Hikino T, Shimizu K, Tanaka S, Ishizuka T, et al. 2009. $CXCR4^{+}FoxP3^{+}CD25^{+}$ lymphocytes accumulate in CXCL12-expressing malignant pleural mesothelioma. Intl J Immunopathol Pharmacol. 22:43–51.
Testa JR, Cheung M, Pei J, Below JE, Tan Y, Sementino E, Cox NJ, Dogan AU, Pass HI, Trusa S, et al. 2011. Germline BAP1 mutations predispose to malignant mesothelioma. Nat Genet. 43:1022–1025.
Toyokuni S. 2009. Role of iron in carcinogenesis: Cancer as a ferrotoxic disease. Cancer Sci. 100:9–16.
Yagi H, Nomura T, Nakamura K, Yamazaki S, Kitawaki T, Hori S, Maeda M, Onodera M, Uchiyama T, Fujii S, et al. 2004. Crucial role of FoxP3 in the development and function of human $CD25^{+}CD4^{+}$ regulatory T-cells. Intl Immunol. 16:1643–1656.

Hindawi Publishing Corporation
Journal of Immunology Research
Volume 2016, Article ID 7484872, 10 pages
http://dx.doi.org/10.1155/2016/7484872

Research Article

The Suppressed Induction of Human Mature Cytotoxic T Lymphocytes Caused by Asbestos Is Not due to Interleukin-2 Insufficiency

Naoko Kumagai-Takei,[1] Yasumitsu Nishimura,[1] Hidenori Matsuzaki,[1] Suni Lee,[1] Kei Yoshitome,[1] Hiroaki Hayashi,[2] and Takemi Otsuki[1]

[1]*Department of Hygiene, Kawasaki Medical School, Kurashiki 701-0192, Japan*
[2]*Department of Dermatology, Kawasaki Medical School, Kurashiki 701-0192, Japan*

Correspondence should be addressed to Yasumitsu Nishimura; yas@med.kawasaki-m.ac.jp

Received 1 September 2016; Revised 19 October 2016; Accepted 30 October 2016

Academic Editor: Nejat K. Egilmez

We previously reported that exposure to chrysotile B (CB) asbestos suppressed the induction of mature cytotoxic T lymphocytes (CTLs) during mixed lymphocyte reaction assays (MLRs) with a decrease in the proliferation of immature CTLs. However, the mechanism responsible for the effect of asbestos fibers on the differentiation of CTLs remains unclear. Since interleukin-2 (IL-2) is a regulator of T lymphocyte proliferation, we examined the effect of IL-2 addition on suppressed CTL differentiation in CB-exposed cultures using flow cytometry (FCM). When IL-2 was added at 1 ng/mL on the second day of MLRs, the asbestos-caused decreases in the proliferation and percentages of $CD25^+$ and $CD45RO^+$ cells in $CD8^+$ lymphocytes were not recovered by IL-2 addition, although the decrease in percentage of granzyme B^+ cells was partially recovered. $CD8^+$ lymphocytes from the IL-2-treated culture with asbestos showed the same degree of cytotoxicity as those in cultures without IL-2 or asbestos. These findings indicate that IL-2 insufficiency is not the main cause for the suppressed induction of CTLs by asbestos exposure, although they suggest a potential for the improvement of such suppressed CTL functions. Secretory factors other than IL-2 in addition to membrane-bound stimulatory molecules may play a role in asbestos-caused suppressed CTL differentiation.

1. Introduction

The term "asbestos" is derived from the Greek meaning unquenchable and is now utilized as a generic term for a family of naturally occurring fibrous silicate minerals with a crystalline structure [1, 2]. These minerals have been greatly valued for their thermal resistance, flexibility, and durability. Asbestos minerals which consist of a silicate core are subclassified into two groups, amphibole and serpentine, according to the fiber morphology. Amphibole asbestos consists of sharp brittle javelin-shaped fibers with a high length-to-width ratio. This group includes crocidolite, amosite, tremolite, actinolite, and anthophyllite. In contrast, serpentine asbestos, such as chrysotile, comprises long curved fibers [1].

While asbestos possesses beneficial properties, as described above, the association between mesothelioma and asbestos exposure is undisputed [3, 4]. Wagner et al. reported the first association between asbestos exposure and mesothelioma in 1960 [5]. Following Wagner et al.'s study of mesothelioma subsequent to environmental and occupational exposure to asbestos, epidemiological and case-control studies from many industrialized nations have documented rising rates of malignant mesothelioma (MM) following the heavy commercial use of asbestos [3]. Studies have largely focused on the properties of asbestos fibers that are important in the development of MM and the mechanisms of action of asbestos in the multistage carcinogenic process. Asbestos fibers at cytotoxic concentrations cause chromosomal changes, DNA damage, and oxidative DNA lesions in mesothelial cells *in vitro* [6, 7]. The physical and chemical properties of asbestos are influenced by the type and proportion of other metals within the core structure, which

may explain the differing carcinogenic potential of various fibers [1].

In fact, the induction of malignant mesothelioma by exposure to asbestos is not a rapid process and takes a long period to develop [8–10]. This suggests the possibility that the development of malignant mesothelioma might be related to other functional alterations, such as those implicated by the idea that exposure to inhaled asbestos might gradually impair the immune response. On the basis of this hypothesis, we have thus far revealed several findings that include alteration in the expression profile of natural killer (NK) cell-activating receptors on human NK cells and functional alterations of $CD4^+$ T cells following exposure to asbestos [11, 12].

Recently we reported that asbestos exposure suppressed the differentiation of human mature CTLs during MLRs and was accompanied by decreases in the proliferation of immature CTLs [13]. $CD8^+$ lymphocytes in culture following exposure to asbestos showed impaired cytotoxicity with decreases in the proliferation and percentages of $CD25^+$ and $CD45RO^+$ cells in $CD8^+$ lymphocytes and an increase in percentage of $CD45RA^+$ cells, compared with those in control cultures. Additionally, we reported that patients with mesothelioma showed a decrease in $perforin^+$ cell levels in $CD8^+$ lymphocytes following stimulation with phorbol 12-myristate 13-acetate and ionomycin, whereas most of the healthy and plaque-positive individuals retained those cell levels following stimulation [14].

In the present study, we focused on investigating the mechanism of the previously reported phenomenon, asbestos-caused suppressed differentiation of mature CTLs with decreased proliferation of immature CTLs. IL-2 is a necessary cytokine for immature CTLs to proliferate during development into mature CTLs [15]. Therefore, we investigated whether IL-2 insufficiency might contribute to the suppressed induction of CTL upon exposure to asbestos. Previously we examined the production of IL-2 during MLRs upon exposure to asbestos [13]. However, after 7 days of the MLRs, the amount of IL-2 was very low in all culture supernatants assayed, and there were no differences in the production of IL-2 between the control culture and the culture with CB asbestos. We hypothesized that IL-2 may play an earlier role in the MLRs. Therefore, in the present study, we examined the production of IL-2 at the early period during MLRs. Additionally, IL-2 was added at 1 ng/mL on the second day of the MLRs to examine the effect of IL-2 addition on suppressed CTL differentiation in cultures exposed to CB asbestos.

2. Materials and Methods

2.1. MLRs. Peripheral blood mononuclear cells (PBMCs), isolated from heparinized blood by using a Ficoll-Hypaque density gradient (Separate-L, Muto Pure Chemicals Co. Ltd., Tokyo, Japan), were suspended in RPMI 1640 medium (Sigma-Aldrich, St. Louis, MO, USA) supplemented with 10% heat-inactivated fetal bovine serum (Medical and Biological Laboratories Co., Ltd., Nagoya, Japan), 100 μg/mL streptomycin, and 100 U/mL penicillin (Meiji Seika Pharma Co., Ltd., Tokyo, Japan). For the MLRs, 1.5×10^5 PBMCs were cultured with 5.0×10^4 allogenic PBMCs, which had been treated with irradiation of 40 Gy according to a previous method [16], and CB asbestos at 5 μg/mL. Following 2 days of the MLRs, IL-2 (Peprotech, Rocky Hill, NJ, USA) was added at 100 pg/mL or 1 ng/mL for 5 days. International Union Against Cancer (UICC) standard CB was kindly provided by the Department of Occupational Health at the National Institute for Occupational Health of South Africa [17]. All blood samples were taken from healthy volunteers who provided informed consent. The project was approved by the Institutional Ethics Committees of Kawasaki Medical School.

2.2. Enzyme-Linked Immunosorbent Assays (ELISA). After 2, 4, and 7 days of the MLRs, the culture supernatants were collected and assayed for the production of IL-2 using Quantikine ELISA kit (R&D Systems, Inc., Minneapolis, MN, USA). Four independent experiments were performed from three individuals.

2.3. Measurement of Cytotoxicity. Cytotoxicity against allogenic target cells was evaluated using FCM as previously described [8]. Allogenic PBMCs were stained using Vybrant™ DiO Cell-Labeling Solution (Molecular Probes, Inc., Eugene, OR, USA) during incubation for 20 mins at 37°C. After DiO-stained cells were washed with phosphate-buffered saline (PBS), effector cells (PBMCs harvested after MLRs) were incubated with 5000 DiO-labeled allogenic PBMCs in 96-well round bottom plates at several different effector/target (E/T) ratios for 5 h at 37°C in 5% CO_2. Three wells were prepared for each experimental group. Following incubation, cells were collected and stained with propidium iodide (PI) and then analyzed for the percentage of PI^+ cells among the total DiO-labeled cells (representing the percentage of lysed cells) using FACS Calibur™ (Becton Dickinson, Franklin Lakes, NJ, USA). Two independent experiments were performed. In part of the experiments, $CD8^+$ lymphocytes were stained and sorted with phycoerythrin-cychrome 5- (PC5-) conjugated anti-CD8 antibody (Ab) (Beckman Coulter, Inc., Brea, CA, USA) and FACSAria™ (Becton Dickinson) and then purified from the cells harvested after 7 days of the MLRs and assayed for cytotoxicity as described above. Two independent experiments were performed.

2.4. Assay for Expression Level of Cell-Surface and Intracellular Molecules. To examine the expression level of molecules on the cell surface, cells harvested after the MLRs were washed with PBS containing 2% FBS and then stained with the following Abs: PC5-conjugated anti-CD8 and fluorescein isothiocyanate- (FITC-) conjugated anti-CD3, FITC-conjugated anti-CD25 (Becton Dickinson), phycoerythrin- (PE-) conjugated anti-CD45RA, or PE-conjugated anti-CD45RO (BioLegend, San Diego, CA, USA) at room temperature in the dark for 30 min. Cells were then washed with PBS containing 2% FBS and resuspended in 0.3 mL of PBS containing 2% FBS for FCM analysis. To examine the expression level of intracellular granzyme B, cells were harvested after the MLRs and surfaces were stained with PC5-conjugated anti-CD8 Ab as described above. Surface stained cells were washed with PBS containing 2% FBS and

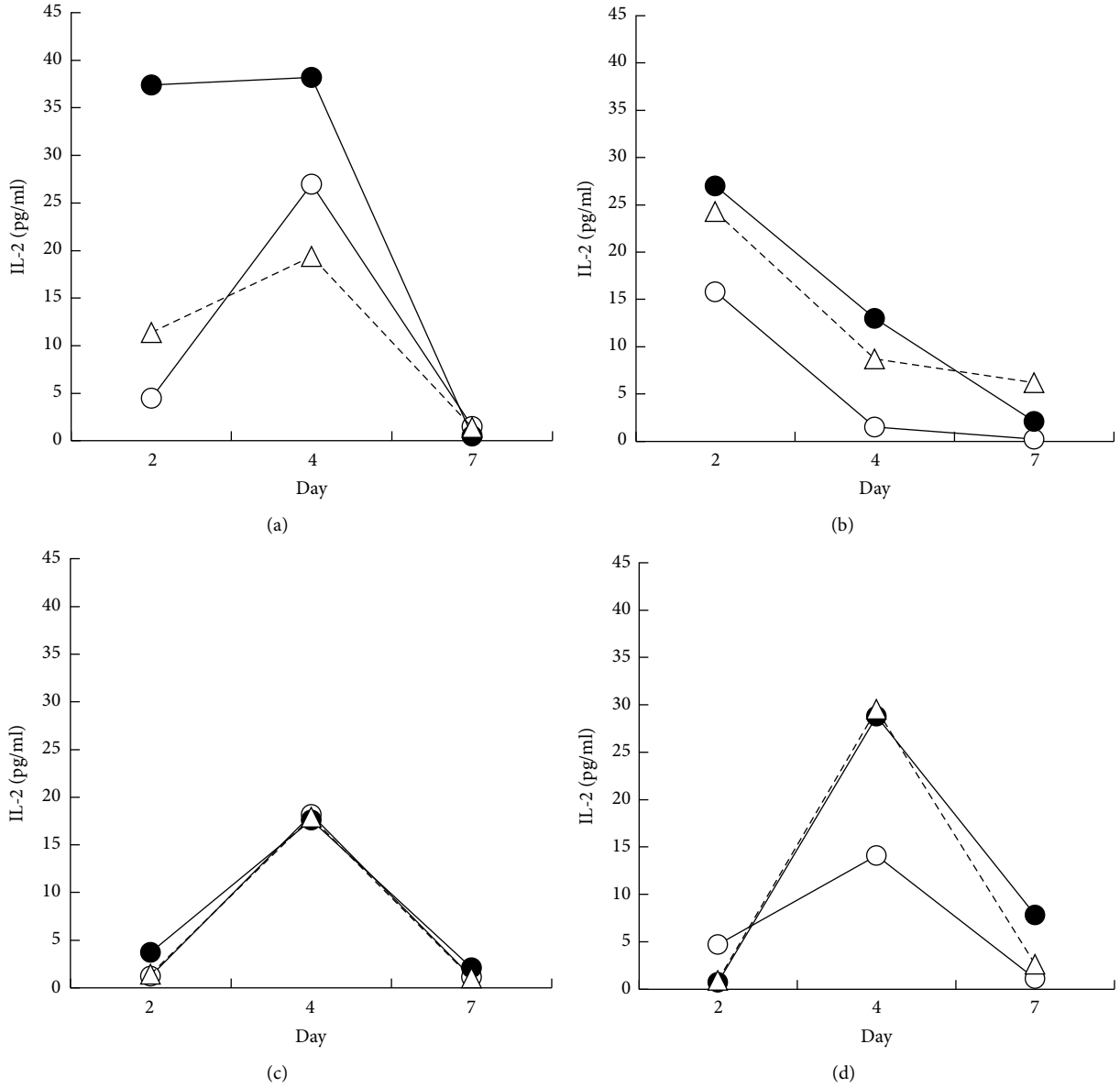

Figure 1: Production of IL-2 during the MLRs upon exposure to asbestos. After 2, 4, and 7 days of the MLRs, culture supernatants were harvested from the three groups, representing no stimulation (open circle), allostimulation (closed circle), and CB-exposed allostimulation (open triangle), and assayed for the production of IL-2 by ELISA. Data (a–d) from one of four independent experiments using PBMCs from three individuals.

then fixed with 3.7% formaldehyde for 15 min. Fixed cells were washed with PBS containing 2% FBS. Fixed cells were permeabilized with 0.1% Triton 100 and stained with R-phycoerythrin- (RPE-) conjugated anti-granzyme B Ab (AbD Serotec, Oxford, UK) at room temperature in the dark for 30 min. Cells were then washed and resuspended as described above. The percentage of cells positive for each parameter was analyzed using FCM. Four independent experiments were performed.

2.5. Analysis of Granzyme B Production in Proliferating and Nonproliferating CD8$^+$ Lymphocytes. To examine the effect of IL-2 on the expression level of intracellular granzyme B in proliferating and nonproliferating CD8$^+$ lymphocytes, PBMCs were stained using carboxyfluorescein diacetate succinimidyl ester (CFSE) (Molecular Probes) and then washed and used for MLRs. After MLRs, cells were harvested and stained with PC5-conjugated anti-CD8 and RPE-conjugated anti-granzyme B Abs as described above. The percentage of granzyme B$^+$ cells in proliferating CFSE-negative CD8$^+$ lymphocytes or nonproliferating CFSE$^+$ CD8$^+$ cells was analyzed using FCM. Four independent experiments were performed.

2.6. Statistical Analysis. Significance of difference ($p < 0.05$) was determined using an analysis of variance with the post hoc test of Student-Newman-Keuls or paired Student's t-test.

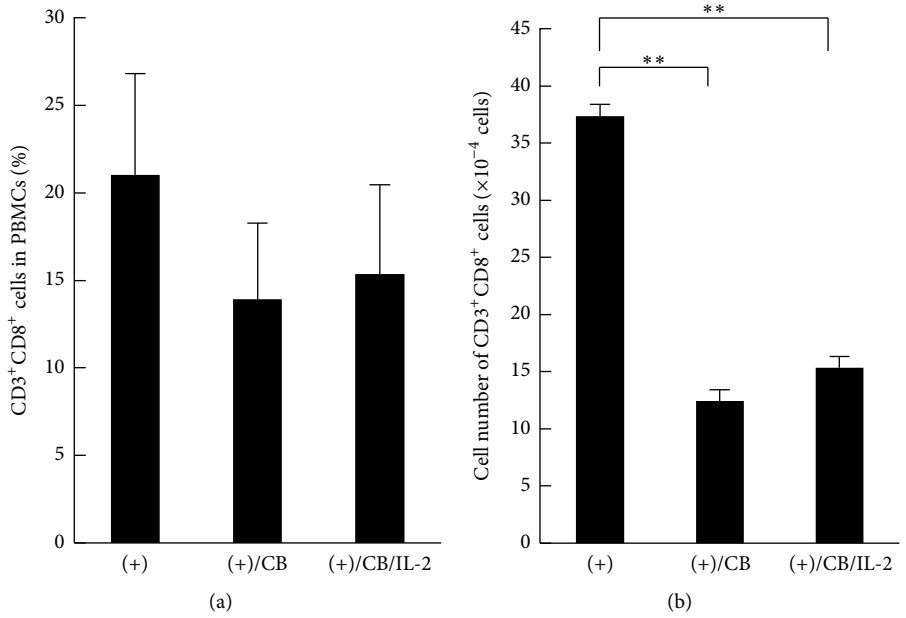

Figure 2: The percentage and number of $CD3^+CD8^+$ cells in PBMCs stimulated with allogenic PBMCs upon exposure to CB with IL-2. Freshly purified PBMCs were cultured with irradiated allogenic stimulator PBMCs in the presence of CB and the absence ((+)/CB) or presence ((+)/CB/IL-2) of IL-2. PBMCs were also cultured with allogenic PBMCs as a control group ((+)) without asbestos and IL-2. The percentage (a) and number (b) of $CD3^+CD8^+$ cells were measured by FCM in PBMCs harvested from 10 wells after culturing. Data represent the mean + SD from four independent experiments using PBMCs. Significant differences are indicated by asterisks ($^{**}p < 0.01$). (+), the culture with allogenic PBMCs without CB; (+)/CB, the culture with allogenic PBMCs with CB; (+)/CB/IL-2, the culture with allogenic PBMCs with CB and IL-2.

3. Results

3.1. Production of IL-2 during MLRs upon Exposure to Chrysotile B Asbestos. To examine the production of IL-2 at days 2, 4, and 7 after the MLRs, the supernatants from cultures of PBMCs stimulated allogenically in the absence or presence of CB asbestos were harvested. For part of the cultures, PBMCs were cultured alone and the supernatants were used as a group without allogenic stimulation. In 3 of the 4 experiments, the production of IL-2 tended to increase following allogenic stimulation to reach a peak at day 4 (Figures 1(a), 1(c), and 1(d)). Some of the CB-exposed cultures showed a decrease in IL-2 compared with the control culture without CB at day 4 (Figures 1(a) and 1(b)). In contrast, in the other CB-exposed cultures, the level of IL-2 production was the same as the control culture (Figures 1(c) and 1(d)). Thus, there were no differences in the production of IL-2 between trials involving the absence or presence of exposure to CB.

3.2. Effect of IL-2 on Percentage and Number of $CD3^+CD8^+$ Cells in PBMCs Stimulated upon Exposure to Asbestos. Although there were no significant differences in the production of IL-2 among the culture groups, the consumption of IL-2 by expanding T lymphocytes would mask the difference in IL-2 production. If insufficient production of IL-2 caused suppressed proliferation of $CD3^+CD8^+$ cells upon exposure to asbestos, exogenous IL-2 should restore such suppressed proliferation. Therefore, IL-2 was added to the asbestos-exposed culture at day 2 after the MLRs, and cells were harvested at day 7 to measure the percentage and number of $CD3^+CD8^+$ cells, since our previous study showed that the number of CFSE-negative cells, proliferating or going to the end of proliferation, increased markedly in $CD8^+$ lymphocytes by stimulation with allogenic PBMCs from day 6 to day 7 of the MLRs [13]. There was no statistically significant difference in the percentages of $CD3^+CD8^+$ cells between cultures with and without CB, which was similar to our previous report [13] (Figure 2(a)). The percentage of $CD3^+CD8^+$ cells in the IL-2-treated culture was the same as that present in the CB-exposed culture. It was also reconfirmed that exposure to CB causes a significant decrease in the number of $CD3^+CD8^+$ cells. Furthermore, the addition of IL-2 did not restore the asbestos-caused decrease in the number of $CD3^+CD8^+$ cells (Figure 2(b)). These results indicate that the addition of IL-2 to CB-exposed cultures did not affect either the percentage or the number of $CD3^+CD8^+$ cells.

3.3. Effect of IL-2 on Differentiation of Naïve $CD8^+$ T Cells into CTLs. To examine the effect of IL-2 addition on asbestos-caused suppressed differentiation of naïve $CD8^+$ T cells into effector/memory cells, we analyzed the expression of several cell-surface molecules on $CD8^+$ lymphocytes in the culture of PBMCs exposed to CB supplemented with IL-2. The percentage of cells positive for CD45RA and CD45RO, expressed on naïve and effector/memory cells, respectively [18, 19], as well as CD25 cells, expressed on activated cells [20], in $CD8^+$ lymphocytes was measured after 7 days of the MLRs, the time point that had also been utilized to confirm the differentiation of effector/memory cells in our previous study [13] (Figure 3(a)). The decrease in $CD45RA^+$ naïve cells in

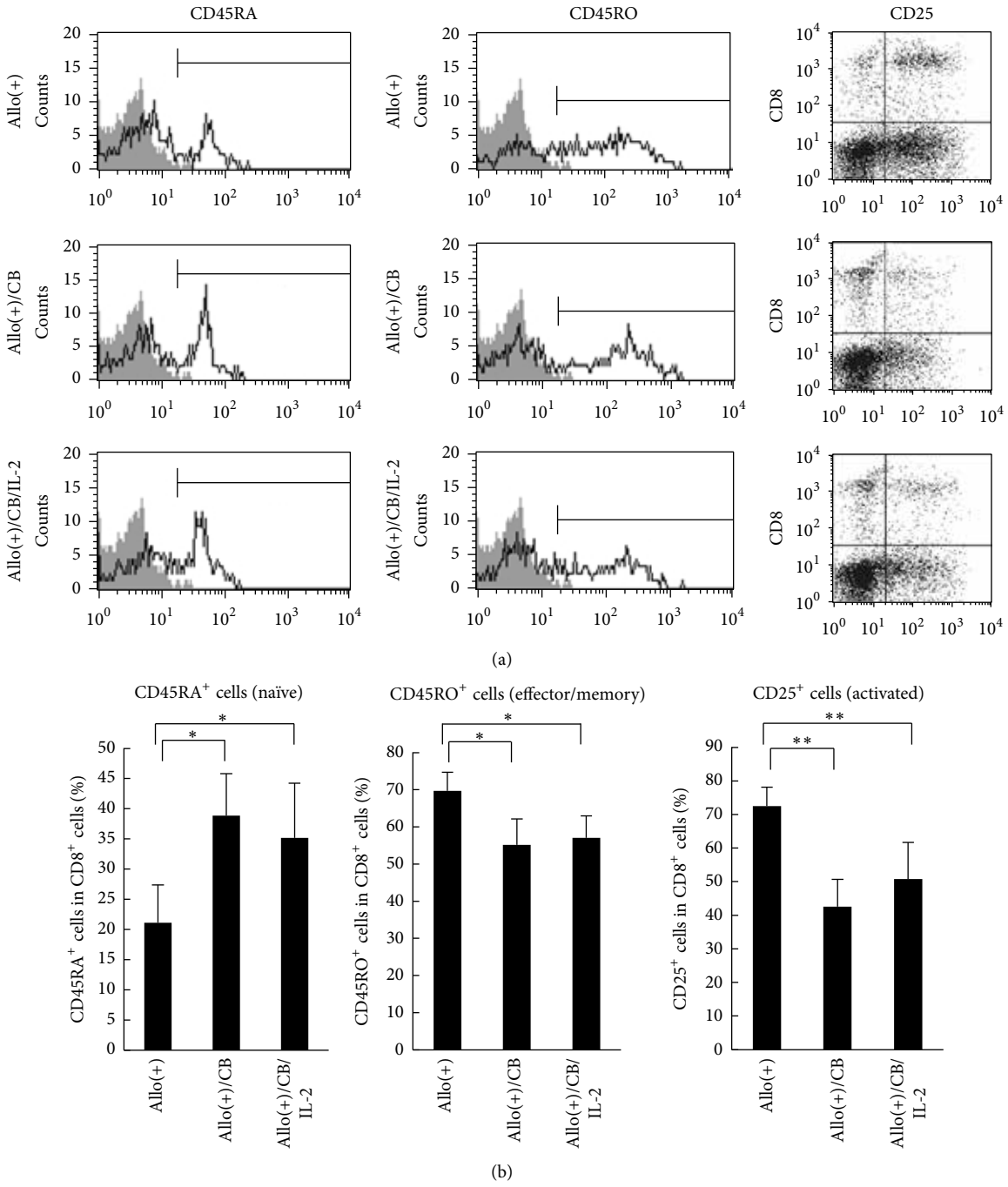

Figure 3: The percentage of cell-surface CD45RA-, CD45RO-, and CD25-positive cells in $CD8^+$ lymphocytes stimulated with allogenic cells upon exposure to CB with IL-2. PBMCs were harvested from the three groups, representing allostimulation, CB-exposed allo-stimulation, and CB-exposed allostimulation with IL-2, and assayed for the percentage of cells positive for CD45RA, CD45RO, and CD25 using FCM. (a) Representative histograms of cell-surface CD45RA and CD45RO expressed on $CD8^+$ lymphocytes. Representative dot plots of CD25 versus CD8 on PBMCs. (b) Cumulative data showing percentage of CD45RA-, CD45RO-, and CD25-positive cells in $CD8^+$ lymphocytes. Data represent the mean + SD from four independent experiments using PBMCs. Significant differences are indicated by asterisks ($^*p < 0.05$, $^{**}p < 0.01$). Allo(+), the culture with allogenic PBMCs without CB; allo(+)/CB, the culture with allogenic PBMCs with CB; allo(+)/CB/IL-2, the culture with allogenic PBMCs with CB and IL-2.

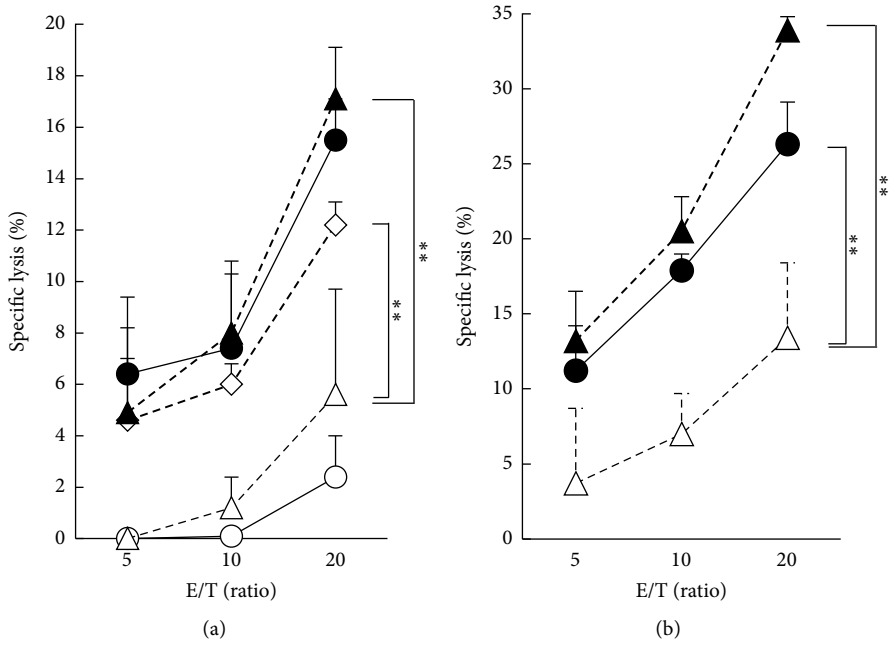

Figure 4: Cytotoxicity of PBMCs or $CD8^+$ lymphocytes stimulated with allogenic cells upon exposure to asbestos with IL-2. PBMCs were harvested after the MLRs and assayed for allogenic cytotoxicity using FCM. (a) Dose-dependent allogenic cytotoxicity of cultured PBMCs. PBMCs cultured alone (open circle) or with allogenic PBMCs in the absence (closed circle) or presence of CB (open triangle) or with CB and IL-2 at 100 pg/mL (open diamond) or with CB and IL-2 at 1 ng/mL (closed triangle) as effectors are shown. The percentage of specific lysis induced by effector cells was calculated as follows: (percentage of lysed cells − percentage of spontaneously dead cells)/(100 − percentage of spontaneously dead cells) × 100, where the percentage of spontaneously dead cells represented the percentage of dead cells in target cells harvested from the well without effector cells. Representative data from one of two independent experiments using PBMCs. Data represent the mean + SD from three wells at each E/T ratio. A significant difference is indicated by asterisks ($^{**}p < 0.01$). (b) Cytotoxicity of $CD8^+$ lymphocytes purified from PBMCs cultured with allogenic cells (closed circles), or with allogenic cells in the presence of CB (open triangles), or with CB and IL-2 at 1 ng/mL (closed triangle). The percentage of specific lysis induced by effector cells was calculated in the same manner as in (a). Representative data from one of two independent experiments using PBMCs. Data represent the mean + SD from three wells at each E/T ratio. A significant difference is indicated by asterisks ($^{**}p < 0.01$).

$CD8^+$ lymphocytes, resulting from stimulation with allogenic PBMCs, was suppressed upon exposure to CB (Figure 3(b)). The increases in $CD45RO^+$ effector/memory cells and $CD25^+$ activated cells in $CD8^+$ lymphocytes were also suppressed by exposure to CB. These results agree with those previously reported in which exposure to CB during MLRs suppressed differentiation into CTLs [13]. In the present study, the addition of IL-2 did not restore the suppression of increased levels of $CD25^+$ and $CD45RO^+$ cells in $CD8^+$ lymphocytes or the suppressed decrease in $CD45RA^+$ cell levels. These results indicate that exogenous supplementation of IL-2 did not lead to appropriate differentiation of CTLs upon exposure to CB during the MLRs.

3.4. Effect of IL-2 on Asbestos-Caused Suppression of Allogenic Cytotoxicity. To examine for the effect of IL-2 addition on asbestos-caused suppressed cytotoxicity, we analyzed the cytotoxicity of PBMCs or purified $CD8^+$ lymphocytes derived from cultures with allogenic PBMCs and CB supplemented with IL-2. Figure 4 shows the allogenic cytotoxicity of PBMCs (a) and sorted $CD8^+$ lymphocytes (b) in an E/T-ratio-dependent manner. PBMCs cultured with allogenic cells showed obvious cytotoxicity, whereas decreased cytotoxicity was observed in PBMCs exposed to CB during the MLRs. Contrary to our expectation, PBMCs cultured in media supplemented with 100 pg/mL IL-2 exhibited significantly increased allogenic cytotoxicity. Moreover, cells cultured in 1 ng/mL IL-2 showed the same degree of cytotoxicity as those of the allogenic control culture without IL-2 and asbestos (Figure 4(a)). Thus, as shown in Figure 2(b), although exposure to CB regardless of IL-2 treatment resulted in a decreased number of total $CD8^+$ T cells in PBMCs, the addition of IL-2 restored the suppressed allogenic cytotoxicity of PBMCs exposed to CB. To remove the difference in the number of total $CD8^+$ T cells among the cell groups within PBMCs and to clarify the effect of IL-2 on the allogenic cytotoxicity of $CD8^+$ lymphocytes themselves, we purified $CD8^+$ lymphocytes from cultured PBMCs and examined the allogenic cytotoxicity of $CD8^+$ T cells after the MLRs. $CD8^+$ cells purified from PBMCs exposed to CB during the MLRs showed decreased cytotoxicity compared with $CD8^+$ cells from PBMCs after the MLRs without CB, which was similar to the results in our previous report [13] (Figure 4(b)). Similar to the results obtained concerning the cytotoxicity of whole PBMCs, $CD8^+$ lymphocytes from a 1 ng/mL IL-2-treated culture with asbestos showed the same degree of cytotoxicity as those of the control culture without IL-2 or asbestos (Figure 4(b)). These results indicate that the addition of IL-2

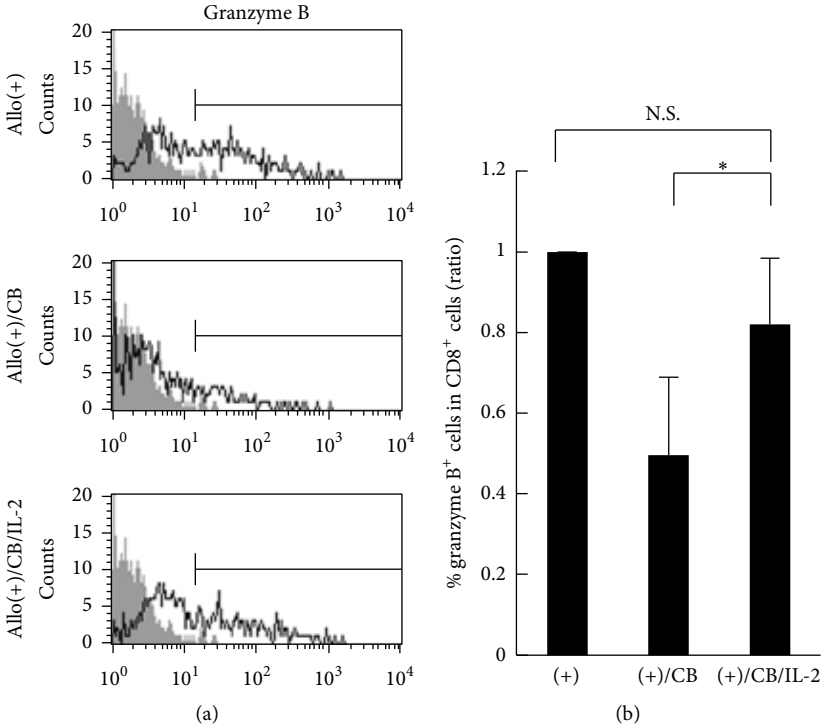

Figure 5: The percentage of granzyme B-positive cells in $CD8^+$lymphocytes stimulated with allogenic cells upon exposure to CB with IL-2. PBMCs were harvested from the three groups, representing allostimulation, CB-exposed allostimulation, and CB-exposed allostimulation with IL-2, and assayed for the percentage of cells positive for intracellular granzyme B using FCM. (a) Representative histograms of intracellular granzyme B in $CD8^+$lymphocytes. A nonstained control (gray) is shown in each panel. (b) Cumulative data showing the ratio of each group to the allostimulation control was calculated and compared among the groups. Data represent the mean + SD from four independent experiments using PBMCs. Significant differences are indicated by an asterisk ($^*p < 0.05$). No significant difference (N.S.) is also indicated. (+), the culture with allogenic PBMCs without CB; (+)/CB, the culture with allogenic PBMCs with CB; (+)/CB/IL-2, the culture with allogenic PBMCs with CB and IL-2.

to CB-exposed cultures led to recovery of the cytotoxicity of $CD8^+$ lymphocytes for allogenic targets.

3.5. Effect of IL-2 on Percentage of Granzyme B-Positive Cells in $CD8^+$ Lymphocytes. We analyzed the percentage of $CD8^+$ lymphocytes positive for intracellular granzyme B, a representative mediator of target cell death accomplished by CTLs, since our previous study showed that $CD8^+$ lymphocytes from PBMCs exposed to CB during the MLRs displayed suppressed cytotoxicity with a decrease in percentages of granzyme B^+ cells in our previous study [13]. It was again confirmed that the percentage of granzyme B^+ cells in $CD8^+$ lymphocytes increased following allogenic stimulation, whereas the percentage of granzyme B^+ cells in $CD8^+$ lymphocytes was significantly lower following exposure to CB during the MLRs (0.5 ± 0.2 ratio (mean ± S.D.)), which was similar to the results in our previous report [13]. In accordance with the increase in cytotoxicity of $CD8^+$ lymphocytes (Figure 4(b)), the addition of IL-2 partially, but not fully, restored the asbestos-caused decrease in the percentage of granzyme B^+ cells (0.8 ± 0.2 ratio) (Figures 5(a) and 5(b)).

3.6. Effect of IL-2 on Induction of Granzyme B in Proliferating or Nonproliferating $CD8^+$ Lymphocytes. As mentioned above, the number of $CD8^+$ lymphocytes following exposure to CB did not increase by the addition of IL-2, whereas the cytotoxicity and granzyme B^+ cell levels increased. Therefore, we set out to determine whether the restored increase in granzyme B^+ cell levels induced by the addition of IL-2 might be accompanied by a recovery of cell proliferation. PBMCs were stained using CFSE before the MLRs to detect CFSE-negative proliferating cells. After 7 days of the MLRs, PBMCs were collected and stained using granzyme B and CD8 antibodies. As shown in Figure 6(a), addition of IL-2 did not restore the asbestos-caused suppressed proliferation of $CD8^+$ lymphocytes during the MLRs. As shown in Figures 6(b) and 6(c), the percentage of CFSE-positive (nonproliferating) and granzyme B-positive cells in $CD8^+$ lymphocytes was 35.2% in asbestos-exposed cultures with exogenous IL-2, which tended to be higher than that observed in cultures without IL-2, being 19.3% ($p = 0.057$). In contrast, the level of CFSE-negative (proliferating) and granzyme B-positive cells did not increase with the addition of IL-2 in 3 of the 4 experiments. These results, together with the results mentioned above, indicate that exogenous addition of IL-2 did not result in appropriate CTL differentiation with cell proliferation but improved asbestos-caused suppressed cytotoxicity and partially restored intracellular granzyme B.

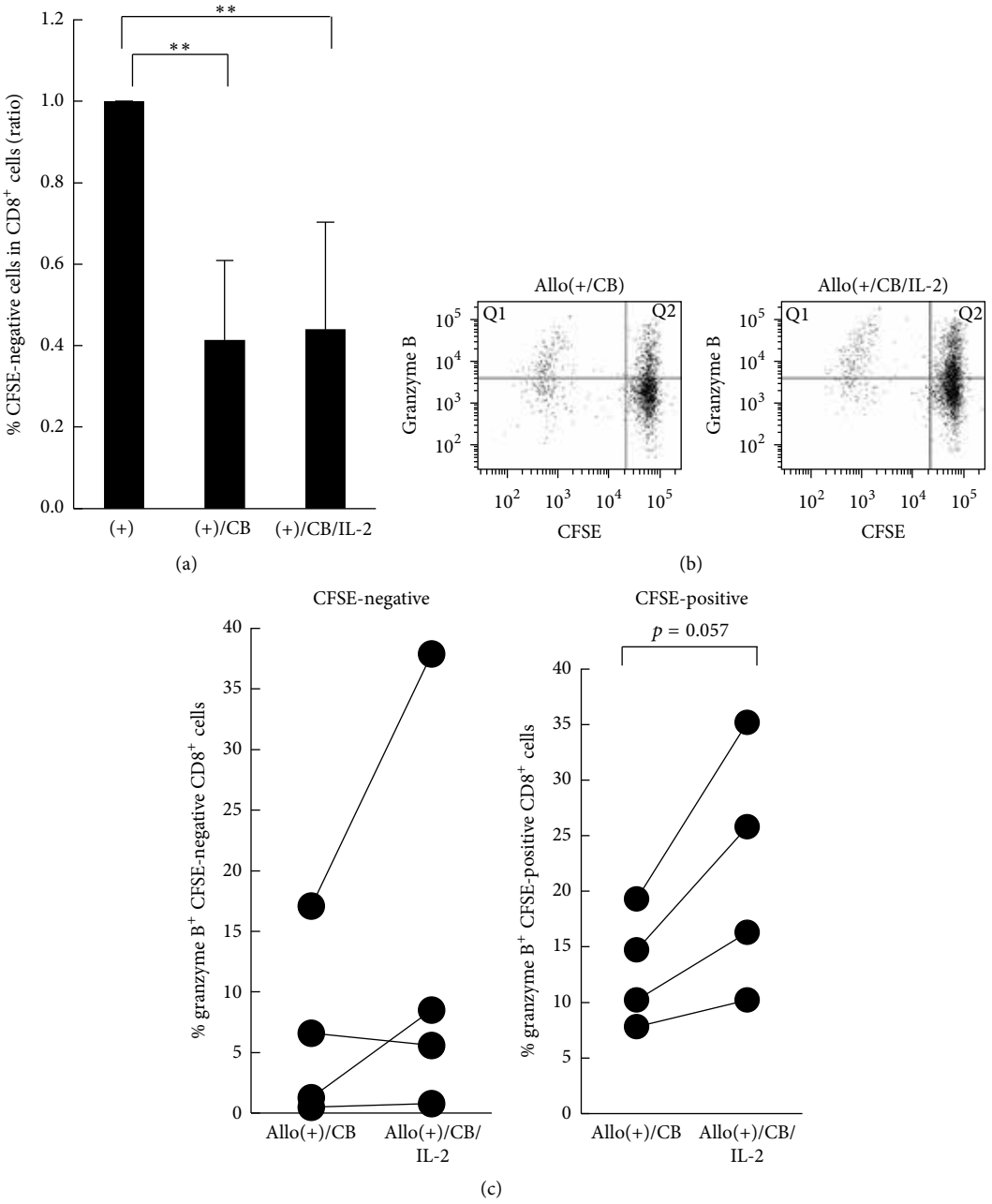

Figure 6: The induction of granzyme B in proliferative and nonproliferative $CD8^+$ lymphocytes in the presence of asbestos with IL-2. PBMCs were harvested from the two groups, representing CB-exposed allostimulation and CB-exposed allostimulation with IL-2, and assayed for the percentage of cells positive for granzyme B in CFSE-negative proliferating or CFSE-positive nonproliferating $CD8^+$ lymphocytes using FCM. (a) Cumulative data showing the ratio of each group to the allostimulation control was calculated and compared among the groups. Data represent the mean + SD from four independent experiments using PBMCs. Significant differences are indicated by asterisks ($^{**}p < 0.01$). (b) Representative dot plots of granzyme B versus CFSE in $CD8^+$ lymphocytes. Granzyme B-positive cells of CFSE-negative $CD8^+$ lymphocytes (Q1) and granzyme B-positive nondividing cells of $CD8^+$ lymphocytes (Q2) were gated for analysis. (c) Cumulative data showing the percentage of granzyme B-positive cells in CFSE-negative or CFSE-positive $CD8^+$ lymphocytes. Data represent values from four independent experiments using PBMCs. (+), the culture with allogenic PBMCs without CB; (+)/CB or Allo(+/CB), the culture with allogenic PBMCs with CB; (+)/CB/IL-2 or Allo(+/CB/IL-2), the culture with allogenic PBMCs with CB and IL-2.

4. Discussion

Previously, we demonstrated that asbestos exposure suppressed the differentiation of mature CTLs and was accompanied by a decrease in the proliferation of immature CTLs [13]. However, the mechanism responsible for the effect of asbestos fibers on the differentiation of cytotoxic T cells has hitherto remained unknown. In this study, IL-2 addition partially recovered the percentage of granzyme B and the same degree of cytotoxicity as those of the control culture without IL-2 or asbestos, although it did not restore the number of $CD3^+CD8^+$ cells, the proliferation of $CD8^+$ lymphocytes, or the percentage of $CD45RA^+$, $CD45RO^+$, and $CD25^+$ cells in $CD8^+$ lymphocytes after the MLRs. These findings indicate that IL-2 addition did not restore the asbestos-caused suppressed differentiation and proliferation of $CD8^+$ lymphocytes by stimulation with allogenic PBMCs. The present study suggests a potential for improvement of such suppressed CTL functions, whereas it demonstrated that IL-2 insufficiency is not the main cause for the suppressed induction of CTLs with decreased proliferation of $CD8^+$ lymphocytes upon exposure to asbestos.

$CD8^+$ lymphocytes from IL-2-treated cultures with asbestos showed the same degree of cytotoxicity as those in cultures without IL-2 or asbestos, although IL-2 addition did not restore the suppressed proliferation of $CD8^+$ lymphocytes and CTL differentiation upon exposure to asbestos. Therefore, there remains the possibility that the increase in cytotoxicity is not specific against the allogenic target. However, it is known that noncognate antigen or some cytokines such as IL-2 without any antigens can bystander-activate polyclonal memory phenotype cells, but not naïve CD8 cells. Another group also reported that cultures with IL-2, and without antigen, induced the cytotoxic capacity in $CD8^+$ T cells by anti-CD3 antibody redirected lysis of Fc IgG-receptor-bearing P815 cells [21]. These findings indicated that bystander-activated $CD8^+$ T cells could kill targets if they make contact with target cells. Thus, in this study, polyclonal memory $CD8^+$ T cells included in PBMCs before the MLRs might be bystander-activated and kill targets by the addition of IL-2. It is noteworthy that asbestos-exposed $CD8^+$ lymphocytes showed a potential to recover cytotoxicity, although this was not accompanied by appropriate proliferation and CTL differentiation. The results of our present study can contribute towards the development of a strategy for the improvement of antitumor immunity in asbestos-exposed patients to avoid the development of malignant mesothelioma.

Thus, the partial recovery of granzyme B expression and enhanced cytotoxicity in $CD8^+$ lymphocytes by IL-2 addition indicate that memory $CD8^+$ T cells were activated in a TcR-independent manner (bystander activation), as described above. With such bystander activation, some memory $CD8^+$ T cells are known to be activated to engage in cell division [21]. However, in our present study, IL-2 addition did not restore the suppressed proliferation of $CD8^+$ lymphocytes exposed to asbestos during the MLRs. This question might be explained as follows. Tamang and coworkers reported that $CD8^+$ T cells can be partially activated to express granzyme B without being activated to engage in cell division by IL-2 in the absence of antigens [21]. Recently, Arneja et al. reported that the proliferation of $CD8^+$ T cells requires continuous Janus kinase (JAK) signal transduction from IL-2 receptor, but not its signal strength [22]. In contrast, cell size and metabolic activity increased with increasing cytokine dose (JAK signal strength) independent of time period in culture with IL-2 [22]. Although we have no data to account for the fact that IL-2 addition did not restore asbestos-caused suppressed proliferation of $CD8^+$ lymphocytes, it is possible that such incomplete recovery caused by IL-2 addition might be due to a mechanism related to the aforementioned findings.

5. Conclusion

Our present investigation demonstrated that the suppressed induction of CTLs upon exposure to asbestos is not attributed to IL-2 insufficiency, whereas addition of IL-2 improved the cytotoxicity of asbestos-exposed $CD8^+$ lymphocytes, even though in an incomplete manner. The former motivates us to explore a mechanism for suppressed CTL differentiation upon exposure to asbestos, in which secretory factors other than IL-2 in addition to membrane-bound stimulatory molecules might play a role. This approach could facilitate delineation of asbestos-caused suppressed CTL function. These issues will be examined in future studies.

Competing Interests

The authors declare that they have no conflict of interests.

Acknowledgments

Grant support from JPSS KAKENHI Grants (20890270, 25860470), Kawasaki Medical School Project Grant (21-107, 26B39), and Strategic Research Foundation Grant-Aided Project for Private Universities from Ministry of Education, Culture, Sport, Science, and Technology in Japan (S1291010) is gratefully acknowledged. The authors thank Ms. Tamayo Hatayama and Shoko Yamamoto for their technical help.

References

[1] J. E. King and P. S. Hasleton, "The epidemiology and aetiology of malignant mesotheliom," in *Malignant Pleural Mesothelioma*, K. O'Byrne and V. Rusch, Eds., pp. 1–18, Oxford University Press, New York, NY, USA, 2006.

[2] J. E. Craighead, A. R. Gibbs, and F. Pooley, "Mineralogy of asbestos," in *Asbestos and Its Diseases*, J. E. Craighead and A. Gibbs, Eds., pp. 23–38, Oxford University Press, New York, NY, USA, 2008.

[3] T. A. Sporn and V. L. Roggli, "Mesothelioma," in *Pathology of Asbestos-Associated Diseases*, V. L. Roggli, T. D. Oury, and T. A. Sporn, Eds., pp. 104–168, Springer, New York, NY, USA, 2004.

[4] B. T. Mossman, D. W. Kamp, and S. A. Weitzman, "Mechanisms of carcinogenesis and clinical features of asbestos-associated cancers," *Cancer Investigation*, vol. 14, no. 5, pp. 466–480, 1996.

[5] J. C. Wagner, C. A. Sleggs, and P. Marchand, "Diffuse pleural mesothelioma and asbestos exposure in the North Western

Cape Province," *British Journal of Industrial Medicine*, vol. 17, pp. 260–271, 1960.

[6] M. Dušinská, A. Collins, A. Kazimirova et al., "Genotoxic effects of asbestos in humans," *Mutation Research*, vol. 553, no. 1-2, pp. 91–102, 2004.

[7] J. Topinka, P. Loli, P. Georgiadis et al., "Mutagenesis by asbestos in the lung of λ-lacI transgenic rats," *Mutation Research/Fundamental and Molecular Mechanisms of Mutagenesis*, vol. 553, no. 1-2, pp. 67–78, 2004.

[8] A. D. McDonald and J. C. McDonald, "Mesothelioma after crocidolite exposure during gas mask manufacture," *Environmental Research*, vol. 17, no. 3, pp. 340–346, 1978.

[9] I. J. Selikoff, E. C. Hammond, and H. Seidman, "Mortality experience of insulation workers in the United States and Canada, 1943–1976," *Annals of the New York Academy of Sciences*, vol. 330, pp. 91–116, 1979.

[10] I. J. Selikoff, E. C. Hammond, and H. Seidman, "Latency of asbestos disease among insulation workers in the United States and Canada," *Cancer*, vol. 46, no. 12, pp. 2736–2740, 1980.

[11] Y. Nishimura, Y. Miura, M. Maeda et al., "Impairment in cytotoxicity and expression of NK cell-activating receptors on human NK cells following exposure to asbestos fibers," *International Journal of Immunopathology and Pharmacology*, vol. 22, no. 3, pp. 579–590, 2009.

[12] M. Maeda, Y. Nishimura, H. Hayashi et al., "Reduction of CXC chemokine receptor 3 in an *in vitro* model of continuous exposure to asbestos in a human T-cell line, MT-2," *American Journal of Respiratory Cell and Molecular Biology*, vol. 45, no. 3, pp. 470–479, 2011.

[13] N. Kumagai-Takei, Y. Nishimura, M. Maeda et al., "Effect of asbestos exposure on differentiation of cytotoxic t lymphocytes in mixed lymphocyte reaction of human peripheral blood mononuclear cells," *American Journal of Respiratory Cell and Molecular Biology*, vol. 49, no. 1, pp. 28–36, 2013.

[14] N. Kumagai-Takei, Y. Nishimura, M. Maeda et al., "Functional properties of CD8+ lymphocytes in patients with pleural plaque and malignant mesothelioma," *Journal of Immunology Research*, vol. 2014, Article ID 670140, 10 pages, 2014.

[15] Y.-P. Lai, C.-C. Lin, W.-J. Liao, C.-Y. Tang, and S.-C. Chen, "CD4+ T cell-derived IL-2 signals during early priming advances primary CD8+ T cell responses," *PLoS ONE*, vol. 4, article e7766, 2009.

[16] E. M. Bluman, G. S. Schnier, B. R. Avalos et al., "The c-kit ligand potentiates the allogeneic mixed lymphocyte reaction," *Blood*, vol. 88, no. 10, pp. 3887–3893, 1996.

[17] N. Kohyama, Y. Shinohara, and Y. Suzuki, "Mineral phases and some reexamined characteristics of the International Union against cancer standard asbestos samples," *American Journal of Industrial Medicine*, vol. 30, no. 5, pp. 515–528, 1996.

[18] D. Hamann, M. T. L. Roos, and R. A. W. van Lier, "Faces and phases of human $CD8^+$ T-cell development," *Immunology Today*, vol. 20, no. 4, pp. 177–180, 1999.

[19] H. Tomiyama, T. Matsuda, and M. Takiguchi, "Differentiation of human CD8+ T cells from a memory to memory/effector phenotype," *Journal of Immunology*, vol. 168, no. 11, pp. 5538–5550, 2002.

[20] W. L. Redmond, C. E. Ruby, and A. D. Weinberg, "The Role of OX40-mediated Co-stimulation in T-cell activation and survival," *Critical Reviews in Immunology*, vol. 29, no. 3, pp. 187–201, 2009.

[21] D. L. Tamang, D. Redelman, B. N. Alves, L. Vollger, C. Bethley, and D. Hudig, "Induction of granzyme B and T cell cytotoxic capacity by IL-2 or IL-15 without antigens: multiclonal responses that are extremely lytic if triggered and short-lived after cytokine withdrawal," *Cytokine*, vol. 36, no. 3-4, pp. 148–159, 2006.

[22] A. Arneja, H. Johnson, L. Gabrovsek, D. A. Lauffenburger, and F. M. White, "Qualitatively different T cell phenotypic responses to IL-2 versus IL-15 are unified by identical dependences on receptor signal strength and duration," *The Journal of Immunology*, vol. 192, no. 1, pp. 123–135, 2014.

Accelerated cell cycle progression of human regulatory T cell-like cell line caused by continuous exposure to asbestos fibers

SUNI LEE[1], HIDENORI MATSUZAKI[1], MEGUMI MAEDA[2], SHOKO YAMAMOTO[1], NAOKO KUMAGAI-TAKEI[1], TAMAYO HATAYAMA[1], MIHO IKEDA[1], KEI YOSHITOME[1], YASUMITSU NISHIMURA[1] and TAKEMI OTSUKI[1]

[1]Department of Hygiene, Kawasaki Medical School, Kurashiki, Okayama 701-0192; [2]Department of Biofunctional Chemistry, Division of Bioscience, Okayama University Graduate School of Natural Science and Technology, Kita-Ku, Okayama 700-8530, Japan

Received September 21, 2016; Accepted November 18, 2016

DOI: 10.3892/ijo.2016.3776

Abstract. Asbestos exposure causes malignant tumors such as lung cancer and malignant mesothelioma. Based on our hypothesis in which continuous exposure to asbestos of immune cells cause reduction of antitumor immunity, the decrease of natural killer cell killing activity with reduction of NKp46 activating receptor expression, inhibition of cytotoxic T cell clonal expansion, reduced CXCR3 chemokine receptor expression and production of interferon-γ production in $CD4^+$ T cells were reported using cell line models, freshly isolated peripheral blood immune cells from health donors as well as asbestos exposed patients such as pleural plaque and mesothelioma. In addition to these findings, regulatory T cells (Treg) showed enhanced function through cell-cell contact and increased secretion of typical soluble factors, interleukin (IL)-10 and transforming growth factor (TGF)-β, in a cell line model using the MT-2 human polyclonal T cells and its sublines exposed continuously to asbestos fibers. Since these sublines showed a remarkable reduction of FoxO1 transcription factor, which regulates various cell cycle regulators in asbestos-exposed sublines, the cell cycle progression in these sublines was examined and compared with that of the original MT-2 cells. Results showed that cyclin D1 expression was markedly enhanced, and various cyclin-dependent kinase-inhibitors were reduced with increased S phases in the sublines. Furthermore, the increase of cyclin D1 expression was regulated by FoxO1. The overall findings indicate that antitumor immunity in asbestos-exposed individuals may be reduced in Treg through changes in the function and volume of Treg.

Correspondence to: Dr Takemi Otsuki, Department of Hygiene, Kawasaki Medical School, 577 Matsushima, Kurashiki, Okayama 701-0192, Japan
E-mail: takemi@med.kawasaki-m.ac.jp

Key words: asbestos, regulatory T cell, cell cycle, FoxO1, cyclin D1

Introduction

Asbestos exposure causes lung fibrosis known as asbestosis, one of the most typical forms of pneumoconiosis, as well as pleural plaque (PP), benign pleural effusion, and diffuse pleural thickening (1-3). In addition to these benign diseases, the occurrence of malignant tumors such as lung cancer and malignant mesothelioma (MM) is an important consideration for the understanding and development of disease prevention methods, early diagnosis and treatment (4-6). The carcinogenic potential of asbestos fibers has been recognized. Initial DNA damage caused by production of reactive oxygen species (ROS) mainly derived from iron-including asbestos such as crocidolite (CRD) and amosite is considered the dominant cause of asbestos-induced carcinogenesis (7,8). Next, physiological DNA damage caused by asbestos fibers to pulmonary epithelial cells and pleural mesothelial cells is the other cause of malignant transformation because of the rigid and thin physical features of fibers with more than a 3 aspect ratio for fibers defined as a 'fiber' (9,10). In addition to these causes, the easy absorbance of other carcinogenic substances inhaled into the lung, such as tobacco smoke and air pollutants on the surface of asbestos fibers, may enhance the synergistic effects for malignant transformation, especially for lung epithelial cells, since the odds ratio for lung cancer caused by asbestos inhalation and tobacco smoking showed synergistic effects according to various epidemiological studies (9-11).

We have been investigating the immunological effects of asbestos fibers because asbestos is a mineral silicate possessing Si and O as the core chemicals, and silica (SiO_2) has been shown to affect immune competent cells. The evidence of dysregulation of the immune system caused by silica was confirmed epidemiologically by frequent complications of autoimmune diseases, as well as cell biological investigations which revealed chronic activation of responder and regulatory T cells (Treg; $CD4^+$, $CD25^+$ and forkhead box P3 (FoxP3) positive inhibitory cells) caused by silica particles (12-14). Considering the malignant complications in asbestos-exposed patients, it is possible that asbestos exposure promotes the

reduction of tumor immunity in these patients (15,16). It is on the basis of this viewpoint that we examined the effects of asbestos on human immune cells. Investigations involving human natural killer (NK) cells, a cell line and freshly isolated NK cells derived from healthy donors (HD) and stimulated *ex vivo*, showed reduction of NK cell killing activity with decreased expression of some NK cell-activating receptors such as NKG2D and 2B4, with the suppression of the mitogen-activated protein kinase (MAPK) signaling pathway (17,18). In addition, the most remarkable reduction among these activating receptors was NKp46 when comparing its expression to freshly isolated NK cells derived from HD, PP and MM patients (17,18). The expression of NKp46 on the surface of NK cells was well correlated with NK cell killing activities in these patients. Differentiation and clonal expansion of $CD8^+$ cytotoxic T lymphocytes (CTLs) were inhibited when chrysotile asbestos was co-cultured in a mixed lymphocyte reaction (MLR) assay with reduction of cell attacking molecules such as granzyme B and perforin (19,20).

Experiments involving T cells have been developed using cell line models with continuous exposure to chrysotile A (ChA), chrysotile B (ChB) or CRD for more than one year *in vitro*, with cells derived from the human T cell leukemia/lymphoma (HTLV)-1 virus immortalized human polyclonal cell line, MT-2. The original MT-2 cells (Org) showed apoptosis with activation of pro-apoptotic MAPK, mitochondrial apoptotic pathway and ROS production, when exposed transiently to ChA, ChB or CRD with relatively high doses of these fibers (21-24). However, when Org cells (MT-2 cells that never encountered asbestos fibers) were exposed continuously with relatively low doses of fibers (doses that do not yield apoptosis in less than half of the cells) for more than one year, these sublines (designated as CB1 to 3, CA1 to 3, and CR1 exposed to ChB, ChA and CRD, respectively, and established independently) exhibited changes in cell features (15,22,24). The cells showed acquisition of asbestos-induced apoptosis, alteration of cytokine production, excess production of interleukin (IL)-10 and transforming growth factor (TGF)-β, reduced production of interferon (IFN)-γ, resistance to TGF-β-induced growth inhibition, and enhanced phosphorylation and expression of β-actin on their cell surface (15,22-25). In addition to these alterations, the cell surfaces in these sublines showed reduction of C-X-C motif chemokine receptor 3 (CXCR3), which is known to be important to attract IFN-γ-producing and tumor attacking T cells near tumor cells (26-28). Coupled with reduced secretion of IFN-γ, these sublines were characterized by reduced antitumor immunity. These findings were confirmed in freshly isolated $CD4^+$ T cells derived from patients with PP or MM (26-28). Thus, considering these results and those obtained from NK cells and CTLs indicated that asbestos exposure causes reduction of antitumor immunity in asbestos-exposed individuals.

Since it was reported that MT-2 cells possess Treg function (29) and exhibit excess production of typical soluble factors such as Treg, IL-10 and TGF-β in CB1-3, CA1-3 and CR sublines continuously exposed to asbestos fibers such as ChB, ChA and CRD (15,22-25), it was thought that asbestos exposure of the MT-2 cell line causes enhanced Treg function. This possibility was investigated together with the increase in Treg function of sublines through cell cell contact, as well as the reported excess production of soluble factors (30).

It was also found that sublines continuously exposed to asbestos showed remarkably reduced expression of forkhead transcriptional factor 1 (FoxO1) (31). We reported that this reduced FoxO1 caused reduction of pro-apoptotic molecules such as Puma, Bim and Fas ligand in exposed sublines (CB1-3, CA1-3 and CR1), in addition to Bcl-2 overexpression induced by phosphorylation of signal tranducer and activator of transcription 3 (STAT3) caused by autocrine usage of overproduced IL-10 (31). FoxO1 is known to regulate various cell cycle regulators such as cyclins and cyclin-dependent kinase-inhibitors (CDK-Is) (32-36). Therefore, in this study we analyzed the expression of these cell cycle regulators and the status of cell cycle progression in sublines continuously exposed to asbestos, and compared the results with those obtained for Org cells.

Materials and methods

Cell lines and asbestos. Details of MT-2, Org and the asbestos-induced apoptosis resistant sublines (CA1-3, CB1-3 and CR1) have been reported previously (22-24). These cells were maintained in a humidified atmosphere of 5% CO_2 at 37˚C in RPMI-1640 medium supplemented with 10% fetal calf serum (FCS), streptomycin and penicillin. Seven asbestos-resistant sublines, CA1-3, CB1-3 and CR1, were generated by continuous exposure to ChA, ChB, and CRD, respectively. As previously reported (22-24), the doses of asbestos fibers for continuous exposure were 5-10 μg/ml. These doses induced less than half of the cells to proceed to apoptosis when transiently exposed (22-24). The International Union Against Cancer standard ChA and ChB were kindly provided by the Department of Occupational Health at the National Institute for Occupational Health, South Africa. In addition, ChA, ChB and CRD were kindly provided as standard fibers from the Japan Association for the Study of Fiber Materials. The mineralogical features of fibers used have been reported previously (37).

Real-time RT-PCR. The expression levels of various cell cycle regulators such as CDK-Is including $p21^{Cip1}$, $p27^{Kip1}$, $p57^{Kip2}$, $p16^{ink4a}$, $p15^{ink4b}$, $p18^{ink4c}$, and $p19^{ink4d}$, and cyclins including cyclin A, B, D1, D2 and E, were analyzed in Org and continuously exposed sublines (CA1-3, CB1-3 and CR) using the real-time RT-PCR method. All the primers used are listed in Table I. Total cellular mRNA from ORG, CA1-3. CB1-3 and CR1 cells was extracted using the RNeasy Mini kit (Qiagen GmbH, Hilden, Germany). After synthesis of the first strand of cDNA, real-time RT-PCR was performed using the SYBER Green method (Takara Bio Inc., Kusatsu, Japan) with the Mx3000P QPCR System (Agilent Technologies, Inc., Santa Clara, CA, USA) according to the manufacturer's instructions.

Western blotting. The procedures for western blotting were performed according to the previously reported methods (31). Briefly, MT-2Org cells and cells from asbestos continuously exposed sublines were lysed in 20 mM Tris-HCl (pH 7.5) containing 1 mM EDTA, 1 mM EGTA, 10 mM 2-mercaptoethanol, 1% Triton X-100, 1% sodium deoxycholate, 0.1% sodium lauryl sulfate, 150 mM NaCl and 1% protease

Table I. Primers used for real-time RT-PCR.

Gene	Sequences	
	Forward	Reverse
GAPDH	5'-GAGTCAACGGATTTGGTCGT -3'	5'-TTGATTTTGGAGGGATCTCG-3'
Cyclin A	5'-ATGTGTGCAGAAGGAGGTCC-3'	5'-GAAGGTCCATGAGACAAGGC-3'
Cyclin B	5'-CGAAGATCAACATGGCAGG-3'	5'-CTTGGAGAGGCAGTATCAACC-3'
Cyclin D1	5'-ATGTGTGCAGAAGGAGGTCC-3'	5'-CCTTCATCTTAGAGGCCACG-3'
Cyclin D2	5'-TGCAGAAGGACATCCAACC-3'	5'-AGGAACATGCAGACAGCACC-3'
Cyclin E	5'-TAAATGTCCCGCTCTGAGCC-3'	5'-ACGTTTGCCTTCCTCTTCCT-3'
p21Cip1	5'-AGCAGAGGAAGACCATGTGG-3'	5'-AGGCAGAAGATGTAGAGCGG-3'
p27Kip1	5'-AACGTGCGAGTGTCTAACGG-3'	5'-CTTCCATGTCTCTGCAGTGC-3'
p57Kip2	5'-AGAGATCAGCGCCTGAGAAG-3'	5'-TTGCTGCTACATGAACGGTC-3'
$p16^{ink4a}$	5'-ACCAGAGGCAGTAACCATGC-3'	5'-CACATGAATGTGCGCTTAGG-3'
$p15^{ink4b}$	5'-CGTTAAGTTTACGGCCAACG-3'	5'-CATCATCATGACCTGGATCG-3'
$p18^{ink4c}$	5'-AGTTCCTGGTGAAGCACACG-3'	5'-GGCTAACAACCTCATTCCTCC-3'
$p19^{ink4d}$	5'-ATGTCAACGTGCCTGATGG-3'	5'-GGAGATCAGATTCAGCTGCC-3'

inhibitor cocktail (Sigma) and briefly sonicated. After centrifugation at 18,000 x g for 10 min, the supernatant was collected and measured using a BCA protein assay kit (Pierce, Rockford, IL, USA). Cell lysate containing 50 μg protein was boiled in SDS-sample buffer and then subjected to SDS-PAGE separation. The resolved proteins were subsequently electrotransferred onto Immobilon P membranes (Millipore, Bedford, MA, USA). After initial blocking with Tris-buffered saline containing 0.2% Tween-20 (TBS-T) supplemented with 5% BSA for 2 h membranes were then incubated with each primary antibody in TBS-T containing 1% BSA at dilutions recommended by the manufacturers for 1-2 h at room temperature (RT). Thereafter, the membrane was gently rinsed with TBS-T and then incubated with horseradish peroxidase-conjugated anti-mouse or anti-rabbit secondary antibodies in TBS-T at dilutions recommended by the manufacturers for 1 h at RT. After a final set of rinsing with TBS-T, the presence of the proteins of interest was evaluated using a chemiluminescence reaction mediated by an ECL Plus chemiluminescence detection kit (GE Healthcare, Little Chalfont, UK) and each was then visualized with Chemi-Stage (Toyobo, Osaka, Japan).

Western blotting for some of the cell cycle regulators was performed using mouse anti $p21^{Cip1}$ (F-5) (Santa Cruz Biotechnology), rabbit anti $p16^{ink4a}$ (C-20) (Santa Cruz Biotechnology), rabbit anti-cyclin D1 (M-20) (Santa Cruz Biotechnology), and rabbit anti-β-actin as the control (Cell Signaling Technology, Danvers, MA, USA).

Flow cytometric analysis of the cell cycle. The individual cell cycle phases in logarithmically proliferating ORG, CA1-3, CB1-3 and CR1 cells were analyzed using flow cytometry. For the continuously exposed sublines CA1-3, CB1-3 and CR1, supplemented asbestos fibers were removed using density gradient centrifugation and cells without fibers were then cultured for one week before the analysis. All of these sublines and the Org MT-2 cells were cultured with bromodeoxyuridine (BrdU) for 30 min, and after being washed twice with PBS the cells were incubated with fluorescence-labelled anti-BrdU antibody and 7-amino-actinomycin D (7AAD) for detection of DNA indices. The G1 phase in the cell cycle was then determined as BrdU-negative, DNA indices = 2n fraction, the S phase was BrdU-positive, and DNA indices = 2n< <4n fraction, while the G2/M phases were BrdU-negative and DNA indices = 4n fraction.

Knock-down of FoxO1 in the MT-2Org cell line. Procedures regarding knock-down of FoxO1 in MT-2Org with lentivirus have been described (31). Lentivirus plasmid vectors pLKO.1-puro-Control having scramble shRNA sequence and pLKO.1-puro containing shRNA sequence targeting human FoxO1 (TRCN0000039579 and TRCN0000039580), and the packaging plasmids kit of pLP1, pLP2 and pLP/VSVG, were obtained from Sigma and Invitrogen (Carlsbad, CA, USA), respectively. Recombinant lentivirus was produced in HEK293T cells and MT-2Org cells were infected with recombinant lentivirus. Sublines having the shRNA expression cassette with puromycin resistance were established after culture with medium containing 1 μg/ml puromycin (Sigma) for 2 weeks. Resultant cell lines were designated Org-Ctrl (Scramble), Org-KD#1 (TRCN0000039579) or Org-KD#2 (TRCN0000039580). The amount of FoxO1 protein was determined with immunoblot analysis using anti-FoxO1 monoclonal antibody (Cell Signaling Technology).

Results

mRNA expression of cell cycle regulators. As shown in Figs. 1 and 2, various cell cycle regulators in the cells of Org, CA1-3, CB1-3 and CR1 were analyzed. FoxO1 transcription factor is

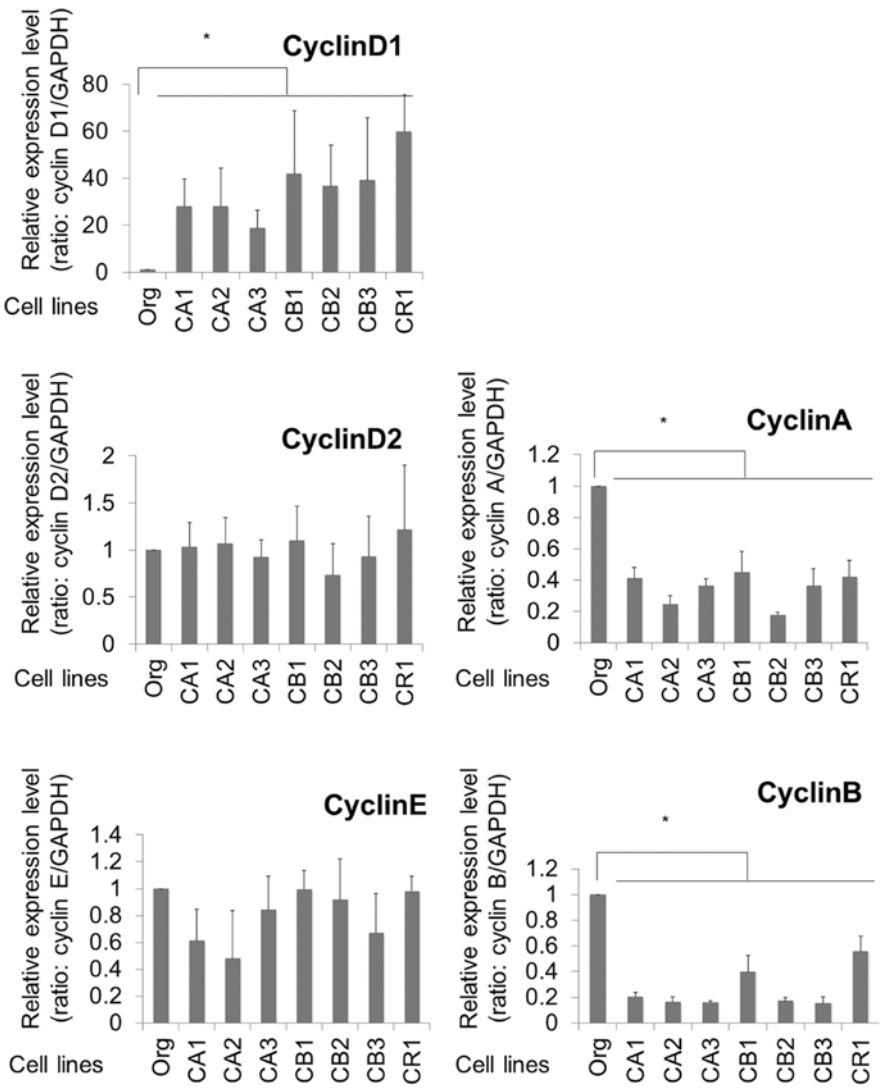

Figure 1. The gene expression of various cyclins in MT-2Org and sublines. The mRNA expression of cyclin D1, D2, E, A and B was analyzed using real-time RT-PCR in MT-2 Org and its sublines CA1-3, CB1-3 and CR1 continuously exposed to ChA, ChB and CRD, respectively. Graphs show mRNA expression level relative to MT-2 Org cells with a value of 1.0. Asterisk indicates a P-value (significance) <0.05.

known to negatively regulate cyclin D1 among the various cyclins. In addition, the sublines continuously exposed to asbestos (MT-2 Org, CA1-3, CB1-3 and CR1) showed remarkably reduced expression of the FoxO1 gene. As expected, cyclin D1 expression was remarkably enhanced in all the sublines by ~20-60-fold when compared with that of Org cells. For other cyclins, expressions of cyclin D2 and E showed no differences between Org and sublines. Although cyclins A and B showed decreased expression in sublines compared to Org cells, the reduction rate was 0.2-0.5-fold in the sublines. The excess expression of cyclin D1 in the sublines was a remarkable finding among the cyclins examined.

In contrast to results for the cyclins, various CDK-Is exhibited reduced expression in sublines compared to MT-2 Org cells. As shown in Fig. 2, $p21^{Cip1}$, $p57^{Kip2}$, $p18^{ink4c}$ and 9\$p19^{ink4d}$ showed significantly reduced expression in the sublines.

Protein expression of cyclin D1 and CDK-Is. The representative protein expression of $p21^{Cip1}$, $p16^{ink4a}$ and cyclin D1 are shown in Fig. 3. Similar to findings for mRNA expression, cyclin D1 was expressed highly in sublines when compared to that in MT-2 Org cells. In addition, expressions of $p21^{Cip1}$ and $p16^{ink4a}$ were reduced in the sublines. Although $p16^{ink4a}$ mRNA was not representative because of the lower quality of real-time RT-PCR, it was clear that the expression of $p16^{ink4a}$ decreased remarkably in sublines at the protein level.

Cell cycle phases in MT-2Org and sublines continuously exposed to asbestos fibers. As shown in Fig. 4A, cell cycle phases in MT-2 Org cells and the seven sublines continuously exposed to asbestos fibers (CA1-3, CB1-3 and CR1) were analyzed using staining with anti-BrdU antibody and DNA indices using 7AAD. The percentages of the S phase (cells with BrdU-positive and 2n< <4n in DNA indices) were then divided by the percentage of the G1 phase (cells with BrdU-negative and 2n in DNA indices). The results for all cell lines and MT-2 Org are shown in Fig. 4B, and S/G1 phase-population ratios are relative to a ratio of 1.0 for MT-2 Org. All sublines showed a higher ratio ranging from 2.6 to 4.3. This indicated that the cell cycle in sublines had progressed rapidly compared to that

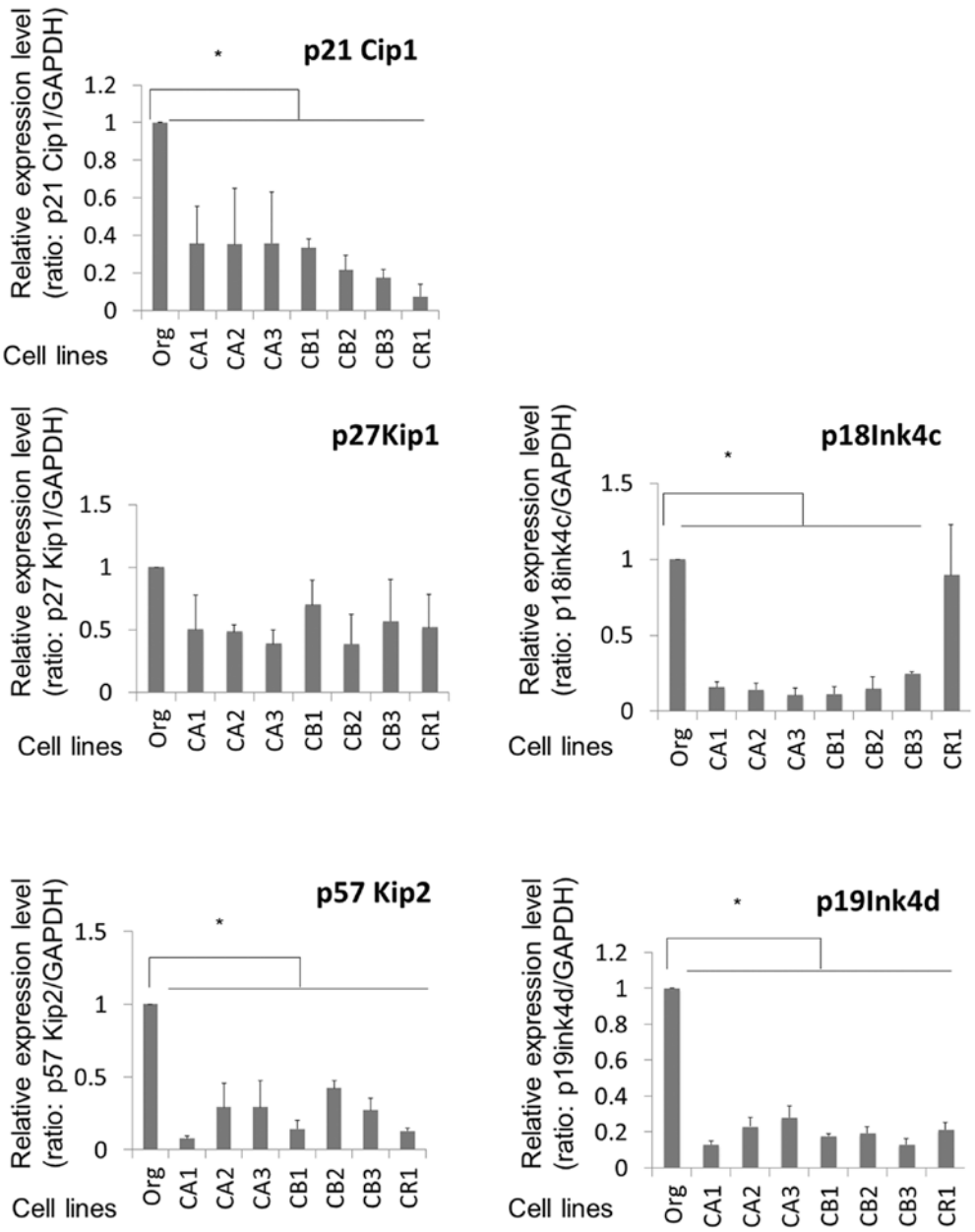

Figure 2. The gene expression of various cyclin-dependent kinase-inhibitors (CDK-Is) in MT-2Org and sublines. The mRNA expression of CDK-Is including $p21^{Cip1}$, $p27^{Kip1}$, $p57^{Kip2}$, $p18^{ink4c}$, and $p19^{ink4d}$ was analyzed using real-time RT-PCR in MT-2 Org and its sublines CA1-3, CB1-3 and CR1 continuously exposed to ChA, ChB and CRD, respectively. Graphs show mRNA expression level relative to MT-2Org cells with a value of 1.0. Asterisk indicates a P-value (significance) <0.05.

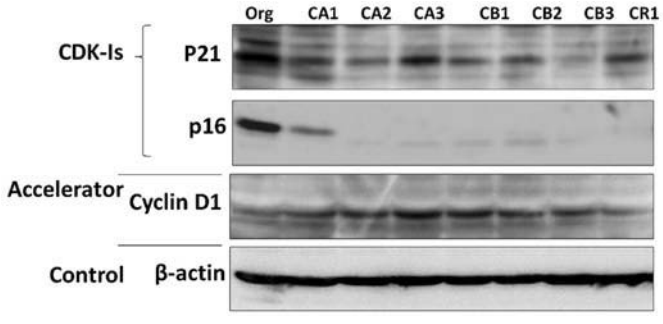

Figure 3. The protein expression of cell cycle regulators. Representative data regarding protein expression of $p21^{Cip1}$, $p16^{ink4a}$ and cyclin D1 analyzed by western blotting for MT-2 Org and its sublines CA1-3, CB1-3 and CR1 continuously exposed to ChA, ChB and CRD, respectively.

of MT-2 Org cells, as suggested from the data of cell cycle regulator expression, the remarkable excess expression of cyclin D1, and the reduced expression of CDK-Is.

Cyclin D1 expression in MT-2 Org knocked down forcibly by FoxO1. The sublines of MT-2 Org, which were continuously exposed to asbestos fibers, showed a remarkably decreased expression of FoxO1 as we reported previously. In addition, cyclin D1, which is negatively regulated by FoxO1, showed recovered expression in the sublines, and a similar pattern was observed for CDK-Is, which are positively regulated by FoxO1 and showed reduced expression in the sublines. To confirm the direct effects of reduced FoxO1 in MT-2 Org for the expression of cyclin D1, lentivirus-derived shRNA for FoxO1 was

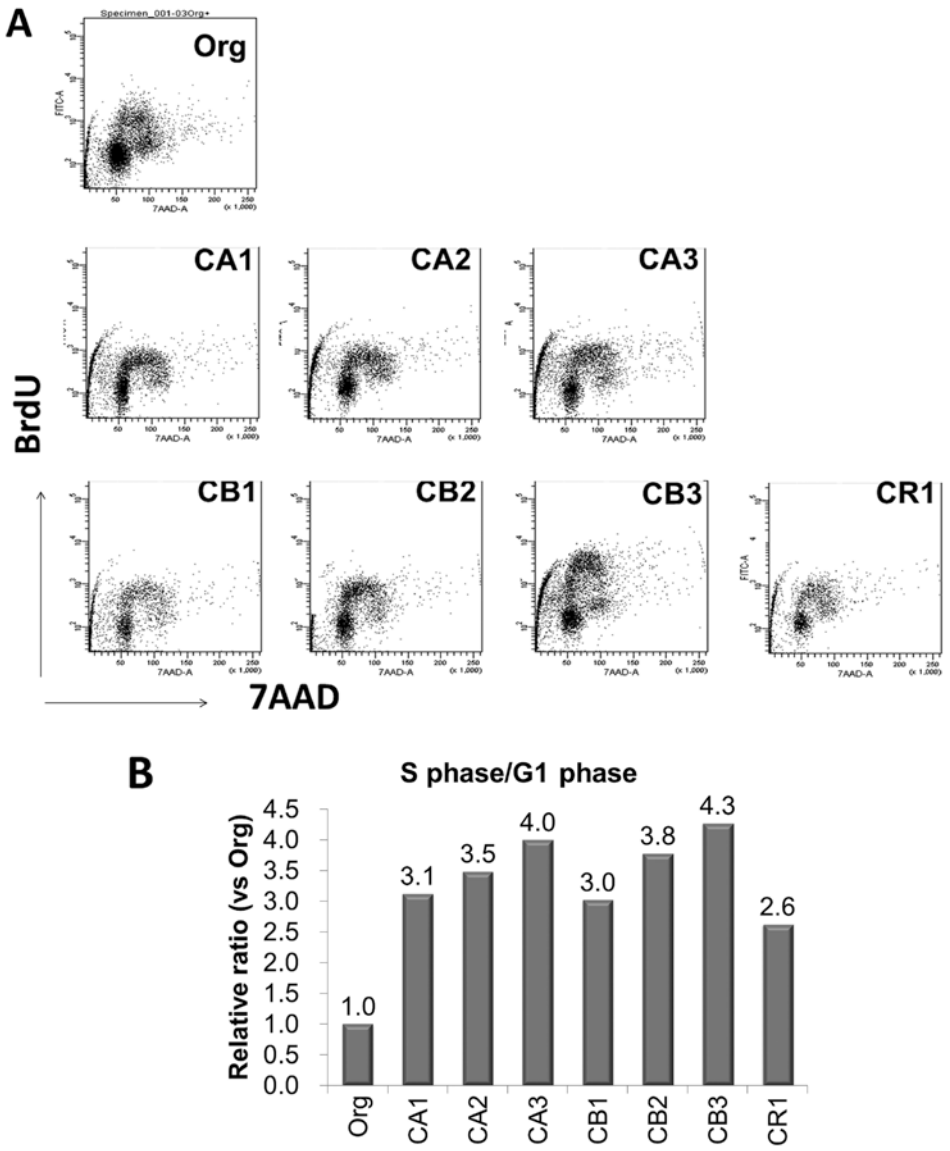

Figure 4. Cell cycle analyses. Cell cycle phases were analyzed using BrdU incorporated cells in MT-2 Org and its sublines CA1-3, CB1-3 and CR1 continuously exposed to ChA, ChB and CRD, respectively. (A) Representative flow cytometry findings for all cell lines examined. (B) The S phase population (percentage) divided by the G1 phase population (percentage) in individual cell lines including MT-2 Org, CA1-3, CB1-3 and CR, with ratios being relative to a value of 1.0 for the MT-2 Org line.

induced in MT-2Org, and the expression of cyclin D1 in MT-2 Org and the knocked-down subline was analyzed. As shown in Fig. 5A, two of the knocked-down cells (KD#1 and KD#2) showed reduced expression of FoxO1. Additionally, the mRNA expression of cyclin D1 was assayed using KD#1 cells and scrambled sequence transfected cells. Although the expression level in KD#1 was not enhanced remarkably, as we observed in sublines continuously exposed to asbestos fibers for more than one year, the expression of cyclin D1 was significantly upregulated in KD#1 compared to that in scrambled transfected cells.

Discussion

Asbestos-exposed patients show complications comprising malignant tumors such as lung cancer and malignant mesothelioma (4-6). In addition, these individuals might have an increased risk of developing other tumors such as laryngeal, gastrointestinal and bladder cancers (38,39). Pulmonary regions are also affected by carcinogenic activities such as ROS production, physical impairment of cellular DNA due to the mineralogical features of the asbestos fibers, and absorption of other carcinogenic substances inhaled into the lung, all of which may lead to the development of malignant tumors. However, a consideration of other cancers and the long latent period (30-50 years) for pulmonary and pleural occurrence of cancers suggest that reduction of antitumor immunity may be an important factor in the development of asbestos-induced tumors (4-6). It is from this viewpoint that we have been investigating the immunological effects of asbestos fibers on immune competent cells. Our results showed that NK cells exhibited reduced killing activity and expression of various activating receptors, as well as a decrease of MAPK signaling in experiments involving an asbestos-exposed human NK cell line, freshly isolated NK cells exposed to asbestos *in vitro*, and

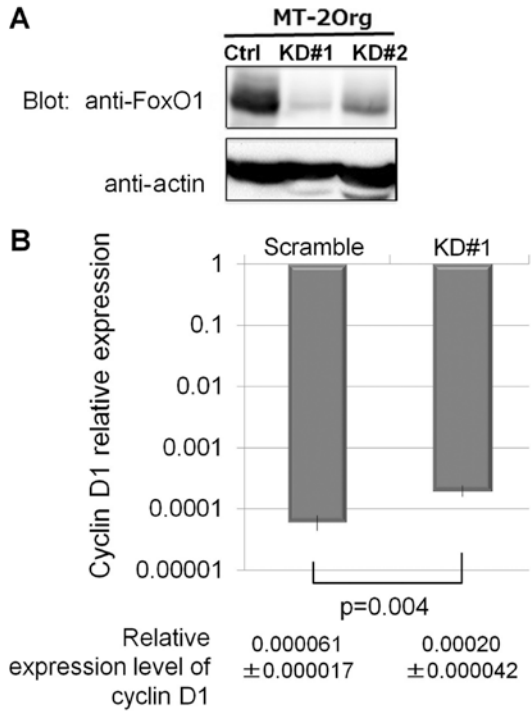

Figure 5. The effects of FoxO1 knock-down on the expression of cyclin D1. (A) Artificial knock-down of the FoxO1 gene in the MT-2 Org line was performed using lentivirus-mediated shRNA transfection. The reduction of FoxO1 protein in two clones (KD#1 and KD#2) is shown via immunoblotting. (B) Cyclin D1 mRNA expression assayed using real-time RT-PCR in MT-2 Org and the KD#1 clone silenced by shRNA for FoxO1. The relative expression level of cyclin D1 was enhanced significantly in KD#1 cells.

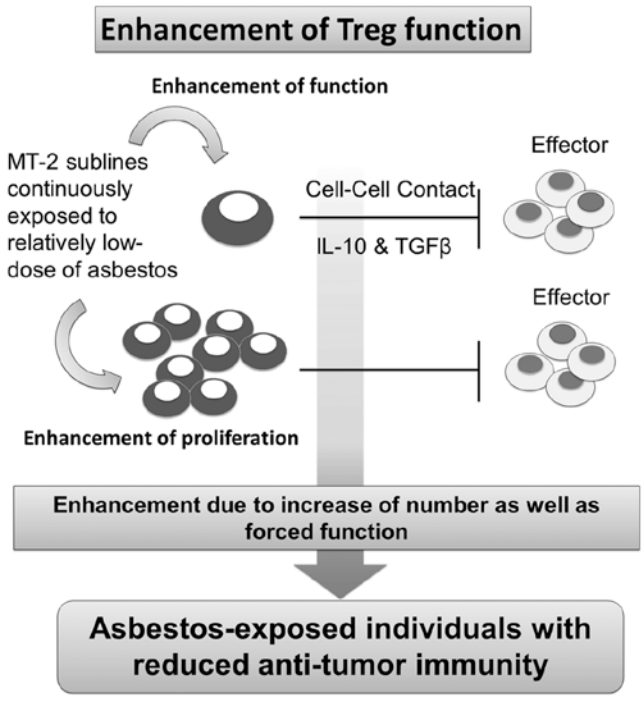

Figure 6. Schematic summary of the effects on Treg following continuous exposure to asbestos fibers, the 'enhancement of Treg function'. The function of Treg was enhanced through cell-cell contact and excess production of typical soluble factors such as IL-10 and TGF-β. In addition to these functional enhancements, the volume of Treg may increase following asbestos exposure through the remarkable reduction of the FoxO1 transcription factor. Both effects of asbestos exposure on Treg reduces antitumor immunity in asbestos-exposed individuals.

in NK cells derived from asbestos-exposed patients with PP or MM (17,18). CTLs showed reduced differentiation and clonal expansion when $CD8^+$ T cells were put into the MLR assay with reduction of cell attacking molecules such as granzyme B and perforin (19,20). Investigation of T helper cells showed that CXCR3 expression and IFN-γ production were reduced in trials involving the cell line model, freshly isolated cells from HD and continuously exposed to asbestos *in vitro*, and in $CD4^+$ cells derived from patients with PP or MM (15,26,27).

The other immune cell that plays an important role in antitumor immunity is Treg. If the function and volume of Treg are enhanced, the activity of tumor-killing T cells is suppressed, particularly in the area surrounding tumor cells, and antitumor immunity is subsequently reduced (40-42). To investigate the possibility of enhanced Treg function following its continuous exposure to asbestos, we investigated Treg function using MT-2 cells, which were reported to possess Treg function (29,30). Our findings indicated that MT-2 cells exposed continuously to asbestos with a relatively low dose did not exhibit apoptosis when exposed transiently, showed enhancement of Treg function via cell-cell contact, and revealed an increase of soluble factors to function as Treg, namely, IL-10 and TGF-β, as we reported previously (22,24,30).

The next goal was to determine how asbestos alters cell proliferation or cell cycle progression in Treg. A key fact for this investigation was the remarkably reduced expression of FoxO1 transcription factor found in MT-2 sublines exposed continuously to asbestos fibers such as ChA, ChB, and CRD. These sublines showed resistance against the asbestos-induced apoptosis via upregulation of IL-10, increased phosphorylation of STAT3 by autocrine usage of IL-10, and subsequent upregulation of Bcl-2 located downstream of STAT3 (22). Moreover, our recent study revealed that reduced FoxO1 caused reduction of other apoptosis-related molecules such as Bim, Puma, and Fas ligand, which are known to be regulated by FoxO1 (31).

FoxO1 is known to regulate various cell cycle regulators, such as cyclin D1 and CDK-Is. Since cyclin D1 is negatively regulated and CDK-Is are positively regulated, it seems that FoxO1 control of the cell cycle does not proceed quickly. However, if continuous asbestos exposure causes massive downregulation of FoxO1, the cell proliferating activity might be accelerated in such cells. Therefore, the expression of cell cycle regulators in MT-2 Org and its sublines was examined. Results showed an overall tendency toward acceleration of cell cycle progression, since cyclin D1 was highly expressed, CDK-Is showed reduced expression, and the S phase in sublines increased in comparison to MT-2 Org cells. The increased expression of cyclin D1 was regulated by FoxO1, since artificially silenced cells from MT-2 Org showed increased cyclin D1 expression.

A consideration of the overall results and our previous findings reveals that MT-2 sublines continuously exposed to asbestos fibers such as ChA, ChB and CRD showed enhanced Treg function via cell-cell contact and excess secretion of typical two soluble factors, namely, IL-10 and TGF-β, and examination of Treg in the asbestos-exposed population may reflect enhancement of function and proliferation, quality and volume (Fig. 6). However, it is difficult to examine these facts in asbestos-exposed patients because the function and volume of Treg needs to be analyzed in the tumor-surrounding area

instead of peripheral blood. This evaluation therefore needs time. Notwithstanding these considerations, our cell line model clearly showed that asbestos causes a reduction of antitumor immunity in asbestos-exposed individuals and makes them more sensitive to the development of tumors after a long-term latent period following the initial exposure to asbestos.

Future studies are needed to evaluate Treg function and volume in the surrounding areas of asbestos-induced tumors, and to develop preventive procedures to neutralize asbestos-induced enhancement of Treg through the use of natural products in foods or plants. These approaches may be helpful for chemoprevention of asbestos-induced tumorigenesis.

Acknowledgements

This study was supported by the Private University Strategic Research Base Formation Support Project (2011 to 2016), Kakenhi 15K08788, the Japanese Society for the Promotion of Science, and Research Grants from Kawasaki Medical School (27B058, 26B53, 25B67, 24S4 and 23S6).

References

1. Parkes WR: Asbestos-related disorders. Br J Dis Chest 67: 261-300, 1973.
2. Mossman BT and Gee JB: Asbestos-related diseases. N Engl J Med 320: 1721-1730, 1989.
3. Peacock C, Copley SJ and Hansell DM: Asbestos-related benign pleural disease. Clin Radiol 55: 422-432, 2000.
4. Morinaga K, Kishimoto T, Sakatani M, Akira M, Yokoyama K and Sera Y: Asbestos-related lung cancer and mesothelioma in Japan. Ind Health 39: 65-74, 2001.
5. O'Reilly KM, Mclaughlin AM, Beckett WS and Sime PJ: Asbestos-related lung disease. Am Fam Physician 75: 683-688, 2007.
6. Lazarus A, Massoumi A, Hostler J and Hostler DC: Asbestos-related pleuropulmonary diseases: Benign and malignant. Postgrad Med 124: 116-130, 2012.
7. Kamp DW, Graceffa P, Pryor WA and Weitzman SA: The role of free radicals in asbestos-induced diseases. Free Radic Biol Med 12: 293-315, 1992.
8. Shukla A, Gulumian M, Hei TK, Kamp D, Rahman Q and Mossman BT: Multiple roles of oxidants in the pathogenesis of asbestos-induced diseases. Free Radic Biol Med 34: 1117-1129, 2003.
9. Toyokuni S: Mechanisms of asbestos-induced carcinogenesis. Nagoya J Med Sci 71: 1-10, 2009.
10. Toyokuni S: Role of iron in carcinogenesis: Cancer as a ferrotoxic disease. Cancer Sci 100: 9-16, 2009.
11. Lemen RA, Dement JM and Wagoner JK: Epidemiology of asbestos-related diseases. Environ Health Perspect 34: 1-11, 1980.
12. Lee S, Matsuzaki H, Kumagai-Takei N, Yoshitome K, Maeda M, Chen Y, Kusaka M, Urakami K, Hayashi H, Fujimoto W, *et al*: Silica exposure and altered regulation of autoimmunity. Environ Health Prev Med 19: 322-329, 2014.
13. Hayashi H, Miura Y, Maeda M, Murakami S, Kumagai N, Nishimura Y, Kusaka M, Urakami K, Fujimoto W and Otsuki T: Reductive alteration of the regulatory function of the CD4(+) CD25(+) T cell fraction in silicosis patients. Int J Immunopathol Pharmacol 23: 1099-1109, 2010.
14. Lee S, Hayashi H, Maeda M, Chen Y, Matsuzaki H, Takei-Kumagai N, Nishimura Y, Fujimoto W and Otsuki T: Environmental factors producing autoimmune dysregulation - chronic activation of T cells caused by silica exposure. Immunobiology 217: 743-748, 2012.
15. Otsuki T, Matsuzaki H, Lee S, Kumagai-Takei N, Yamamoto S, Hatayama T, Yoshitome K and Nishimura Y: Environmental factors and human health: Fibrous and particulate substance-induced immunological disorders and construction of a health-promoting living environment. Environ Health Prev Med 21: 71-81, 2016.
16. Kumagai-Takei N, Maeda M, Chen Y, Matsuzaki H, Lee S, Nishimura Y, Hiratsuka J and Otsuki T: Asbestos induces reduction of tumor immunity. Clin Dev Immunol 2011: 481439, 2011.
17. Nishimura Y, Miura Y, Maeda M, Kumagai N, Murakami S, Hayashi H, Fukuoka K, Nakano T and Otsuki T: Impairment in cytotoxicity and expression of NK cell- activating receptors on human NK cells following exposure to asbestos fibers. Int J Immunopathol Pharmacol 22: 579-590, 2009.
18. Nishimura Y, Maeda M, Kumagai N, Hayashi H, Miura Y and Otsuki T: Decrease in phosphorylation of ERK following decreased expression of NK cell-activating receptors in human NK cell line exposed to asbestos. Int J Immunopathol Pharmacol 22: 879-888, 2009.
19. Kumagai-Takei N, Nishimura Y, Maeda M, Hayashi H, Matsuzaki H, Lee S, Hiratsuka J and Otsuki T: Effect of asbestos exposure on differentiation of cytotoxic T lymphocytes in mixed lymphocyte reaction of human peripheral blood mononuclear cells. Am J Respir Cell Mol Biol 49: 28-36, 2013.
20. Kumagai-Takei N, Nishimura Y, Maeda M, Hayashi H, Matsuzaki H, Lee S, Kishimoto T, Fukuoka K, Nakano T and Otsuki T: Functional properties of CD8 (+) lymphocytes in patients with pleural plaque and malignant mesothelioma. J Immunol Res 2014: 670140, 2014.
21. Hyodoh F, Takata-Tomokuni A, Miura Y, Sakaguchi H, Hatayama T, Hatada S, Katsuyama H, Matsuo Y and Otsuki T: Inhibitory effects of anti-oxidants on apoptosis of a human polyclonal T-cell line, MT-2, induced by an asbestos, chrysotile-A. Scand J Immunol 61: 442-448, 2005.
22. Miura Y, Nishimura Y, Katsuyama H, Maeda M, Hayashi H, Dong M, Hyodoh F, Tomita M, Matsuo Y, Uesaka A, *et al*: Involvement of IL-10 and Bcl-2 in resistance against an asbestos-induced apoptosis of T cells. Apoptosis 11: 1825-1835, 2006.
23. Maeda M, Yamamoto S, Chen Y, Kumagai-Takei N, Hayashi H, Matsuzaki H, Lee S, Hatayama T, Miyahara N, Katoh M, *et al*: Resistance to asbestos-induced apoptosis with continuous exposure to crocidolite on a human T cell. Sci Total Environ 429: 174-182, 2012.
24. Maeda M, Chen Y, Hayashi H, Kumagai-Takei N, Matsuzaki H, Lee S, Nishimura Y and Otsuki T: Chronic exposure to asbestos enhances TGF-β1 production in the human adult T cell leukemia virus-immortalized T cell line MT-2. Int J Oncol 45: 2522-2532, 2014.
25. Maeda M, Chen Y, Kumagai-Takei N, Hayashi H, Matsuzaki H, Lee S, Hiratsuka J, Nishimura Y, Kimura Y and Otsuki T: Alteration of cytoskeletal molecules in a human T cell line caused by continuous exposure to chrysotile asbestos. 218: 1184-1191, 2013.
26. Maeda M, Nishimura Y, Hayashi H, Kumagai N, Chen Y, Murakami S, Miura Y, Hiratsuka J, Kishimoto T and Otsuki T: Reduction of CXC chemokine receptor 3 in an in vitro model of continuous exposure to asbestos in a human T-cell line, MT-2. Am J Respir Cell Mol Biol 45: 470-479, 2011.
27. Maeda M, Nishimura Y, Hayashi H, Kumagai N, Chen Y, Murakami S, Miura Y, Hiratsuka J, Kishimoto T and Otsuki T: Decreased CXCR3 expression in $CD4^+$ T cells exposed to asbestos or derived from asbestos-exposed patients. Am J Respir Cell Mol Biol 45: 795-803, 2011.
28. Matsuzaki H, Maeda M, Lee S, Nishimura Y, Kumagai-Takei N, Hayashi H, Yamamoto S, Hatayama T, Kojima Y, Tabata R, *et al*: Asbestos-induced cellular and molecular alteration of immunocompetent cells and their relationship with chronic inflammation and carcinogenesis. J Biomed Biotechnol 2012: 492608, 2012.
29. Hamano R, Wu X, Wang Y, Oppenheim JJ and Chen X: Characterization of MT-2 cells as a human regulatory T cell-like cell line. Cell Mol Immunol 12: 780-782, 2015.
30. Ying C, Maeda M, Nishimura Y, Kumagai-Takei N, Hayashi H, Matsuzaki H, Lee S, Yoshitome K, Yamamoto S, Hatayama T, *et al*: Enhancement of regulatory T cell-like suppressive function in MT-2 by long-term and low-dose exposure to asbestos. Toxicology 338: 86-94, 2015.
31. Matsuzaki H, Lee S, Maeda M, Kumagai-Takei N, Nishimura Y and Otsuki T: FoxO1 regulates apoptosis induced by asbestos in the MT-2 human T-cell line. J Immunotoxicol 13: 620-627, 2016.
32. Arden KC: FoxO: Linking new signaling pathways. Mol Cell 14: 416-418, 2004.
33. Accili D and Arden KC: FoxOs at the crossroads of cellular metabolism, differentiation, and transformation. Cell 117: 421-426, 2004.

34. Huang H and Tindall DJ: CDK2 and FOXO1: A fork in the road for cell fate decisions. Cell Cycle 6: 902-906, 2007.
35. Liu P, Kao TP and Huang H: CDK1 promotes cell proliferation and survival via phosphorylation and inhibition of FOXO1 transcription factor. Oncogene 27: 4733-4744, 2008.
36. Eijkelenboom A and Burgering BM: FOXOs: Signalling integrators for homeostasis maintenance. Nat Rev Mol Cell Biol 14: 83-97, 2013.
37. Kohyama N, Shinohara Y and Suzuki Y: Mineral phases and some reexamined characteristics of the International Union Against Cancer standard asbestos samples. Am J Ind Med 30: 515-528, 1996.
38. Gao FF and Oury TD: Other neoplasia. In: Pathology of Asbestos-Associated Diseases. Roggi VL, Oury TD and Sporn TA (eds.) 3rd edit. Springer, Berlin, pp177-192, 2014.
39. Craighead JE: Nonthoracic cancers possibly resulting from asbestos exposure. In: Asbestos and its Diseases. Craighead JE and Gibbs AR (eds). Oxford University Press, New York, NY, pp230-252, 2008.
40. Sakaguchi S, Ono M, Setoguchi R, Yagi H, Hori S, Fehervari Z, Shimizu J, Takahashi T and Nomura T: Foxp3^{+} CD25^{+} CD4^{+} natural regulatory T cells in dominant self-tolerance and autoimmune disease. Immunol Rev 212: 8-27, 2006.
41. Nishikawa H and Sakaguchi S: Regulatory T cells in tumor immunity. Int J Cancer 127: 759-767, 2010.
42. Yamaguchi T and Sakaguchi S: Regulatory T cells in immune surveillance and treatment of cancer. Semin Cancer Biol 16: 115-123, 2006.

Toxicology 338 (2015) 86–94

Contents lists available at ScienceDirect

Toxicology

journal homepage: www.elsevier.com/locate/toxicol

Enhancement of regulatory T cell-like suppressive function in MT-2 by long-term and low-dose exposure to asbestos

Chen Ying[a,c,1], Megumi Maeda[b,c,1], Yasumitsu Nishimura[c], Naoko Kumagai-Takei[c], Hiroaki Hayashi[a,d,1], Hidenori Matsuzaki[c], Suni Lee[c], Kei Yoshitome[c], Shoko Yamamoto[c], Tamayo Hatayama[c], Takemi Otsuki[c,*]

[a] Division of Pneumoconiosis, School of Public Health, China Medical University, Shenyang, PR China
[b] Department of Biofunctional Chemistry, Division of Bioscience, Okayama University Graduate School of Natural Science and Technology, Okayama, Japan
[c] Department of Hygiene, 4: Department of Dermatology, Kawasaki Medical School, Kurashiki, Okayama, Japan
[d] Department of Dermatology, Kawasaki Medical School, Kurashiki, Japan

ARTICLE INFO

Article history:
Received 7 September 2015
Received in revised form 8 October 2015
Accepted 13 October 2015
Available online 23 October 2015

Keywords:
Asbestos
Regulatory T cell
IL-10
TGF-β1
CTLA-4

ABSTRACT

Asbestos exposure causes lung fibrosis and various malignant tumors such as lung cancer and malignant mesothelioma. The effects of asbestos on immune cells have not been thoroughly investigated, although our previous reports showed that asbestos exposure reduced anti-tumor immunity. The effects of continuous exposure of regulatory T cells (Treg) to asbestos were examined using the HTLV-1 immortalized human T cell line MT-2, which possesses a suppressive function and expresses the Treg marker protein, Foxp3. Sublines were generated by the continuous exposure to low doses of asbestos fibers for more than one year. The sublines exposed to asbestos showed enhanced suppressive Treg function via cell–cell contact, and increased production of soluble factors such as IL-10 and transforming growth factor (TGF)-β1. These results also indicated that asbestos exposure induced the reduction of anti-tumor immunity, and efforts to develop substances to reverse this reduction may be helpful in preventing the occurrence of asbestos-induced tumors.

1. Introduction

Asbestos exposure causes not only lung fibrosis, which is a typical form of pneumoconiosis known as asbestosis, but also malignant tumors such as lung cancer and malignant mesothelioma (MM) (Brody, 2010; Jamrozik et al., 2011; Liu et al., 2013; Stayner et al., 2013). In addition, cancers of the larynx, gastrointestinal tracts and bladder have frequently been found in asbestos-exposed individuals (Friedman, 2011). The causes of asbestos-induced cancer are thought to include (i) DNA damage induced by reactive oxygen species (ROS) and produced mainly by the Fenton reaction due to the iron present in asbestos fibers, (ii) direct chromosomal and genomic injury caused by the firm and rigid physical characteristics of asbestos fibers, and (iii) adsorption of various carcinogenic substances around asbestos fibers inhaled into the respiratory system (Barrett et al., 1989; Kamp et al., 1992; Toyokuni 2014).

The core chemical component of asbestos fibers is silica (SiO_2). It is well known that exposure to silica particles also causes a type of lung fibrosis known as silicosis, another typical form of pneumoconiosis, as well as various disorders of autoimmunity such as rheumatoid arthritis (known as Caplan's syndrome), systemic lupus erythematosus (SLE), systemic sclerosis (SSc), and ailments detailed in many recent reports involving complications of anti-neutrophil cytoplasmic antibody-induced vasculitis/nephritis in silicosis patients (Steenland and Goldsmith, 1995; Wichmann et al., 1996; D'Cruz, 2000; Mulloy, 2003; Gómez-Puerta et al., 2013). Although silica-induced dysregulation of autoimmunity has been considered an adjuvant disease, we have

Abbreviations: MM, malignant mesothelioma; ROS, reactive oxygen species; SLE, systemic lupus erythematosus; SSc, systemic sclerosis; Teff, effector T cells; Treg, regulatory T cells; DcR3, decoy receptor 3; HTLV, human T-lymphotropic virus; PP, pleural plaque; IL, interleukin; TGF, transforming growth factor; STAT3, signal transducer and activator of transcription 3; CXCR3, C-X-C chemokine receptor type 3; IFN, interferon; NK, natural killer; CTL, cytotoxic T lymphocytes; MLR, mixed lymphocyte reaction; FCS, fetal calf serum; PBMCs, peripheral blood mononuclear cells; FITC, fluorescein isothiocyanate; Tresp, responder T cells; iDCs, immature dendritic cells; GM-CSF, granulocyte macrophage-colony stimulating factor; CBA, cytometric bead array; ELISA, enzyme-linked immunosorbent assay; DC, dendritic cells; PLSD, parametric least significant difference; TCR, T cell receptor; SMRP, soluble mesothelin-related peptide.

* Corresponding author at: Department of Hygiene, Kawasaki Medical School, 577 Matsushima, Kurashiki 701-0192, Japan. Fax: +81 86 464 1125.
E-mail address: takemi@med.kawasaki-m.ac.jp (T. Otsuki).

[1] These two authors contributed equally to this study.

http://dx.doi.org/10.1016/j.tox.2015.10.005
0300-483X/

been investigating the direct effects of silica particles on immunocompetent cells and found unbalanced levels of effector T cells (Teff) and regulatory T cells (Treg). Silica particles induce chronic activation of both Teff and Treg. Activated Teff showed escape from Fas/CD95-mediated apoptosis by producing inhibitory molecules such as soluble Fas and decoy receptor 3 (DcR3) that resulted in its long survival. As a consequence of the chronic activation of Treg, these cells enhanced their Fas/CD95 expression and experienced early death. Finally, the unbalance of Teff/Treg leads to subsequent dysregulation of autoimmunity (Hayashi et al., 2010; Lee et al., 2012, 2014).

Given that silica affects immunocompetent cells, it is supposed that asbestos fibers, which possess SiO_2 as the core chemical, also affect immune cells. Considering the above-mentioned complications exhibited by asbestos-exposed patients, exposure to asbestos is likely to decrease anti-tumor immunity. It is on this basis that we have been investigating the immunological effects of asbestos fibers on human T cells using the human T-lymphotropic virus (HTLV)-1 immortalized polyclonal T cell line MT-2 as Treg-like cells (Chen et al., 2006), and freshly isolated human T cells from healthy volunteers, as well as cells from asbestos-exposed patients such as those with pleural plaque (PP), who only show the plaque without any clinical evidence of cancers, and patients with MM (Otsuki et al., 2007; Maeda et al., 2010).

The results of our investigations revealed apoptosis of MT-2 cells through production of ROS, activation of the mitochondrial apoptotic pathway by transient high-dose exposure to asbestos (Hyodoh et al., 2005), acquisition of asbestos-induced apoptosis by continuous and low-dose exposure to asbestos in MT-2 cells through Src-activation, enhanced production of interleukin (IL)-10, activation of signal transducer and activator of transcription 3 (STAT3), and upregulation of bcl-2 located downstream of STAT3 activation (Miura et al., 2006). Furthermore, asbestos-resistant strains of MT-2 cells produced transforming growth factor TGF-β1 at high levels (Maeda et al., 2014). Continuously exposed MT-2 cells showed reduction of C-X-C chemokine receptor type 3 (CXCR3) expression with reduced production of interferon (IFN)-γ (Maeda et al., 2011a,b). These reductions of CXCR3 and IFN-γ were also found in patients with PP and MM (Maeda et al., 2011a,b). Furthermore, the natural killer (NK) cell line, freshly isolated peripheral blood NK cells, and NK cells isolated from asbestos-exposed patients showed decreased expression of NK cell activating receptors. In particular, reduction of NKp46 was the significant effect of asbestos exposure and caused a decrease in the tumor-killing function of experimental asbestos-exposed NK cells and of patient NK cells (Nishimura et al., 2009a,b, 2013). Moreover, asbestos exposure caused inhibition of differentiation and proliferation of CD8+ cytotoxic T lymphocytes (CTL) in vitro when CTL from healthy volunteers were examined in a mixed lymphocyte reaction (MLR) with or without chrysotile asbestos (Kumagai-Takei et al., 2013, 2014). The overall findings indicate that asbestos affects human immune cells and causes a reduction of anti-tumor immunity.

In this study, we assessed whether exposure to asbestos affects Treg function. We have independently established six asbestos-resistant sublines as a model of continuous (more than one year) and low-dose (10 μg/mL) exposure to asbestos in the MT-2 cell line (Org), which has Treg functionality and has never been exposed to asbestos fibers. The asbestos-resistant sublines were designated CA 1, 2 and 3, which were exposed to chrysotile A, and CB 1, 2 and 3, which were exposed to chrysotile B. The difference between chrysotile A and B concerns the amounts of mineralogical minor components such as TiO_2, Al_2O_3 and Fe_2O_3 (Kohyama et al., 1996). Finally, we compared the Treg suppressive function regarding the cell-to-cell contact manner, as well as soluble molecules such as IL-10 and TGF-β1 as typical soluble factors that reflect Treg functionality (Horwitz et al., 2003; Chattopadhyay et al., 2005; Linehan and Goedegebuure, 2005; Taylor et al., 2006).

2. Materials and methods

2.1. Cell lines and asbestos

MT-2Org and the asbestos-resistant sublines were cultured as reported previously (Miura et al., 2006; Maeda et al., 2011a,b, 2014). These cells were maintained in a humidified atmosphere of 5% CO_2 at 37 °C in RPMI-1640 medium supplemented with 10% fetal calf serum (FCS), streptomycin and penicillin. The International Union Against Cancer standard chrysotile-A and -B were kindly provided by the Department of Occupational Health at the National Institute for Occupational Health of South Africa. The mineralogical features of these fibers were reported previously (Kohyama et al., 1996). Six asbestos-resistant sublines (CA 1–3 and CB 1–3) were generated by continuous exposure to CA or CB (10 μg/ml, for more than eight months) of MT-2Org, as described previously. 293FT cells were cultured in Dulbecco's modified Eagle's medium (Invitrogen, Carlsbad, CA) supplemented with 10% FCS.

2.2. Lentiviral transduction

IL-10 and TGF-β1-targeting double-stranded oligonucleotides 5′- GATCCCCGCCTACATGACAATGAAGATTCAAGAGATCTTCATTGTCATGTAGGCTTTTTGGAAA -3′ (IL-10) and 5′- GATCCCCGGAGGTCACCCGCGTGCTATTCAAGAGATAGCACGCGGGTGACCTCCTTTTTGGAAA-3′ (TGF-β1) were subcloned into pSUPER digested by BglII-HindIII (Brummelkamp et al., 2002). Resulting constructs were digested with BamHI/SalI, and short hairpin RNA (shRNA) containing human H1 RNA polymerase III promoter subcloned into the BamHI-SalI site of the lentiviral vector pRDI292 that expresses shRNA and a protein associated with puromycin resistance as described previously (Naldini et al., 1996). The vesicular stomatitis virus G protein (VSV-G)-pseudotyped HIV-1-based vector system was generated as described previously (Bridge et al., 2003). The replication-defective lentiviral vector particles were produced by transient cotransfection of the second-generation packaging construct pCMV-DR8.91 (Zufferey et al., 1997), the VSV-G envelope plasmid pMDG2 and the lentiviral vector into 293FT cells with FuGene6 (Roche Diagnostics, Mannheim, Germany). The supernatant containing the virus was collected 48 h and 72 h after transfection. The lentivirus-containing supernatants were added to MT-2Org or the subline CB 1 (0.5×10^5 in 2 mL of medium) in a six-well plate. After 3 days, cells were treated with 1 μg/mL of puromycin to select stable clones expressing shRNA.

2.3. Purification of monocytes and primary T cells

Human peripheral blood was obtained from healthy donors after informed consent was received in accordance with procedures approved by the human ethics committee of Kawasaki Medical School, Kurashiki, Japan (#883). Peripheral blood mononuclear cells (PBMCs) were isolated by density gradient centrifugation (Separate-L®, Muto Pure Chemical Co., Ltd., Tokyo, Japan). $CD14^+$ monocytes were isolated by positive selection using anti-CD14-coated beads (Miltenyi Biotec GmbH, Bergisch Gladbach, Germany) in accordance with manufacturer's instructions. The remaining cells were labeled with anti-CD4-phycoerythrin (PE) (clone RPA-T4) and anti-CD25-fluorescein isothiocyanate (FITC) (clone M-A251) for 30 min at room temperature. After washing, $CD4^+CD25^-$ responder T cells (Tresp) and $CD4^+CD25^{high}$ Treg were sorted using a FACS Aria cell sorter (BD Biosciences, San Jose, CA) (Fig. 1A).

2.4. Treg functional assays using the allogeneic MLR

Purified Tresp cells (5×10^3) were stimulated with irradiated allogeneic PBMCs (5×10^4) in the absence or presence of an increasing number of irradiated MT-2Org or the sublines CA 1–3 and CB 1–3. Cell culture in 96-well U-bottom plates was performed in 200 μl of RPMI 1640 supplemented with 10% FCS, streptomycin and penicillin for six days. 10 μL of ^{3}H-thymidine (3.7 KBq, 0.1 μCi) (G.E. Healthcare U.K. Ltd., Buckinghamshire, England) was then added to each well and incubated for 16 h. The ^{3}H-thymidine incorporation was measured using a liquid scintillation counter (LSC-5100, Aloka, Japan).

2.5. CFSE-based suppression assay

Purified Tresp were labeled with 1 μM CellTrace™ CFSE (Molecular Probes, Eugene, OR) according to manufacturer's instructions. The CFSE-labeled Tresp (1×10^5) were stimulated with 1 μg/mL of plate-bound anti-CD3 monoclonal antibody (mAb) (clone UCHT1) and 1 μg/mL of anti-CD28 mAb (clone CD28.2) (Beckman Coulter, Inc., Fullerton, CA) in the absence or presence of an increasing number of irradiated MT-2Org or the subline CB 1. Cell culture in 96-well flat plates was performed in 100 μL of RPMI 1640 supplemented with 10% FCS, streptomycin and penicillin for three days. Cell division was analyzed using a flow cytometer (FACSCalibur™; BD Biosciences, Franklin Lakes, N. J.).

For stimulation through cell–cell contact, CFSE-labeled Tresp (1×10^5) were stimulated with 1 μg/mL of plate-bound anti-CD3 mAb and irradiated autologous monocyte-derived immature dendritic cells (iDCs) (1×10^4) in the absence or presence of an increasing number of irradiated MT-2Org or the subline CB 1. Cell culture in 96-well flat plates was performed in 100 μL of RPMI 1640 supplemented with 10% FCS, streptomycin and penicillin for five days. Cell division was analyzed using a FACSCalibur™. The differentiation from CD14$^+$ monocytes to iDCs in a 6-well plate was performed in 3 mL of RPMI 1640 supplemented with 10% FCS, streptomycin and penicillin under 50 ng/mL of granulocyte

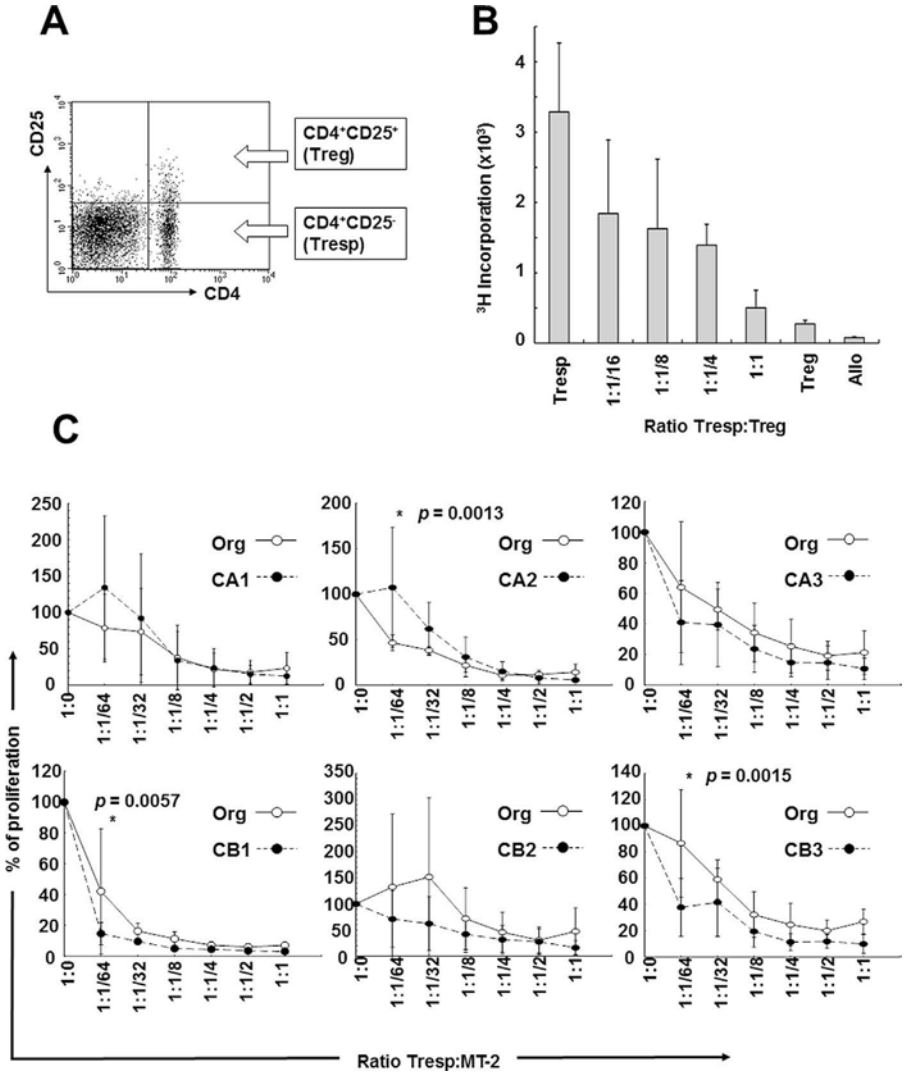

Fig. 1. *Invitro* assay of Treg suppressive function. (A) Treg and Tresp were defined by surface expression of CD4 and CD25, and were isolated by a FACS Aria cell sorter. (B) Tresp were stimulated with irradiated allogeneic PBMCs. These cells were cocultured with Treg at Tresp:Treg ratios of 1:1, 1:1/4, 1:1/8, 1:1/16, 1:0 (Tresp only), 0:1 (Treg only) and 0:0 (allogeneic PBMC only). The Treg suppressive function was monitored by ^{3}H thymidine incorporation. (C) MT-2Org and the sublines (CA 1–3 and CB 1–3) showed a suppressive function on the proliferation of allostimulated Tresp. Tresp (5×10^3) were stimulated with irradiated allogeneic PBMCs (5×10^4) in the absence or presence of irradiated MT-2Org or the sublines (CA 1–3 and CB 1–3). The ratios of Tresp to irradiated MT-2Org or the sublines were 1:1, 1:1/2, 1:1/4, 1:1/8, 1:1/32 1:1/64 and 1:0 (Tresp only). The proliferation of Tresp only was set at 100%. Data shown are the mean ± SD from three independent experiments. *P*-values were obtained using Fisher's PLSD test. *: $p < 0.01$.

macrophage-colony stimulating factor (GM-CSF) and 50 ng/mL IL-4 for seven days. Before being applied to the culture, the differentiation of iDCs was confirmed by surface expression of CD14 using a FACSCalibur™.

2.6. Soluble cytokines in culture supernatants

Levels of IL-10 were quantified by a BD™ cytometric bead array (CBA) assay and an enzyme-linked immunosorbent assay (ELISA) using a CBA Kit (BD Biosciences, San Diego, CA) and an Endogen® Human IL-10 ELISA Kit (Pierce Biotechnology, Inc., Rockford, IL), respectively. Levels of activated TGF-β1 in the culture supernatant were quantified by ELISA using the Quantikine Human TGF-β1 Immunoassay kit (R&D Systems, Minneapolis, MN).

2.7. Transwell assay

CFSE-labeled Tresp cells (1×10^5) in 24-well plates were stimulated with plate-bound anti-CD3 mAb (1 μg/mL) and irradiated autologous dendritic cells (DC) (1×10^4) as described above, and non-irradiated control subline CB 1, IL-10 or TGF-β1 knocked down cells (2×10^5) were cultured using a transwell assay. After six days of culture in 1 mL of RPMI1640 containing 10% FCS, cell division was analyzed using a FACSCalibur™.

2.8. Flow cytometry

Cell surface antigens were detected with anti-CTLA4-PE (clone 48815) and anti-GITR-PE (clone 110416) antibodies (R&D Systems). Intracellular FOXP3 was stained using the Human Foxp3 Buffer Set and anti-FOXP3-PE antibody (clone 259D/C7) (BD Biosciences Pharmingen, San Diego, CA) according to manufacturer's instructions. Cells were analyzed on a FACS system.

2.9. Statistical analyses

Fisher's parametric least significant difference (PLSD) test, the unpaired *t*-test, and Dunnett's test were used to determine the statistical significance of differences between experimental groups.

3. Results

3.1. Exposure to chrysotile-B enhances the suppressive function of MT-2Org

To determine the effects of asbestos exposure on Treg cells, we investigated the suppressive function of MT-2Org and the sublines (CA 1–3 and CB 1–3). To evaluate the suppressive function of these cells, we used an allogeneic mixed lymphocyte reaction (allo-MLR) system. Cultures of MT-2Org and the sublines were purified using the Ficoll density gradient method to remove dead cells and chrysotile completely, and then cultured for two to four days in the absence of chrysotile before the allo-MLR assay. After irradiation, MT-2Org and the sublines were cocultured with Tresp cells under allogeneic irradiated PBMCs. After 6 days of culture, the proliferation of Tresp cells was measured using [^{3}H]-thymidine incorporation. Results showed that all cell lines exhibited a potent suppressive function compared with that of autologous Treg, and fully inhibited the proliferation of Tresp cells at the ratio of 1:4, 1:2 and 1:1 (Fig. 1B and C). This result suggests that the enhanced function of MT-2Org and the sublines is due to immortalization and culture over a long period. Interestingly, all three CB sublines (CB 1–3) and CA 3 presented a greater potent suppressive function compared with that of MT-2Org, while CB 1 and CB 3 were significant at the ratio of 1:64 ($p = 0.0057$ and $p = 0.0015$, respectively). On the other hand, CA 1 and CA 2 showed a poor suppressive function compared with that of MT-2Org. Given that chrysotile-A contains 2% fibrous anthophyllite, and that chrysotile-B does not contain any fibrous impurities, it seems that chrysotile itself enhances the suppressive function in MT-2Org. Furthermore, the standard deviation was relatively large.

3.2. The subline CB 1 does not exhibit a greater potent suppressive function when Tresp cells are stimulated with anti-CD3/CD28 Abs

To determine the effect of chrysotile-B on MT-2Org, we evaluated the suppressive function of the subline CB 1 in regard to the proliferation of Tresp cells with T cell receptor (TCR)-based simulation using the CFSE-based assay. To assess the suppressive function of CB 1, irradiated MT-2Org or CB 1 cells were co-cultured with CFSE-labeled Tresp cells stimulated by plate-bound anti-CD3 mAbs and soluble anti-CD28 mAbs. After three days of culture, cell proliferation of Tresp was measured using FACSCalibur™, and the suppressive function was assessed by determining the percentage of non-proliferated cells. Results showed that both cells exhibited a suppressive function of the same intensity in contrast to the results of allo-MRL, and fully inhibited the differentiation of Tresp at the ratio of 1:4 and 1:1 (Fig. 2A and C). These results suggest that cell–cell contact may be necessary for the strong suppressive function of CB 1.

3.3. The enhanced suppressive function of the subline CB 1 depends on cell–cell contact

Given that there was no significant difference in suppressive function between MT-2Org and the subline CB 1 when TCR on these cells were stimulated with antibodies, Tresp were stimulated with plate-bound anti-CD3 mAbs and iDC to investigate the suppressive function via cell–cell contact, such as allo-MLR. After 5 days of culture, cell proliferation of Tresp was analyzed. In contrast to the outcome following stimulation with anti-CD3/CD28 mAbs, the results showed that the suppressive function of CB 1 was higher than that of MT-2Org, and was significantly high at the ratio of 1:64 and 1:16 ($p = 0.04$ and $p = 0.037$, respectively) (Fig. 2B and D). These findings suggested that exposure of Tresp to chrysotile-B enhances the suppressive function by stimulation through cell–cell contact.

3.4. Expression of Foxp3, CTLA-4 and GITR in MT-2Cells

Foxp3 is well known as the master transcription factor of Treg. CTLA4 and GITR are cell surface molecules that can be used to monitor the suppressive function of Treg. These Treg molecular markers were therefore examined using FACSCalibur™ since exposure to chrysotile-B enhanced the suppressive function of the sublines (CB 1–3). Results showed that intracellular expression of Foxp3 and cell surface expression of GITR were high in MT-2Org and the sublines (CB 1–3), although there were no significant differences (Fig. 3). On the other hand, cell surface expression of CTLA4 tended to increase slightly in the sublines (CB 1–3) (only significant in the CB 3 subline), although the expression was not as high in MT-2Org (Fig. 3). It seems that cell surface expression of CTLA4 in the sublines (CB 1–3) may be involved in the suppressive function via cell–cell contact.

3.5. Suppressive function depends on the soluble factors IL-10 and TGF-β1 produced by the subline CB 1

It is known that the soluble factors IL-10 and TGF-β1 produced by Treg cells suppress the proliferation of Tresp cells. To examine the production of IL-10 and TGF-β1 from MT-2Org and the subline

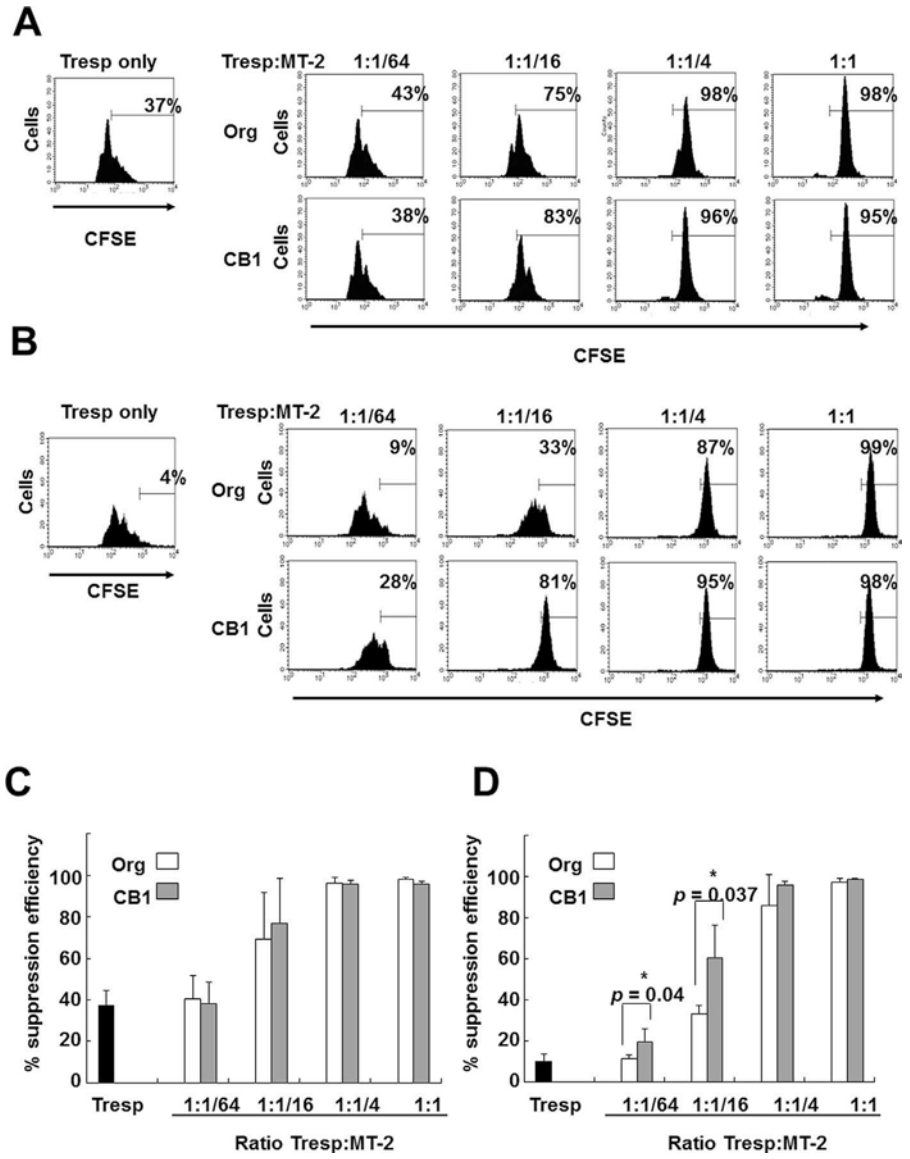

Fig. 2. (A) Suppressive function of MT-2Org and the subline CB1 on the proliferation of Tresp stimulated with anti-CD3 and anti-CD28 antibodies. Histograms show a representative example of the suppressive function. Non-dividing cells were gated and are indicated as a suppression efficiency (%). CFSE-labeled Tresp cells (1×10^5) were stimulated with plate-bound anti-CD3 mAb (1 μg/mL) and soluble anti-CD28 mAb (1 μg/mL) in the presence of irradiated MT-2Org or the subline CB 1. The ratios of Tresp to irradiated MT-2Org or the subline CB1 were 1:1, 1:1/4, 1:1/16 and 1:1/64. (B) Suppressive function of MT-2Org and the subline CB 1 on the proliferation of Tresp stimulated with anti-CD3 antibody and iDC. Histograms show a representative example of the suppressive function. Non-dividing cells were gated and are indicated as a suppression efficiency (%). CFSE-labeled Tresp cells (1×10^5) were stimulated with plate-bound anti-CD3 mAb (1 μg/mL) and irradiated autologous iDC (1×10^4) in the presence of irradiated MT-2Org or the subline CB1. The ratios of Tresp to irradiated MT-2Org or the subline CB 1 were 1:1, 1:1/4, 1:1/16 and 1:1/64. (C and D) The suppressive function of the subline CB 1 was enhanced through cell–cell contact. The graph shows the suppression efficiency. (C) Suppression efficiency obtained from the experiment shown in panel A. (D) Suppression efficiency obtained from the experiment shown in panel B. Data shown are the mean + SD from four independent experiments. The *p*-value was obtained using an unpaired *t*-test. $^*p < 0.05$.

CB 1, dead cells and chrysotile-B were removed using density-gradient centrifugation. Cells (2×10^5/mL) were cultured in 24-well plates in RPMI 1640 medium supplemented with 10% FBS for IL-10 detection or 10% 1× Serum Replacement 1 for TGF-β1 detection (Sigma–Aldrich, Saint Louis, MO). After three days, the level of IL-10 and TGF-β1 in the culture supernatants was determined using ELISA. As described in our report previously, the production of IL-10 and TGF-β1 increased significantly in the subline CB 1 compared with MT-2Org (Fig. 4A). Consequently, to examine the suppressive function of IL-10 and TGF-β1 in the subline CB 1, gene expression of IL-10 or TGF-β1 was knocked down with shRNA including a specific gene sequence. The production of IL-10 and TGF-β1 decreased significantly in the IL-10 or TGF-β1 knocked-down subline CB 1 compared with that of the control CB 1 subline ($p = 0.013$ and $p < 0.001$, respectively) (Fig. 4B).

These cells were then applied to the CFSE assay with transwell to investigate the suppressive function via IL-10 and TGF-β1 of the subline CB 1. When CFSE-labeled Tresp cells were cultured with the control CB 1 subline under transwell conditions, the proportion of non-divided Tresp cells was approximately 45% (Fig. 4C). On the other hand, non-divided Tresp cells decreased to 15% or 30% by culture with the IL-10 or TGF-β1 knocked-down subline CB 1, respectively. These findings indicated that approximately half of the enhanced suppressive function of the subline CB 1 was due to the increased production of soluble factors such as IL-10 and TGF-β1, whereas the remaining half of the suppressive function was due to the mediated cell–cell contact.

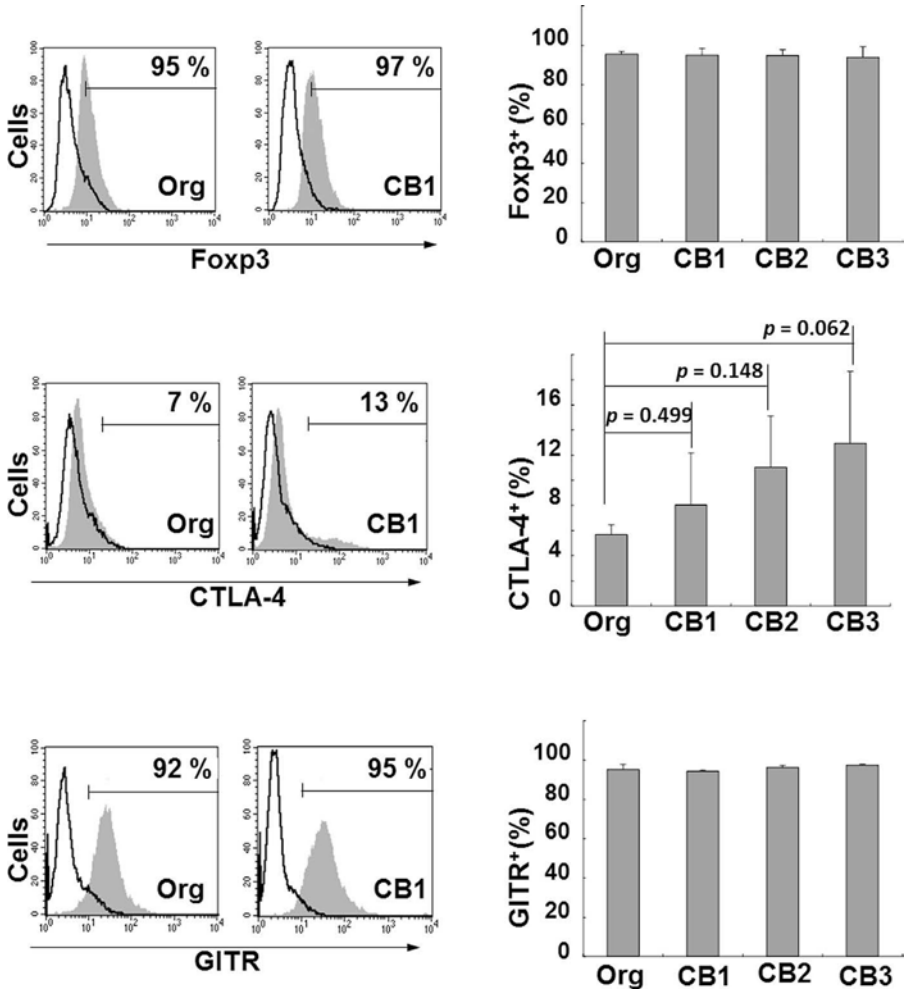

Fig. 3. Expression of the Treg-related molecules Foxp3, CTLA-4, and GITR in MT-2Org and the sublines CB 1–3. Histograms show a representative example of intracellular Foxp3, cell surface CTLA-4 and GITR in MT-2Org and the subline CB 1. The graphs show the percentage of $Foxp3^+$, $CTLA\text{-}4^+$, and $GITR^+$ cells. Data shown are the mean + SD from three independent experiments. The *p*-value was obtained using Dunnett's test.

4. Discussion

Asbestos exposure and the subsequent development of various cancers are an important problem not only from a medical aspect, but also from a social viewpoint. This is highlighted by the fact that patients with asbestos-induced malignancies such as MM and lung cancer were exposed to asbestos approximately 30–40 years ago (Brody, 2010; Jamrozik et al., 2011; Liu et al., 2013; Stayner et al., 2013). The banning of asbestos or restrictions concerning its use should have been the responsibility of manufacturers and governments decades ago in order to safeguard occupational health. Furthermore, it is alarming that people who lived in areas surrounding the asbestos handling industry also exhibit a high incidence of MM (Kurumatani and Kumagai, 2008; Kumagai and Kurumatani, 2009). These issues still exist in various countries, particularly in developing nations.

Since we discovered alteration of immune cells following silica (SiO_2) exposure (Hayashi et al., 2010; Lee et al., 2012, 2014), it is thought that asbestos, which is a mineral silicate, may also affect immune cells. The reduction of anti-tumor immunity may have occurred because the most important complication exhibited by asbestos-exposed individuals is the occurrence of cancers such as MM and those related to the lung (Camus, 2001; Bertino et al., 2009; Baratti et al., 2011; Frank and Joshi, 2014) with a long latency period of 30–40 years (Fig. 5).

It is on the basis of these findings that we have been investigating the immunological effects of asbestos fibers. As reported previously, the human HTLV-1 immortalized polyclonal T cell line MT-2 was utilized in this investigation (Hyodoh et al., 2005; Miura et al., 2006; Otsuki et al., 2007; Maeda et al., 2010). Although MT-2 progressed to apoptosis following a transient and relatively high dose of exposure, subjecting the subline to continuous asbestos exposure with a relatively low dose (doses with which transient exposure yielded less than half the level of apoptosis) resulted in certain changes that included upregulation of IL-10, activation of STAT3 following upregulation of Bcl-2, and acquisition of resistance to asbestos-induced apoptosis. These cellular features were also confirmed following examination of plasma and peripheral blood CD4+ T cells derived from patients with MM (Miura et al., 2006; Otsuki et al., 2007).

Investigations using this cell line model revealed that asbestos exposure caused reduction of CXCR3 expression with a decrease in the production potential for IFNγ secretion in asbestos-exposed T cells (Maeda et al., 2011a,b). These findings were later confirmed using specimens from asbestos-exposed PP and MM patients (Maeda et al., 2011a,b). As both CXCR3 and IFNγ are important molecules for anti-tumor immunity (Musha et al., 2005; Yoon et al., 2009; Billottet et al., 2013), individuals exposed to asbestos may possess reduced anti-tumor immunity.

We examined Treg function in this study to determine whether it is altered by asbestos exposure. The results indicated that Treg

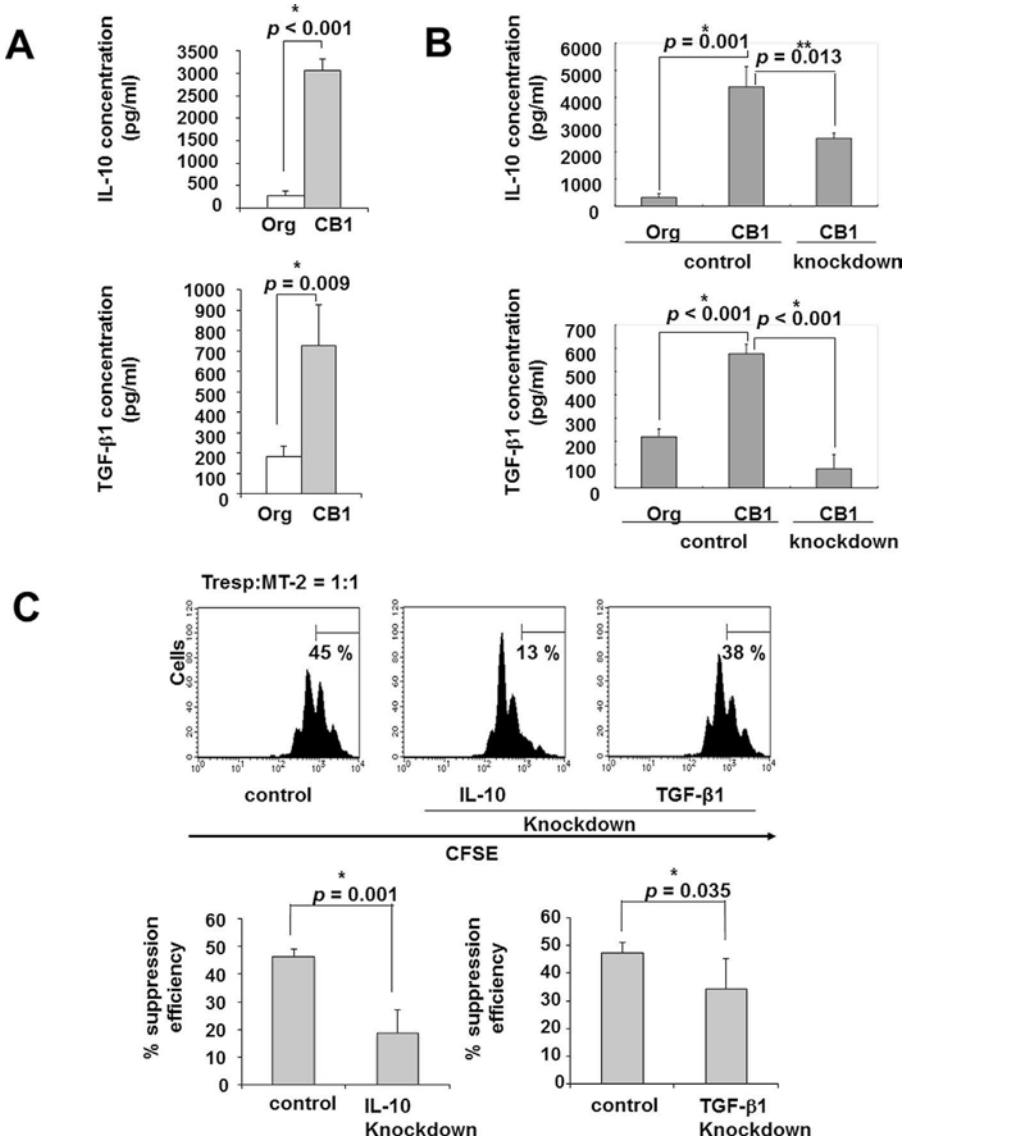

Fig. 4. The suppressive function of the subline CB 1 was enhanced through the soluble factors IL-10 and TGF-β1. (A) IL-10 (top) and activated TGF-β1 (bottom) levels in culture supernatants of MT-2Org and the subline CB 1 were assessed by ELISA. Error bars represent SD from three independent experiments. The *p*-value was obtained using an unpaired t-test. $^{*}p < 0.01$, $^{**}p < 0.05$. (B) IL-10 and TGF-β1 were knocked down in the subline CB 1 using lentiviral vector-mediated RNA interference as described in Section 2. IL-10 (top) and activated TGF-β1 (bottom) levels in culture supernatants were assessed by ELISA. Error bars represent SD from three independent experiments. The *p*-value was obtained using an unpaired *t*-test. $^{*}p < 0.01$, $^{**}p < 0.05$. (C) The effects of both soluble factors on the suppressive function of the subline CB 1 were analyzed by a transwell assay. CFSE-labeled Tresp cells (1×10^5) were stimulated with plate-bound anti-CD3 mAb (1 μg/mL) and irradiated autologous iDC (1×10^4). The subline CB 1 (control cells), the knockdown of IL-10 in CB 1, or the knockdown of TGF-β1 in CB 1 were cultured at 2×10^5 in transwell. Histograms show a representative example of the suppressive function (top). Non-dividing cells were gated and are indicated as a suppression efficiency (%). The graph shows the suppression efficiency (bottom). Data shown are the mean + SD from three independent experiments. The *p*-value was obtained using an unpaired *t*-test. $^{*}p < 0.01$, $^{**}p < 0.05$.

function caused by cell–cell contact and production of soluble factors such as IL-10 and TGF-β1 was enhanced following continuous exposure to asbestos. This also strongly indicated that asbestos exposure diminishes anti-tumor immunity in asbestos-exposed individuals. The overall level of anti-tumor immunity as represented by Treg, tumor-attacking T cells, NK cells and CTL tended to decrease. We have demonstrated that CXCR3 and IFNγ were reduced in T cells (Maeda et al., 2011a,b), that the expression of NKp46, the cell activating receptor, was reduced in asbestos-exposed patients such as those with PP and MM, and that in individual patients a positive correlation was found between the expression level of NKp46 and NK cell cytotoxicity (Nishimura et al., 2009a,b, 2013). In addition, differentiation and proliferation of CD8+ CTL were suppressed by co-culturing with asbestos, and the CTL function in peripheral blood from mesothelioma patients was reduced (Kumagai-Takei et al., 2013, 2014). This may provide an insight into part of the mechanisms associated with the occurrence of malignant tumors in asbestos-exposed patients and involving a long-term latency period (30–40 years).

We investigated the effects on Treg of silica, which is the core chemical component of asbestos. However, the physical features of silica and asbestos differ since asbestos is a fibrous substance and silica comprises particulate matter. The effect of silica on Treg was characterized as induction of chronic activation. The results of the chronic activation indicated that Treg express Fas/CD95 earlier and easily, which results in early cell death. Since chronic exposure to silica particles of Tresp also induces chronic activation, and Tresp may survive longer and acquire cellular features for resistance to

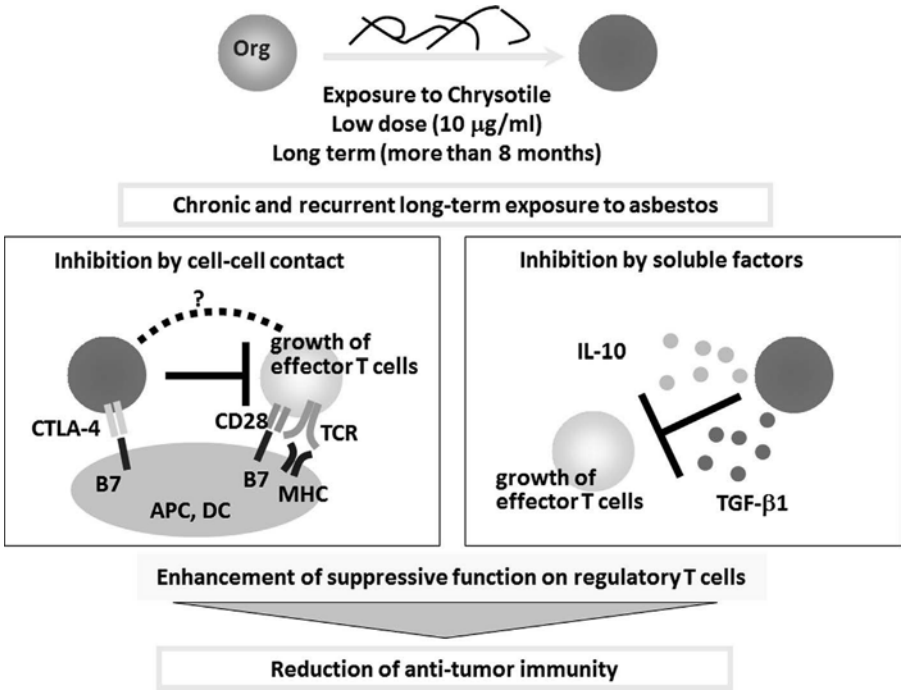

Fig. 5. Schematic summary of the predicted effects of continuous exposure of Treg to asbestos. A long-term exposure to asbestos at a low dose induces enhancement of the Treg suppressive function through cell–cell contact and production of the soluble factors IL-10 and TGF-β1, indicating that this enhanced Treg function leads to the reduction of anti-tumor immunity in individuals exposed to asbestos.

Fas/CD95-mediated apoptosis, an unbalance (less Treg and more Tresp) of Treg/Tresp occurs in silicosis patients, and this unbalance may partly explain the frequent occurrence of complications involving autoimmune diseases in silicosis patients (Wu et al., 2006; Hayashi et al., 2010; Lee et al., 2014, 2012).

When we focused on changes in Treg concerning the immunological effect of silica and the mineral silicate (asbestos), the effects caused by silica and asbestos tended to result in opposite outcomes. Silica caused the reduction of Treg and asbestos induced an enhancement of Treg function. Future investigations should therefore be performed to determine how both materials affect Treg to yield different cellular alterations, including reductions or increases of the Treg cell population.

Investigation of asbestos-exposed patients such as those with PP and MM did not clarify whether their circulating Treg showed enhancement of function as revealed in the cell line model, since Treg usually work in the surrounding area of tumors. The next step is therefore to confirm our findings by collecting tumor-surrounding Treg derived from asbestos-induced mesothelioma in order to analyze their functions.

A consideration of Treg function in terms of cell–cell contact indicates that the expression of CD103 (αEβ7 integrin) is important. Although we did not investigate the expression level of Cd103 at either the surface or mRNA level in this study, we previously employed cDNA microarray analysis using the original MT-2 cell line and the continuously exposed sublines (Maeda et al., 2011a,b). The microarray data revealed that the fold changes of CD103 expression in the six sublines were respectively 0.64, 0.75, 0.80, 1.12, 1.45 and 1.47 when compared with the original MT-2 cell line. Therefore, CD103 expression did not change substantially and showed some variation. In addition, the expression of cell surface CD25 as a typical marker for Treg in the original MT-2 cell line and sublines was sufficiently high to express most of the cells, and no differences were observed between the original line and the sublines. Additionally, it is difficult to detail a shift in the Th1 and Th2 balance in asbestos-exposed patients using our recent findings because we thought the high production of IL-10 may be due to Treg, and not Th2-type helper T cells. Therefore, detailed analyses regarding cytokines for helper T cells, as well as changes in Th17 cells, are necessary in future investigations of asbestos-exposed patients. Finally, since continuously exposed sublines showed resistance to asbestos-induced apoptosis, the relationship between FoxP3 expression and apoptosis-related genes, particularly genes regulated by FoxP3, should form an interesting aspect of future studies.

In conclusion, our studies have revealed that Treg continuously exposed to asbestos fibers showed enhancement of function by cell–cell contact and increased production of soluble factors, and individuals exposed to asbestos appeared to possess a reduction of anti-tumor immunity. These findings may be useful in modifying the immunological status of asbestos-exposed individuals, in whom anti-tumor immunity is reduced, by recovering their anti-tumor immunity through physiologically active substances derived from food sources or other materials such as cytokines. This type of intervention may safeguard asbestos-exposed individuals against the development of malignancies.

Conflict of interest

All the authors have no disclosure of COI for this study.

Acknowledgements

We thank Dr. Yasuo Ariumi for the VSV-G-pseudotyped HIV-1-based vector system (pCMVΔ R8.91 and pMDG2), pSUPER, pRDI292, and 293FT cells. We also thank Ms. Naomi Miyahara, Minako Katoh, Misao Kuroki, Keiko Kimura, Yoshiko Yamashita and Tomoko Sueishi for their technical assistance. The authors thank the former members of our department, Dr. Yoshie Miura, Shuko Murakami, Fuminori Hyodoh, Akiko Takata-Tomokuni and Ayako Ueki, for their contribution to the establishment of the fundamental concepts of this investigation.

This study was supported by Special Coordination Funds for Promoting Science and Technology grant H18-1-3-3-1

(Comprehensive Approach on Asbestos-Related Diseases), grants from the Ministry of Education, Culture, Sports, Science and Technology of Japan (18390186,1965153, 19790411, 20390178 and 22700933), Ryobi Teien Memory Foundation, The Promotion and Mutual Aid Corporation for Private Schools of Japan, Kawasaki Medical School Project Grants (21-201), the Strategic Research Foundation Grant-aided Project for Private Universities from the Ministry of Education, Culture, Sport, Science, and Technology, Japan, and the Program to Disseminate Tenure Tracking System (FY 2011-2013) from the Ministry of Education, Culture, Sports, Science and Technology of Japan.

References

Baratti, D., Kusamura, S., Deraco, M., 2011. Diffuse malignant peritoneal mesothelioma: systematic review of clinical management and biological research. J. Surg. Oncol. 103, 822–831.

Barrett, J.C., Lamb, P.W., Wiseman, R.W., 1989. Multiple mechanisms for the carcinogenic effects of asbestos and other mineral fibers. Environ. Health Perspect. 81, 81–89.

Bertino, P., Carbone, M., Pass, H., 2009. Chemotherapy of malignant pleural mesothelioma. Expert Opin. Pharmacother. 10, 99–107.

Billottet, C., Quemener, C., Bikfalvi, A., 2013. CXCR3, a double-edged sword in tumor progression and angiogenesis. Biochim. Biophys. Acta 1836, 287–295.

Bridge, A.J., Pebernard, S., Ducraux, A., Nicoulaz, A.L., Iggo, R., 2003. Induction of an interferon response by RNAi vectors in mammalian cells. Nat. Genet. 34, 263–264.

Brody, A.R., 2010. Asbestos and lung disease. Am. J. Respir. Cell Mol. Biol. 42, 131–132.

Brummelkamp, T.R., Bernards, R., Agami, R., 2002. A system for stable expression of short interfering RNAs in mammalian cells. Science 296, 550–553.

Camus, M., 2001. A ban on asbestos must be based on a comparative risk assessment. CMAJ 164, 491–494.

Chattopadhyay, S., Chakraborty, N.G., Mukherji, B., 2005. Regulatory T cells and tumor immunity. Cancer Immunol. Immunother. 54, 1153–1161.

Chen, S., Ishii, N., Ine, S., Ikeda, S., Fujimura, T., Ndhlovu, L.C., Soroosh, P., Tada, K., Harigae, H., Kameoka, J., Kasai, N., Sasaki, T., Sugamura, K., 2006. Regulatory T cell-like activity of $Foxp^{3+}$ adult T cell leukemia cells. Int. Immunol. 18, 269–277.

D'Cruz, D., 2000. Autoimmune diseases associated with drugs, chemicals and environmental factors. Toxicol. Lett. 112–113, 421–432.

Frank, A.L., Joshi, T.K., 2014. The global spread of asbestos. Ann. Glob. Health 80, 257–262.

Friedman, G.K., 2011. Malignant diseases attributed to asbestos exposure. In: Dodson, R.E., Hammar, S.P. (Eds.), Risk Assessment, Epidemiology, and Health Effects. CRC Press, Taylor and Francis, New York, pp. 561–592.

Gómez-Puerta, J.A., Gedmintas, L., Costenbader, K.H., 2013. The association between silica exposure and development of ANCA-associated vasculitis: systematic review and meta-analysis. Autoimmun. Rev. 12, 1129–1135.

Hayashi, H., Miura, Y., Maeda, M., Murakami, S., Kumagai, N., Nishimura, Y., Kusaka, M., Urakami, K., Fujimoto, W., Otsuki, T., 2010. Reductive alteration of the regulatory function of the CD4(+)CD25(+) T cell fraction in silicosis patients. Int. J. Immunopathol. Pharmacol. 23, 1099–1109.

Horwitz, D.A., Zheng, S.G., Gray, J.D., 2003. The role of the combination of IL-2 and TGF-beta, IL-10 in the generation and function of CD4+ CD25+ and CD8+ regulatory T cell subsets. J. Leukoc. Biol. 74, 471–478.

Hyodoh, F., Takata-Tomokuni, A., Miura, Y., Sakaguchi, H., Hatayama, T., Hatada, S., Katsuyama, H., Matsuo, Y., Otsuki, T., Katsuyama, H., Matsuo, Y., Otsuki, T., 2005. Inhibitory effects of anti-oxidants on apoptosis of a human polyclonal T-cell line, MT-2, induced by an asbestos, chrysotile-A. Scand. J. Immunol. 61, 442–448.

Jamrozik, E., de Klerk, N., Musk, A.W., 2011. Asbestos-related disease. Intern. Med. J. 41, 372–380.

Kamp, D.W., Graceffa, P., Pryor, W.A., Weitzman, S.A., 1992. The role of free radicals in asbestos-induced diseases. Free Radic. Biol. Med. 112, 293–315.

Kohyama, N., Shinohara, Y., Suzuki, Y., 1996. Mineral phases and some reexamined characteristics of the International Union Against Cancer standard asbestos samples. Am. J. Ind. Med. 30, 515–528.

Kumagai, S., Kurumatani, N., 2009. Asbestos fiber concentration in the area surrounding a former asbestos cement plant and excess mesothelioma deaths in residents. Am. J. Ind. Med. 52, 790–798.

Kumagai-Takei, N., Nishimura, Y., Maeda, M., Hayashi, H., Matsuzaki, H., Lee, S., Hiratsuka, J., Otsuki, T., 2013. Effect of asbestos exposure on differentiation of cytotoxic T lymphocytes in mixed lymphocyte reaction of human peripheral blood mononuclear cells. Am. J. Respir. Cell Mol. Biol. 49, 28–36.

Kumagai-Takei, N., Nishimura, Y., Maeda, M., Hayashi, H., Matsuzaki, H., Lee, S., Kishimoto, T., Fukuoka, K., Nakano, T., Otsuki, T., 2014. Functional properties of CD8(+) lymphocytes in patients with pleural plaque and malignant mesothelioma. J. Immunol. Res. 2014, 670140. doi:http://dx.doi.org/10.1155/2014/670140.

Kurumatani, N., Kumagai, S., 2008. Mapping the risk of mesothelioma due to neighborhood asbestos exposure. Am. J. Respir. Crit. Care Med. 178, 624–629.

Lee, S., Hayashi, H., Maeda, M., Chen, Y., Matsuzaki, H., Takei-Kumagai, N., Nishimura, Y., Fujimoto, W., Otsuki, T., 2012. Environmental factors producing autoimmune dysregulation-chronic activation of T cells caused by silica exposure. Immunobiology 217, 743–748.

Lee, S., Matsuzaki, H., Kumagai-Takei, N., Yoshitome, K., Maeda, M., Chen, Y., Kusaka, M., Urakami, K., Hayashi, H., Fujimoto, W., Nishimura, Y., Otsuki, T., 2014. Silica exposure and altered regulation of autoimmunity. Environ. Health Prev. Med. 19, 322–329.

Linehan, D.C., Goedegebuure, P.S., 2005. CD25+ CD4+ regulatory T-cells in cancer. Immunol. Res. 32, 155–168.

Liu, G., Cheresh, P., Kamp, D.W., 2013. Molecular basis of asbestos-induced lung disease. Annu. Rev. Pathol. 8, 161–187.

Maeda, M., Chen, Y., Hayashi, H., Kumagai-Takei, N., Matsuzaki, H., Lee, S., Nishimura, Y., Otsuki, T., 2014. Chronic exposure to asbestos enhances TGF-β1 production in the human adult T cell leukemia virus-immortalized T cell line MT-2. Int. J. Oncol. 45, 2522–2532.

Maeda, M., Nishimura, Y., Hayashi, H., Kumagai, N., Chen, Y., Murakami, S., Miura, Y., Hiratsuka, J., Kishimoto, T., Otsuki, T., 2011a. Reduction of CXC chemokine receptor 3 in an in vitro model of continuous exposure to asbestos in a human T-cell line MT-2. Am. J. Respir. Cell Mol. Biol. 45, 470–479.

Maeda, M., Nishimura, Y., Hayashi, H., Kumagai, N., Chen, Y., Murakami, S., Miura, Y., Hiratsuka, J., Kishimoto, T., Otsuki, T., 2011b. Decreased CXCR3 expression in CD4+ T cells exposed to asbestos or derived from asbestos-exposed patients. Am. J. Respir. Cell Mol. Biol. 45, 795–803.

Maeda, M., Nishimura, Y., Kumagai, N., Hayashi, H., Hatayama, T., Katoh, M., Miyahara, N., Yamamoto, S., Hirastuka, J., Otsuki, T., 2010. Dysregulation of the immune system caused by silica and asbestos. J. Immunotoxicol. 7, 268–278.

Miura, Y., Nishimura, Y., Katsuyama, H., Maeda, M., Hayashi, H., Dong, M., Hyodoh, F., Tomita, M., Matsuo, Y., Uesaka, A., Kuribayashi, K., Nakano, T., Kishimoto, T., Otsuki, T., 2006. Involvement of IL-10 and Bcl-2 in resistance against an asbestos-induced apoptosis of T cells. Apoptosis 11, 1825–1835.

Mulloy, K.B., 2003. Silica exposure and systemic vasculitis. Environ. Health Perspect. 111, 1933–1938.

Musha, H., Ohtani, H., Mizoi, T., Kinouchi, M., Nakayama, T., Shiiba, K., Miyagawa, K., Nagura, H., Yoshie, O., Sasaki, I., 2005. Selective infiltration of CCR5(+)CXCR3(+) T lymphocytes in human colorectal carcinoma. Int. J. Cancer 116, 949–956.

Naldini, L., Blömer, U., Gallay, P., Ory, D., Mulligan, R., Gage, F.H., Verma, I.M., Trono, D., 1996. In vivo gene delivery and stable transduction of nondividing cells by a lentiviral vector. Science 272, 263–267.

Nishimura, Y., Maeda, M., Kumagai, N., Hayashi, H., Miura, Y., Otsuki, T., 2009a. Decrease in phosphorylation of ERK following decreased expression of NK cell-activating receptors in human NK cell line exposed to asbestos. Int. J. Immunopathol. Pharmacol. 22, 879–888.

Nishimura, Y., Maeda, M., Kumagai-Takei, N., Lee, S., Matsuzaki, H., Wada, Y., Nishiike-Wada, T., Iguchi, H., Otsuki, T., 2013. Altered functions of alveolar macrophages and NK cells involved in asbestos-related diseases. Environ. Health Prev. Med. 18, 198–204.

Nishimura, Y., Miura, Y., Maeda, M., Kumagai, N., Murakami, S., Hayashi, H., Fukuoka, K., Nakano, T., Otsuki, T., 2009b. Impairment in cytotoxicity and expression of NK cell- activating receptors on human NK cells following exposure to asbestos fibers. Int. J. Immunopathol. Pharmacol. 22, 579–590.

Otsuki, T., Maeda, M., Murakami, S., Hayashi, H., Miura, Y., Kusaka, M., Nakano, T., Fukuoka, K., Kishimoto, T., Hyodoh, F., Ueki, A., Nishimura, Y., 2007. Immunological effects of silica and asbestos. Cell. Mol. Immunol. 4, 261–268.

Stayner, L., Welch, L.S., Lemen, R., 2013. The worldwide pandemic of asbestos-related diseases. Annu. Rev. Public Health 34, 205–216.

Steenland, K., Goldsmith, D.F., 1995. Silica exposure and autoimmune diseases. Am. J. Ind. Med. 28, 603–608.

Taylor, A., Verhagen, J., Blaser, K., Akdis, M., Akdis, C.A., 2006. Mechanisms of immune suppression by interleukin-10 and transforming growth factor-beta: the role of T regulatory cells. Immunology 117, 433–442.

Toyokuni, S., 2014. Iron overload as a major targetable pathogenesis of asbestos-induced mesothelial carcinogenesis. Redox Rep. 19, 1–7.

Wichmann, I., Sanchez-Roman, J., Morales, J., Castillo, M.J., Ocaña, C., Nuñez-Roldan, A., 1996. Antimyeloperoxidase antibodies in individuals with occupational exposure to silica. Ann. Rheum. Dis. 55, 205–207.

Wu, P., Miura, Y., Hyodoh, F., Nishimura, Y., Hatayama, T., Hatada, S., Sakaguchi, H., Kusaka, M., Katsuyama, H., Tomita, M., Otsuki, T., 2006. Reduced function of CD4 +25+ regulatory T cell fraction in silicosis patients. Int. J. Immunopathol. Pharmacol. 19, 357–368.

Yoon, S.H., Yun, S.O., Park, J.Y., Won, H.Y., Kim, E.K., Sohn, H.J., Cho, H.I., Kim, T.G., 2009. Selective addition of CXCR3(+) CCR4(−) CD4(+) Th1 cells enhances generation of cytotoxic T cells by dendritic cells in vitro. Exp. Mol. Med. 41, 161–170.

Zufferey, R., Nagy, D., Mandel, R.J., Naldini, L., Trono, D., 1997. Multiply attenuated lentiviral vector achieves efficient gene delivery in vivo. Nat. Biotechnol. 15, 871–875.

労災疾病臨床研究事業

胸膜中皮腫の的確な診断方法に関する研究
―鑑別診断方法と症例収集―

平成 26～28 年度　総括・分担研究報告書

平成 29 年 3 月 31 日発行

発行：研究代表者　岸本　卓巳

〒702-8055　岡山市南区築港緑町 1-10-25
独立行政法人　労働者健康安全機構　岡山労災病院